Evaluation of Liquefaction Potential on Selected Sites of Hawassa City

By:

Tewodros Tadesse

Addis Ababa University

Addis Ababa, Ethiopia

November, 2017

Addis Ababa University

Addis Ababa Institute of Technology

School of Civil and Environmental Engineering

Evaluation of Liquefaction Potential on Selected Sites of Hawassa City

by

Tewodros Tadesse

Advisor: Asrat Worku (Dr.-Ing)

Sponsor: Ethiopian Road Authority (ERA)

November, 2017

A thesis submitted to the School of Graduate Studies of Addis Ababa University in Partial fulfillment of the Degree of Master of Science in Geotechnical Engineering.

UNDERTAKING

I certify that the research work titled "**Evaluation of Liquefaction Potential on Selected Sites of Hawassa City**" is my own work. The work has not been presented elsewhere for assessment. Where material has been used from other sources, it has been properly acknowledged/referred.

_____

Tewodros Tadesse

ABSTRACT

A city of high population growth and rapid development founded on top of soft, lacustrine and alluvial deposit, Hawassa is located in a seismically active area of the country. On top of this, the fact that it is a lakeside city makes liquefaction a potential hazard that calls for serious consideration. This thesis evaluates the potential of liquefaction of Hawassa city based on data acquired after selecting sites in and around the city. Based on these data, the level of hazard with respect to magnitudes of earthquakes and vulnerable layers thickness with depth is assessed. SPT and shear-wave velocity based simplified procedure methods are used to evaluate the liquefaction potential of the study area. This study evaluates liquefaction resistance of the soil against earthquake induced loads expressed in terms cyclic shear stress of the study area. The results of the analyses are compared with factor of safeties recommended by ES-EN1998:2015 and BSSC 2000. Majority of the results indicated liquefaction hazard is minimal within the city with some parts showing marginal signs of liquefaction, leading to the recommendation of site specific studies for important structures.

Key words: Liquefaction, Simplified procedure, Hawassa

ACKNOWLEDGMNET

I would like to express my deepest gratitude to my advisor, Dr. Asrat Worku, Chairman of Geotechnical Engineering Unit, School of Civil and Environmental Engineering, Addis Ababa University. His office doors were always open whenever I needed to talk to him, in addition to the amount of time he dedicated to consult and review this work. I would like to thank him for his patience and valuable advice.

I would like to thank Ethiopian Road Authority (ERA) for the financial support and Addis Ababa University for giving this wonderful chance to pursue my postgraduate study in geotechnical engineering program.

I would also like to acknowledge Besrat Eshetu, School of Civil and Environmental Engineering at AAiT, for his valuable comment on this thesis and continuous support on acquiring the required data.

I would like to thank the experts of Institute of Geophysics, Space Science and Astronomy (IGSSA), AAU: Dr. Getnet Mewa, Dr. Genet Tamiru, Dr. Atalay Ayele, Birhanu Abera, Daniel Mamo and Sisay Alemayehu for their kind cooperation in conducting geophysical survey.

I would like to thank the Ethiopia Construction Design and supervision Works Corporation, Building and Urban Design and Supervision Works Sector geotechnical and IT department Heads and their staff, M.H. Engineering Plc, and Addis Geosystems Plc for providing access to the geotechnical investigations reports of various projects.

I would like to thank the City Administration of Hawassa and Mayor office, Ato Belayneh Teshome, Chief advisor of Mayor, for their positive and immediate response on giving permission to conduct the investigations in the city. Moreover the author would like to thankfully acknowledge, Hawassa University Agricultural College Dean Office, Hawassa City Police Commission, Menaheria sub-city Police, Haikdar Sub-city Police Offices, Amora-Gedel Park Administration, for their cooperation during the field survey.

I would like to acknowledge the developers of PEER data base, DEEPSOIL software, and GSHAP map for providing a free access and use of their respective tools and database for this thesis. Moreover, the author is also thankful for the valuable contribution by Zesteat Gashaye, Fasika worku, Seyfu Tefera, Yeneneh Atnafu.

Finally, I must express my very profound gratitude to my wife Frehiwot Mesfin and my beloved daughters Ruth and Yedidya for providing me with unfailing support and continuous encouragement throughout my years of study and through the process of researching and writing this thesis. This accomplishment would not have been possible without them. Thank you

TABLE OF CONTENTS

LIST OF TABLES

LIST OF FIGURES

ACRONYMS

α_{max}	Maximum ground surface acceleration
CSR	Cyclic stress ratio
CRR	Cyclic resistance ratio
Dsr	Significant duration
EQL	Equivalent linear analysis
FLS	Flow liquefaction surface
FS	Factor of Safety
G_{max}	Small strain shear modulus
GSHAP	Global Seismic Hazard assessment program
GWT	Ground water table
I	Current
K'_o	Coefficient of earth pressure at rest
K_σ	Overburden stress correction factor
M	Moment magnitude
MER	Main Ethiopian rift
MSF	Magnitude scaling factor
P_α	Atmospheric pressure
PEER	Pacific Earthquake Engineering Research center
PGA	Peak ground acceleration

PSHA	Probabilistic seismic hazard analysis
r_d	Depth reduction factor
SER	Southern Ethiopian rift
SPT	Standard penetration test
V_P	Primary velocity
V_S	Shear wave velocity
V_{Sd}	Timed average shear wave velocity from top to depth, d
V_{S30}	Timed average shear wave velocity of the top 30m depth
μ	Poisson's ratio
ρ_a	Apparent resistivity
ΔV	Potential difference

CHAPTER ONE

INTRODUCTION

1.1 General

Natural disasters like earthquake can neither be predicted nor prevented. However, the severity of the damage can be minimized by proper infrastructure and development planning based on proper studies. The consequence of an earthquake nowadays could be distressing because of the alarming rate, at which development of infrastructures and urbanization in most seismically active regions of Ethiopia, is taking place. High rise buildings, highway bridges, dams and other infrastructures enhance the catastrophic effect of earthquakes and endanger human life as well as potentially having significant impact on the country's economy.

Hawassa is one of the cities found in the seismic active zone of the country. Being the seat of the regional government, a popular tourist destination, a rapidly industrializing city, its population and infrastructure are booming at an alarming rate. It is one of the four cities in the country that expect a population growth that will approximately be four-times the current estimate by 2040 (Lamson-Hall et al. 2015).

The Ministry of Construction of Ethiopia has updated the country building code in 2015 which will be used for design of earthquake resistant structures by adopting the level of risk and current practiced worldwide (ES EN 1998:2015). However the risk of liquefaction is not addresses in the document.

Hawassa city is built on thick lacustrine deposits which can amplify the earthquake shaking intensity significantly. The percentage of silt is high in all sampled sites indicating that there could be a chance of the soil to liquefy under the action of earthquake ground motions. The ground water table (perched or free) is found at different depths during borehole investigations performed in different sites.

The purpose of this thesis is, therefore, to evaluate the potential of liquefaction in and around Hawassa with current knowledge of the phenomena based on subsurface data at some selected sites and seismic hazard expected in the region. Since strong ground motion record is scarce in the region, the seismicity of the region is considered from the revised code (ES EN 1998:2015) and Global Seismic Hazard Assessment Program (GSHAP) map (Giardini et al. 2003). The subsurface data are gathered from geotechnical investigation performed by different companies and geophysical surveys conducted for this study.

1.2 Description of the Study Area

1.2.1 Location

Hawassa is the seat of Southern Ethiopia Nation Nationality Regional State Government found 275km south of Addis Ababa with approximate geographical coordinates of 7^0 North and 38.5^0 East (Figure1.1).

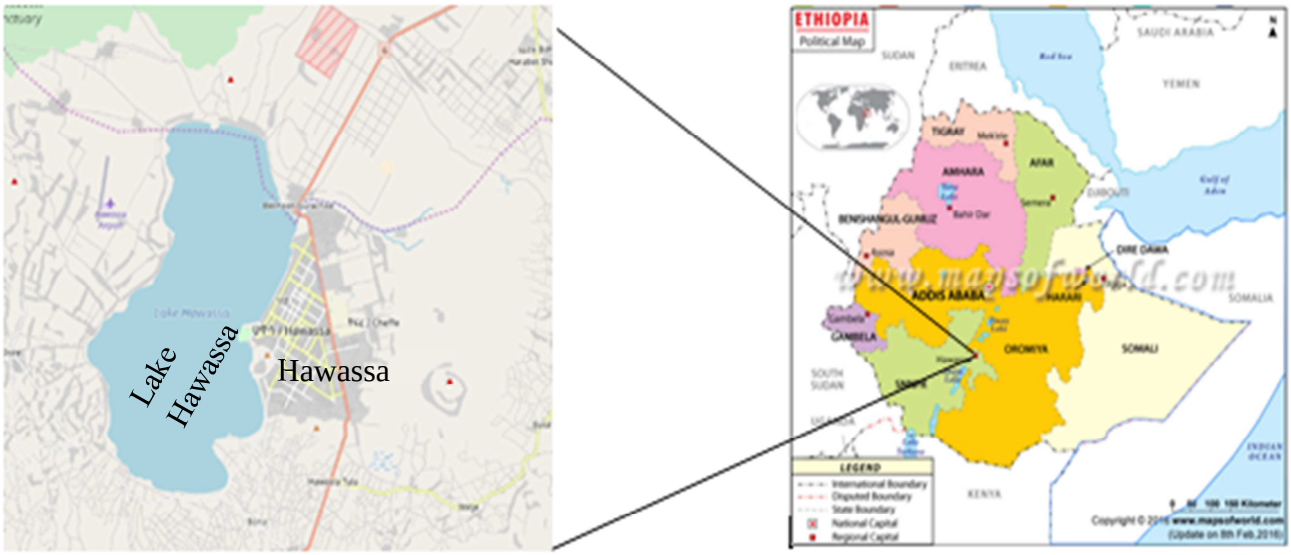

Figure 1.1 Location map of the study Area (www.mapsoftworld.com)

1.2.2 Current and Projected Demographics of Hawassa

Hawassa is one of the thriving metropolises in the country. The city administration has planned to build a new waterfront city on and around the lake which covers 2,000 hectares with a distance of 11 km by land and 6-7 km by water. The new waterfront development will have a 500m buffer zone with luxurious landscape design. The main purpose of the development is making Hawassa the center for recreation and tourism among Ethiopian cities (Tekalign 2013).

Among commercial land use types, the hospitality sector is developing at a fast rate in Hawassa lake waterfront. The rate of development along the shore is so high that almost all plots are already occupied by investors for construction of resorts and luxury hotels (Tekalign, 2013).

Since the launch of the Ethiopia Urban Expansion Initiative (UEI) in mid-2013, the first group of four cities has approved plans that will allow them to accommodate their projected spatial growth to 2040. These four cities -Hawassa, Adama, Mekele, and Bahir Dar- have approved plans for over 1700km of 30m wide arterial roads, along with 81,000 hectares of land for expansion–enough to accommodate a 4-fold increase in the current built-up area of

these cities. These cities have also expanded their administrative boundaries, increasing the area under their control in response to estimates of their growth. According to the approved plan, the future expansion plan of Hawassa is prepared, which encircle the Hawassa lake Figure 1.2 (Lamson-Hall et al. 2015).

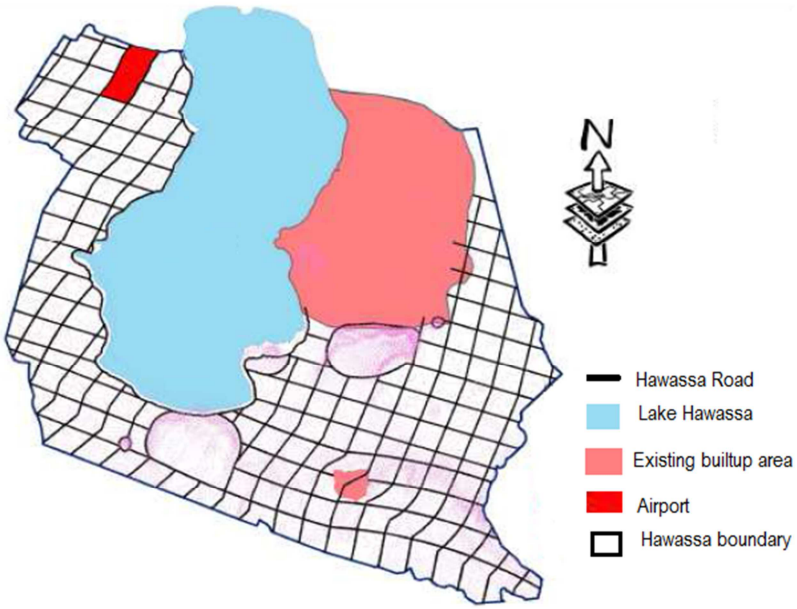

Figure 1.2 Expansion plan of Hawassa (Lamson-Hall et al. 2015)

1.2.3 Geomorphology of Hawassa basin and Hawassa city

Recent lacustrine and alluvial deposits, scoria cones, rhyolite lava flows and associated ignimbrites, tuffs and volcanic ash form the Hawassa basin. The rhyolite lava flows and the associated ignimbrites, tuffs and ash belong to the recent rhyolite volcanic centers and the scoria cones to the recent plateau basalts. Hawassa basin is made up of Nazeret series, which is composed of ignimbrite, unwelded tuff, ash flow, rhyolite flow, domes and trachyte. The northern, south western and western margins are made up of the Dino formation, which is characterized by ignimbrite, tuff, coarse pumice, water lain pyroclastic rocks with intercalation of lacustrine sediments. Either Dino Formation or Nazret series underlies the Hawassa basin deposits (Mengesha et al. 1996).

Moreover, Hawassa city was built on Early Pleistocene Hawassa Caldera and in the shade of two silicic volcanoes emerging from the floor of Middle Pleistocene Corbetti Caldera. Lake Hawassa and its surrounding areas are within a caldera basin, surrounded by steep caldera walls. Late Miocene to Pleistocene volcanic rocks are exposed toward the wall. Holocene sediments are distributed on the floor of the caldera. The lowest unit is Wendo Genet Rhyolite, which is thickly exposed at the foot of caldera wall, may have erupted from Hawassa caldera. Western and southern parts of the caldera are dominated by Wendo-Genet

Rhyolite. Corbetti Volcano is prominent in Holocene volcanic activity. This volcano was active around 20,000 years ago (JICA 2012).

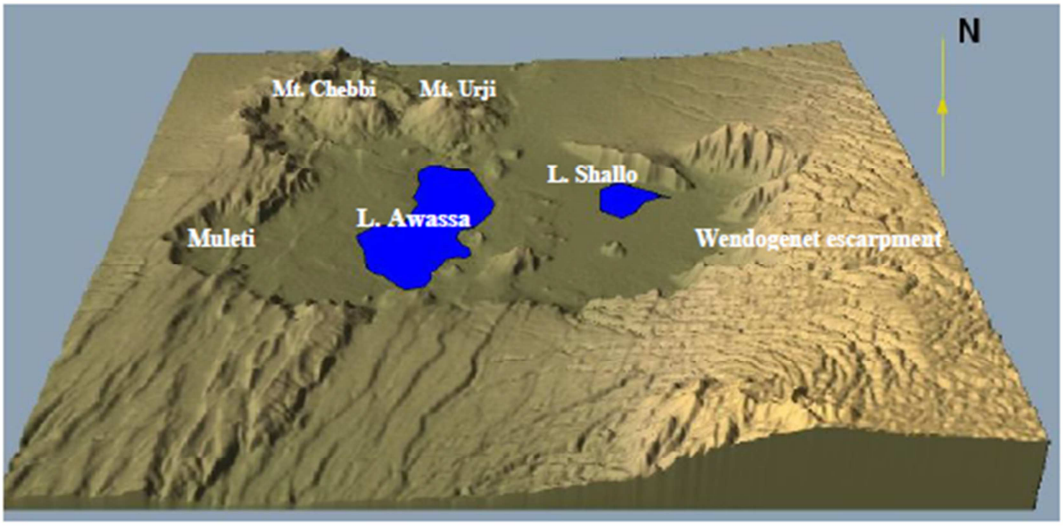

Figure 1.3 Digital Elevation Model showing the topography of the area (Global Mapper 2015)

1.2.4 Geological structure

The closed basin of the nested Hawassa-Corbetti caldera complex is a giant elliptical depression 30-40 kms wide as shown on Figure 1.3. There are a number of rift system faults with north and north-east trend along which the length of Lake Hawassa is oriented. These faults are expansion (normal faults) forming step faults, which are mainly dominant in the regions found south and south west of the lake (see Figure 1.3). The volcanic collapse structure (caldera) forms elliptical structure around Lake Hawassa basin. This collapse shifts some of the MER fault systems showing that the collapse has taken place subsequent to the rifting. In the Hawassa caldera a line of young faults affect the rift floor. These faults, the Wonji fault Belt shattered the rift floor into several relatively small horst and graven. Lakes or swamps occupy the more depressed areas. The Corbetti caldera, which is found north-west of Hawassa Lake, is a nested caldera within Hawassa caldera (Desse et al. 2003). The corbetti caldera has two volcanic centers of Urgi and Chebbi. The Urgi center is a source for the formation of pumice in the vicinity and Chebbi is a center for the formation of obsidian, which covers the Chebbi Mountain (Williams 2016)

1.2.5 Seismic hazard

The Ethiopian rift system is part of the East African Rift System, widely believed to have been formed by diverging lithospheric plates, which is active since the early tertiary times. The Ethiopian Rift system is commonly used to designate the three rift segments namely, the Afar depression, the Main Ethiopian Rift (MER), and the Southern Ethiopian Rift (SER). The

Probabilistic Seismic Hazard Analyses (PSHA) study in the region has revealed that the study area is located in high seismic hazard zone (Kebede and van Eck. 1997; Ayele 2017). The seismicity of the Horn of Africa region for the period from 1900 to 2012 compiled by Ayele (2017) show a concentration of earthquake sources around the study area (Figure 1.4).

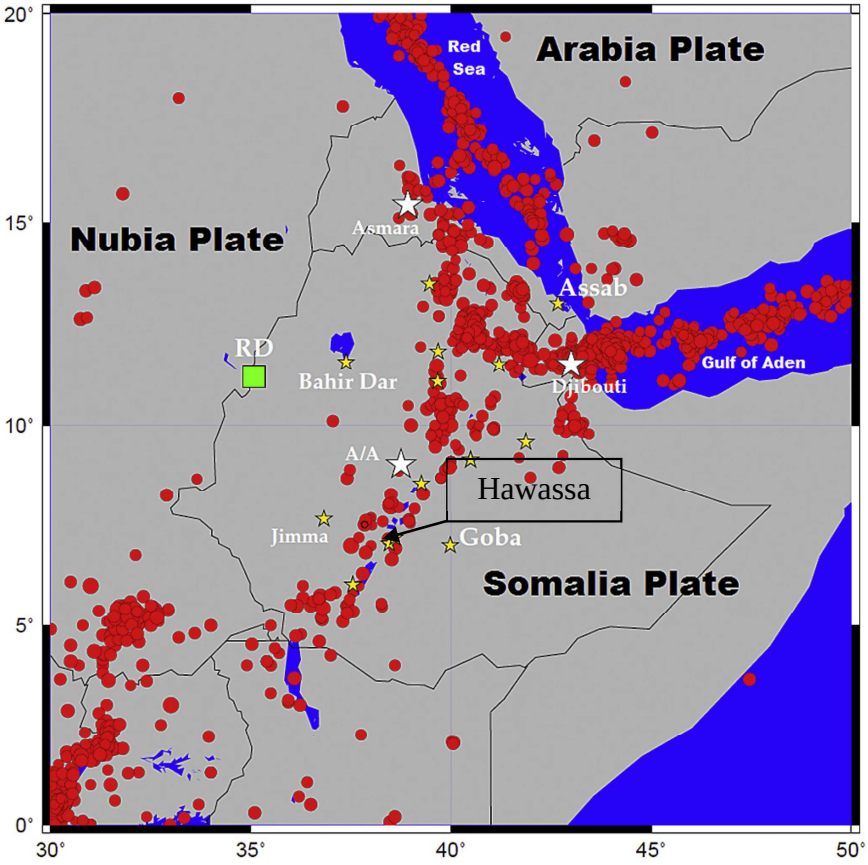

Figure 1.4 Seismicity of the Horn of Africa region for the period from 1900 to 2012 (after Ayele 2017)

1.3 The Research Problem

Around the lakes inside the rift, intensive urban development has been taking place, which is a very worrying process, considering seismic hazard. The subsoil at most populated localities is covered by lake sediments with low shear-wave velocities, which can potentially amplify the amplitude of seismic waves several times comparing to bedrock level intensities.

In the 20th century alone, a study done by Pierre Gouin reported that as many as 15,000 tremors, strong enough to be felt by humans, had occurred in Ethiopia and the Horn of Africa. A similar study indicated that there were a total of 16 recorded earthquakes of magnitude 6.5 and higher in some of Ethiopia's seismically active areas. The most significant earthquakes of the 20th and 21st centuries such as the 1906 Langano earthquake, the 1961 Kara Kore earthquake, the 1983 Wondo Genet earthquake, the 1985 Langano earthquake, the 1989 Dobi graben earthquake in central Afar, the 1993 Nazret earthquake, and the 2011 Hosanna earthquake were all felt in some of the major cities in the country such as Addis Ababa, Jimma, Nazret and Hawassa (Kassegne et al. 2012).

Different infrastructure and high rise buildings for hotels and resort, mixed use, residential, schools, hospitals and utilities like water supply pipes, telecom cables, storm drainage pipes, electric ducts, septic tanks, and other infrastructure are expanding in the study area, Hawassa city. Studies have been carried out in the study area related to geological, hydro-geological, geophysical investigation related to thermal springs and seismic hazard assessment. However, the shallow geological formation can significantly influence the shaking intensity, which can potentially trigger liquefaction of the uppermost loose soil deposit, especially with the shallow water level in sight.

In this thesis work, the potential of liquefaction of Hawassa and the surrounding area will be assessed using available and first-hand conducted investigations.

1.4 Objectives of the Study

1.4.1 General Objective of the study

The general objective of this research is assessing the liquefaction potential on selected sites of Hawassa and nearby the city.

1.4.2 Specific objectives of the study

- Evaluating the potential of liquefaction of the study area by the stress-based approach using the secondary and primary data from the city and around the city
- Identify range of magnitudes of earthquake that can potentially trigger liquefaction in the study area
- Identify the depth and thickness of layer which are vulnerable to liquefaction in the study area

1.5 Significance of the Study

Liquefaction phenomena can affect buildings, bridges, buried pipe lines, and other constructed facilities in many different ways. Liquefaction can also influence the nature of ground surface motions. Flow liquefaction can produce massive flow slide and contribute to the sinking or tilting of heavy structures, the floating of light buried structures, and to the failure of retaining structures. Cyclic mobility can cause slumping of slopes, settlement of buildings, lateral spreading, and retaining wall failure. Substantial ground oscillation, ground settlement, sand boils, post-earthquake stability failures can develop at level-ground sites.

Assessment of the liquefaction potential of the city will help the city administration to incorporate prevention and mitigation measures on future developmental plan of the city for the possible damage to occur due to liquefaction and related phenomena.

1.6 Previous Work

As far as previous works are concerned, the area has been a major interest for local and foreign researchers in the past. Different studies related to seismic hazard, geology, hydro-

geology, geothermal potential and ground water interaction have been conducted in the area. Out of these studies some are presented as follow;

The seismic hazard of southern Ethiopia has been studied by Malek (2014), Czech Republic Development Cooperation in conjunction with Ethiopian Geological Survey. The study compiled previous earthquake data for the purpose of seismic hazard analysis and asses the seismic risk level qualitatively.

The hydrogeology and engineering geology of the MER study has been conducted by the Geological Survey of Ethiopia (GSE) (Dessie and Tesema 2003). The study addresses the risk of Hawassa lake level rise and the remedial measures to be taken. It pointed out that the lacustrine deposit and fractured ignimbrite are the water bearing formation covers the area.

Characterization of ground water – lake water interaction in Lake Hawassa basin has been studied by Atnafu (2014). It studies the Lake water level variation effect on the groundwater of the city and also addressed the pollution of ground water on the lake.

More works were conducted in relations to the rise of lake level by Water Works Design and Supervision Enterprise (WWDSE 1999). This work includes land use/land cover and soils, water balance, analysis of lake level rise and storage change, as well as giving short and long-term remedial measures and socio-economic and environmental impact assessment of the remedial measures.

Nevertheless, as far as liquefaction assessment is concerned, no previous studies have been conducted in in the region as well as other earthquake-prone area of the country.

1.7 Limitations of the Study

Liquefaction potential assessment has to be conducted based on strong data base of earthquakes, subsurface geotechnical investigations, and soil parameters of the study area. This study has limited access to strong motion database recorded from the study area. Hence, the study used strong motion records from alternative sources. The available geophysical investigation used for subsurface investigation has limitation with respect to energy efficiency to explore deeper depth. Borehole data gathered are limited in number and most of them are shallow in depth of investigation. In addition to this, available resource limits the extent and coverage of investigation and laboratory work required to be performed for advanced assessment.

1.8 Organization of the Thesis

This thesis is organized in six chapters. The first chapter is general introduction of the study and the study area. The second chapter covers theoretical background of liquefaction and the science and pioneering research works selected for this study. Chapter Three is data acquisition and processing section. In this chapter the theoretical background of the data acquisition techniques are included. Chapter Four is the data analysis section of the research.

Chapter Five presents the interpretation of the results provided in Chapter Four. The last chapter comprises conclusions and recommendations of the research.

CHAPTER TWO

LITERATURE REVIEW

2.1Theoretical Background of Liquefaction

2.1.1 General

The most precise definition of liquefaction is given by Sladen et al. (1985), which states that liquefaction is a phenomenon wherein a mass of soil loses a large percentage of its shear resistance, when subjected to monotonic, cyclic, or shock loading, and flows in a manner resembling a liquid until the shear stresses acting on the mass are as low as the reduced shear resistance. Moreover, for the earthquake related definition given by the National Research Council (NRC), it is stated that during earthquakes, the shaking of ground may cause a loss of strength or stiffness that results in the settlement of buildings, landslides, the failure of earth dams, or other hazards. The process leading to such loss of strength or stiffness is called soil liquefaction. It is a phenomenon associated primarily, but not exclusively, with saturated cohesionless soils (Housner et al. 1985). Liquefaction typically occurs in cohesionless silt, sand, and fine-grained gravel deposits of Holocene to late Pleistocene age in areas where the groundwater is shallower than about 15 meter (Martin and Lew 1999). The depth of ground water either free or perched influences liquefaction susceptibility (Kramer 1996). At sites where ground water fluctuates significantly, liquefaction susceptibility may also fluctuate (Kramer 1996). It should be noted that the groundwater levels used for the purposes of liquefaction hazard zoning are the historically shallowest (highest) groundwater levels using the results of groundwater studies (Martin and Lew 1999).

2.1.2 Liquefaction hazard zoning

Delineating areas that are susceptible to liquefaction hazards is important for evaluating and reducing the risk from liquefaction through appropriate mitigation. Since, liquefaction generally occurs in areas underlain by low density, saturated fine grained granular sediments, the liquefaction susceptibility can be mapped using specific, well established geologic and geotechnical criteria. Damages caused by liquefaction of saturated soil revealed that after liquefaction the ground failed, sand boiling occurred and the structure subsided unevenly causing tilting, cracking or even collapse. Liquefaction susceptibility can be judged primarily based on four criteria according to Kramer, (1996). These are historical, geological, compositional and state criteria. Liquefaction often occurs in the same location when soil and ground water level condition have remained unchanged. Geological process that sorts soil into uniform grain size distributions and deposit them in loose states produces soil deposit with high liquefaction susceptibility (Kramer, 1996). Areas containing soil of late Holocene age where the ground water is less than 12m deep and anticipated earthquake peak ground acceleration (PGA) having a 475 return period is greater than 0.1g is susceptible to liquefaction (Martin and Lew 1999). Compositional characteristics associated with high

volume change potential tend to be associated with high liquefaction susceptibility (Kramer, 1996). Even if the soil meets all of the criteria described above for liquefaction susceptibility; it doesn't assure that the soil will liquefy. Susceptibility of liquefaction also depend on the initial state of the soil i.e. its stress and density condition at the time of earthquake (Kramer, 1996). Unsaturated soils are not subject to liquefaction because compression does not generate excess pore water pressure (Day 2002). It should be noted during liquefaction susceptibility study that sediments deposited on valley floors are presumed to become saturated during wet seasons and shallow water conditions can occur in narrow stream valleys that can receive an abundance of water runoff from canyon drainages and tributary streams during periods of high precipitation (Martin and Lew 1999).

2.1.3 Depth of Analysis for liquefaction evaluation

Liquefaction resistance of a soil deposit increases with depth as overburden pressure increases. Traditionally, a depth of 15 m has been used as the limit for depth of analysis for the evaluation of liquefaction. Liquefaction has been known to occur during earthquakes at deeper depths than 15m given that proper conditions such as low-density granular soils, presence of ground water, and sufficient cycles of earthquake ground motion prevail (Martin and Lew 1999).

Experience has shown that the 15m depth may be adequate for the evaluation of liquefaction potential in most cases; however, there may be situations where this depth may not be sufficiently deep. For site specific study Southern California Earthquake Center recommended that a minimum depth of 15m below the existing ground surface or lowest proposed finished grade (whichever is lower) be investigated for liquefaction potential (Martin and Lew 1999). Where a structure may have subterranean construction or deep foundations (e.g., caissons or piles), the depth of investigation should extend to a depth that is a minimum of 6 m below the lowest expected foundation level (e.g., caisson bottom or pile tip) or 15m below the existing ground surface or lowest proposed finished grade, whichever is deeper. If, during the investigation, the indices to evaluate liquefaction indicate that the liquefaction potential may extend below that depth, the exploration should be continued until a significant thickness, at least 3 m, or the extent possible of no liquefiable soils is encountered.

2.1.4 Past records of liquefaction

Written records dating back hundreds of years have descriptions of earthquake effects that are now known to be associated with liquefaction. However liquefaction related devastating effects are becoming pronounced with the civilization of 20^{th} century. Its devastating effects sprang to the attention of geotechnical engineers in the three month period in 1964 when the Good Friday earthquake (Mw=9.2) in Alaska was followed by the Niigata earthquake (Ms=7.5) in Japan. Both earthquakes produced spectacular examples of liquefaction- induced damages, including slope failures, bridge and building foundation failures, and flotation of buried structures. Among the 310 damaged reinforced concrete buildings during the 1964 Niigata earthquake, 200 tilted or excessively settled due to liquefaction (Kramer, 1996).

The upstream slope of the Lower San Fernando Dam, California, failed due to the liquefaction of a zone of a hydraulic sand fill during the 1971, 6.6-magnitude, San Fernando earthquake (Beaty et al. 2001). Excessive movement of a retaining wall at a sea shore due to liquefaction during the 6.9 magnitude 1995 Kobe earthquake was also recorded. More recently, sever earthquake effects of liquefaction such as sand boil happened in the 2010/11 Christchurch earthquake, New Zealand (McSayeney 2011).

2.1.5 Ground Failures associated with liquefaction

Liquefaction phenomena can affect buildings, bridges, buried pipelines, and other constructed facilities in many different ways. Flow liquefaction can produce massive flow slides and contribute to the sinking of heavy structures, the floating of light structures, and to the failure of retaining structures. Cyclic mobility can cause slumping of slopes, settlement of buildings, lateral spreading, and retaining wall failure. Substantial ground oscillation, ground surface settlement, sand boils, and post-earthquake stability failures can develop at ground sites (Kramer, 1996). Some of the major effects are discussed below briefly.

1. Alteration of ground motion

A deposit of liquefiable soil that is relatively stiff at the beginning of earthquake may be much softer by the end of the motion. The alteration of frequency content and decreasing of amplitude will be accompanied by excessive lateral displacement. This displacement may be of a particular concern for buried structures, utilities and pile foundation that extended in liquefiable layer.

2. Development of sand boil

Liquefaction is often accompanied by the development of sand boil. During and following earthquake shaking, seismically induced excess pore pressure are dissipated predominantly by the upward flow of pore water. This flow produces upward acting force on soil particles. This phenomenon will be manifested on the surface as sand boil (Kramer 1996).

3. Settlement

Dissipation of the excess pore pressures will be accompanied by densification of the soil and settlement of the surface. If the site affected by subsidence is close to river, lake or water body, permanent flooding may result.

4. Instability

Liquefaction induced instabilities are among the most damaging of all earthquake hazards. The effects have been observed in the form of flow slide, lateral spreads, retaining wall failures, and foundation failures in countless earthquakes throughout the world.

2.2 Initiation of Liquefaction

The generation of excess pore water pressure under undrained loading is a hallmark of all liquefaction phenomena. When cohesionless saturated soil is loading under undrained condition, the tendency to densification will cause pore pressure to increase and the effective stress to decrease. Liquefaction phenomena resulted from this process can be divided in to two major groups. These are flow liquefaction and cyclic mobility (Kramer 1996).

Flow liquefaction can occur when the shear stress required for static equilibrium of a soil mass (the static shear stress) is greater than the shear strength of the soil in its liquefied state. In contrast to flow liquefaction, cyclic mobility occurs when the static shear stress is less than the shear strength of liquefied soil. Hence, initiation of both type of liquefaction requires identification of the state of soil when liquefaction is triggered. As studied by Hanzawa et al. (1979) and cited by Kramer (1996) flow liquefaction is initiated at the peak of each stress path as shown on Figure 2.1 during undrained triaxial consolidated to the same void ratio at different initial effective confining pressure. Since all the specimens have the same initial void ratio, they will reach the same effective stress condition at the steady state. Flow liquefaction surface (FLS) shall be the surface connecting those peaks as marked on the broken line with an asterisk (*). The FLS marks the boundary between stable and unstable states in undrained shear.

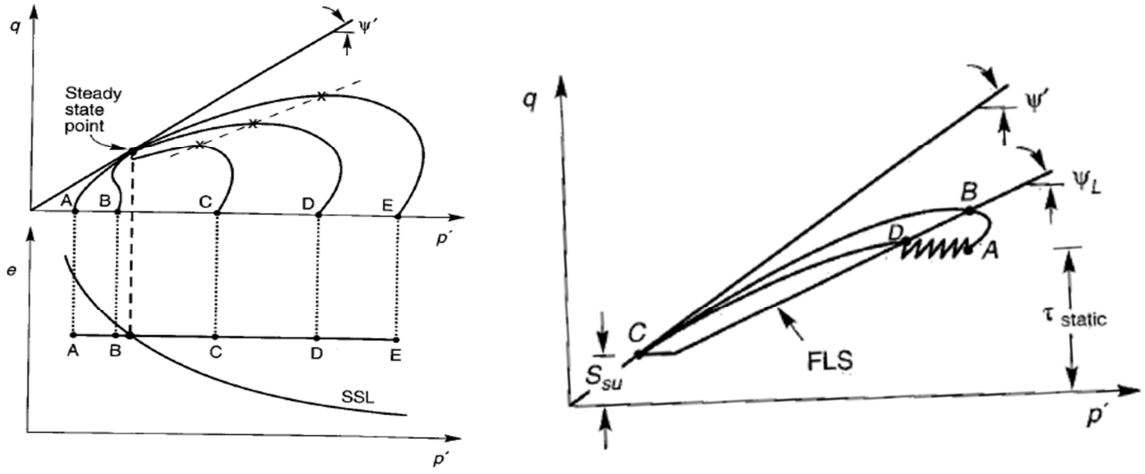

Figure 2.1 (a) Monotonically loaded five specimens isotropically consolidated to the same initial void ratio at different initial effective confining pressure (b) cyclically loaded specimens (Kramer 1996)

Flow liquefaction can be initiated by cyclic loading only when the shear stress required for static equilibrium is greater than the steady state strength.

Flow liquefaction occurs in two stages. The first stage involves generation of excess pore pressure to move the stress path from its initial position to FLS. This excess pore pressure may be generated by undrained cyclic loading. When the effective stress path reaches the FLS, the soil becomes inherently unstable and second stage begins. The second stage involves strain softening that is driven by the shear stress required for static equilibrium. If

the first stage takes the soil to the FLS under undrained, stress controlled conditions, the second stage is inevitable (Kramer 1996).

Flow liquefaction to occur requires an undrained disturbance strong enough to move the effective stress path from initial points in the shaded region to FLS (Figure 2.2 (a).

As stated above, soil could also liquefy by cyclic mobility. Cyclic mobility can develop when the static shear stress is smaller than the steady state strength. Initial liquefaction can only occur during stress reversal as shown in Figure 2.2 (b).

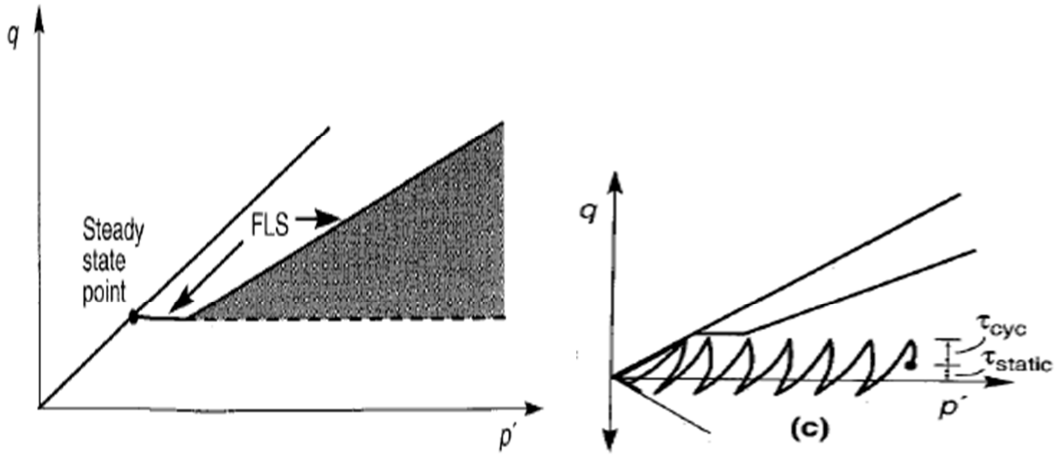

Figure 2.2 (a) Zone of flow liquefaction (b) Cyclic mobility with stress reversal (Kramer 1996)

In both cases, flow liquefaction and cyclic mobility, the influence of excess pore pressure generation is important. Seed and Lee (1966) as cited by Kramer (1996) defined initial liquefaction as the point at which increase in pore pressure (U_{EXCESS}) is equal to the initial effective confining pressure, (σ'_{3c}) i.e. when $U_{EXCESS} = \sigma'_{3c}$ or when $r_u = \frac{U_{EXCESS}}{\sigma'_{3C}} = 100\%$.

The level of excess pore pressure required to initiate liquefaction is related to the amplitude and duration of earthquake induced cyclic loading. The loading can be predicted by a detail ground response analysis or by the use of simplified approach.

Liquefaction Potential

A number of approaches to evaluation of potential for liquefaction have been developed over the years. It is common practice to evaluate liquefaction potential by different approaches. But for this study a cyclic stress approach is discussed due to its simplicity and robustness to accurately model earthquake induced stress with in the ground. Because of these reasons, over the years many design charts and correlations were developed based on cyclic stress approach for the estimation of liquefaction resistance of soils through laboratory as well as in situ tests. Application of the cyclic stress approach requires careful attention to the manner in which the loading conditions and liquefaction resistance are considered.

2.2.1 Earthquake loading

Comparison of earthquake induced loading with laboratory determined resistance requires conversion of irregular time history of shear stress to an equivalent series of uniform stress cycles (Kramer 1996). A factor of 65% of the peak shear stress that would produce an increase in pore pressure equivalent to that of irregular time history has been recommended by Seed, Haldar and Tang (1981) as cited by Kramer (1996).

i.e.

$$\tau_{cyc} = 0.65\tau_{\max} \tag{2.1}$$

Referring Figure 2.3 the maximum shear stress $\tau_{\max}$ is given by

$$\tau_{\max} = \frac{a_{\max}}{g}\sigma_v r_d \tag{2.2}$$

τ_{cyc} is given by

$$\tau_{cyc} = 0.65\frac{a_{max}}{g}\sigma_v . r_d \tag{2.3}$$

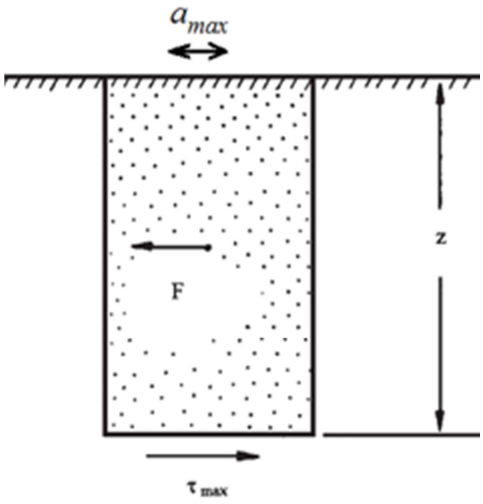

Figure 2.3 Schematic sketch of soil column during dynamic load

Therefore, the seismic demand on a soil layer, expressed in terms of Cyclic Shear Stress (CSR) is given by

$$CSR = 0.65 \frac{a_{max}}{g} \frac{\sigma_v}{\sigma_v'} . r_d \quad (2.4)$$

Where

a_{max} = peak ground surface acceleration, g acceleration of gravity, σ_v total vertical stress, σ_v' is effective stress, and r_d is the value of a stress reduction factor at the depth of interest. The two important quantities are discussed below.

I) Peak ground acceleration, a_{max}

a_{max} is defined as the peak value in a horizontal ground acceleration record that would occur at the ground surface of a site without the influence of excess pore-water pressures or liquefaction that might develop (Youd et al. 2001).

The 1996/1998 National Center for Earthquake Engineering Research (NCEER) workshop (simplified method review workshop) addressed different issues regarding maximum or peak ground acceleration (Youd et al. 2001). The preferred method for estimating a_{max} is through empirical correlations of a_{max} with earthquake magnitude, distance from the seismic energy source, and local site conditions. Selection of an attenuation relationship should be based on such factors as region of the country, type of faulting, and site condition.

The second recommendation by Youd et al. (2001) to estimate a_{max} for soft soil and other soils that are not compatible to the available attenuation relationships is from local site response analysis. Computer program such as SHAKE shall be used to perform site response analysis. Youd et al. (2001) also suggest that input ground motions in the form of recorded accelerograms are preferable to synthetic records. A suite of plausible earthquake records should be used in the analysis, including as many as feasible from earthquakes with similar magnitudes, source distances, with the study area (Youd et al. 2001).

II) Reduction factor, r_d

The term r_d, used in the evaluation of Cyclic Stress Ratio (CSR), is to account for the flexibility of soil. The most widely used technique to calculate the stress reduction factor (r_d) was suggested by Seed and Idriss (1971). Later the depth reduction factor has been revised by incorporating additional liquefaction cases by Idriss and Boulanger 2010. Idriss and Boulanger (2010) updated a relation to evaluate the stress reduction factor as a function of depth and earthquake magnitude.

Hence, r_d is given by (Idriss and Boulanger 2010);

$$\begin{aligned} r_d &= exp\left[\alpha(Z) + \beta(Z).M\right] \\ \alpha(Z) &= -1.012 - 1.126 sin\left(\frac{Z}{11.73} + 5.133\right) \\ \beta(Z) &= 0.106 + 0.118 sin\left(\frac{Z}{11.28} + 5.142\right) \end{aligned} \quad (2.5)$$

Where *Z* is depth and *M* is moment magnitude

2.2.2 Liquefaction Resistance

The liquefaction resistance of an element of soil depends on how close is the initial state of the soil to the state corresponding to "failure" and the nature of loading required to move it from the initial state to the failure state. Characterization of liquefaction resistance can be developed based on the laboratory method and insitu tests and observation of liquefaction behavior of past earthquakes.

For a number of years, liqufaction was commonly charaterized by cyclic stress determined from laboratory tests. However, subsequent works showed that cyclic stress based measurment of liquefaction resisance are influenced by factors other than initial density and stress conditions. For excample it is influenced by soil fabric (Kramer 1996). The history of prior seismic straining also influences the liquefaction resistance. Because of these and other facors, characterizaion of liquefaction resistance by laboratory testing is extremely difficult and has been suplimented by insitu based resisatance (Kramer 1996). Hence, for this thesis work, characterization of liquefaction resistance based on insitu tests will be discussed in detail.

Following the disastrous earthquake in Alska and Nigata, Japan, in 1964 Professor H.B seed and I.M Idriss developed and published a methodology termed the "Simplified Procedure" for evaluation of liquefaction resistance. This approach and the development over the 10 years period since 1985 had been reviewed by the 1996 and 1998 workshops on "Evaluation of Liquefaction Resistance of Soil" convened by T.L. Youd and I.M. Idriss with 20 experts (Youd et al. 2001). In the workshop the following issues have been reviewed:

- Criteria based on standard penetration tests;
- Criteria based on cone penetration tests;
- Criteria based on shear-wave velocity measurements;
- Use of the Becker penetration test for gravelly soil;
- Magnitude Scaling Correction factors.

Though Cone penetration test (CPT) has many advantages in the prediction of liquefaction resistance, SPT based method from geotechnical investigation report is selected for this study for its wide application and availability in the country. On top of that, SPT has the largest case history database of any insitu test (Kramer 1996). Moreover, the shear wave velocity based approach is also employed for the study, as it can be determined by correlation from SPT as well as geophysical survey. Therefore SPT based and Shear wave velocity based liquefaction potential assessments are discussed among the insitu methods.

1. Standard Penetration Test, (SPT)

Factors that tend to increase liquefaction resistance such as density, prior seismic straining, overconsolidation ratio, lateral earth pressure, time under sustained pressure also tend to increase SPT resistance (Youd et al. 2001).

SPT blow counts are affected by a number of procedural details (rod lengths, hammer energy, sampler details, borehole size) and by effective overburden stress. Thus, the correlation to cyclic resistance ratio (CRR) is based on corrected penetration resistance,

$$(N_1)_{60} = C_N C_E C_R C_B C_S N_M \tag{2.6}$$

where C_N is an overburden correction factor, C_E = ER_m/60%, ER_m is the measured value of the delivered energy as a percentage of the theoretical free-fall hammer energy, C_R is a rod correction factor to account for energy ratios being smaller with shorter rod lengths, C_B is a correction factor for nonstandard borehole diameters, C_S is a correction factor for using split spoons with room for liners but with the liners absent, and Nm is the measured SPT blow count. The factors C_B and C_S are set equal to unity if standard procedures are followed.

The cyclic resistance ratio (CRR) also affected by duration of shaking, which is correlated with MSF, magnification scaling factor and effective overburden stress, K_σ .

Therefore,

$$CRR_{M_w,\sigma'_v} = CRR_{M=7.5,\sigma'_v=1atm} * MSF * K_\sigma \tag{2.7}$$

The correlation of CRR to $(N_1)_{60}$ is affected by the soil's fines content (FC) and is expressed as

$$CRR_{M=7.5,\sigma'_v} = f\left[(N_1)_{60}, FC\right] \tag{2.8}$$

This correlation can also be expressed in terms of an equivalent clean-sand (N1)60cs, which is obtained using the following expression:

$$(N_1)_{60CS} = (N_1)_{60} + \Delta(N_1)_{60} \tag{2.9}$$

Where $\Delta(N_1)_{60}$ is a function of FC.

Therefore CRR can be expressed by

Table 2.1.Correction factor for measured SPT (Youd et al. 2001)

Factor	*Equipment variable*	*Term*	*Correction*
Overburden pressure	-	C_N	$(Pa/\sigma'v)^{0.5}$
Overburden pressure	-	C_N	CN<1.7
Energy ratio	Donut hammer	C_E	0.5-1.0
Energy ratio	Safety hammer	C_E	0.7-1.2
Energy ratio	Automatic-trip Donut-type hammer	C_E	0.8-1.3
Borehole diameter	65-115mm	C_B	1
Borehole diameter	150mm	C_B	1.05
Borehole diameter	200mm	C_B	1.15
Rod length	<3m	C_R	0.75
Rod length	3-4m	C_R	0.8
Rod length	4-6m	C_R	0.85
Rod length	6-10m	C_R	0.95
Rod length	10-30m	C_R	1
Sampling method	Standard sampler	C_S	1
Sampling length	Standard sampler	C_S	1.0-1.3

NOTE; increase the estimated rod stick up length to 2.5 m for all cases (Idriss et al. 2010)

- Overburden correction factor

$$C_N = \left(\frac{P_a}{\sigma'_v}\right)^m \leq 1.7$$
$$m = 0.784 - 0.0768\sqrt{(N_1)_{60CS}} \quad (2.11)$$

Where P_a = 1atm ≅100kPa

The limit of 1.7 on the maximum value of C_N is reached at vertical effective stresses less than about 35kPa, which corresponds to depths less than about 2 m. This limit is imposed because these expressions were not derived or validated for very low effective stresses, and the assumed functional form will otherwise produce unrealistically large C_N values as the vertical effective stress approaches zero. Limits of 1.6 to 2.0 have been recommended by various researchers (Idriss et al. 2010).

$$C_N = \left(\frac{100}{\sigma'_v}\right)^{0.5} \quad (2.12)$$

- Short rod correction factor, C_R

The short rod correction factor accounts for the effect of rod length on the energy transferred to the sampling rods during the primary hammer impact.

- Overburden correction factor, K_σ

Idriss and Boulanger (2008) recommends K_σ relationship be expressed in terms of the (N1)60cs values as follows,

$$K_\sigma = 1 - C_\sigma \left(\frac{\sigma'_v}{P_a}\right) \leq 1.1$$
$$C_a = \frac{1}{18.9 - 2.55\sqrt{(N_1)_{60CS}}} \leq 0.3 \quad (2.13)$$

- Magnitude scaling factor, MSF

The magnitude scaling factor (MSF) is used to account for duration effects (i.e., number of loading cycles) on the triggering of liquefaction. MSF factor is applied to the calculated value of CRR for each case to convert to a common value of M (conventionally taken as M = 7.5). The MSF for sands can be calculated by Idriss 1999 relationship (Idriss et al. 2010).

$$MSF = 6.9 * exp\left(\frac{-M}{4}\right) - 0.058 \leq 1.8 \quad (2.14)$$

An upper limit for the MSF is assigned to very-small-magnitude earthquakes for which a single peak stress can dominate the entire time series. MSF given by different researchers are presented in the following Figure 2.4.

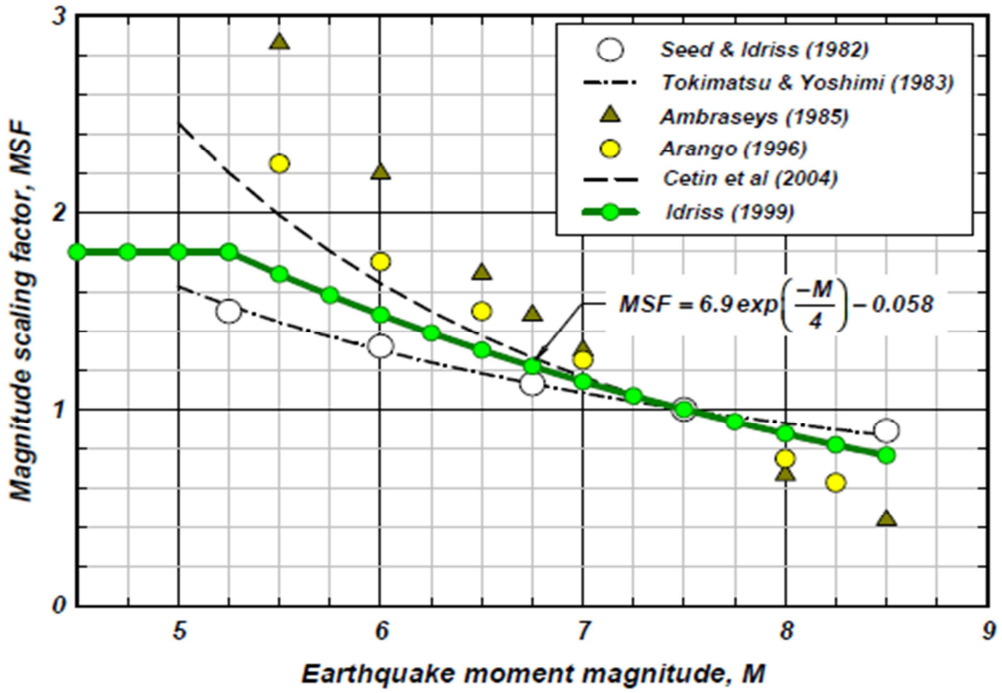

Figure 2.4 Magnitude scaling factor MSF relations with moment magnitude. (After Idriss et al. 2010)

- Equivalent clean sand adjustment, $\Delta(N_1)_{60}$

The equivalent clean sand adjustment, $\Delta(N_1)_{60}$, accounts for the effects that fines content has on both the CRR and the SPT blow count. This effect is conveniently represented by adjusting the SPT $(N_1)_{60}$ values to equivalent clean sand $(N_1)_{60cs}$ values, and then expressing CRR as a function of $(N_1)_{60cs}$. The equivalent clean sand adjustment developed by Idriss et al. (2010) is expressed as,

$$\Delta(N_1)_{60} = EXP\left(1.63 + \frac{9.7}{FC + 0.01} - \left(\frac{15.7}{FC + 0.01}\right)^2\right) \quad (2.15)$$

Where, *FC* is average fines content in percent by mass.

- Liquefaction triggering correlation

The correlation between the cyclic resistance ratio (CRR) adjusted to M = 7.5 and σ'v = 1 atm and the equivalent clean sand $(N_1)60cs$ value for cohesionless soils, as developed by Idriss and Boulanger (2004, 2008), is expressed as,

$$CRR_{M=7.5,\sigma'_v=1atm} = EXP\left(\frac{(N_1)_{60CS}}{14.1} + \left(\frac{(N_1)_{60CS}}{126}\right)^2 - \left(\frac{(N_1)_{60CS}}{23.6}\right)^3 + \left(\frac{(N_1)_{60CS}}{25.4}\right)^4 - 2.8\right) \quad (2.16)$$

2. Shear Wave Velocity, V_S

Improved methods of insitu shear wave velocity measurment and studies related to cyclic strain approach have contributed to the recognition of shear wave velocity as the useful measure of liquefaction resistance. However, the insensitiveness to factors such as Soil fabric, OCR, prior cyclic straining, that are known to influence liquefaction resistance suggests that shear wave velocity measurment alone may not be sufficient to evaluate liquefaction potential of soil deposits (Kramer 1996). In some cases, where only seismic measurements are possible, it may be the only alternative to the penetration-based approach (Andrus et al. 2004). Similar to SPT based, the shear wave velocity procedure also share the procedure termed as simplified procedure (Youd et al. 2001).

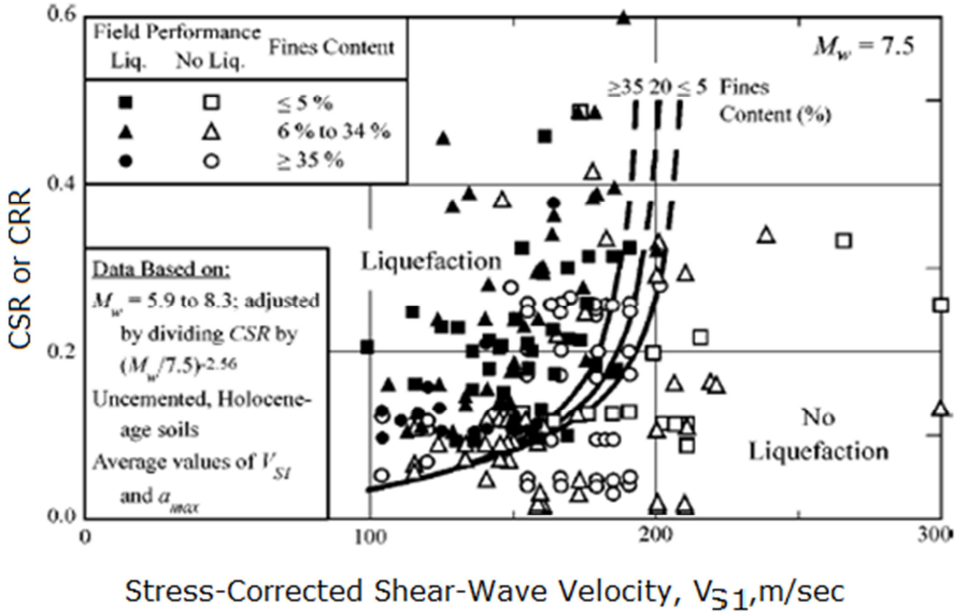

Figure 2.5 Cyclic stress ratio (CSR) or cyclic resistance ratio (CRR) Vs Shear wave velocity case history for magnitude 7.5 earthquakes (After Andrus et al. 2004)

Unlike SPT based Shear wave velocity based liquefaction prediction has been verified by limited number of case history. As can be seen in Figure 2.5, CRR beyond 0.35 and shear wave velocity below 100m/s are not confirmed by the case history studies (Andrus et al. 2004).

Similar to correcting penetration resistance, V_S should be corrected to a reference overburden stress as given by Andrus et al. (2004) as follows

$$V_{S1} = V_S \left(\frac{P_a}{\sigma'_v}\right)^{0.25} \left(\frac{0.5}{K'_0}\right)^{0.125} \quad (2.17)$$

Where, V_{S1} is stress-corrected shear-wave velocity, P_a is a reference stress of 100 kPa, K'_0 is coefficient of effective earth pressure at rest, and σ'_v is initial effective overburden stress in kPa. For level ground where K'_0 =0.5, V_{S1} becomes

$$V_{S1} = V_S \left(\frac{P_a}{\sigma'_v} \right)^{0.25} \tag{2.18}$$

- Cyclic resistance ratio, CRR

Andrus et al. (2004) develop the CRR – V_{S1} Relation as follows.

$$CRR = MSF \left\{ 0.022 \left(\frac{K_{a1} V_{S1}}{100} \right)^2 + 2.8 \left(\frac{1}{V^*_{S1} - (K_{a1} V_{S1})} - \frac{1}{V^*_{S1}} \right) \right\} K_{a2} \tag{2.19}$$

Where

MSF is the magnitude scaling factor,

V^*_{S1} is the limiting upper value of VS1 for liquefaction occurrence,

K_{a1} is a factor to correct for high VS1 values caused by aging, and

K_{a2} is a factor to correct for influence of age on CRR.

- MSF Magnitude scaling factor

Different researchers suggested various MSF depend on magnitude. Youd et al. (2001) reported that the workshop participant agreed on the conservative MSF given by Idriss for engineering practice.

$$MSF = \frac{10^{2.24}}{M_W^{2.56}} \tag{2.20}$$

- Limiting Upper Value of V_{S1}

The assumption of a limiting (or maximum) upper value of V_{S1} for liquefaction occurrence is equivalent to the assumption commonly made in the penetration-based procedures dealing with clean sands, where liquefaction is considered not possible above a corrected SPT blow count of about 30 Seed (Andrus et al. 2004).

Andrus et al. (2004) suggested the following relationship;

$$\begin{aligned} V^*_{S1} &= 215 m/s && \text{for } FC \le 5\% \\ V^*_{S1} &= 215 - 0.5(FC - 5) m/s && \text{for } 5\% \le FC \le 35\% \\ V^*_{S1} &= 200 m/s && \text{for } FC \ge 35\% \end{aligned} \tag{2.23}$$

- Age Correction Factors

The factors K_{a1} and K_{a2} are included in the equation to extend the original CRR-V_{S1} equation by Andrus and Stokoe (2000) for uncemented Holocene-age soils to older soils. K_{a1} and K_{a2} are 1.0 for uncemented soils of Holocene age. For older soil, the suggested method for approximating K_{a1} involves using SPT-V_{S1} relationships to estimate V_{S1} in Holocene-age soil for a similar $(N_1)_{60}$ value, and dividing the estimated V_{S1} value by the measured V_{S1} value. This approach assumes SPT measurements are not affected by aging and cementation, and K_{a1} is the ratio of the estimated value to the measured value of V_{S1}.

Approximate lower-bound values of K_{a2} are presented in Table 2.2. It is suggested in this paper that lower-bound values of these results be used as estimates of K_{a2}. Use of the lower-bound value provides a lower estimate of CRR (Andrus et al. 2004).

Table 2.2 Lower-bound of K_{a2} based on study of Arango et al. (2000) as cited by Andrus et al. (2004)

Time (years)	**Lower-bound Estimate of K_{a2}**
<10,000	1.0
10,000	1.1
100,000	1.3
1,000,000	1.5

2.2.3 Evaluation of liquefaction potential

1. Factor of safety

Once the cyclic loading imposed and liquefaction resistance of the soil have been characterized, liquefaction potential can be evaluated by factor of safety, FS.

Liquefaction can be expexted at depths if

$$FS_L = \frac{CSR_L}{CSR} or \frac{CRR}{CSR} \tag{2.24}$$

is less than 1 (Kramer 1996).

The zone of liquefaction can be best described by plotting CSR/CRR Vs depth as shown in Figure 2.6

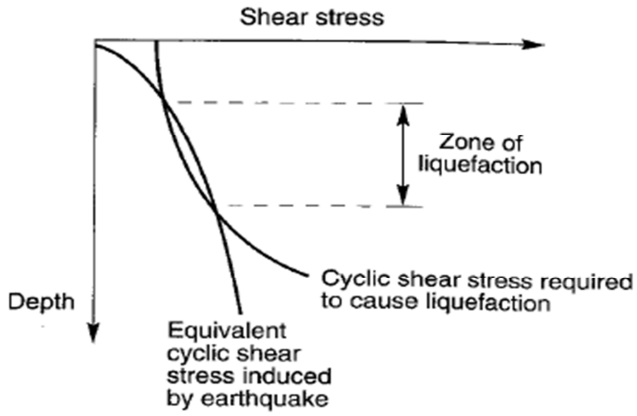

Figure 2.6 Process by which the zone of liquefaction is identified (Kramer 1996)

2. Probability of liquefaction

A second way to quantify the potential for liquefaction is in terms of probability. One advantage of expressing liquefaction potential in terms of probability is that probability of liquefaction can be derived in a more objective manner than the deterministic bounding curves, which traditionally have been visually drawn. Another important advantage is that probability of liquefaction is required information for making risk-based design decisions (Andrus et al. 2004). Juang method as cited by Andrus et.al (2004) is

$$P_L = \frac{1}{1+\left(\frac{FS}{0.72}\right)^{2.4}} \tag{2.25}$$

BSSC (2000) has suggested that a FS value of 1.2 to 1.5 is appropriate when applying the Seed-Idriss simplified procedure in engineering design. The same range of FS is recommended for the VS-based procedure. When applying the V_S-based procedure, these FS values are equivalent to P_L values of 0.16 to 0.08, respectively.

CHAPTER THREE

DATA ACQUISITION AND PROCESSING

3.1 Introduction

Identification of subsurface conditions (geometry, stratification, and depth to bedrock) and dynamic soil properties including ground water table are the primary tasks to perform for liquefaction potential assessment. Subsurface condition of the Hawassa city has been studied by gathering the available geotechnical investigation data for different parts of the city and by directly performing geophysical investigations at four selected sites in and around the city. As the southern parts of the city are founded on shallow rhyolite, the sites are selected from the central and northern parts of the city. Most of the geotechnical investigations data gathered are for buildings in the city. They are mainly comprised of shallow depth investigation, ranging from 10m to 17m with the exception of the 25m depth conducted for NIB international bank. All available data consisted of standard penetration test data (SPT) and basic laboratory test results. Dynamic soil properties are missing from these reports. In order to obtain primary data, which complement the missing information with respect to depth and variety, geophysical investigations, consisting of seismic refraction and electrical resistivity, have been conducted at four selected sites in and around the city. Subsurface information gathered and their sources are summarized in Table 3.1.

Table 3.1 Sources of subsurface data gathered for the study

		Data source			
				Geophysical	
Item No	Description	Secondary data from BH	Literature/ Previous study	Seismic refraction	Vertical electrical sounding
1	SPT	X			
2	Unit weight	X			
3	Specific gravity	X			
4	Moisture content	X			
5	Ground water table	X	X		X
6	Shear wave velocity	X (by correlation)		X	
7	Layering, stratification	X		X	X

3.2 Subsurface Data Collected from Geotechnical Investigation Reports

3.2.1 Selection of Sites

The site selections have been performed based on availability of secondary data, accessibility to geophysical survey, and upon consideration of the analysis to the already built up high-rise

building area. Four sites have been selected as shown in Figure 3.1. These are Progress International Hotel, Hawassa Industry Park, Nib International Bank and South Ethiopia People Democratic Movement (SEPDM) Office building sites, hereafter referred to as PIH, HIP, NIB and SEPDM respectively.

(a) (b)

Figure 3.1 Selected analysis sites of Hawassa city (Google Earth), (a) Borehole investigation sites (b) Geophysical investigation sites

3.2.2 Summary of data acquired from secondary data sources

The geotechnical investigations data gathered by different companies have been used for construction of industry shades and medium height buildings. Among the gathered borehole data,the PIH, HIP, NIB and SEPDM selected due to their good representation of the city subsurface conditions. The pertinent boreholes investigation data are enclosed in appendix A.

1. Progress International Hotel (PIH)

The PIH study area is found at the shore of the Hawassa Lake. About 12 boreholes of different depth ranging from 15 to 20m are investigated. Among them, four boreholes, which represent a wider area beyond the hotel, are selected for the study (Appendix A). Ground water table is recorded at 3.6m during the investigation. The first 15 m is covered with loose to medium dense silty-sand interbedded by 1.9 to 3m thick moderately weathered ignimbrite. As confirmed by the Construction Design and Supervision Corporation (CDSCo), who performed the investigation, an energy efficiency of the SPT machine is 70%.

2. Hawassa Industry Park

The HIP site investigation has been performed to 10m depth. No ground water has been recorded to this depth. About 30 boreholes are drilled in total. The 10m depth of investigation

shows that the area is layered with thick deposit of loose to dense, silty-sand with SPT ranging from 8 to 42 before correction. As the investigation has been made by CDSCo, SPT machine efficiency of 70% has been considered.

3. NIB International Bank

The NIB investigation data represent the most built up area in the center of the city. The investigation is performed for a 2B+G+11 building of the bank. Four boreholes of depth ranging from 20 to 25m have been drilled. Ground water table has been recorded at 13.6m during the investigation. The investigation reveals that the area is dominated by loose to medium dense, silty-sand soil interbedded with 1.4 to 2m thick moderately-weathered ignimbrite at around 6m below the ground surface.

4. SEPDM Office Building

As shown in Figure 3.1, the SEPDM office site is selected to represent south-east part of the developed area of the city. The investigation has been conducted for the office building. Though a total of four boreholes were investigated, only two have SPT information. Both boreholes are drilled up to a depth of 10m. The 10m investigation shows about 4m slightly-weathered tuff extending from 3m to 7m interbedded between clayey silt and silty sand layers. The shallowest ground water table recorded is 3m from the ground surface.

3.2.3 Data processing

3.2.3.1 SPT Correction

The SPT has historically been the most widely used insitu geotechnical test throughout the world. It is common geotechnical practice to correct field SPT N values for variations from standard practice as stated in Chapter Two Section 2.2.1.2.

As the correction is done primarily for correlation of shear-wave velocity, overburden correction factor is ignored at this stage (Youd et al. 2001). Referring to Table 2.1 (correction factors for measured SPT) and Equation 2.6, corrections of SPT have been done for all sites and given in Table 3.2 through Table 3.5.

Table 3.2 SPT correction based on Youd et al 2001 for PIH investigation

BH9				***Correction OF SPT (Youd et al.2001)***						
Depth (m)	Description	Layer thick-ness	SPT, N rec.	Depth, m	C_E	C_B	Rod length m	C_R	C_S	N_{60}
0-3.3	L. to M. dense Sandy silt	3.3	10	3.3	1.17	1.00	5.80	0.85	1.00	10.00
3.3-6.4	Slightly weat. Igni.	3.1		6.4						
6.4-7.0	M. dense sand	0.6	12	7	1.17	1.00	9.50	0.95	1.00	13.00
7.0-9.0	M. dense sand	2	23	9	1.17	1.00	11.50	1.00	1.00	27.00
9.0-11.0	M. dense sand	2	21	11	1.17	1.00	13.50	1.00	1.00	25.00
11.0-15.	M. dense sand	4	21	15	1.17	1.00	17.50	1.00	1.00	25.00

Table 3.3 SPT correction based on Youd et al 2001 for HIP investigation

BHB35C				Correction of SPT						
Depth (m)	Description	Layer Thickness	SPT, N rec.	Depth, m	C_E	C_B	Rod length, m	C_R	C_S	N_{60}
0-1.5	Red Ash	1.5	8	1.50	1.17	1.00	4.00	0.85	1.00	8.00
1.5-3.0	Silty Sand	1.5	15	3.00	1.17	1.00	5.50	0.85	1.00	15.00
3.0-6.0	Silty Sand	3	25	6.00	1.17	1.00	8.50	0.95	1.00	28.00
6-7.5	Silty Sand	1.5	26	7.50	1.17	1.00	10.00	1.00	1.00	30.00
7.5-10	Silty Sand	2.5	38	10.00	1.17	1.00	12.50	1.00	1.00	44.00

Table 3.4 SPT correction based on Youd et al 2001 for Nib investigation

BH1		Layer Thickness	SPT,	Depth	Correction of SPT					
Depth	Description				C_E	C_B	Rod length, m	C_R	C_S	N_{60}
0-0.5	Top soil	0.5		0.50	0.92	1.00	3.00	0.80	1.00	
0.5-3.45	M. dense to silty sand (ash deposit)	2.95	20	3.45	0.92	1.00	5.95	0.85	1.00	16
3.45-5	M. dense to silty sand (ash deposit)	1.55		5.00	0.92	1.00	7.50	0.95	1.00	
5.0-6.4	Moderate weath. Ign.	1.4		6.40	0.92	1.00	8.90	0.95	1.00	
6.4-8.45	M. dense sandy silt	2.05	24	8.45	0.92	1.00	10.95	1.00	1.00	22
8.45-10.45	M. dense sandy silt	2	20	10.45	0.92	1.00	12.95	1.00	1.00	18
10.45-12.45	M. dense sandy silt	2	23	12.45	0.92	1.00	14.95	1.00	1.00	21
12.45-14.45	M. dense sandy silt	2	27	14.45	0.92	1.00	16.95	1.00	1.00	25
14.45-16.45	M. dense sandy silt	2	20	16.45	0.92	1.00	18.95	1.00	1.00	18
16.45-20	M. dense sandy silt	3.55		20.00	0.92	1.00	22.50	1.00	1.00	

Table 3.5 SPT correction based on Youd et al 2001 for SEPDM investigation

BH3					Correction of SPT					
Depth (m)	Description	Layer Thickness	SPT rec	Depth, m	C_E	C_B	Rod length, m	C_R	C_S	N_{60}
0-1.2	Organic Clayey Silt	1.2	6	1.20	1.17	1.00	3.70	0.80	1.00	6.00
1.2-3.0	Stiff Clayey silt	1.8	15	3.00	1.17	1.00	5.50	0.85	1.00	15.00
3.0-4.5	Slightly Weathered	1.5		4.50	1.17	1.00	7.00	0.95	1.00	

4.5-7.0	Tuff Fresh Welded Tuff	2.5		7.00	1.17	1.00	9.50	0.95	1.00	
7.0-10.0	Soft silty sand	3	12	10.00	1.17	1.00	12.50	1.00	1.00	14.00

3.2.3.2 SPT -V_S correlations

Characterization of the small-strain shear modulus and the shear-wave velocity of soils is an integral component of various seismic analyses, including site classification, hazard analysis, site response analysis, soil–structure interaction and most importantly, liquefaction. The Next Generation Attenuation ground motion prediction equations use the shear-wave velocity of the top 30m of the subsurface profile (V_{S30}) as the primary parameter for characterizing the effects of sediment stiffness on ground motions (Wair et al. 2012). The SPT practices vary significantly from region to region due to differences in equipment and procedures, It has to be corrected for standard practice before used in correlation to shear wave velocity.

Normalization of penetration data i.e. overburden correction is not required for estimation of V_S, and/or calculation of V_{S30} (Wair et al. 2012). For some applications, such as liquefaction triggering assessment, it may be necessary to normalize V_S estimates to a reference stress level. In such cases, V_S can be estimated from non-normalized penetration resistance, and then normalized for overburden (Wair et al. 2012).

Estimation of V_S from penetration test, SPT, is improved when additional parameters such as confining stress (depth), geology (depositional environment, aging, etc.), and soil type are considered (Wair et al. 2012).

Ohta and Goto (1978) identified four index properties that were related to shear-wave velocity, $V_{S,}$ with SPT-N value, depth, geologic age, and soil type. Data points were divided among categories based on geologic age (Holocene and Pleistocene) and soil type (clay, fine sand, medium sand, coarse sand, sand and gravel, and gravel). Silts were placed under the clay category. Moreover Wair et al. (2012) recommended correlation equations after studying plenty of SPT vs shear-wave velocity correlations since 1960. For this study, Ohta and Goto (1978) and PEER NGA 2 recommendations by Wair et al. (2012) are adopted. The equations suggested by Ohta and Goto (1978) are given as follows.

For clays and silts without overburden Holocene age alluvium deposition,

$$V_S = 90.6 N_{60}^{0.25} \tag{3.1}$$

For clays and silts with overburden Holocene age alluvium deposition,

$$V_S = 67.5 N_{60}^{0.17} D^{0.20} \tag{3.2}$$

For sand without overburden,

$$V_S = 95.6 N_{60}^{0.25} \quad (3.3)$$

For sand with overburden,

$$V_S = 73.3 N_{60}^{0.17} D^{0.20} \quad (3.4)$$

Where *D* is depth measured down from the surface.

PEER recommendation for correlation of SPT with Shear-wave velocity is described in Table 3.6.

Table 3.6: Recommended SPT–stress–V_S correlation equations by PEER (after Wair et al. 2012)

Soil type	Vs for Quaternary soils(m/s)	Age scaling factors	
		Holocene	Pleistocene
All soils	$30 N_{60}^{0.215} \sigma'_v{}^{0.275}$	0.87	1.13
Clay & Silts	$26 N_{60}^{0.17} \sigma'_v{}^{0.32}$	0.88	1.12
Sands	$30 N_{60}^{0.23} \sigma'_v{}^{0.32}$	0.9	1.17
Gravels - Holocene	$53 N_{60}^{0.19} \sigma'_v{}^{0.18}$	------	-----
Gravels- Pleistocene	$115 N_{60}^{0.17} \sigma'_v{}^{0.12}$	------	-----

Where σ'_v is the effective overburden stress measured in kPa

Based on Ohta and Goto (1978) and PEER correlation equations four selected SPT profiles with shear-wave velocity correlation is tabulated in Table 3.8 through Table 3.11. For layers below ground water table saturated unit weight have been computed from their corresponding specific gravity and moisture content (Appendix A)

3.2.3.3 Shear wave velocity of the ignimbrite

For moderately weathered fractured tuff, the small strain shear modulus shall be computed according to Choi (2008).

$$G_{max} = 13.13 e^{0.00307 \gamma_t} \quad (3.5)$$

Where G_{max} in MPa and γ_t in Kg/m^3

Hence shear wave velocity shall be derived from the relation

$$G_{max} = \rho V_S^2 \quad (3.6)$$

Where ρ is bulk density of soil

Table 3.7 Shear-wave velocity of Ignimbrite layer (after Choi 2008)

SITE	***Depth range, m***	***Unit Weight, Kg/m^3***	***G_{max}, MPa***	***V_S, m/sec***
PIH	3.3-6.4	2423	22326	3035
NIB	5-6.4	2267	13830	2470
SEPDM	3.0-4.5	2267	13830	2470
SEPDM	4.5-7	2456	24706	3172

3.2.3.4 Ground water table, GWT

The Hawassa lake level has been rising time to time due to different reasons. The record between 1969 and 1998 revealed the lake level raised by 3.82m (Dessie and Tesema 2003). The lake level rise obviously raises the ground water table to the ground level of the city. Recent investigation performed on ground water table level shows that the water table is found at shallower depth (Tefera 2004).

Based on the information available from the geotechnical investigations, GWT levels have been recorded at PIH, NIB and SEPDM sites. However, no ground water showed up in the 10m depth of investigation in the HIP site. Previous studies have been referred to assess the historically shallowest (highest) groundwater levels for the selected sites. According to Tefera's (2004) research the HIP area GWT level ranged from 1698 to 1703 above sea level as shown on Figure 3.2 and ground elevation is between 1704 and 1712 above sea level. Hence, a GWT at 10m from the ground surface is adopted for Hawassa Industry Park area.

The GWT level has been recorded at NIB site at 13.6m during the borehole drilling. At SEPDM site water table record at 3m depth from ground surface. Moreover, the Vertical Electrical Sounding (VES) survey showed that a highly conductive layer is found at shallow depth above and below the ignimbrite layers on SEPDM and NIB sites (Section 3.3.3). Considering the seasonal fluctuation and the aquiclude behavior of welded-tuff, the GWT of NIB is projected to 3m depth from the ground surface.

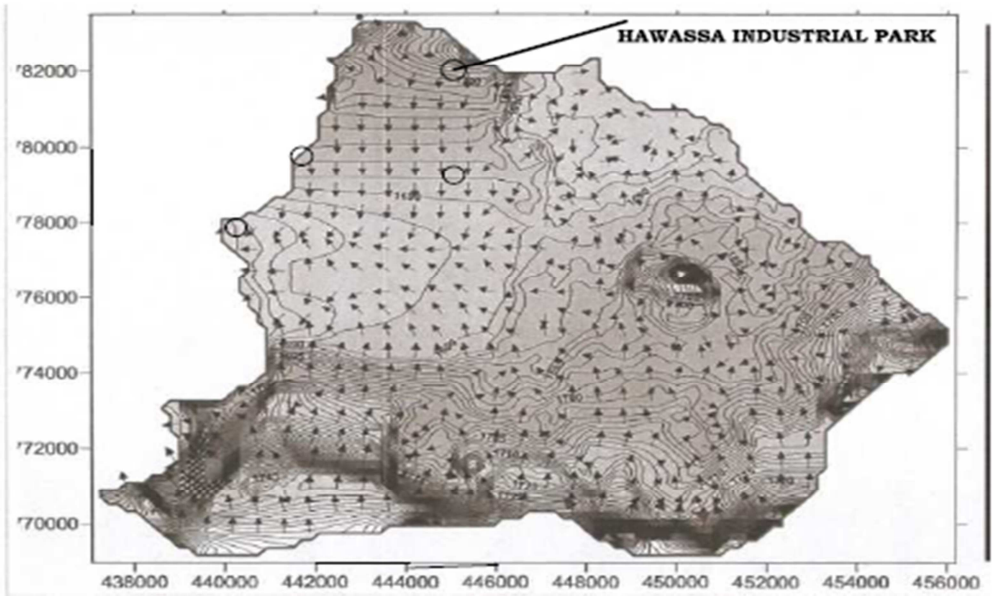

Figure 3.2 Hawassa city ground water table. After Tefera (2004)

Table 3.8 SPT – shear wave velocity correlation of PIH

BH9						***Vs***				***Vs***
Depth (m)	Description	Unit Weight	Layer Thick.	Depth, m	N_{60}	Ohta and Goto	U	σ	σ'	PEER
`	Loose to medium dense Sandy silt	18.33	3.3	3.3	10	138	0	60	60	118
3.3-6.4	Slightly weathered ignimbrite	24.23	3.1	6.4	-	-	10	136	126	-
6.4-7	Medium dense sand	19.54	0.6	7	13	167	33	147	114	145
7-9	Medium dense sand	19.54	2	9	27	199	53	186	133	178
9-11	Medium dense sand	19.54	2	11	25	205	73	225	153	180
11-15	Medium dense sand	19.76	4	15	25	218	112	305	193	190

Table 3.9 SPT – shear wave velocity correlation of HIP

BH-B35C						***Vs***				***Vs***
Depth (m)	Description	Unit Weight	Layer Thick.	Depth, m	N_{60}	Ohta and Goto	U	σ	σ'	PEER
0-1.5	Red Ash	12.81	1.5	1.5	8	113	0	19	19	86
1.5-3.	Silty Sand	14.29	1.5	3	15	145	0	41	41	118
3.0-6.	Silty Sand	14.29	3	6	28	185	0	84	84	161
6-7.5	Silty Sand	14.29	1.5	7.5	30	196	0	105	105	172
7.5-10	Silty Sand	14.29	2.5	10	44	221	0	141	141	201

Table 3.10 SPT – shear wave velocity correlation of NIB

NIB- BH1						***Vs***				***Vs***
Depth (m)	Description	Unit Wt.	Layer Thick.	Depth, m	N_{60}	Ohta and Goto	U	σ	σ'	PEER
0-0.5	Top soil	17	0.5	0.5			0	9	9	
0.5-3.0	M. dense to silty sand	17	2.5	3	16	146		51	51	126
3.0-5	M. dense to silty sand	17	2	5	16	162	20	85	65	134
5.0-6.4	Mod. weath. Igni.	22.67	1.4	6.4	-	-	33	117		-
6.4-8.45	M. dense sandy silt	17	2.05	8.45	22	190	53	152	98	158
8.45-10.45	M. dense sandy silt	17	2	10.45	18	192	73	186	113	156
10.45-12.45	M. dense sandy silt	17	2	12.45	21	204	93	220	127	166
12.45-14.45	M. dense sandy silt	17	2	14.45	25	216	112	254	141	177
14.45-16.45	M. dense sandy silt	17	2	16.45	15	203	132	288	156	161
16.45-20	M. dense sandy silt	17	3.55	20		0	167	348	181	0

Table 3.11 SPT – Shear wave velocity correlation of SEPDM

BH3						***Vs***				***Vs***
Depth (m)	Description	Unit Wt.	Layer Thick	Depth, m	N_{60}	Ohta& Goto	U	σ	σ'	PEER
0-1.2	Organic silty clay	15	1.2	1.2	6	95	0	18	18	78
1.2-3.0	Stiff silty clay	18	1.8	3	15	133	0	50	50	127

3.0-4.5	Slightly Weathered Tuff	22.67	1.5	4.5	-	-	0	84	84	0
4.5-7.0	Fresh Welded Tuff	24.56	2.5	7	-	-	0	146	146	-
7.0-10.0	Soft silty sand	14	3	10	14	182	69	197	128	151

3.2.3.5 Extrapolation of shear wave velocity

In many cases, V_S data (either measured or estimated from geotechnical data) does not extend to a depth of 30 m. In these cases, extrapolation of shallow velocity data is required to estimate the V_{S30} (Boore 2004 as cited by Wair et al 2012). Boore (2004) proposed an extrapolation method based on statistical analysis of borehole data in California. And the extrapolation has been verified by different parts of the world, Europe, turkey, and Japan (Boore et al. 2011). According to the study regional differences in geology or geomorphology do not affect the equation. Hence the extrapolation equation of Boore (2004) has been used to compute time average of the upper 30m shear-wave velocity. The extrapolation Equation 3.7 also used to compute the shear-wave velocity of intermediate layers.

$$\log V_{S30} = a + b \log V_{Sd} \quad (3.7)$$

Where VS30 and V_{Sd} are timed average shear-wave velocity of the top 30m depth and to the depth of known shear-wave velocity respectively. a and b are regression coefficients as given by Boore (2004) on Table 3.12

Four representative boreholes from each site are selected for extrapolation and for further analysis. The PIH site investigation revealed that the vesicular basalt was found at 20m depth. Therefore the PIH site extrapolation is performed to 20m depth. The remaining three sites are computed for 30m depths. See Table 3.13.

Table 3.12 Regression coefficients of Boore (2004)

Depth (m)	***Regression Coefficients***			***Depth (m)***	***Regression Coefficients***	
	a	b			a	b
10	0.042062	1.0292		20	0.025436	1.0095
11	0.02214	1.0341		21	0.025311	1.0072
12	0.012571	1.0352		22	0.0269	1.0044
13	0.014186	1.0318		23	0.022207	1.0042
14	0.0123	1.029		24	0.016891	1.0043
15	0.013795	1.0263		25	0.011483	1.0045
16	0.013893	1.0237		26	0.006565	1.0045
17	0.019565	1.019		27	0.002519	1.0043
18	0.024879	1.0144		28	0.000773	1.0031
19	0.025614	1.0117		29	0.000431	1.0015

Table 3.13 V_{S30} and intermediate layer V_S by extrapolation equation 3.7 of four sites

PHI	***BH9***	***HIP***	***BH-B35C***	***NIB***	***BH1***	***SEPDM***	***BH3***
Depth (m)	V_S	Depth (m)	V_S	Depth (m)	V_S	Depth (m)	V_S
0	138	1.5	113	0.5	146	1.2	95
3.3	138	3	145	3	146	3	133
6.4	181*	6	185	5	162	4.5	141*
7	167	7.5	196	6.4	181*	7	141*
9	199	10	221	8.45	190	10	182
11	205	11	217	10.45	192	11	182
15	218	12	214	12.45	204	12	178
16	228	13	213	14.45	216	13	175
17	226	14	239	16.45	203	14	197
18	234	15	215	17	224	15	177
19	244	16	232	18	230	16	190
20**	248	17	230	19	240	17	187
		18	238	20	244	18	193
		19	248	21	254	19	203
		20	252	22	252	20	206
		21	263	23	265	21	214
		22	261	24	271	22	212
		23	274	25	276	23	225
		24	280	26	283	24	231
		25	285	27	280	25	235
		26	292	28	288	26	241
		27	290	29	283	27	239
		28	298	30	286	28	243
		29	293			29	238
		30	295			30	241

*Dummy value (for computation purpose only)

** The geotechnical investigation report revealed that at PHI site massive rhyolite was found at 20m depth from the ground surface.

3.3 Subsurface Data Collected from Direct Geophysical Investigations

3.3.1 Introduction

All the geotechnical investigation data available are penetration based insitu and basic laboratory tests. The available information gathered are standard penetration test (SPT), laboratory results and engineering soil classification of shallow depth extended from 10m to 17m . For liquefaction potential analysis, the upper 30m shear-wave velocities and related dynamic soil properties are required. Based on this fact, further investigations were

performed in and around the city by seismic refraction and vertical electrical sounding (VES) survey in the vicinity of boreholes stated in Section 3.2.1 Figure 3.1 (b).

- Objective of the investigation

The objective of the investigation is to get primary data on shear-wave velocity, ground water level and bedrock level if it is found in the extent of investigation and stratification of the soil deposit for the application of liquefaction potential assessment.

- Prior information

Prior information has been gathered from geotechnical investigation reports, geological maps, JICA maps and previous studies. The documents showed that the study area is founded on thick lacustrine deposit with scattered islands of rhyolite outcrops in the southern and south west of the city. The interbedded layer of ignimbrite between the thick lacustrine deposits shows an aquiclude behavior. Hence, ground water was expected at shallow depths in most parts of the city. The survey was conducted inorder to confirm this proposition. Moreover, repeated site visits were made to see the possible places to conduct geophysical investigations, and to get permission from the city administration. Of the available and proposed open spaces in and around the city, four sites have been selected to conduct the survey.

3.3.2 Geophysical methods

Seismic refraction and vertical electrical sounding methods have been performed alternatively at four different selected sites of the city to supplement the secondary data. The seismic refraction helps to establish the stratification and provides primary (compressional) velocity data. The electrical resistivity method has been used to locate ground water table in addition to mapping the stratification and resistivity of layers for further correlations.

3.3.2.1 Seismic refraction

1. Theoretical background of seismic refraction survey

The seismic refraction method is well suited for general site investigations for soil dynamics and earthquake engineering purposes. This technique provides for the determination of elastic wave velocities of a layered soil profile. Wave velocities and thickness of each layer are determined as long as the wave velocities increase with each successively deeper layer. The test aims to accurately measure the arrival-times of the seismic body waves, which consists of Compression P- and shear S- waves, produced by a near-surface seismic source. The waves travel through the soil to a linear array of detectors (geophones) placed at the ground surface. Compression P-waves arrive at a receiver faster than shear S-waves, thus obscuring the arrival of the latter waves i.e. the S-waves. Therefore the P-waves have been widely used in seismic refraction tests (Luna et al. 2000).

Seismic refraction surveys are useful in obtaining preliminary information about the thickness of the layering of various soils and the depth to rock or hard soil at a site. P-wave refraction is used to locate underlying bedrock formations and S-wave refraction can be used to obtain the small strain stiffness profiles. However; as stated above, S-waves are usually obscured by P-wave. Hence a rich source of shearing energy is needed to generate shear wave velocity. Alternatively it can be derived from the relation between the two wave velocities assuming an elastic medium.

2. Mechanism

The refraction method consists of measuring the travel times of the compressional waves generated by an impulsive energy source. The choice of energy sources are usually dependent on the depth and material type to be surveyed. The impulse energy is detected, amplified, and recorded by special equipment designed for this purpose (Figure 3.3).

(a)

(b)

(c)

Figure 3.3 some of the equipment used for seismic refraction (a) geophones (b) Seismograph (c) energy source

Some of the seismic energy travels along the surface in the form of a direct wave. Parts of body waves propagate to the inner surface. However, when a seismic wave encounters an interface between two different soil and/or rock layers, a portion of the energy is reflected and the remainder will propagate through the layer boundary at a refracted angle according to Snell's law (Figure 3.4 (a). At a critical angle of incidence the wave is critically refracted and will travel parallel to the interface at the speed of the underlying layer. Energy from this critically refracted wave returns to the surface in the form of a head wave, which may arrive at the more distant geophones before the direct wave. By picking the time of the first arrival of seismic energy at each geophone, a plot of travel-time against distance along the survey line can be generated as described in Figure 3.4b.

Another approach available for the interpretation of refraction data is the modeling and inversion of the acquired seismic velocities. By modeling the paths taken through the subsurface by the seismic energy, or 'ray tracing', the thickness of each layer in the model can be adjusted in an iterative manner until a solution is achieved. This produces a cross-sectional velocity model of the subsurface.

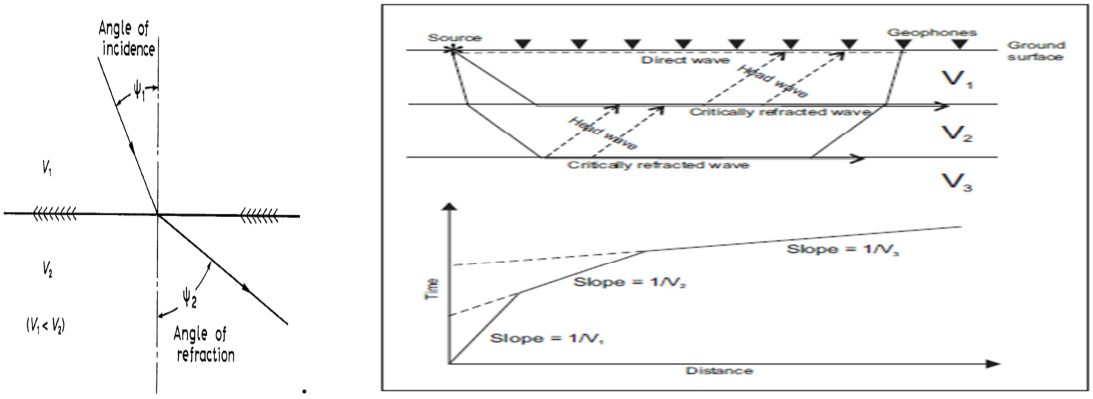

(a) (b)

Figure 3.4 Seismic refraction survey (a) Snell's law (b) Schematics of seismic refraction survey

3. Limitation of refraction methods

The two major potential problem areas in refraction surveys are the phenomenon of a "blind zone" and the effect of a velocity reversal (Redpath 1973). The term blind zone refers to the possible existence of a hidden layer, i.e. the inability of the refraction seismograph to differentiate the existence of certain beds or layers because of insufficient velocity contrast or thickness. Another functional problem that can occur in refraction surveys is the existence of

a velocity reversal that will result in erroneous computations of depths to underlying beds. A velocity reversal can exist because of a low-velocity layer or because of a high-speed layer (Redpath 1973).

4. Field work

The crew has been organized to perform the test in the possible short period of time to optimize the cost with the quality of data required. Therefore, one person is assigned at the data logger to give order for triggering crew at the moment of lower noise and when the data logger is ready for recording. And the triggering crew will perform the maximum effort to trigger the plate for maximum depth of investigation. The vertical electrical sounding crew also organized in the same way. Both methods are performed one after the other in the similar locations.

The seismic refraction method has been used at four sites. Three of the sites were studied by an in-line spread of 24 geophones and the HIP site was studied with 36 in-line spread of geophones with 4m spacing. The triggering units are 10kg hammer, triggering cables, 15cm^2 metallic plate as shown in Figure 3.3. In the 24 in-line spread geophones the shot points are located at 2m, 22m, 42m, 50m, 70m, and 90m. And in the 36 in-line spread geophones the shot points at 98m, 118m and 138m are included in addition to the 24 geophone spread shot points. At each shot point 6 to 8 shots with a 10kg hammer were performed. Some of the actevities are presented in Figure 3.5.

(a)

(b)

(c) (d)

Figure 3.5 Geophysical investigation sites a) Site 1 Amora gedel site (close to progress Int. hotel) (b) Hawassa Industry Park (c) Agricaltural college of Hawassa University. (closer Nib Bank) (d) Hawassa Meskel square (SEPDM office)

5. Output of seismic refraction survey

While interpreting Seismic refraction output, its limitation should be well addressed. Velocity reversal is expected in three sites, which have ignimbrite layer interbedded between the lacustrine deposits. A velocity reversal can exist because of a low-velocity layer or because of a high-speed layer. In either case velocities do not increase progressively with depth, and at some point in the stratigraphy there is downward transition to a relatively lower velocity. This has the effect of refracting the seismic ray downwards towards the vertical as shown in Figure 3.6. Refractions from such a low-velocity layer cannot be detected at the surface, and the existence of this layer cannot be determined from the time-distance curve. The ray will not return to the surface until it encounters a layer with a velocity higher than any layer previously encountered in its downward travel (Redpath 1973). The output is presented in Figure 3.7 to Figure 3.10. The procedure needs special care and good experience in geophysical interpretation because differentiating pulse like waves from refracted wave is difficult in a survey like Hawassa which have thick loose deposit. For analysis the ignimbrite

layer will be inserted at their respective depth from the borehole as well as vertical electrical resistivity output.

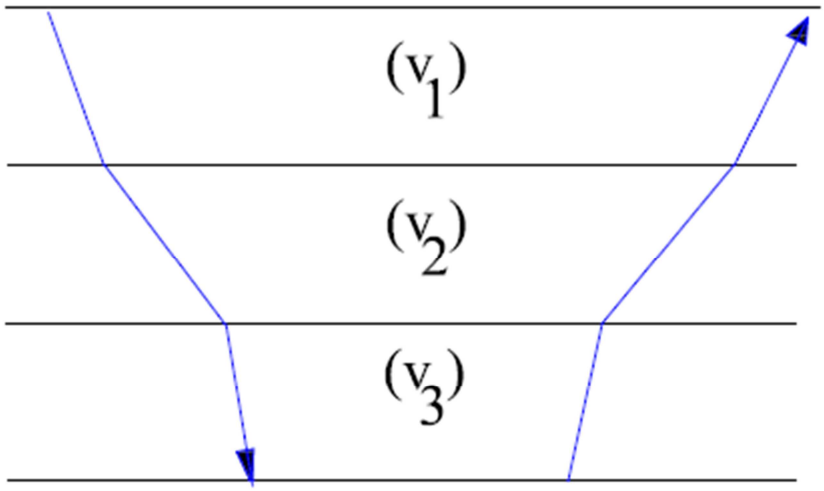

Where $V_1<V_2>V_3$

Figure 3.6 Velocity reversal

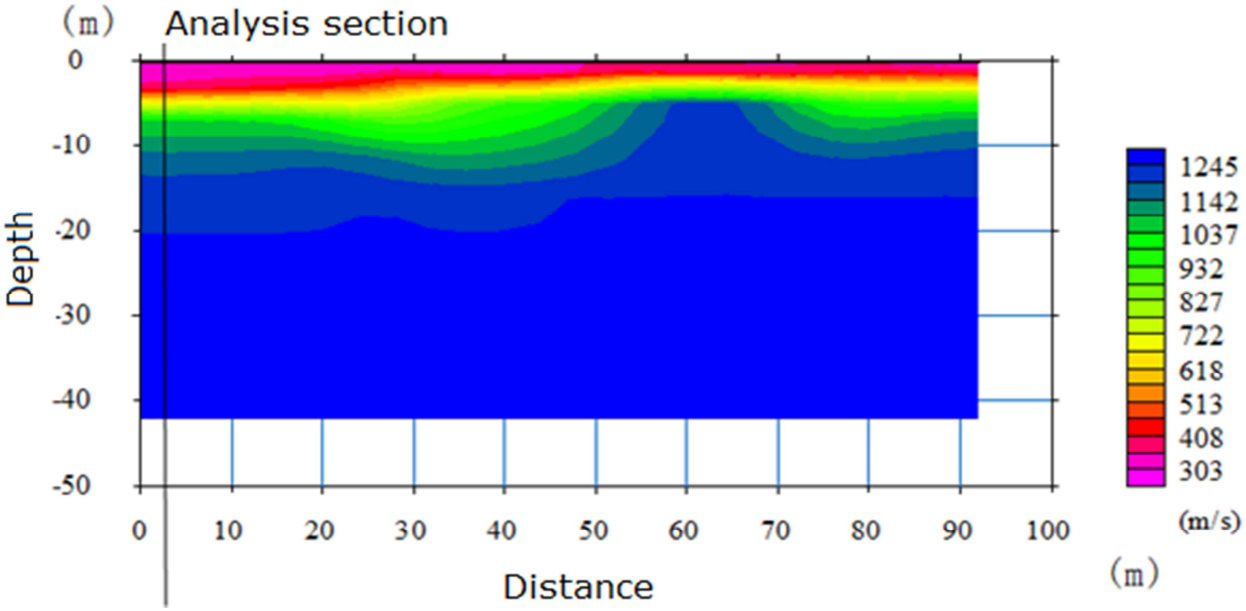

Figure 3.7 Seismic refraction output of site 1 (AMORA GEDEL)

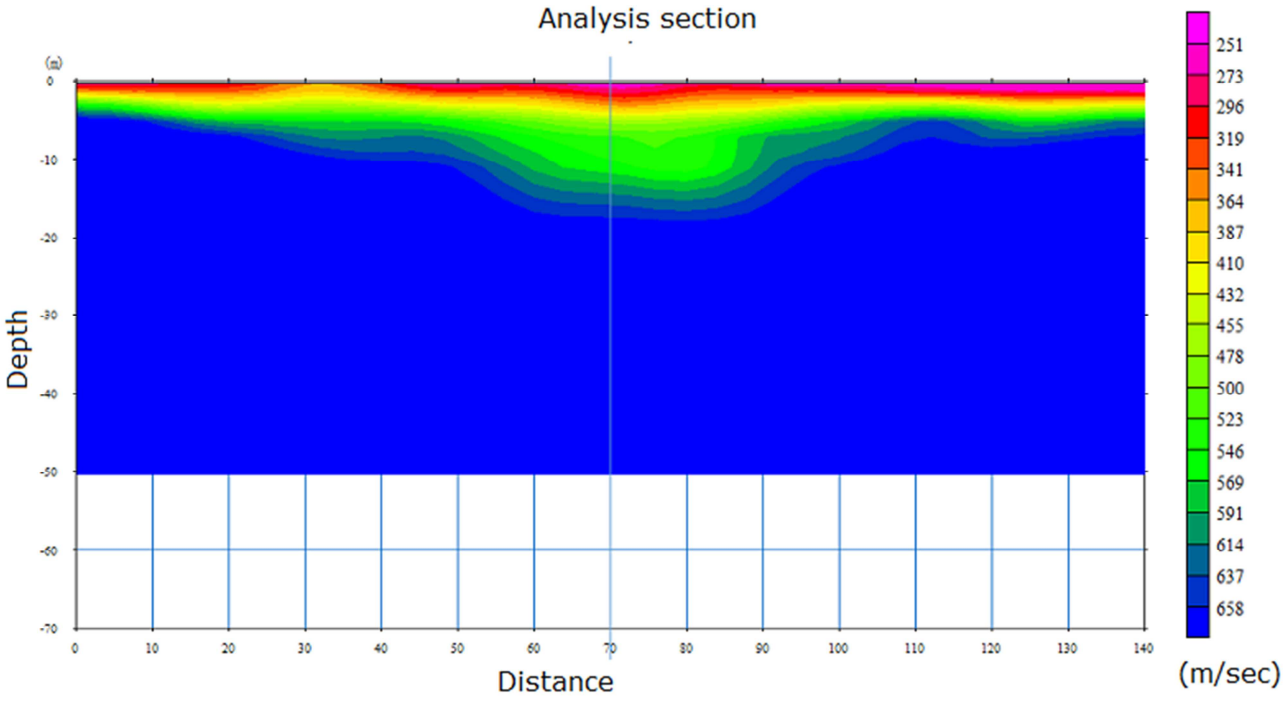

Figure 3.8 Seismic refraction output of site 2(HIP)

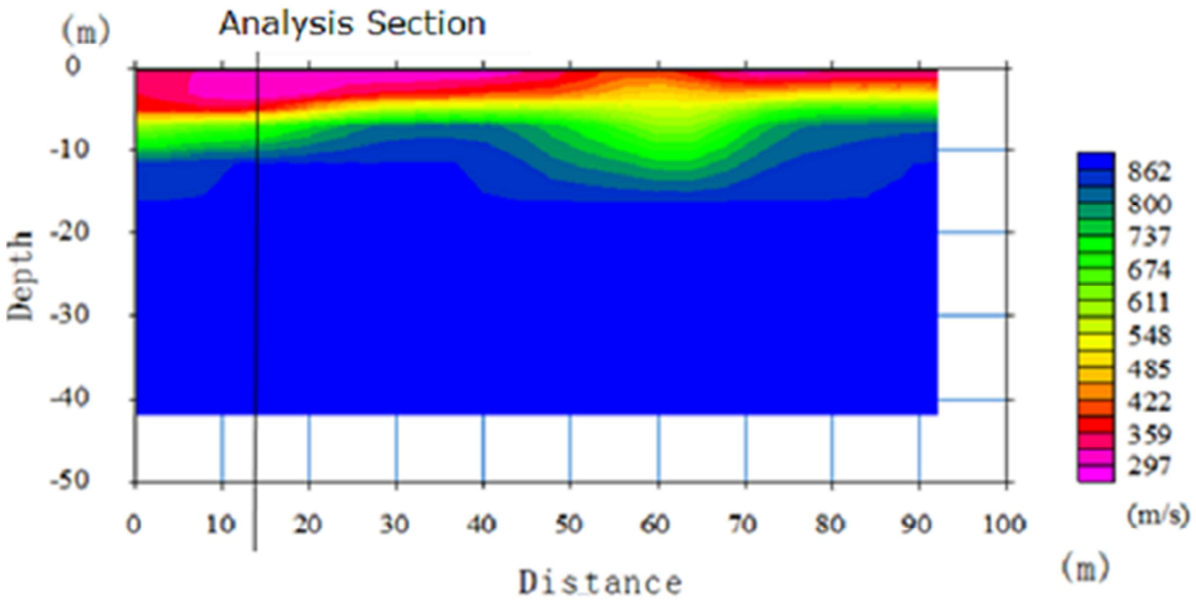

Figure 3.9 Seismic refraction output of site 3 (AGRICULTURAL COLLEGE)

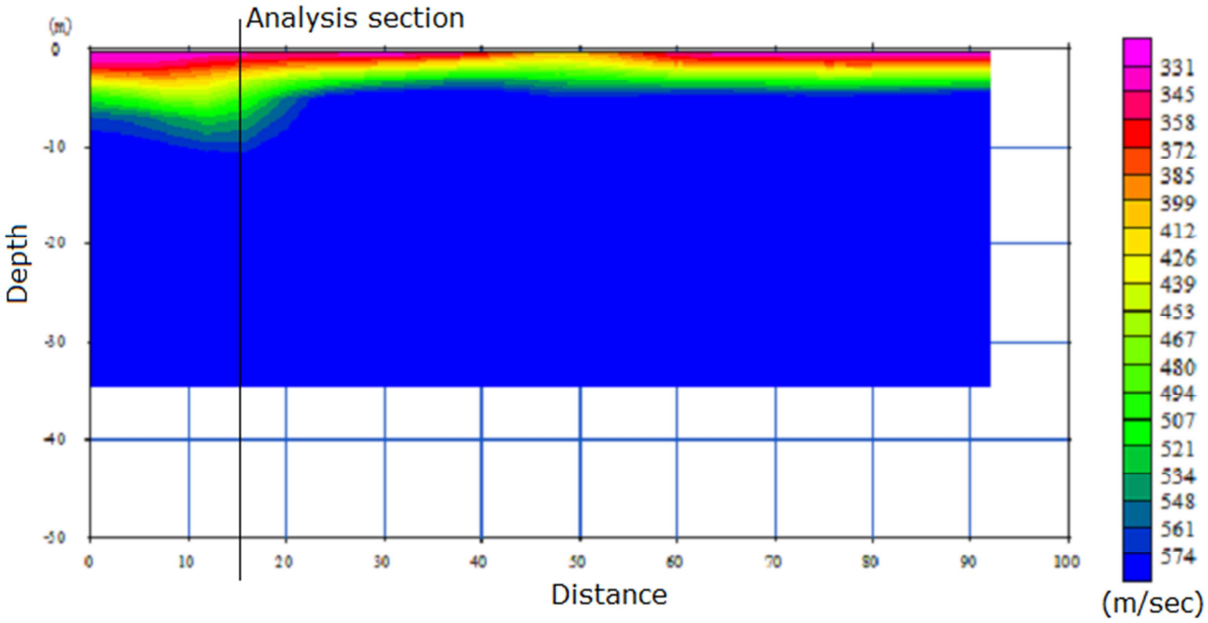

Figure 3.10 Seismic refraction output of site 4 (MESKEL SQUARE)

6. Shear-wave velocity computation

Shear-wave velocity can be determined from any of the elastic constant and primary wave velocity relation. Relative variations between any three independent elastic constants can be related to variations of V_p/V_s as shown in Figure 3.11 (Uyanik, 2010).

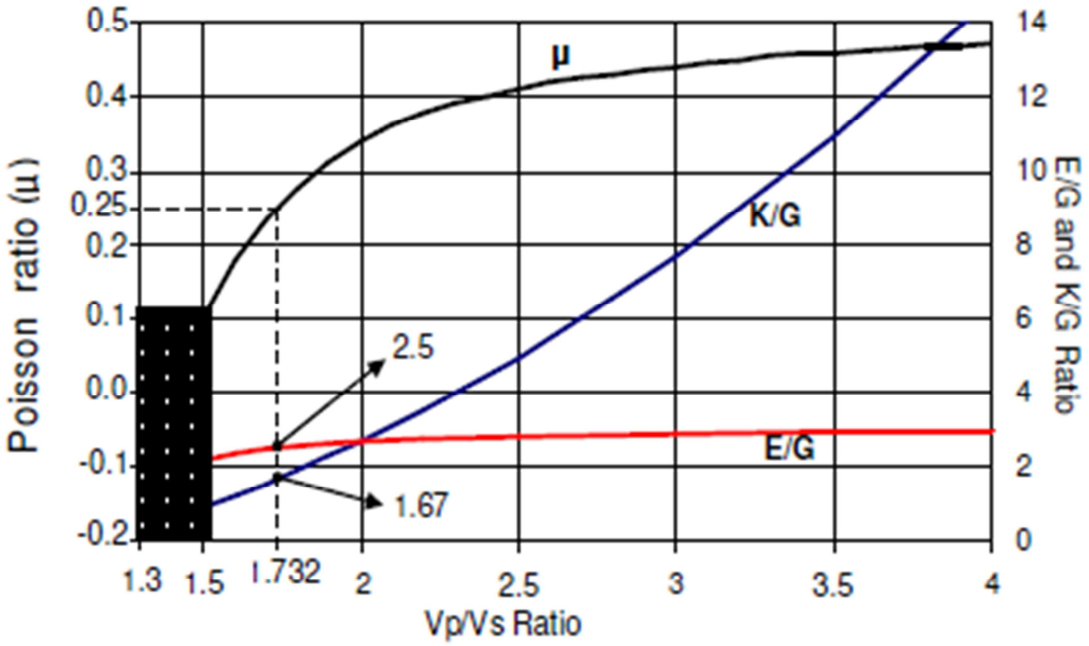

Figure 3.11 E/G (the ratio of elasticity and rigidity), K/G (the ratio of incompressibility and rigidity) and ν (Poisson's ratio) changes versus V_P/V_S (the velocity ratio) (Uyanik 2010)

From Navier's equations for dynamic equilibrium the relation between shear-wave (V_S) and compression-wave (V_P) velocities is given by

$$\frac{V_P}{V_S} = \sqrt{\left[\frac{1-2\mu}{2(1-\mu)}\right]} \tag{3.8}$$

Where μ is Poisson's ratio

Poisson's Ratio

Fine particles in soil play a significant role in defining the mechanical properties and deformation characteristics. So, investigation of fine contents of soil is important to estimate Poisson's ratio. Poisson's ratio values are found to be influenced by amount of fines in sand. Increasing amount of fines tend to increase the Poisson's ratio (Suwal and Kuwano 2012).

Considering the fine content in the boreholes and the range of values given for silty sand and sandy soil by Essien et al. (2014), a Poisson's ratio of 0.35 is adopted for shear-wave velocity computation using equation 3.8. The values are provided in Table 3.14.

7. Shear wave velocity extrapolation

The depth of investigation doesn't reach 30m because of loose deposit and low energy efficiency. Hence extrapolations of shear-wave velocities have been performed for all sites except Amora-Gedel site because it has measured data to the depth of analysis. Similar to section 3.2.3.5, extrapolation of shear-wave velocity has been carried out based on Boore's proposed method for three sites in Table 3.15 (Boore 2004)

Table 3.14 Shear-wave velocity computation from seismic refraction output a) Amora-gedel, b) HIP c) Agricultural College d) Meskel square

AMORA-GEDEL (PIH) SITE 1			***HIP SITE SITE 2***			***AGRI-COLLEGE (NIB) SITE 3***			***MESKEL SQUARE (SEPDM)- SITE4***		
μ, =0.35	0.35	GWT @ 3.6m	μ, =0.35	0.35	GWT @ 10m	μ=0.35	0.35	GWT @ 3m	μ, =0.35	0.35	GWT @ 3m
Depth (m)	V_P, m/s	Vs, m/s	Depth (m)	V_P, m/s	Vs, m/s	Depth (m)	V_P, m/s	Vs, m/s	Depth (m)	V_P, m/s	Vs, m/s
1	290	139	1	251	121	1	297	143	1	331	159
2	290	139	2	273	131	2	297	143	2	345	166
3	290	139	3	319	153	3	297	143	3	372	179
4	408	196	4	341	164	4	318	153	4	399	192
5	408	196	5	364	175	5	338	163	5	412	198
6	670	322	6	387	186	6	359	172	6	439	211
7	670	322	7	410	197	7	422	203	7	453	218
8	827	397	8	432	208	8	485	233	8	480	231
9	827	397	9	455	219	9	611	294	9	521	250

10	827	397	10	478	230	10	674	324	10	548	263
11	1037	498	11	500	240	11	737	354	11	574	276
12	1037	498	12	500	240	12	800	384			
13	1087	522	13	523	251	13	862	414			
14	1087	522	14	546	262						
15	1087	522	15	569	273						
16	1142	549	16	591	284						
17	1142	549	17	614	295						
18	1168	561	18	658	316						
19	1168	561									
20	1168	561									

Table 3.15 Shear-wave velocity extrapolation for intermediate layers of HIP, Agricultural-College, and Meskel Square sites

HIP			***AGRI-COLLEGE (nearby NIB)***			***MESKEL SQUARE (SEPDM)***	
Depth (m)	V_S, m/sec		Depth (m)	V_S, m/sec		Depth (m)	V_S, m/sec
1	121		1	143		1	159
2	131		2	143		2	166
3	153		3	143		3	179
4	164		4	153		4	192
5	175		5	163		5	198
6	186		6	172		6	211
7	197		7	203		7	218
8	208		8	233		8	231
9	219		9	294		9	250
10	230		10	324		10	263
11	240		11	354		11	276
12	240		12	384		12	254
13	251		13	414		13	256
14	262		14	278		14	288
15	273		15	250		15	258
16	284		16	270		16	279
17	295		17	270		17	279
18	316		18	279		18	289
19	267		19	290		19	300
20	271		20	295		20	305
21	282		21	307		21	318
22	281		22	306		22	317
23	293		23	317		23	328
24	300		24	324		24	335

25	305		25	330		25	340
26	313		26	338		26	349
27	310		27	336		27	347
28	320		28	347		28	359
29	315		29	342		29	354
30	318		30	346		30	358

3.3.2.2 Electrical resistivity method

The electrical resistivity method involves the measurement of the apparent resistivity of soils and rock as a function of depth or position. The resistivity of soils is a complicated function of porosity, permeability, ionic content of the pore fluids, and clay mineralization. Regardless of electrodes spread, there are two methods employed in electrical resistivity methods these are vertical electrical soundings (resistivity soundings) and resistivity profiling (Telford et al. 1990).

1. Vertical electric sounding

Vertical electric sounding (VES) employs collinear arrays designed to output a 1-D vertical apparent resistivity versus depth model of the subsurface at a specific observation point. In this method a series of potential differences are acquired at successively greater electrode spacing while maintaining a fixed central reference point. The two most common arrays used for VES are the Wenner array and the Schlumberger array. Schlumberger array has been used for this study.

2. Mechanism of Schlumberger array methods

In Schlumberger array only two of four electrodes are moved between successive readings. The potential electrodes are fixed except when the current electrodes become relatively distant, the potential electrode spacing need to be expanded in order to have measurable potentials.

The apparent resistivity is the bulk average resistivity of all soils and rock influencing the current flow. It is calculated by dividing the measured potential difference by the input current and multiplying by a geometric factor specific to the array being used and electrode spacing.

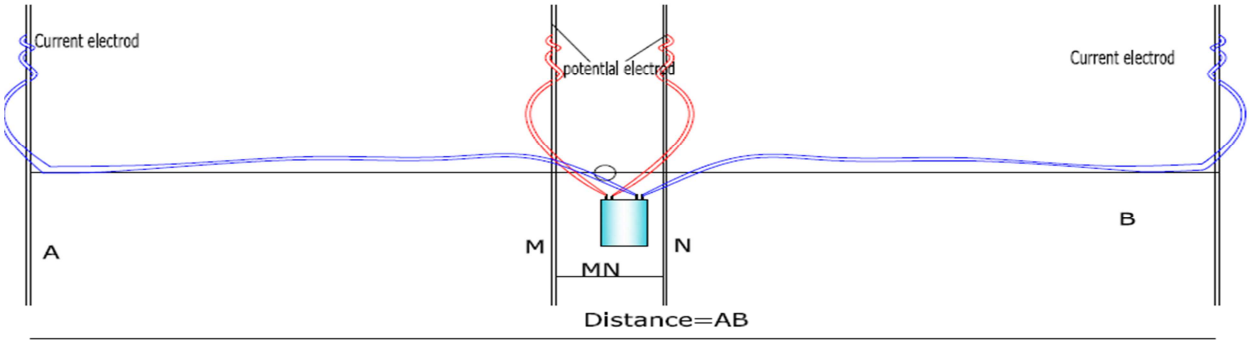

Figure 3.12 Schlumberger array VES schematics

The apparent resistivity of Schlumberger array is given by

$$\rho a = \pi \frac{(AB/2)^2}{2MN}\left(\frac{\Delta V}{I}\right) \tag{3.9}$$

Where AB is distance measured between current electrodes, MN is distance between potential electrodes as shown in Figure 3.12, ΔV is potential difference and I is current measured.

3. Field work

The purpose of this survey was to characterize the location of bedrock if it is found in shallower depth and depth of ground water table and getting information for backing the seismic investigation. The survey was made at the same sites as the seismic refraction survey sites. Locations of the study are presented in Figure 3.13.

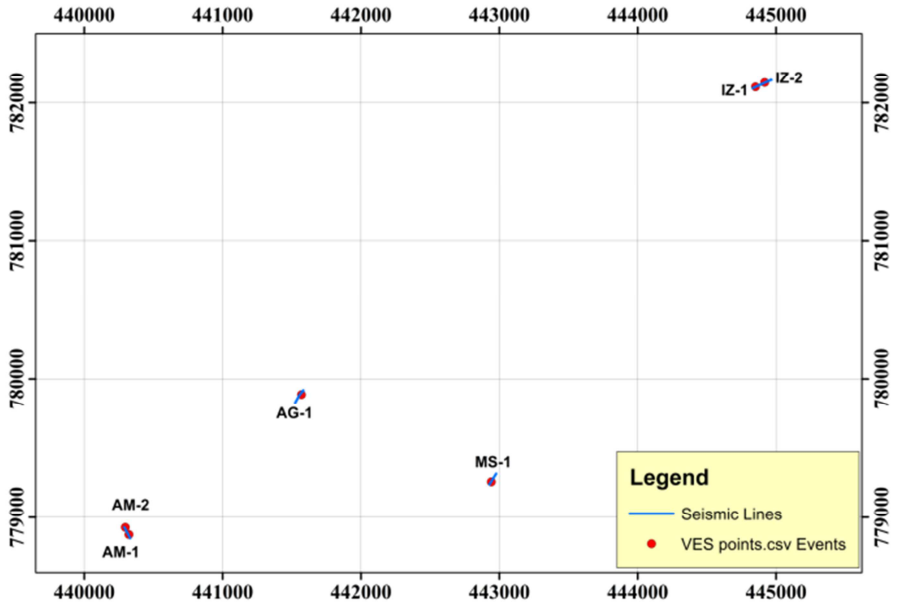

Figure 3.13 Geophysical investigation location and orientation

4. Interpretation and output

Interpretations of multi-layer VES survey performed by using IPI 2win software are presented from Figure 3.14 to Figure 3.17.

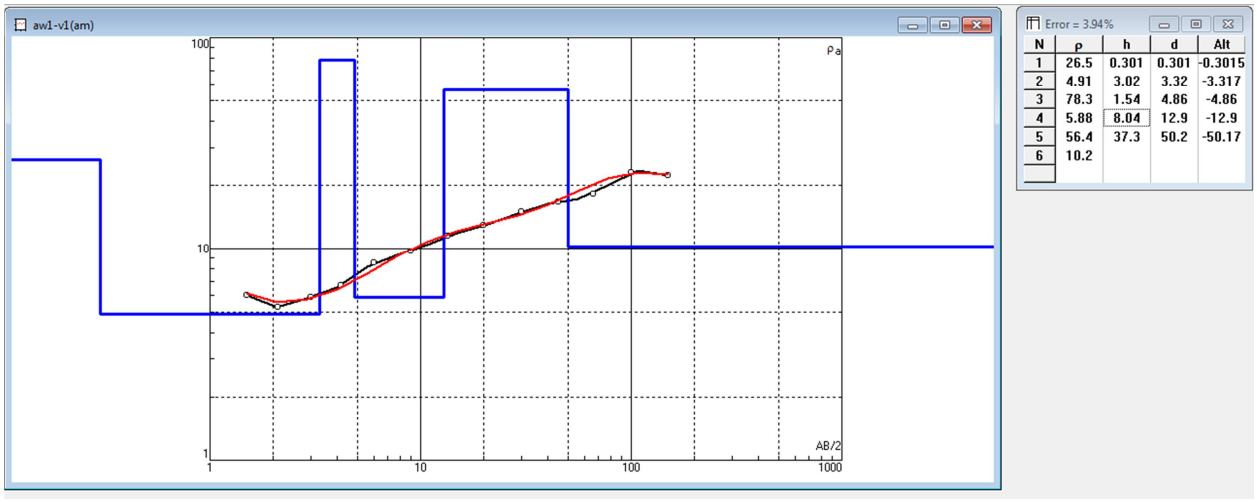

(a)

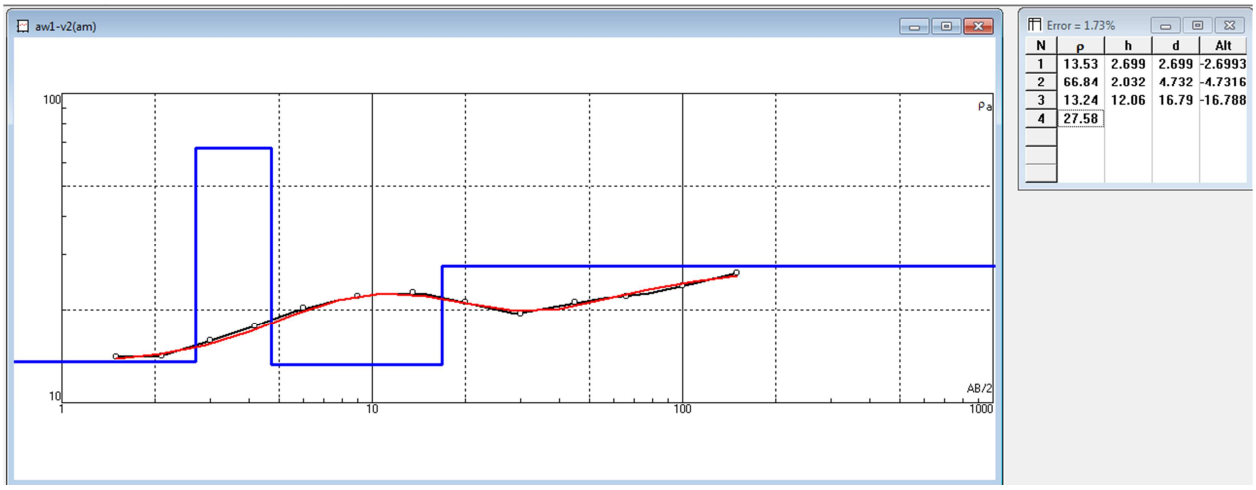

(b)

Figure 3.14 vertical electrical sounding test result of Amora-Gedel (a) VES –V1 profile (b) VES- V2 profile


IZV1
IZV2
8
Hawassa University
Image © 2017 CNES / Airbus
© 2017 Google
Google Earth

(a)

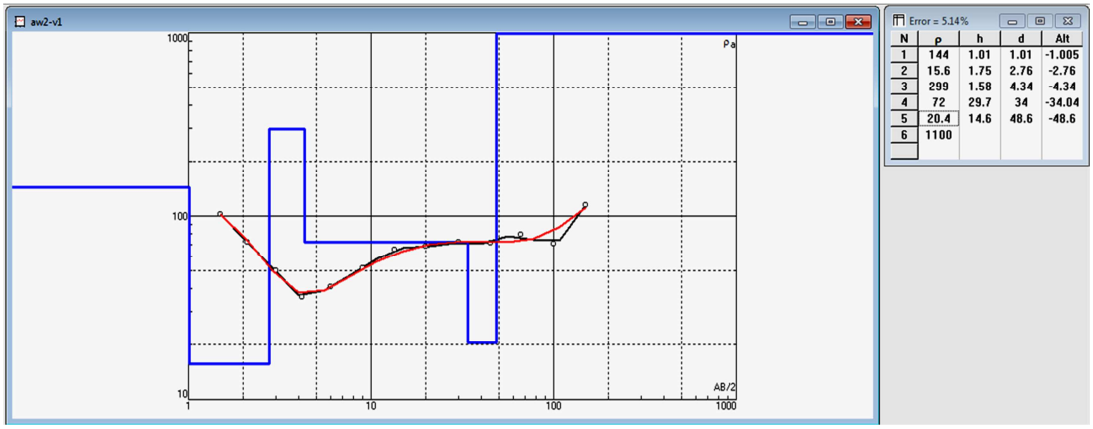
aw2-v1
Error = 5.14%
N ρ h d Alt
1 144 1.01 1.01 -1.005
2 15.6 1.75 2.76 -2.76
3 299 1.58 4.34 -4.34
4 72 29.7 34 -34.04
5 20.4 14.6 48.6 -48.6
6 1100
1000
100
10
1
10
100
1000
ρa
AB/2

(b)

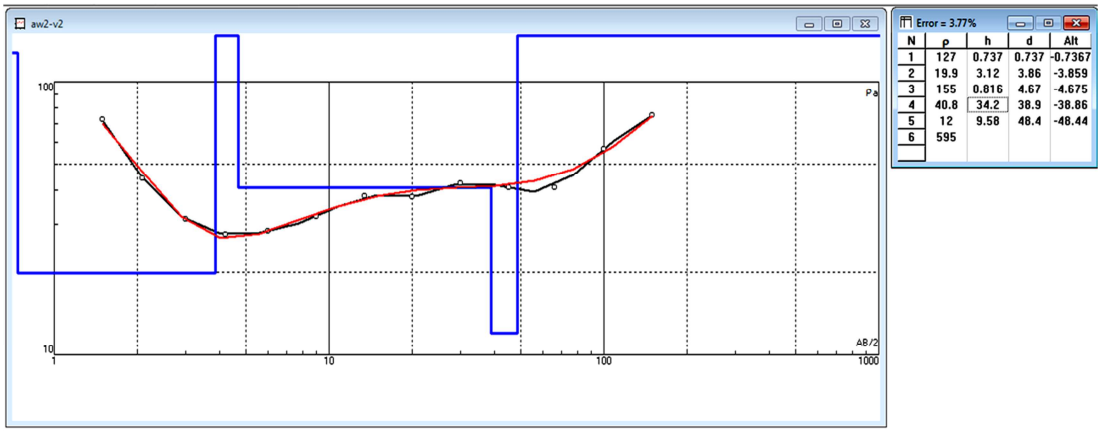
aw2-v2
Error = 3.77%
N ρ h d Alt
1 127 0.737 0.737 -0.7367
2 19.9 3.12 3.86 -3.859
3 155 0.816 4.67 -4.675
4 40.8 34.2 38.9 -38.86
5 12 9.58 48.4 -48.44
6 595
100
10
1
10
100
1000
ρa
AB/2

(c)

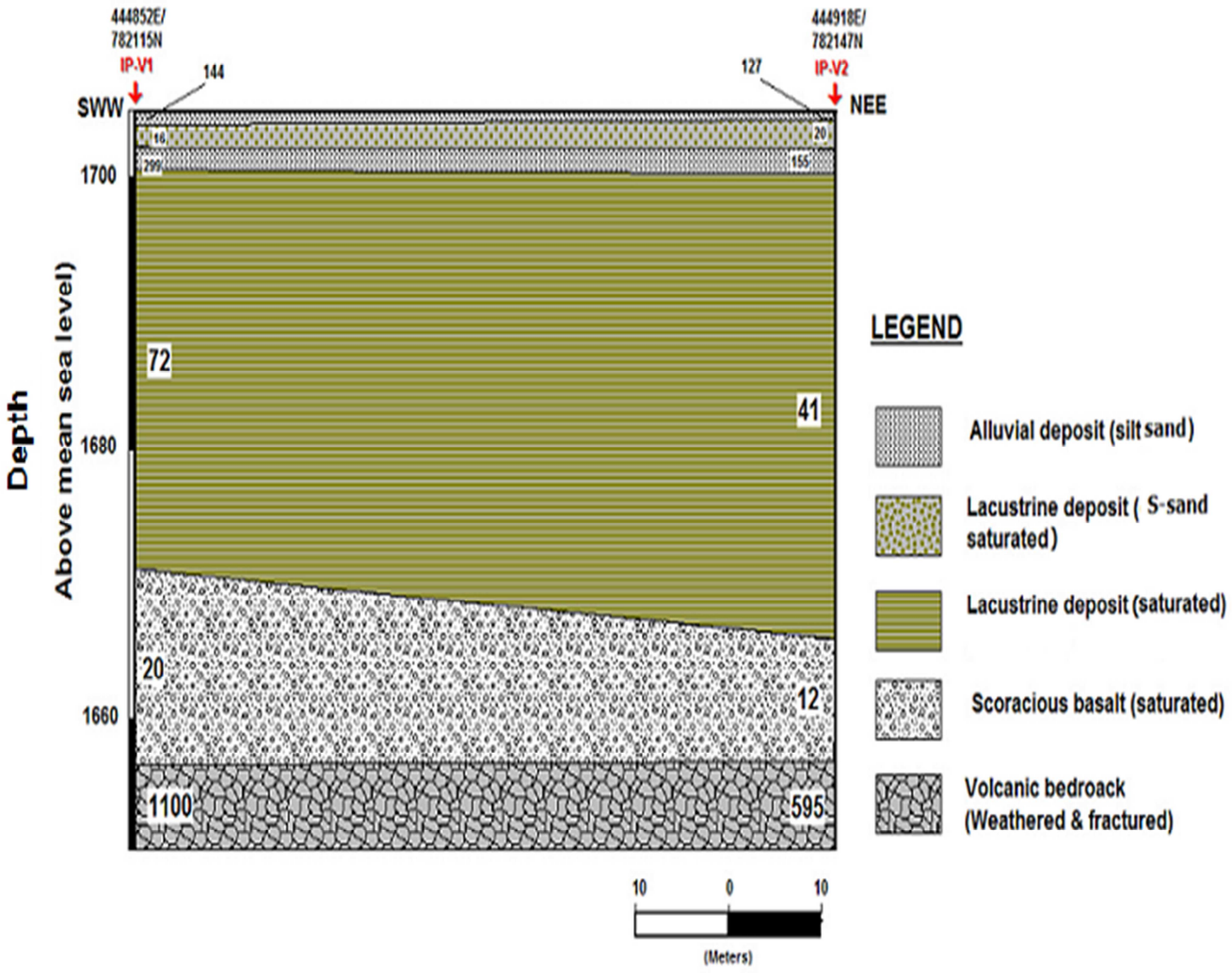

(d)

Figure 3.15 vertical electrical sounding test result of Hawassa industry park (HIP) (a) investigation site location (Google Earth), (b) VES –V1 profile (C) VES- V2 profile (d) vertical section of HIP to the depth of investigation

(a)

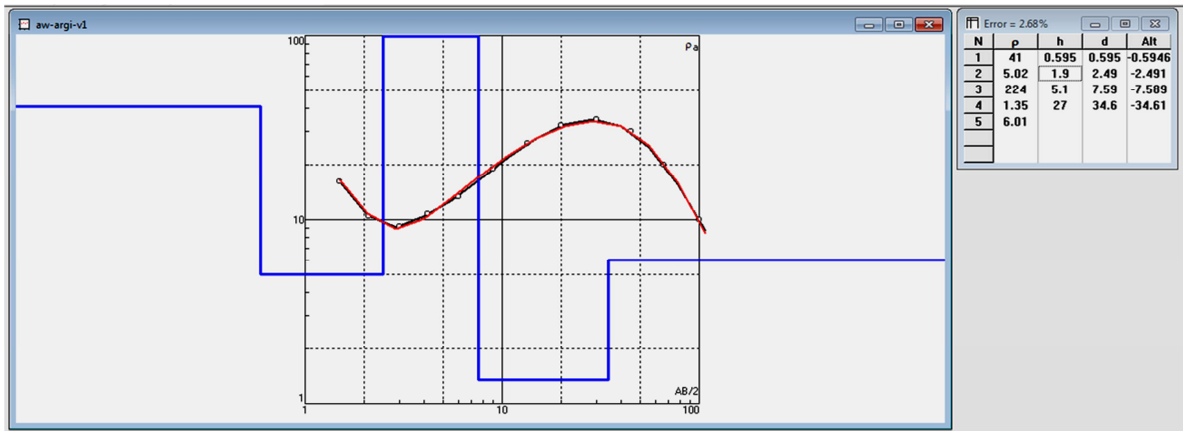

(b)

Figure 3.16 vertical electrical sounding test result of Agricultural college (a) investigation site location (Google Earth), (b) VES –V1 profile

(a)

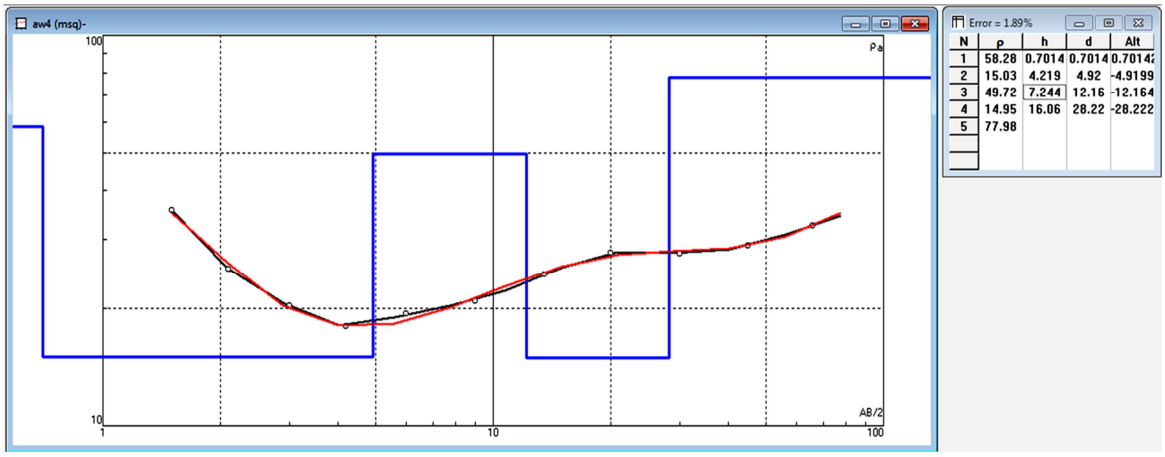

(b)

Figure 3.17 vertical electrical sounding test result of Meskel Square (Near SEPDM site), (a) investigation site location (Google Earth) (b) VES –V1 profile

The vertical electrical sounding test output revealed that there is conductive layer at shallower depth followed by thin layer high electrical resistant layer at 3.m,3.3m,2.50m, and 4.9m from ground surface in Amora-Gedel, HIP, Agricultural college and Meskel square sites respectively . These result confirmed the interbedded ignimbrite layer found in borehole investigation except Industry park site, which is relatively dense layer instead. The highly conductive layer above the ignimbrite and dense layer of HIP shows that the aquiclude behavior of the ignimbrite layer observed during borehole investigations.

CHAPTER FOUR

DATA ANALYSES

4.1 Introduction

Liquefaction potential is generally evaluated by comparing consistent measures of earthquake loading and liquefaction resistance of soil. It is a common practice to compare cyclic shear stress amplitude usually normalized by initial vertical effective stress and expressed in the form of a Cyclic Stress Ratio (CSR), for loading and a Cyclic Resistance Ratio (CRR), for resistance. The potential for liquefaction is then described in terms of a factor of safety against liquefaction, FS_L=CRR/CSR (Kramer 1996). Simplified method of liquefaction potential analyses involves the determination of ground surface maximum acceleration (a_{max}), SPT value, shear-wave velocity, fines content etc... The ground surface maximum acceleration, a_{max}, shall be determined from site response analyses. For this purpose, input ground motion selection from past recorded ground motion is a common practice. A total of seven ground motions are selected for a_{max} determination in this study. Three motions from the crustal earthquake database of PEER NGA west -2 and four commonly recommended (Yoshida 2015) and deconvolved ground motions by Haile (1996) from four different events i.e. Elcentro, Hachinohe, Kobe and Taft are selected for the analyses. The soil models are adopted from literature. And the soil profiles for the analyses are extracted from processed data presented in Chapter Three. Knowing the ground surface maximum acceleration from different combination of the above input parameters, liquefaction potential assessment of the study area is conducted using SPT based and Shear wave velocity based simplified methods. The flow of work is presented in Figure 4.1.

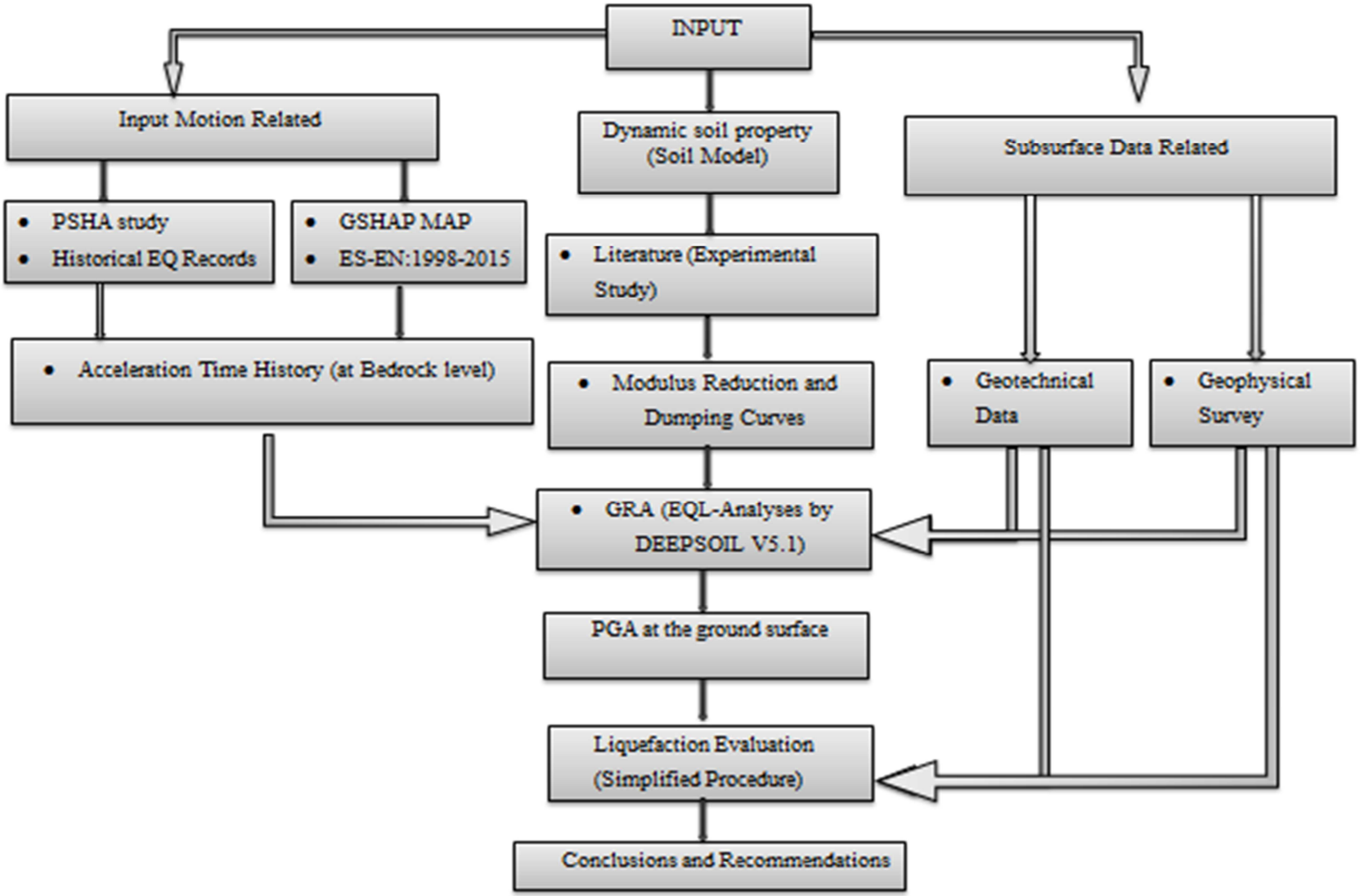

Figure 4.1 Methodology used for liquefaction potential assessment of Hawassa

4.2 Liquefaction Potential Analysis using Simplified procedure

A simplified method based on both a liquefaction resistance factor (FL) and liquefaction potential factors (PL) have been proposed for evaluating soil liquefaction potential. As a result of various detailed studies on the liquefaction of sandy soils, several simplified and complex methods have been proposed to evaluate the liquefaction potential. Based on the simplified method, the liquefaction potential of cohessionless soils can be estimated from SPT N-values or Vs, unit weights, mean particle diameters, and the maximum acceleration at the ground surface. The determination of the maximum ground surface acceleration involves an intensive computation process in liquefaction potential evaluation in a site specific study where there is no attenuation relation.

The preferred method for estimating a_{max} is through empirical correlations of a_{max} with earthquake magnitude and distance from the seismic energy source and local site conditions. Selection of an attenuation relationship should be based on factors such as seismicity of the country, type of faulting, and site condition (Youd et al. 2001). The East African Rift is one of the places where recorded strong motion data are rare and thus there is in effect no Ground Motion Prediction Equations (GMPE), that are directly based on strong-motion data (Ayele 2017). Therefore, estimation of a_{max} for soft soil and other soils from local site response analysis is mandatory. The Computer program DEEPSOIL V5.1 of Hashash et al. (2012) is used for the analysis conducted in this work.

Peak ground acceleration prediction from site response analysis by DEEPSOIL requires selection of input ground motion, soil profile data shear wave velocity of the upper 30m, suitable soil model and ground water level.

4.2.1 Input Motion Selection

Input motion records are available in free-access internet databases, such as Italian Accelerometric Archive (ITACA)(http://itaca.mi.ingv.it/ItacaNet/), Pacific Earthquake Engineering Research Center (PEER) (http://peer.berkeley.edu/) and ITSAK (Greek for Institute of Engineering Seismology and Earthquake Engineering Research and Technical Institute) (http://www.itsak.gr), etc. Compared to other strong-motion databases, the PEEER Next Generation Attenuation (NGA) west 2 database is particularly rich in site characterizations, like V_{S30} (Chiou et al. 2008). The input motions used in this study are extracted from PEER NGA 2 west database, because it avails shallow crustal earthquake records, which the study area is characterized by. This selection is based on matching record characteristics in terms of magnitude and source distances. Tectonic class and site class are also considered in the selection process. The selection process is carried out based on the recent proposed Stewart et al. (2014) procedure. The steps are summarized as follows:

1. The first step involves pre-selecting the ground motion records from the PEER –NGA west 2 website having reasonable magnitude, fault distance, source mechanisms, and site conditions with respect to the study area. As suggested by Stewart et al. (2014),

the site condition used in the pre-selection should be roughly compatible with that for the reference site condition for GRA.

2. The next step involves selecting motion that provided good matches to a target spectrum, which implicitly accounts for many of the above issues.

4.2.1.1 Pre-selection of Input Motion

During the pre-selection step the site compatibility is assured by matching the following characteristics

- Tectonic regime
- Magnitude and distance
- Duration of earthquake
- Site condition

Typically, the input time histories for site response analyses are specified as rock outcrop acceleration time histories that are then modified by the program to represent time histories in bedrock underlying the site.

I) Tectonic Regime

One of the criteria to comply site condition compatibility is the selection of motion from similar tectonic regimes. Since Western United States and the Horn of Africa earthquakes hypo-central depth is constrained to shallow crust (Kebede and van Eck. 1997; Ayele 2017), the database of western USA is considered for the selection of motions.

II) Magnitude and Distance (for duration estimation)

Seismic hazard analyses and historical records are the two sources of magnitudes of earthquake and their corresponding distances.

The PSHA by Kebede and van Eck (1997) shows that Hawassa is located in zone 2 having lower bound of moment magnitude of 4 and upper bound of 7±0.2. The more recent PSHA study conducted by Ayele (2017) revealed that the study area has a moment magnitude of 4.1 and 6.61±0.15 as a lower and upper bound, respectively. On top that, the United States Geological Survey (USGS) report and the seismicity study conducted by Gouin (1979) confirms that the study area has been frequently visited by earthquake magnitudes of 4.4 to 6.3 since 1906. Some of the selected earthquakes are plotted on the Google Earth map Figure 4.2. The seismic epicenters closest to Hawassa are summarized in the Table 4.1.

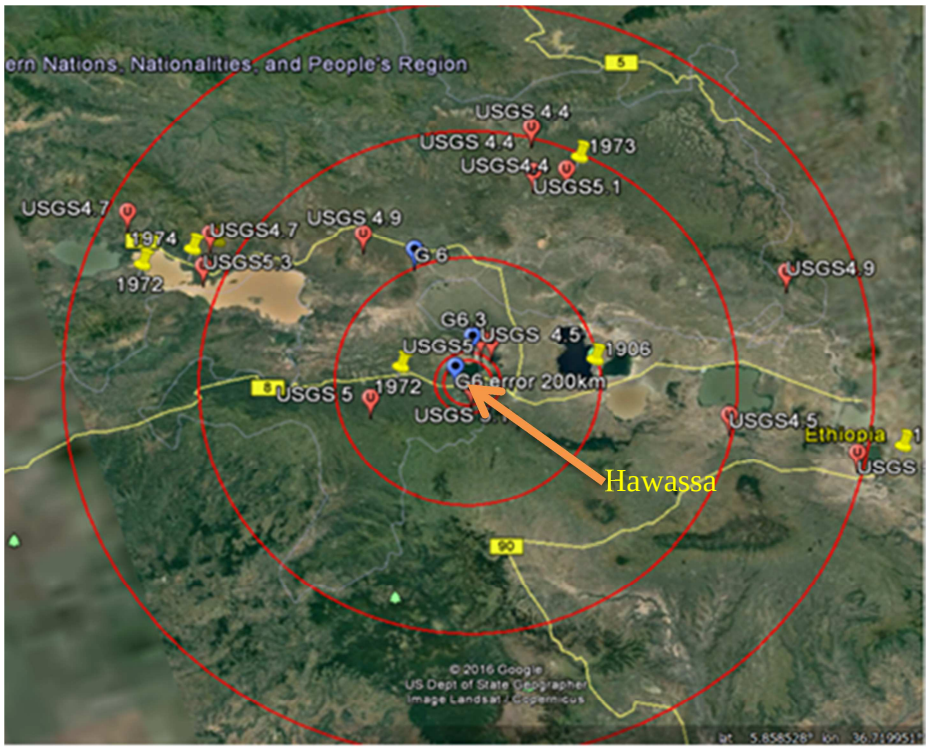

Circle 1 R=10km, Circle 2 R= 13.6km, Circle 3 R=55km,
Circle 4 R=114km, Circle 5 R=170km
Where R is radius of the circles
Note that all circles are drawn with repect to Hawassa

Figure 4.2 Historical recorded earthquakes from USGS and Seismicity study of Gouin (1979)

Table 4.1 Historical earthquake record of Hawassa area (USGS and Gouin 1979)

Year	Date	Time	Latitude	Longitude	Distance from Hawassa*	Magnitude
1944	6-sep.		**7^0	38.5^0	5Km	6
1960	4-Jul.	18:39UT	7.1^0	38.4^0	12Km	6.3
1983	2-Dec.	23:08:39.49UT	7.03^0	38.599^0	11.6Km	5.1
1995	20-Jan.	7:14:27.20UT	7.16^0	38.441^0	14Km	5
2017	24-Jan.	6:34:35 PM/9:34 Local time	7.125^0	38.4184^0	11.9Km	4.5

* Hawassa location $N7.05^o$, $E38.495^o$ **most probable location of epicenter (P. Gouin)

It can be seen from the PSHA study as well as the historical records that, Hawassa city is found in high seismically vulnerable region.

Selecting ground motions having reasonably similar magnitude and distance with the study area is intended to provide generally compatible durations and spectral contents.

Duration Estimation

For strong magnitude, duration is more related to magnitude than distance. So distance criteria need not be strict as far as motion selection is concerned. Selecting a record set with a representative range of durations is especially important in motion selection. Table 4.2 is prepared for 5%-95% significant duration of different earthquake based on magnitude distance pairs from Table 4.1 and considering the PSHA study upper bound of 7.2 (moment magnitude) of Kebede and van Eck. (1997). The Chart in Figure 4.3 is used for significant duration estimation (Bommer et al 2008).

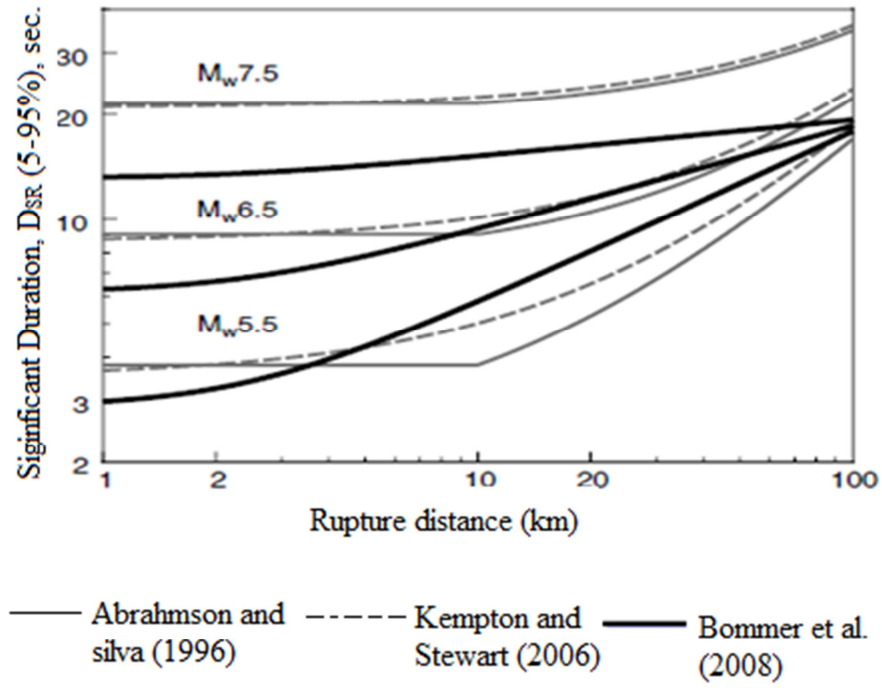

Figure 4.3 Significant duration estimation (after Bommer et al. 2008)

As can be seen in the Figure 4.3, one can read duration of approximately 17 sec. for a distance of 20km and a moment magnitude of 7.5, while the duration is 19 sec for a distance of 100km for the same magnitude, showing the small effect distance has on duration on large magnitudes.

Table 4.2 Magnitude distance pair of selected records

No	Moment Magnitude	R (rupture)	D_{SR}(5-95%) **
1	6	5	5.75
2	6.3	12	9.2
3	5.1	11.6	4.4
4	5	14	5
5	4.5	11.9	3.19
6	7.2	20*	16

Note: *20km distance is taken arbitrarily considering rupture distance has a lesser effect on determination of duration for large moment magnitude.

** Predicted duration as per Boomer et al. (2008) recommendation

III) Site Conditions

A site condition is best represented by average shear wave velocity of the upper 30m (V_{S30}) as far as site class is concerned for motion selection. In order not to be too restrictive in motion selection and as to unnecessarily limit the number of candidate input motions, the motion pre-selection was carried out from all classes of soil at this stage.

4.2.2.2 Selection Based on Target Spectrum

After the pre-selection, additional parameters such as elastic response spectra and scaling factor are also considered. The shape of the response spectrum should be the final consideration when filtering ground motions. The ground motions that provide good match to target spectra will be selected at this stage.

I) Elastic response spectra

According to the revised building code of Ethiopia ES EN 1998:2015, the horizontal elastic response spectrum, $S_e(T)$, for seismic design of buildings is given by equation 4.1.

$$\begin{aligned} S_e(T) &= a_g.S\left[1+\frac{T}{T_B}\left(\eta\,(2.5)-1\right)\right] && 0 \le T \le T_B \\ S_e(T) &= a_g.\,S.\,\eta.\,(2.5) && T_B \le T \le T_C \\ S_e(T) &= a_g.S.\eta.2.5.\left[\frac{T_C}{T}\right] && T_C \le T \le T_D \\ S_e(T) &= a_g.S.\eta.(2.5)\left[\frac{T_C\,T_D}{T^2}\right] && T_D \le T \le 4S \end{aligned} \qquad (4.1)$$

Where

$S_e(T)$ = Elastic Response Spectrum;

a_g - Peak ground acceleration at site class A (rock);

T_B - Lower limit of the period of constant spectral acceleration branch;

T_C- Upper limit of the period of constant spectral acceleration branch;

T_D -The value defining the beginning of the constant displacement response range of the spectrum;

S - site soil factor;

η – Damping correction factor (η=1 for 5% damping).

The soil factor and T_B, T_C, and T_D are given by the code for Type 1 and Type 2 design spectra depending on maximum anticipated magnitude range (Type 2 recommended only for M_W<5.5 and Type 1 spanning across all magnitude ranges). Anticipated moment magnitude for the study area exceeds 5.5 as confirmed by the studies described earlier. Furthermore, the moment magnitude that is believed to cause liquefaction is usually greater than 6 (Ambraseys 1988 as cited in Kramer 1996). For these reasons, Type 1 spectrum is selected and is presented as follows.

Table 4.3 Type 1 factors for acceleration response spectra (ES EN 1998:2015)

soil class	S	TB	TC	TD
A	1.00	0.15	0.4	2
B	1.20	0.15	0.5	2
C	1.15	0.20	0.6	2
D	1.35	0.20	0.8	2
E	1.40	0.15	0.5	2

The bedrock level peak ground acceleration from the new code has not been considered for this study because of the inconsistency of the PGA values in the document. The PGA of Hawassa from the seismic risk/hazard map of the code is read as less than 0.8g. While in the accompanying table the city is assigned a PGA of 0.15g. Due to this serious contradiction, the PGA of Hawassa is taken from the Global Seismic Hazard Analysis Map (GSHAP) by Giardini et al. (2003). According to GSHAP, Hawassa is located in the region having PGA between 0.1g and 0.13g (Figure 4.4). By linear interpolation between the contours, city may be assigned a PGA of 0.11g.

Using this PGA from the GSHAP Map and based on the basic elastic spectrum of ES EN 1998:2015, design spectra for Hawassa area for different soil classes are plotted and presented in Figure 4.5. The site class A spectrum is used as a target spectrum to select the ground motions.

II) Scaling factor

Candidate input motion can be simply scaled up or down uniformly to best match the target spectrum within a period range of interest, without changing the frequency content. The factor used to match the input motion spectrum with the target spectrum is the scaling factor. The objective of scaling is to select a record suite that is generally compatible with the amplitude and frequency content of the target spectrum. Scaling factor between 0.25 and 4 is recommended by Stewart et al. (2014). The best motion is one having a scaling factor close to unity. The period range for the scaling is adopted from the structural system of Hawassa. Considering the anticipated future development plan of Hawassa, a 20 (twenty) story building have been considered for this study as the upper limit. Hence, the period range is between 0.2 and 2sec.

III) Maximum number of motions

Limiting three to four motions from single event or station is a recommended common practice (Stewart et al. 2014). The motion having maximum peak spectral acceleration (PSA) of the two orthogonal records shall be considered for final filtering.

Thus, Selection of ground motion from PEER west2 NGA database has been carried out according to the above stated steps and criteria. The summery data of selected input motion is presented in Table 4.4.

Table 4.4 Summery of data selected input motion (PEER NGA west 2 database)

RSN	5-95% Duration (sec)	Earthquake Name	Year	Station Name	M_W	Vs30 (m/s)	Hor.-1 Acc. Filename	Hor.-2 Acc. Filename
680	6.2	"Whittier Narrows-01"	1987	"Pasadena - CIT Kresge Lab"	5.99	969.07	RSN680_WHITTIER.A_A-KRE090.AT2	RSN680_WHITTIER.A_A-KRE360.AT2
797	14.2	"Loma Prieta"	1989	"SF - Rincon Hill"	6.93	873.1	RSN797_LOMAP_RIN000.AT2	RSN797_LOMAP_RIN090.AT2
4083	8.8	"Parkfield-02_ CA"	2004	"PARKFIELD - TURKEY FLAT #1 (0M)"	6	906.96	RSN4083_PARK2004_36529270.AT2	RSN4083_PARK2004_36529360.AT2

The selected acceleration time histories and pertinent data are presented in Appendix B.

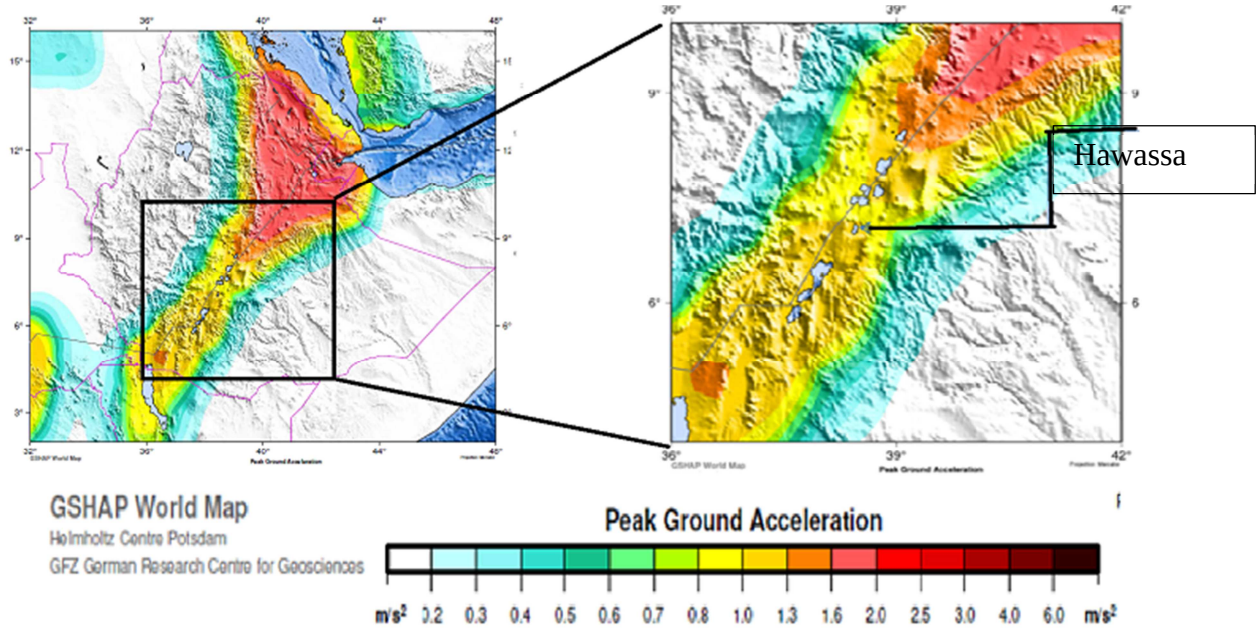

Figure 4.4 GSHAP map of Hawassa regions (Giardini et al. 2003)

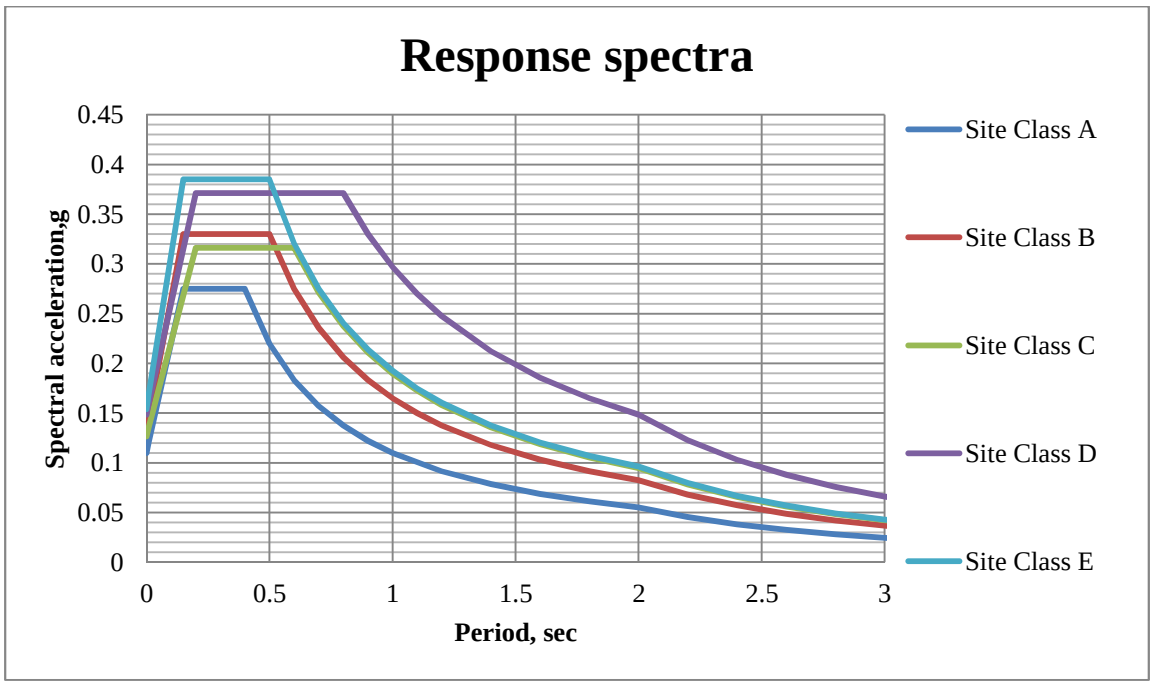

Figure 4.5 Hawassa area elastic response spectra for different class of soil based on ES EN 1998:2015 and GSHAP 475 years return period PGA of 0.11g.

4.2.2 Dynamic Soil Properties

The small strain modulus, G_{max}, of the soil profiles is determined from corresponding density and shear wave velocity of the various layers. The conversion of shear wave velocity to maximum shear modulus and vise-versa of each layer is an integrated process in the DEEPSOIL software. Hence shear wave velocity has been used for the analysis.

Shear-wave velocity determination

The shear wave velocities of the top 30m (V_{S30}) are presented in Chapter 3 as obtained from correlation and direct measurement. The penetration results (SPT) collected from different locations in and around the city have been correlated to shear wave velocity and extrapolated to 30m depths in Chapter 3. The results are presented graphically in Figure 4.6. Direct measurement of shear-wave velocity was also performed at four locations in and around the city by seismic refraction methods. The processed data discussed in Section 3.3 is presented graphically in Figure 4.7.

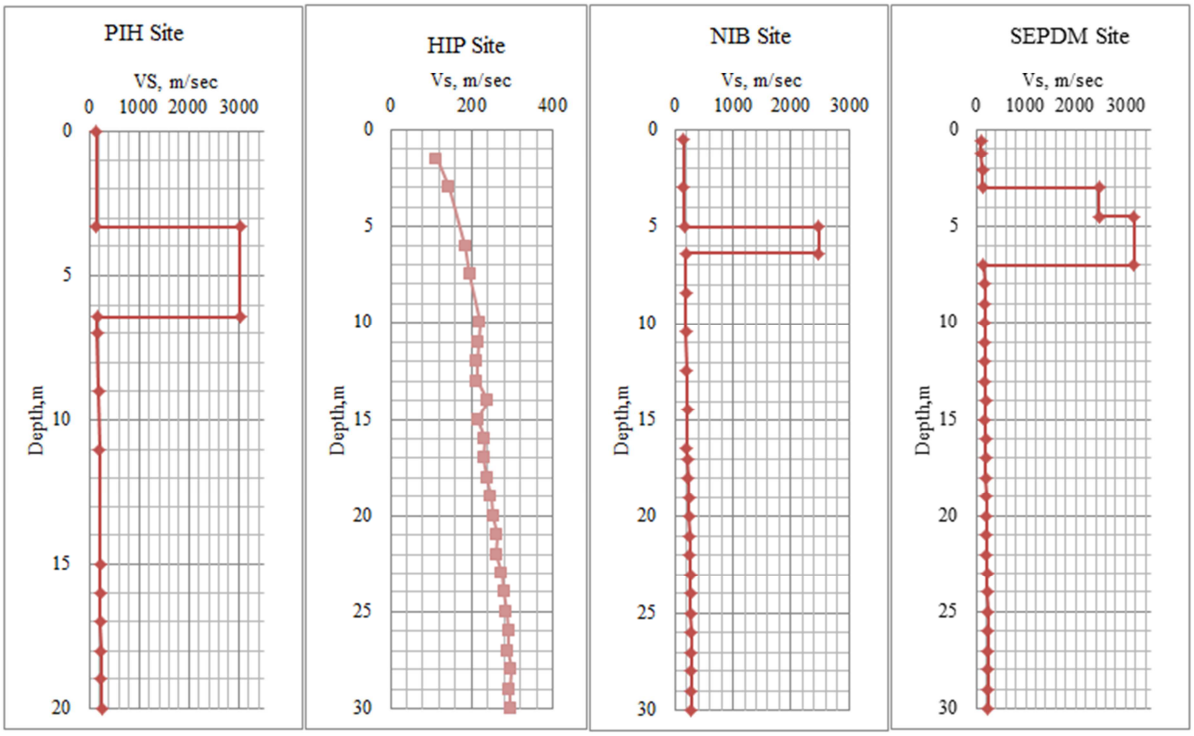

Figure 4.6 Shear wave velocity profiles of sites as computed from geotechnical investigation data

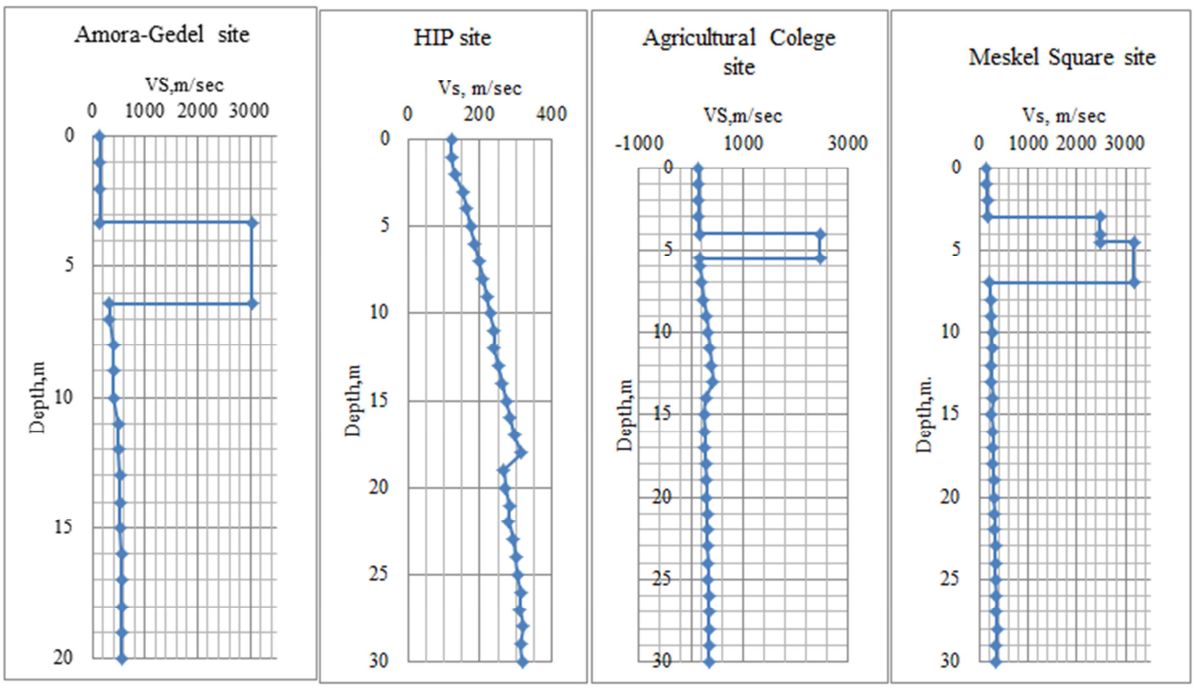

Figure 4.7 Shear wave velocity profiles of sites as measured by using seismic refraction

NOTE; The ignimbrite layer depth is established from the geotechnical investigation and the shear wave velocity as computed by the relation given by Choi (2008) in section 3.2.3.3.

4.2.3 Modulus reduction and Damping Curves

Gashaw (2012) has studied the shear modulus and damping ratio values for the soil in Hawassa city. In his study, he has done good attempt to determine the values at large strain level from 0.01 to 5%. However his result did not match with previous studies of the silty sand modes such as the pioneering work of Seed and Idriss (1970), which is the well accepted curve for sand. Moreover the study lacks small strain range values which are important for Equivalent Linear ground response analyses. Hence, for this study modulus reduction (MR) curves are estimated from relationships from other literature. For sand and clay soils, generic curves are developed as shown on Figure 4.8 by Seed and Idriss (1970). Iwasaki et al. (1978) developed overburden dependent modulus reduction curves for sand. Moreover, PI-dependent MR curves developed by Vucetic and Dobry (1991) as given in Figure 4.9. The MR and damping ratio curves for this study are based on the relations proposed by Seed and Idriss (1970) for the silty-sand layer at the site of PIH, HIP and NIB, and Vucetic and Dobry (1991) PI-dependent MR curves are used for SEPDM silty clay layers.

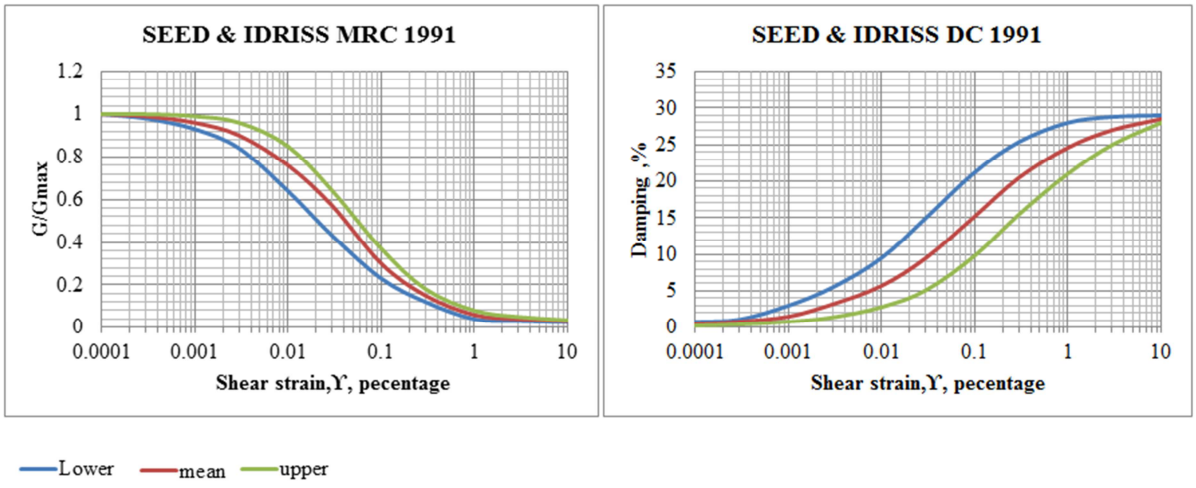

Figure 4.8 (a) Modulus reduction curve (b) Damping curves for different soils (Seed and Idriss 1991)

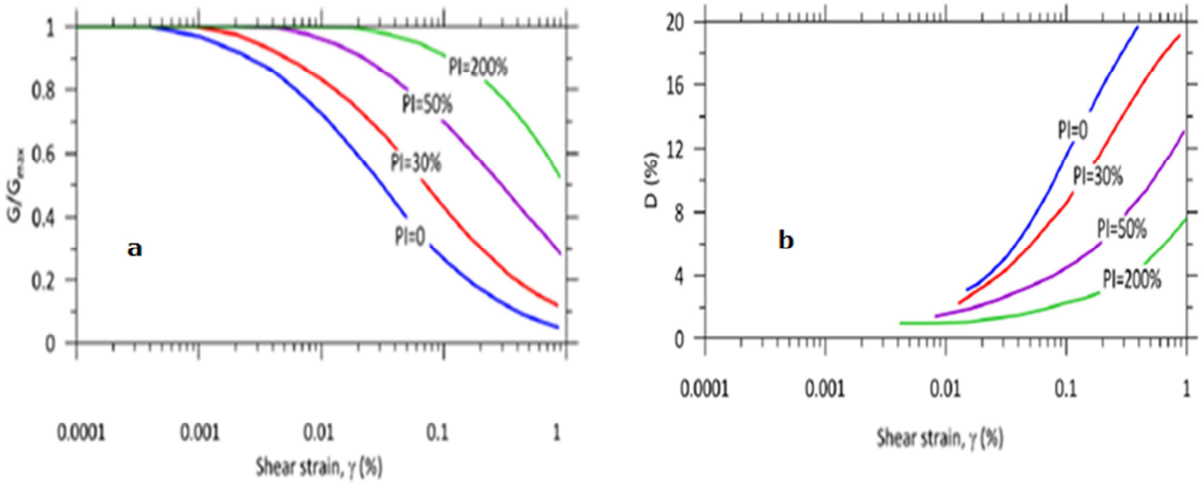

Figure 4.9 (a) Modulus reduction curve (b) Damping curves for different soils with different Plasticity index (Vucetic and Dobry 1991)

4.3 Equivalent Linear Analysis, EQL

The EQL approach is commonly used in practice because it requires straight forward, readily obtainable soil properties and less computational effort since the computation process is performed in the frequency domain (Hashash et al. 2010). The recommended procedure to calculate or estimate a_{max} that would occur at the site is in the absence of increased excess pore pressure or the onset of liquefaction. So that peak acceleration incorporates the influence of site amplification, but neglects the influence of excess pore-water pressure (Youd et al 2001). Hence equivalent linear analysis will be the economic analysis preferred for this study.

The input to EQL site response analyses include;

- ✓ Ground motion time histories (as was discussed in section 4.2.1).

- ✓ Identification of subsurface conditions, including geometry, stratification, and depth to bedrock and groundwater (Chapter 3)
- ✓ Specification of basic and advanced material properties for each layer of subsurface soil and bedrock, such as unit weight and shear wave velocity (or low-strain shear modulus) and shear modulus reduction and damping as a function of shear strain.

4.3.1 Selected Input motions

As discussed in detail in Section 4.2.1, three input motions have been selected from PEER NGA 2 west and scaled to the predicted PGA of Hawassa at bedrock level. Moreover, four ground motions have been selected as recommended by Yohsida (2015) due to their good representation for earthquake resistant design. The four motions have variety with respect to duration, multiple peak in short range of duration and frequency content (Haile 1996). The records are given in Appendix B. For this analysis, their deconvolved versions of acceleration time-histories from Haile (1996) are used after scaling the amplitude to suite to the Hawassa PGA. Therefore, totally 7(seven) acceleration time histories have been used for the analyses. Figure 4.10 shows spectral acceleration of the scaled motions and the target spectrum of Hawassa class A (rock). Their scaled acceleration time history is presented in Figure 4.11 and Figure 4.12.

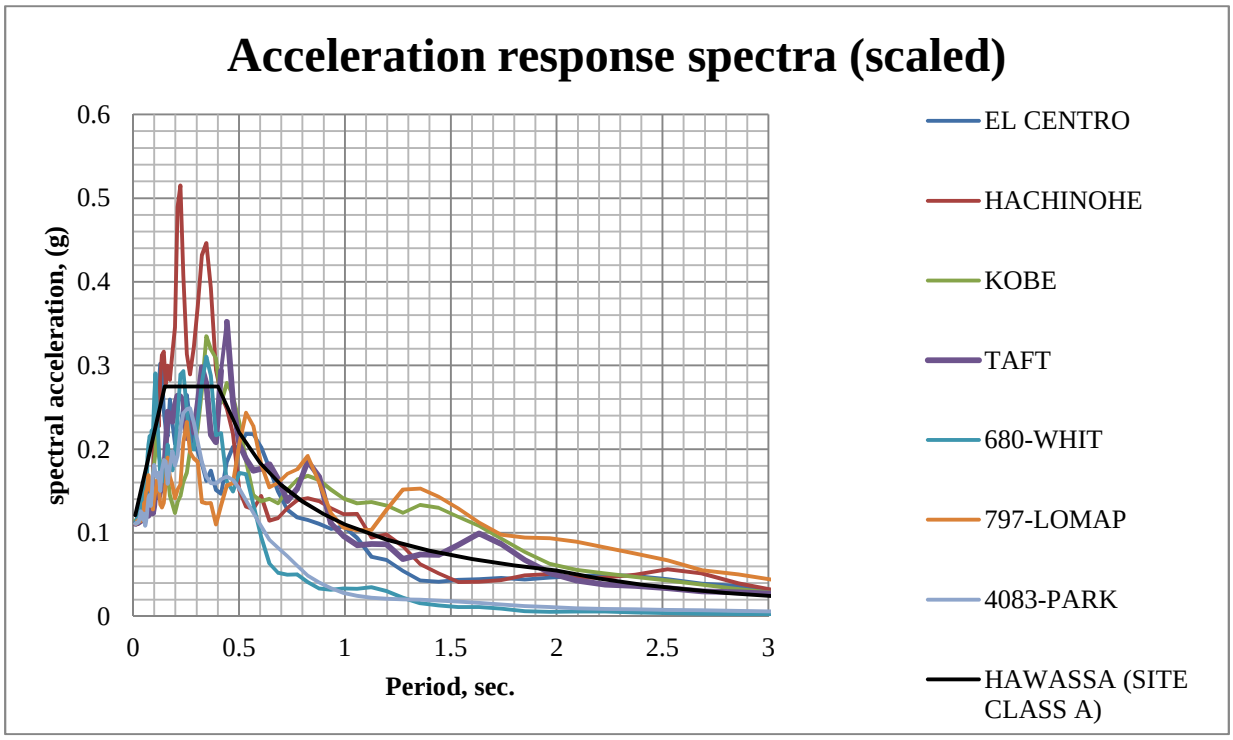

Figure 4.10.Spectral acceleration of seven selected motions and Hawassa acceleration spectra

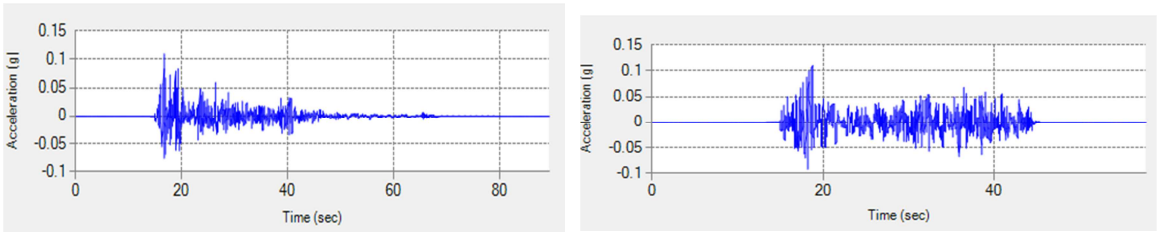

(a) (b)

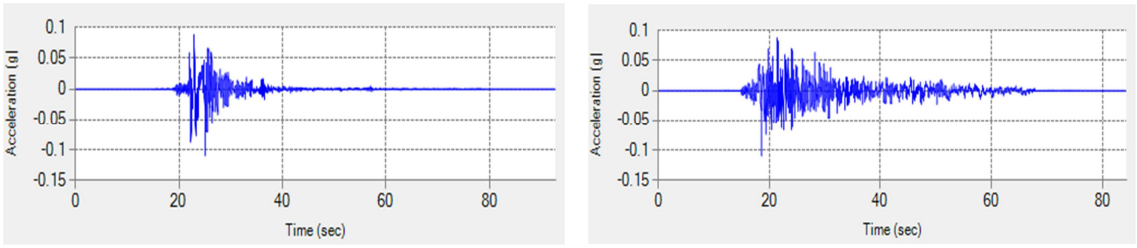

(c) (d)

Figure 4.11 Deconvolved and scaled acceleration time history of (a) Imperial Valley earthquake recorded at Elcentro station 1940. , (b) Tokachi-oki Earthquake, Hachinohe Record, 1968, (c) Hyogoken-nanbu Earthquake, Kobe university station 1995 (d) Kern County Earthquake, Taft Lincoln school Station, 1952 (Haile 1996)

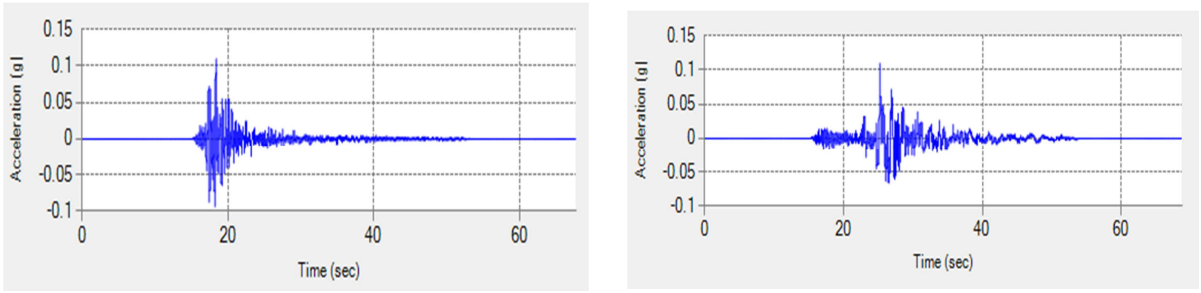

(a) (b)

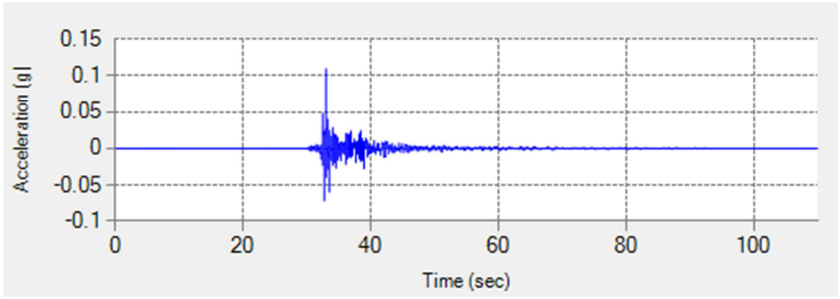

(c)

Figure 4.12 Scaled acceleration time histories of: (a) RSN 680- Whittier narrows-01 EQ recorded at St. Pasadena - CIT Kresge Lab (b) RSN 797 Loma prieta EQ recorded at St. SF - Rincon Hill (c) RSN 4083 Parkfield-02_ CA EQ recorded at ST. PARKFIELD (PEER, https://ngawest2.berkeley.edu/)

Using the selected input motions and processed sub-surface data in the previous sections, equivalent-linear analyses are performed.

4.3.2. Additional considerations for EQL analysis

EQL is employed to solve the 1D shear wave propagation equation (Kramer, 1996). The function which is used in EQL analysis to determine the amplification mainly depends on the soil column properties (i.e., impedance ratios -controlled by mass density and shear wave velocity- damping ratio and layer thicknesses) that determine the degree to which each frequency of input motion is amplified or deamplified by the soil column. Hence, discretization of layer and half space to be used during modeling for EQL shall be considered.

a) Layer Thickness for discretization

If the layer is too thick, the discretized domain may filter important components of the ground motion and thus may underestimate the ground response. If layer thickness is too small, the computational cost can be too high. The maximum discretization of layer thickness depends on the natural frequency/period of the site given by the equation

$$f_{\max,i} = \frac{V_{S_i}}{4H_i}; T_{\min} = \frac{1}{f_{\max}} \tag{4.2}$$

Where f_{max} is the highest frequency that the layer i can propagate, V_{si} is the shear wave velocity and H_i is the thickness of the layer. The common recommendations for the maximum frequency are between 25 – 50 Hz (Hashash et al. 2015). To increase the maximum frequency of a layer, thinner layer discretization is required.

b) Half space

Stewart et al. (2008) performs site response analyses to study combination of half space with different input motions. Hence, the input motion type with the recommended half space is described as follow:

(1) If a recorded rock outcrop motion is used as input, the motion should be used without any modifications. The base of the 1D soil column should be modeled as an elastic half-space.

(2) If a recorded within motion is used like for the simulation of vertical array recording data, the within motion should be used without modifications in conjunction with a rigid base

4.3.3 Equivalent linear analysis output

The analysis is conducted in two packages based on how the subsurface data source is acquired. The first batch of analysis is conducted with the geotechnical investigation subsurface data, and the second one is run with seismic survey subsurface data.

4.3.2.1 EQL analysis based on geotechnical investigation data

The outputs shown in Figure 4.13 are obtained by using the shear wave velocity, from Section 3.2, which is based on SPT records.

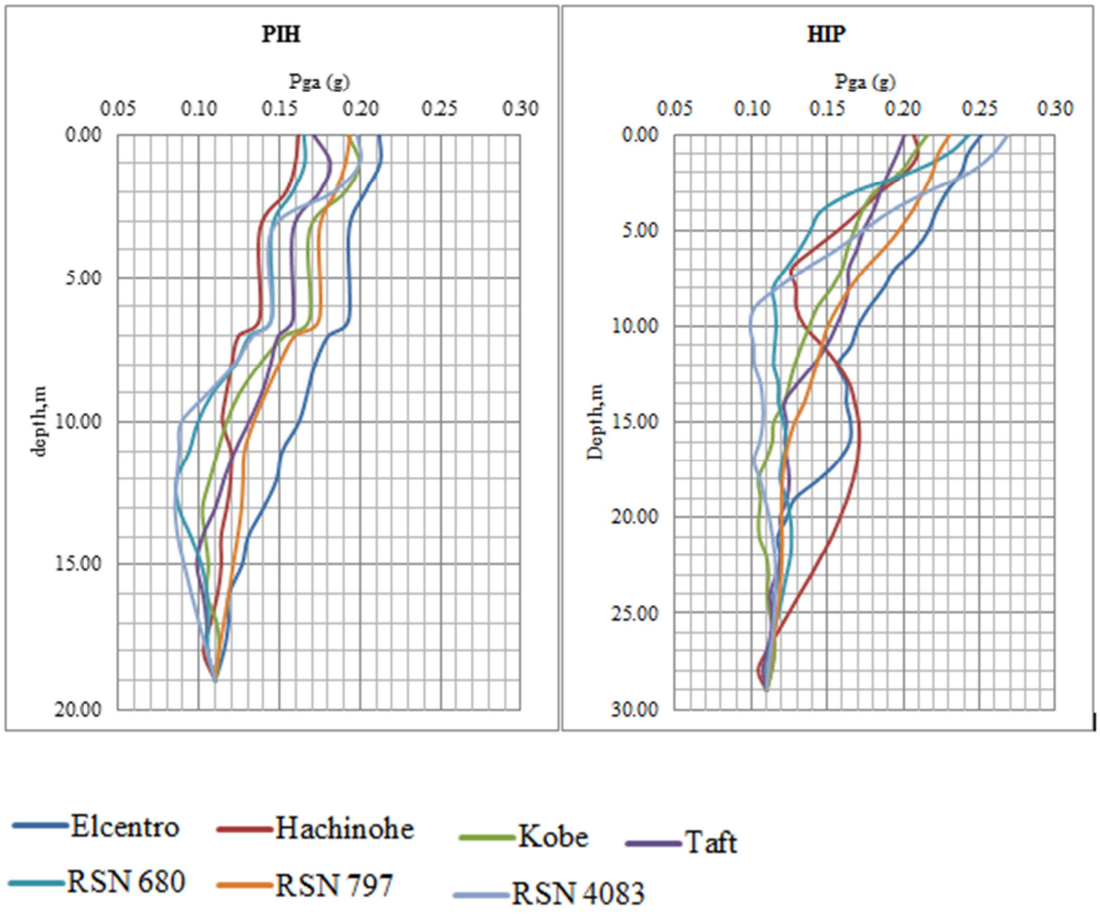

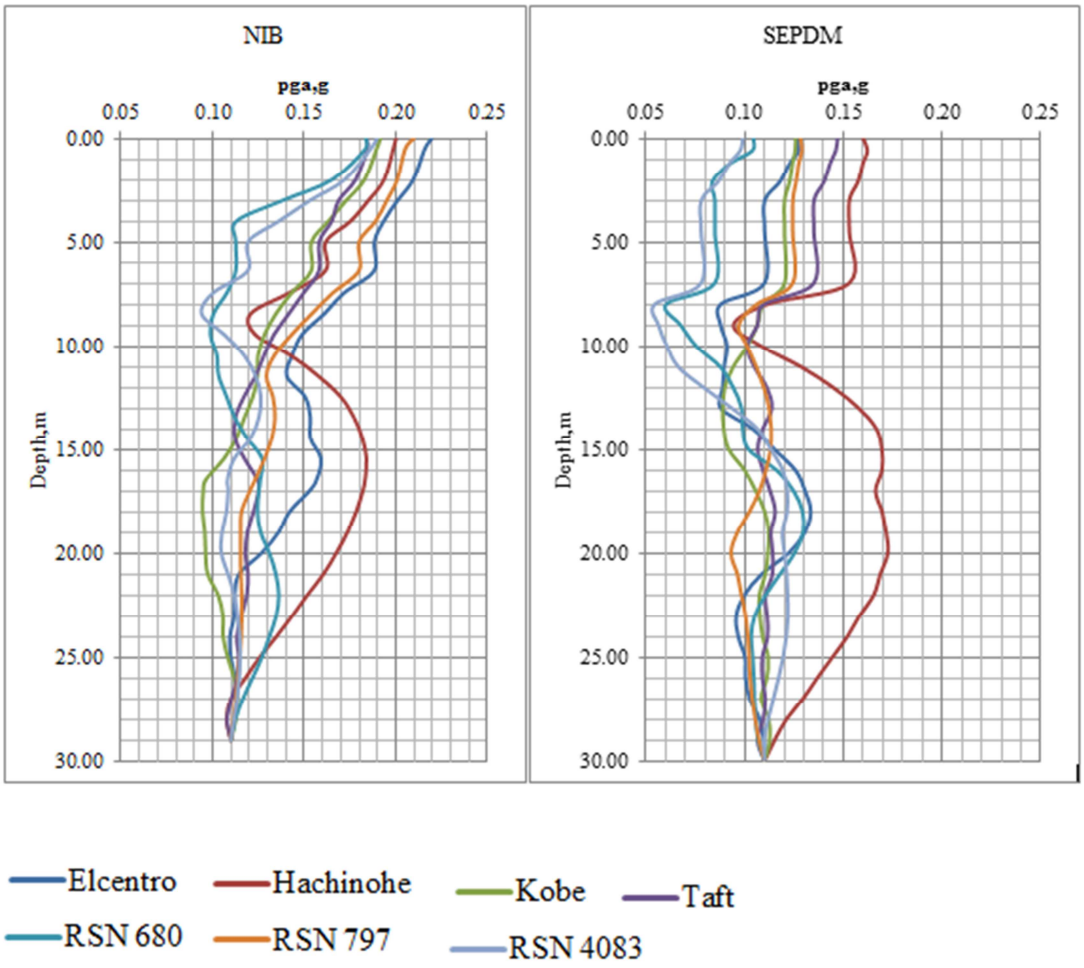

Figure 4.13 Peak ground acceleration profile at four sites for the seven input motions scaled to 0.11g at bedrock using shear wave velocities from geotechnical investigation reports

The peak ground accelerations at the surface have been picked from the profiles and summarized in Table 4.5.

Table 4.5 PGA summery at ground surface from EQL- analysis based on geotechnical investigation data

SITE	***Elcentro***	***Hachinohe***	***Kobe***	***Taft***	***680-whit.***	***797-Lomap***	***4083-park***	***Average***
	Max PGA (g)	Max PGA (g)	Max PGA (g)	Max PGA (g)	Max PGA (g)	Max PGA (g)	Max PGA (g)	Max Pga (g)
PIH	0.21	0.16	0.21	0.18	0.17	0.19	0.21	0.19
HIP	0.25	0.25	0.22	0.21	0.25	0.22	0.27	0.24
NIB	0.22	0.20	0.19	0.18	0.18	0.21	0.19	0.20
SEPDM	0.13	0.16	0.13	0.15	0.10	0.13	0.10	0.13

4.3.2.2 EQL analysis based on seismic survey data

The analyses in this case are performed by using directly measured shear wave velocities and extrapolated to 30m depth as presented in Section 3.3.2.5. The output is presented in Figure 4.14.

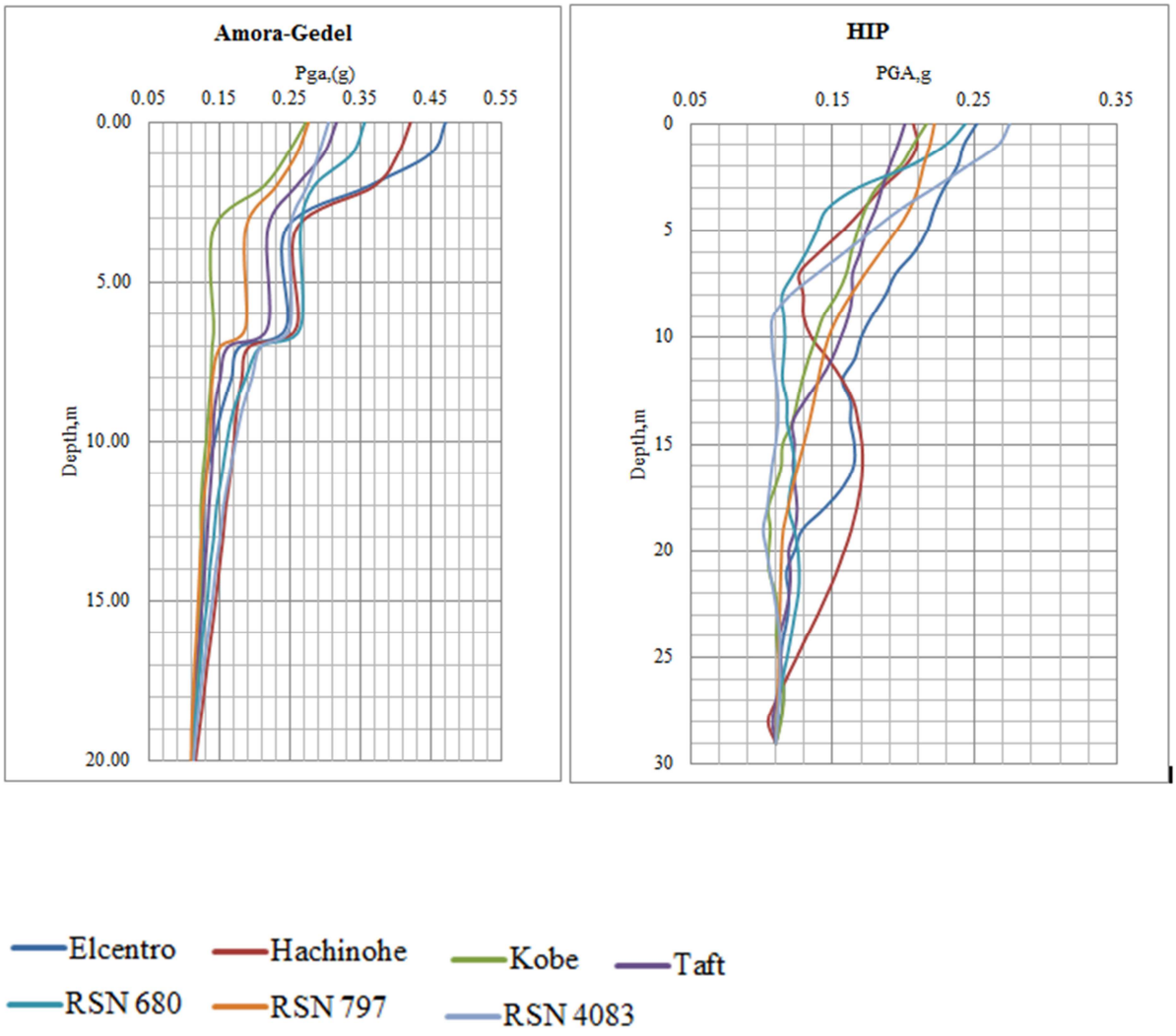

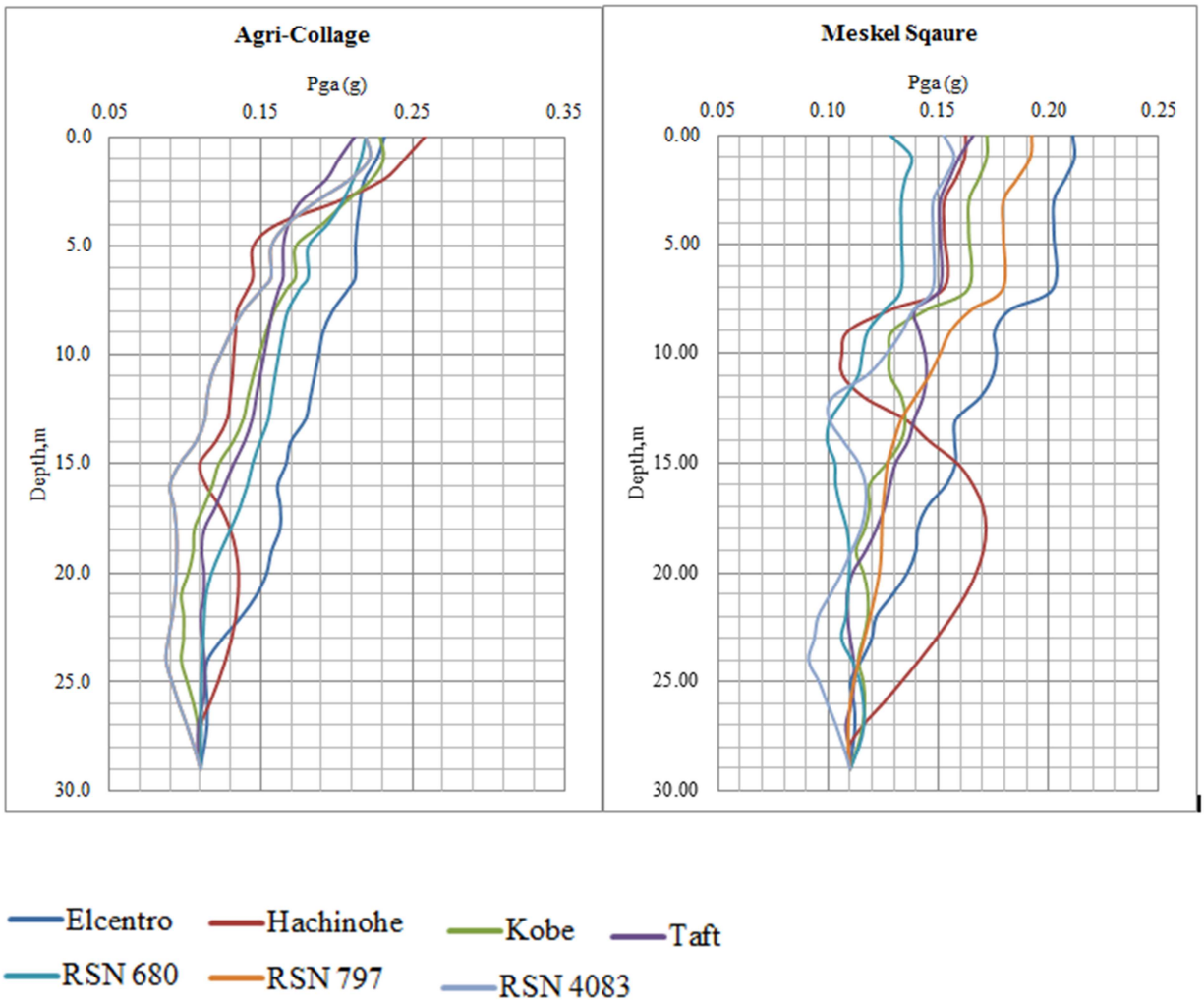

Figure 4.14 Peak ground acceleration profiles at the four sites for the selected seven motions scaled to 0.11g using directly measured shear wave velocities

The PGAs at the surface are presented in Table 4.6.

Table 4.6 PGA summery at ground surface from EQL- analysis based on measured data

	ELC. (0.11g)	***HACH. (0.11g)***	***Kob. (0.11g)***	***Taf. (0.11g)***	***RSN 680 (0.11g)***	***RSN 797 (0.11g)***	***RSN 4083 (0.11g)***	***Average***
	Max PGA, (g)	Max PGA, (g)	Max PGA, (g)	Max PGA, (g)	Max PGA, (g)	Max PGA, (g)	Max PGA, (g)	Max PGA, (g)
Amora- Gedel	0.47	0.42	0.27	0.32	0.36	0.28	0.31	0.35
HIP	0.25	0.21	0.22	0.20	0.24	0.22	0.27	0.23
Agri-college	0.23	0.26	0.23	0.21	0.21	0.22	0.22	0.23
Meskel square	0.21	0.16	0.17	0.17	0.13	0.19	0.15	0.17

As can be noticed from the above table, Elcentro and Hachinohe shows significant amplification at Amora-Gedel sites compared to others motions and sites. The difference

might arise from a resonance effect. The response spectral acceleration peaks of the excitations (Hachinohe and Elcentro motions as shown in Figure 4.10) found in a closer range of the period of Amora-Gedel site (which is 0.24s). This is not the case for other site and motions as observed during the EQL analyses by DEEPSOIL (See Figure 4.10).

The average peak ground acceleration as obtained from both approaches is summarized in Table 4.7 below. These values are used for the forthcoming liquefaction analysis.

Table 4.7 Summary of PGA from two data source

	PGA (g)		
	Geotechnical inv.	Seismic sur.	Average Pga
PIH/Amora-Gedel	0.19g	0.35g	0.27g
HIP	0.24g	0.23g	0.235g
NIB/AGRI. College	0.20g	0.23g	0.215g
SEPDM/ Meskel-Square	0.13g	0.17g	0.15g

As generally expected from the loose formation of the study area, the input motion PGA of 0.11g at the bedrock is significantly amplified at the ground surface.

4.4 Liquefaction Potential Evaluation

Four major in-situ test methods are commonly employed for liquefaction potential evaluation. They are

- ✓ The Standard Penetration Test (SPT)
- ✓ The cone penetration test (CPT)
- ✓ Measurement of in-situ shear wave velocity (VS)
- ✓ The Becker penetration test (BPT).

SPT based and shear wave velocity based methods are used for this study. As discussed in Chapter 3, the shear wave velocities are estimated by correlation from SPT as well as from direct measurement by geophysical survey. Therefore, these two sets of shear wave velocities are available for each site. It creates an opportunity to analyze the liquefaction potential of each site by different combinations of insitu subsurface data. Hence each site is analyzed by three subsurface data combination as described graphically in Figure 4.15.

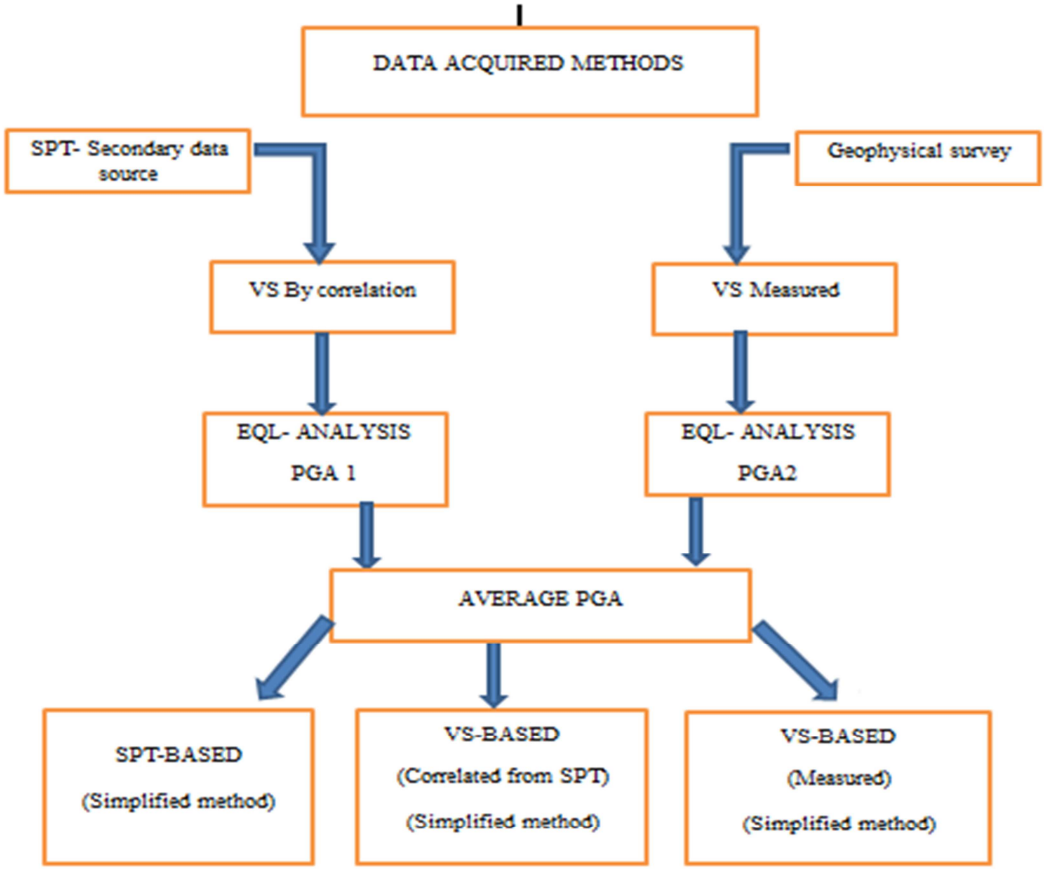

Figure 4.15 Simplified method computation approach used for this study

4.4.1 SPT based simplified Procedure

4.4.1.1 Cyclic Resistance Ratio (CRR)

As discussed in Chapter Two section 2.2.1.2 cyclic resistance ratio, CRR, shall be computed from corrected SPT using Equation 2.16. The corrected SPT $(N_1)_{60}$ presented in Chapter 3 of each site for standard procedures needs to be further corrected for overburden stress in order to be used for simplified procedure (Idriss et al. 2010).

Depth of liquefaction analyses for specific site shall be in accordance with Chapter 2 Section 2.1.3. However, considering reduced finished grade level, for most buildings, septic tank and other structures, depth of investigation up to 20m from ground surface is considered for this study. As described in Chapter 3, SPT values have been recorded up to a depth 15, 10, 20, 10m for PIH, HIP, NIB and SEPDM sites, respectively.

Another criterion which determines depth to be analyzed for susceptibility to liquefaction is its degree of saturation. Normally, the soil located above the water table may be regarded as unsaturated and hence the chances of liquefaction are low (Day 2002). Day (2002) suggests that it is better to consider that the liquefaction will occur only in soil which is located under water. For those locations where the depth of water table is very deep, the liquefaction

susceptibility is generally low. Moreover, if the level of the ground water table keeps on changing, the liquefaction susceptibility of the soil will also fluctuate. The ground water level used for the liquefaction analysis should be the historically shallowest (nearest to the ground surface) groundwater level. In the absence of such information the worst expected ground water level need to be considered. Hence as concluded in section 3.2.3.4 GWTs at 3.6m, 10m, 3m, and 3m for PIH, HIP, NIB and SEPDM are considered, respectively.

As stated above, the SPT based simplified method requires SPT records and below GWT. From this perspective HIP SPT records are above GWT level and SEPDM have few number of SPT records. Hence, SPT based simplified method shall be used for PIH and NIB sites only. HIP and SEPDM will be analyzed by shear wave velocity based simplified method in conjunction with PIH and NIB.

Applying the overburden correction factor given by Equation 2.11, the normalized SPT $(N_1)_{60,}$ is presented in Table 4.8. and Table 4.9.

Table 4.8 PIH site normalized SPT

PIH	***(a)***				*U.Wt, KN/m³*					
Layer	Layer Name	Thick. (m)	Depth, (m)	N60		U	σ	σ'v,	CN	$N_{1(60)}$
1	L. silty sand	1	1	10	18.33	0	18	18	1.7	17
2	L. silty sand	1	2	10	18.33	0	37	37	1.7	16.5
3	L. silty sand	1.3	3.3	10	18.33	0	60	60	1.3	12.9
6	Ignimbrite	3.1	6.4		24.23	27	136	108	1	
6	M. dense sand	0.6	7	13	19.54	33	147	114	0.9	12.2
7	M. dense sand	1	8	27	19.54	43	167	124	0.9	24.3
8	M. dense sand	1	9	27	19.54	53	186	133	0.9	23.4
9	M. dense sand	1	10	25	19.54	63	206	143	0.8	20.9
10	M. dense sand	1	11	25	19.54	73	225	153	0.8	20.2
11	M. dense sand	1	12	25	19.76	82	245	163	0.8	19.6
12	M. dense sand	1	13	25	19.76	92	265	173	0.8	19
13	M. dense sand	1	14	25	19.76	102	285	183	0.7	18.5
14	M. dense sand	1	15	25	19.76	112	305	193	0.7	18

Table 4.9 NIB site normalized SPT

NIB		***GWT @3.0m***			*U. wt. (kN/m³)*					
Layer #	Layer Name	Thick. (m)	Depth (m)	N60		U	σ	σ'v, KPa	CN	$N_{1(60)}$
1	silty sand (ash)	1.5	1	10	17	0	26	26	1.7	17.0
2	silty sand (ash)	1	2	16	17	0	43	43	1.5	24.5
3	silty sand (ash)	1	3	16	17	0	60	60	1.3	20.7
4	silty sand (ash)	1	4	16	17	10	77	67	1.2	19.6
5	silty sand (ash)	1	5	16	17	20	94	74	1.2	18.6
6	Ignimbrite	1.4	6.4		22.67	33	125	92	1.0	0.0
7	M. dense silty	0.6	7	22	17	39	135	96	1.0	22.4

	sand									
8	M. dense silty sand	1	8	22	17	49	152	103	1.0	21.6
9	M. dense silty sand	1	9	18	17	59	169	111	1.0	17.1
10	M. dense silty sand	1	10	18	17	69	186	118	0.9	16.6
11	M. dense silty sand	1	11	21	17	78	203	125	0.9	18.8
12	M. dense silty sand	1	12	21	17	88	220	132	0.9	18.3
13	M. dense silty sand	1	13	25	17	98	237	139	0.8	21.2
14	M. dense silty sand	1	14	25	17	108	254	147	0.8	20.7
15	M. dense silty sand	1	15	15	17	118	271	154	0.8	12.1
16	M. dense silty sand	1	16	15	17	128	288	161	0.8	11.8
17	M. dense silty sand	1	17	20	17	137	305	168	0.8	15.4
18	M. dense silty sand	1	18	20	17	147	322	175	0.8	15.1
19	M. dense silty sand	1	19	20	17	157	339	182	0.7	14.8
20	M. dense silty sand	1	20	20	17	167	356	190	0.7	14.5

Others Factors

The soil's CRR is also affected by the duration of shaking (which is correlated to the earthquake magnitude scaling factor, MSF) and effective overburden stress (which is expressed through an overburden correction factor, $K\sigma$) (Idriss at al. 2010).

- Magnitude scaling factor (MSF)

As discussed in chapter two MSF can be computed by Equation 2.14 for different magnitudes. MSF values used for this study is described in Table 4.10

Table 4.10 MSF computed by Equation 2.14 (after Idriss 1999 as cited by Idriss et al 2010)

M_W	MSF
5.5	1.69
6	1.48
6.5	1.30
6.8	1.20
7	1.14
7.2	1.08

- Overburden correction factor, $K_{\sigma.}$

Idriss and Boulanger (2008) recommended $K\sigma$ relationship expressed in terms of the $(N_1)_{60cs}$ values as follows:

$$K_\sigma = 1 - C_\sigma \left(\frac{\sigma'_v}{P_a}\right) \le 1.1$$
$$C_a = \frac{1}{18.9 - 2.55\sqrt{(N_1)_{60CS}}} \le 0.3 \quad (4.3)$$

- Fine content

When the soil is fine grained or contains some amount of fines, cohesion or adhesion tends to develop between fine particles, thereby making it difficult for them to be separated from each other. Consequently, a greater resistance to liquefaction is generally exhibited by sands containing some fines (Ishara 1996). Furthermore, several studies have shown that the liquefaction resistance of silty sand will initially decreases as the silt content increases until some minimum resistance is reached, and then increase as the silt content continues to increase (Ni et al. 2004). For silty sands and sandy silts, there is a large decrease in cyclic resistance that occurs when the silt content of the soil becomes greater than the limiting silt content. The largest amount of silt that can be accommodated in the voids created by the sand skeleton is referred to as the limiting silt content and occurs between 25 and 45% for most sands (Polito 2001 as cited by Ni et al. 2004). Nevertheless, Boulanger et al. (2006) recommended that fine grained soils (FC exceeding 50%) shall be analyzed by the existing procedure i.e. Simplified procedure as long as the PI not exceed 7. The soil in the study area is cohessionless soil as confirmed by laboratory results provided in Appendix A.

Table 4.11 Average fine content of PIH

PIH					
BH9		BH11		BH12	
Depth, m	FC,%	Depth, m	FC,%	Depth, m	FC,%
2.5	75	2.5	70	2.5	72
8	56	10.5	68	-	-
12.5	67	14.3	62	14	57
				Average	65

Table 4.12 Average fine content of HIP

HIP					
B34B		B34C		B33C	
Depth, m	FC,%	Depth, m	FC,%	Depth, m	FC,%
1	49.12	1	52.46	1	66.98
4	64.26	6	71.04	4	48.6
5.5	47.56	8.5	52.2	6	47.2
-	-	-	-	7	27.02
				Average	53

Table 4.13 Average fine content of NIB

NIB					
BH1		BH2		BH3	
Depth, m	FC,%	Depth, m	FC,%	Depth, m	FC,%
3	57	-	-	4	65
11	-	11	43	-	-
14	45	-	-	-	67
				Average	53

Table 4.14 Average fine content of SEPDM

SEPDM			
BH2		BH4	
Depth, m	FC,%	Depth, m	FC,%
2	58	2	76
3	75	4	71
5.5	78	-	
Average		72	

Hence, cyclic resistance ratio (CRR) can be calculated based on the corrected "N" values using the equation proposed by Idriss and Boulanger (2010) as given in Equation 2.16.

4.4.1.2 Cyclic stress ratio (CSR)

As discussed in Chapter 2 the earthquake-induced CSR, at a given depth, z, within the soil profile, is usually expressed as a representative value (or equivalent uniform value) equal to 65% of the maximum cyclic shear stress ratio. The uniform cyclic shear stress for level (or gently sloping) sites can be estimated from a simplified procedure as given by Seed and Idriss, Equation 2.1 through 2.4. The depth reduction factor of Idriss and Boulanger 2010 using Equation 2.5 is used for the study in the CSR computation.

The depth reduction factors computed to the depth of 20m for a number of earthquake magnitudes are presented in Table 4.15 and graphically in Figure 4.16.

Table 4.15 r_d depth reduction factor for different magnitude (Idriss and Boulanger 2010)

			Mw=5.5	***Mw=6.0***	***Mw=6.5***	***Mw=6.8***	***Mw=7.0***	***Mw=7.2***
Z,m	α(z)	β(z)	$rd_{M=5.5}$	$rd_{M=6.0}$	$rd_{M=6.5}$	$rd_{M=6.8}$	$rd_{M=7.0}$	$rd_{M=7.2}$
0.00	0.016	-0.001	1.000	1.000	1.000	1.000	1.000	1.000
1.00	-0.027	0.003	0.991	0.994	0.996	0.997	0.997	0.998
2.00	-0.077	0.009	0.969	0.978	0.982	0.985	0.987	0.988
3.00	-0.134	0.015	0.945	0.959	0.967	0.971	0.974	0.977
4.00	-0.197	0.022	0.919	0.940	0.950	0.957	0.961	0.965
5.00	-0.266	0.030	0.891	0.918	0.932	0.941	0.946	0.952
6.00	-0.341	0.038	0.862	0.896	0.913	0.924	0.931	0.938
7.00	-0.420	0.047	0.832	0.873	0.893	0.906	0.915	0.924
8.00	-0.504	0.057	0.802	0.848	0.873	0.888	0.898	0.908
9.00	-0.591	0.066	0.771	0.824	0.852	0.869	0.880	0.892
10.00	-0.682	0.076	0.741	0.799	0.830	0.850	0.863	0.876
11.00	-0.775	0.087	0.710	0.774	0.809	0.830	0.844	0.859
12.00	-0.869	0.097	0.681	0.750	0.787	0.810	0.826	0.842
13.00	-0.965	0.107	0.652	0.726	0.766	0.791	0.808	0.825
14.00	-1.061	0.118	0.624	0.702	0.744	0.771	0.789	0.808
15.00	-1.156	0.128	0.597	0.679	0.724	0.752	0.771	0.791
16.00	-1.251	0.138	0.572	0.656	0.703	0.733	0.754	0.775
17.00	-1.344	0.148	0.547	0.635	0.684	0.715	0.736	0.758
18.00	-1.434	0.158	0.525	0.614	0.665	0.697	0.719	0.742
19.00	-1.522	0.167	0.503	0.595	0.647	0.680	0.703	0.727
20.00	-1.605	0.176	0.483	0.576	0.629	0.663	0.687	0.712

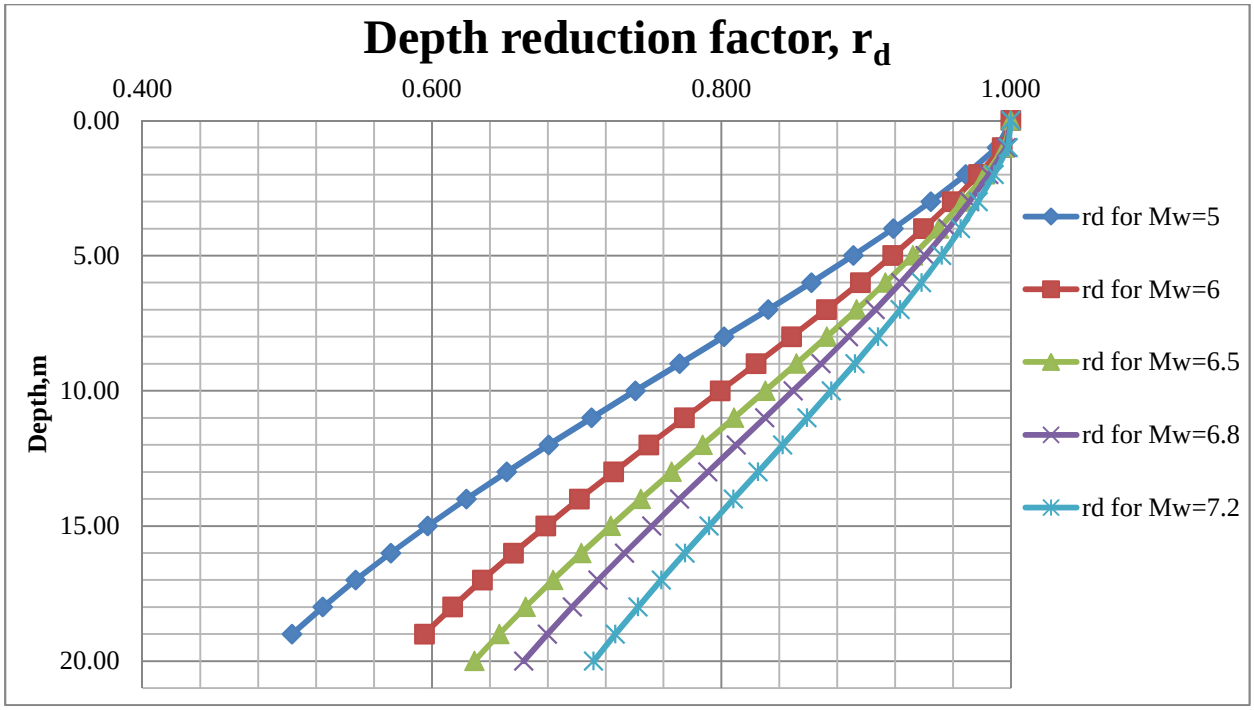

Figure 4.16 Depth reduction factor (Idriss and Boulanger 2010)

4.4.1.3 SPT based simplified procedure computation

After applying the necessary corrections to the SPT 'N' values an excel spread sheet is used to compute CRR. The CSR is computed by using average PGA presented in Table 4.6. The factor of safety for each layer of soil is then calculated as FS = CRR/CSR.

The analysis is conducted for moment magnitudes of 5.5, 6, 6.5, 6.8, 7 and 7.2 for each site. The factor of safety computations are presented in Appendix C. Representative liquefaction analyses from each site are presented in Tables 4.16 and Table 4.17.

Table.4.16 SPT based simplified method liquefaction potential evaluation of PIH site (Mw=7, a_{max} =0.27g)

Layer #	***Layer Name***	***Depth (m)***	σ_v	σ'_v	r_d	***CSR***	$(N_1)_{60cs}$	$CRR_{M=7,\sigma'v}$	***FS= CRR/CSR***
1	Loose silty sand	1.00	18	18	1.000	0.18	22	0.26	
2	Loose silty sand	2.00	37	37	0.987	0.17	22	0.25	
3	Loose silty sand	3.30	60	60	0.970	0.17	18	0.20	
4	Ignimbrite	6.40	136	108	0.925	0.20			
5	M. Dense silty sand	7.00	147	114	0.915	0.21	18	0.18	0.86
6	M. Dense silty sand	8.00	167	124	0.898	0.21	30	0.41	1.92
7	M. Dense silty sand	9.00	186	133	0.880	0.22	29	0.36	1.68
8	M. Dense silty sand	10.00	206	143	0.863	0.22	26	0.28	1.30
9	M. Dense silty sand	11.00	225	153	0.844	0.22	26	0.26	1.20
10	M. Dense silty sand	12.00	245	163	0.826	0.22	25	0.25	1.13
11	M. Dense silty sand	13.00	265	173	0.808	0.22	25	0.23	1.07
12	M. Dense silty sand	14.00	285	183	0.789	0.22	24	0.22	1.02
13	M. Dense silty sand	15.00	305	193	0.771	0.21	24	0.21	0.98

Table.4.17 SPT based simplified method liquefaction potential evaluation of NIB site (Mw=7, a_{max} =0.215g)

Layer #	*Layer Name*	*Depth (m)*	σ_v	σ'_v	r_d	*CSR*	$(N_1)_{60cs}$	$CRR_{M=7,\sigma'v}$	*FS= CRR/CSR*
1	silty sand (ash)	1.00	17	17	1.000	0.14	22	0.26	
2	silty sand (ash)	2.00	34	34	0.987	0.14	30	0.53	
3	silty sand (ash)	3.00	51	51	0.974	0.14	26	0.34	
4	silty sand (ash)	4.00	68	58	0.961	0.16	25	0.30	1.94
5	silty sand (ash)	5.00	85	65	0.946	0.17	24	0.28	1.62
6	Ignimbrite	6.40	117	83	0.925	0.18			
7	M. dense silty sand	7.00	127	88	0.915	0.19	28	0.37	1.99
8	M. dense silty sand	8.00	144	95	0.898	0.19	27	0.34	1.77
9	M. dense silty sand	9.00	161	102	0.880	0.19	23	0.24	1.22
10	M. dense silty sand	10.00	178	109	0.863	0.20	22	0.23	1.15
11	M. dense silty sand	11.00	195	116	0.844	0.20	24	0.26	1.30
12	M. dense silty sand	12.00	212	124	0.826	0.20	24	0.25	1.24
13	M. dense silty sand	13.00	229	131	0.808	0.20	27	0.30	1.51
14	M. dense silty sand	14.00	246	138	0.789	0.20	26	0.28	1.43
15	M. dense silty sand	15.00	263	145	0.771	0.20	18	0.17	0.87
16	M. dense silty sand	16.00	280	152	0.754	0.19	17	0.17	0.86
17	M. dense silty sand	17.00	297	160	0.736	0.19	21	0.19	1.02
18	M. dense silty sand	18.00	314	167	0.719	0.19	21	0.19	1.00
19	M. dense silty sand	19.00	331	174	0.703	0.19	20	0.18	0.98
20	M. dense silty sand	20.00	348	181	0.687	0.18	20	0.18	0.97

As can be seen from the results, liquefiable layers are observed at depths below 15m from the ground surface. By incorporating the results from Appendix C, detail discussion about the results are presented in the next chapter.

4.4.2 Shear-wave Velocity based Simplified Procedure

Shear wave velocity is a basic engineering property of soils in earthquake site response analysis, which directly relates to shear modulus at small shear strain level. Using surface wave velocity measuring techniques, a shear wave velocity profile can be established without boring and penetration. The non-destructive, non-intrusive features make V_S based approach a potentially attractive method for assessing the liquefaction resistance of soils.

Similar to correcting penetration resistance, V_S should be corrected to a reference overburden stress (Andrus et al. 2004) according to equation 2.17 and Equation 2.18.

It should be noted that the procedure is not yet as standardized as that of SPT or CPT and the case histories in the database of validation against field studies are relatively less. Three concerns arise when using V_S for liquefaction-resistance evaluations:

- ✓ Seismic wave velocity measurements are made at small strains, whereas pore-water pressure buildup and the onset of liquefaction are medium- to high-strain phenomena,
- ✓ Seismic testing does not provide samples for classification of soils and identification of non-liquefiable soft clay-rich soils, and

- ✓ Thin, low V_S strata may not be detected if the measurement interval is too large

Because of the limitations of this method, it is best to use the shear wave velocity as a supplement for the penetration based methods (Day 2002). In addition to these, seismic refraction method has its own limitation to map layers interbedded between two lower shear wave velocity layers. The preferred practice is to supplement the shear- wave velocity data by sufficient number of boreholes and conduct in situ tests to detect and delineate thin liquefiable or hard strata. Hence the ignimbrite layer spread in most parts of Hawassa has been integrated in the analysis by inserting the ignimbrite in the position as recorded in boreholes. The shear wave velocity of the layer is assigned from the relation given by Choi (2008) in section 3.2.3.3.

Cyclic resistance ratio, CRR

The CRR shall be computed by Andrus et al. (2004) (Equation 2.19) from V_{S1} as follows by incorporating the following factors;

- Magnitude scaling factor (MSF)

Different researchers suggested various MSF depending on magnitude. After the 1998 workshop Youd et al. (2001) reported that the workshop participants agreed that the greater conservatism embodied in the revised MSF by Idriss should be recommended for engineering practice.

$$MSF = \frac{10^{2.24}}{M_W{}^{2.56}} \tag{4.4}$$

- Limiting Upper Value of V_{S1}

The assumption of a limiting (or maximum) upper value of V_{S1} for liquefaction occurrence is equivalent to the assumption commonly made in the penetration-based procedures dealing with clean sands, where liquefaction is considered not possible above a corrected SPT blow count of about 30 (Andrus et al. 2004).

- Age Correction Factors

The factors K_{a1} and K_{a2} are included in the equation given by Andrus et al. 2004 Equation 2.19. Use of the lower-bound value of K_{a2} provides a lower estimate of CRR (Andrus et al 2004). Hence K_{a2} value of 1 shall be used from Table 2.2. K_{a1} is the ratio of estimated V_S to measure V_S (Andrus et al. 2004). The geomorphology study revealed that the study area is predominantly covered by Holocene sediment. Hence the value of Ka1 of 1.00 is adopted for this study.

V_S based method applied for two sets of subsurface data for each site. The first spread sheet of FS is prepared based on geotechnical investigation data and the second set is analyzed by seismically measured shear wave velocity subsurface data.

I) Estimations Based on geotechnical data

Unlike SPT shear-wave velocity data are extrapolated to the required depth of analysis. Hence liquefaction potential assessment made for all sites. Typical liquefaction analyses from each site are shown Table 4.18 to Table 4.21. FS commuted by excel spread sheet for each site with seven different input motions are presented in appendix C.

Table 4.18 Vs based simplified method liquefaction potential evaluation of PIH site (Mw=7, a_{max} =0.27g)

Layer #	*Layer Name*	*Depth,m*	*σv*	*σ'v*	r_d	*CSR*	*Vs1*	*Ka1*	*Ka2*	*VS1**	*MSF*	*CRR*	*FS*
1	Loose silty sand	1.0	18	18	1.000	0.18	210.9	1.0	1.0	200.0	1.19	NL	
2	Loose silty sand	2.0	37	37	0.987	0.17	177.3	1.0	1.0	200.0	1.19	NL	
3	Loose silty sand	3.3	60	60	0.970	0.17	156.5	1.0	1.0	200.0	1.19	NL	
4	Ignimbrite	6.4	136	108	0.925	0.20		1.0			1.19	NL	
5	M. dense silty sand	7.0	147	114	0.915	0.21	161.6	1.0	1.0	200.0	1.19	0.14	0.67
6	M. dense silty sand	8.0	167	124	0.898	0.21	188.7	1.0	1.0	200.0	1.19	0.37	1.75
7	M. dense silty sand	9.0	186	133	0.880	0.22	185.2	1.0	1.0	200.0	1.19	0.30	1.38
8	M. dense silty sand	10.0	206	143	0.863	0.22	187.4	1.0	1.0	200.0	1.19	0.34	1.56
9	M. dense silty sand	11.0	225	153	0.844	0.22	184.4	1.0	1.0	200.0	1.19	0.29	1.31
10	M. dense silty sand	12.0	245	163	0.826	0.22	193.0	1.0	1.0	200.0	1.19	0.56	2.55
11	M. dense silty sand	13.0	265	173	0.808	0.22	190.1	1.0	1.0	200.0	1.19	0.42	1.92
12	M. dense silty sand	14.0	285	183	0.789	0.22	187.5	1.0	1.0	200.0	1.19	0.34	1.59
13	M. dense silty sand	15.0	305	193	0.771	0.21	185.0	1.0	1.0	200.0	1.19	0.30	1.38

NL used to designate “Non liquefiable”. The layer remarked by NL is due to two cases i.e. either the layer is found above the GWT or the layer shear wave velocity exceeds the threshold shear-wave velocity given by Equation 2.23

Table 4.19 Vs based simplified method liquefaction potential evaluation of HIP site (Mw=7, a_{max} =0.235g)

Layer #	*Layer Name*	*Depth,m*	*σv*	*σ'v*	*rd*	*CSR*	*Vs1*	*Ka1*	*Ka2*	*VS1**	*MSF*	*CRR*	*FS= CRR/CSR*
1	Silty Sand	1	13	13	0.997	0.15	188.9	1.00	1.00	200	1.19	NL	
2	Silty Sand	2	26	26	0.987	0.15	180.0	1.00	1.00	200	1.19	NL	
3	Silty Sand	3	41	41	0.974	0.15	181.6	1.00	1.00	200	1.19	NL	
4	Silty Sand	4	55	55	0.961	0.15	214.9	1.00	1.00	200	1.19	NL	
5	Silty Sand	5	69	69	0.946	0.14	202.8	1.00	1.00	200	1.19	NL	
6	Silty Sand	6	84	84	0.931	0.14	193.5	1.00	1.00	200	1.19	NL	
7	Silty Sand	7	98	98	0.915	0.14	197.1	1.00	1.00	200	1.19	NL	
8	Silty Sand	8	112	112	0.898	0.14	202.6	1.00	1.00	200	1.19	NL	
9	Silty Sand	9	126	126	0.880	0.13	208.4	1.00	1.00	200	1.19	NL	
10	Silty Sand	10	141	141	0.863	0.13	202.9	1.00	1.00	200	1.19	NL	
11	Silty Sand	11	155	145	0.844	0.14	198.1	1.00	1.00	200	1.19	1.80	13.07
12	Silty Sand	12	169	150	0.826	0.14	193.1	1.00	1.00	200	1.19	0.57	3.98
13	Silty Sand	13	184	154	0.808	0.15	191.3	1.00	1.00	200	1.19	0.46	3.16
14	Silty Sand	14	198	159	0.789	0.15	213.4	1.00	1.00	200	1.19	NL	
15	Silty Sand	15	212	163	0.771	0.15	190.3	1.00	1.00	200	1.19	0.42	2.75
16	Silty Sand	16	226	168	0.754	0.16	203.7	1.00	1.00	200	1.19	NL	
17	Silty Sand	17	241	172	0.736	0.16	200.9	1.00	1.00	200	1.19	NL	
18	Silty Sand	18	255	177	0.719	0.16	206.6	1.00	1.00	200	1.19	NL	
19	Silty Sand	19	269	181	0.703	0.16	214.1	1.00	1.00	200	1.19	NL	
20	Silty Sand	20	284	185	0.687	0.16	216.3	1.00	1.00	200	1.19	NL	

Table 4.20 Vs based simplified method liquefaction potential evaluation of NIB site (Mw=7, a_{max} =0.215g)

Layer #	Layer Name	Depth,m	σv	σ'v	r_d	CSR	Vs1	Ka1	Ka2	VS1*	MSF	CRR	FS
1	silty sand (ash)	1.00	17	17	1.000	0.14	227	1.00	1.00	200	1.19	NL	
2	silty sand (ash)	2.00	34	34	0.987	0.14	191	1.00	1.00	200	1.19	NL	
3	silty sand (ash)	3.00	51	51	0.974	0.14	173	1.00	1.00	200	1.19	NL	
4	silty sand (ash)	4.00	68	58	0.961	0.16	185	1.00	1.00	200	1.19	0.30	1.93
5	silty sand (ash)	5.00	85	65	0.946	0.17	180	1.00	1.00	200	1.19	0.24	1.38
6	Ignimbrite	6.40	92	58	0.925	0.20	2470				1.19	NL	
7	M.dense silty sand	7.00	116	72	0.915	0.21	201	1.00	1.00	200	1.19	NL	
8	M.dense silty sand	8.00	133	79	0.898	0.21	201	1.00	1.00	200	1.19	NL	
9	M.dense silty sand	9.00	150	86	0.880	0.21	199	1.00	1.00	200	1.19	4.20	
10	M.dense silty sand	10.00	167	94	0.863	0.21	195	1.00	1.00	200	1.19	0.79	3.66
11	M.dense silty sand	11.00	184	101	0.844	0.22	204	1.00	1.00	200	1.19	NL	
12	M.dense silty sand	12.00	201	108	0.826	0.21	200	1.00	1.00	200	1.19	NL	
13	M.dense silty sand	13.00	218	115	0.808	0.21	209	1.00	1.00	200	1.19	NL	
14	M.dense silty sand	14.00	235	122	0.789	0.21	205	1.00	1.00	200	1.19	NL	
15	M.dense silty sand	15.00	252	129	0.771	0.21	190	1.00	1.00	200	1.19	0.42	2.02
16	M.dense silty sand	16.00	269	137	0.754	0.21	188	1.00	1.00	200	1.19	0.35	1.68
17	M.dense silty sand	17.00	278	141	0.736	0.20	205	1.00	1.00	200	1.19	NL	
18	M.dense silty sand	18.00	295	148	0.719	0.20	208	1.00	1.00	200	1.19	NL	
19	M.dense silty sand	19.00	312	155	0.703	0.20	215	1.00	1.00	200	1.19	NL	
20	M.dense silty sand	20.00	329	162	0.687	0.19	216	1.00	1.00	200	1.19	NL	

Table 4.21 Vs based simplified method liquefaction potential evaluation of SEPDM site (Mw=7, a_{max} =0.15g)

Layer #	***Layer Name***	***Depth,m***	***σv***	***σ'v***	***r_d***	***CSR***	***Vs1***	***Ka1***	***Ka2***	***VS1****	***MSF***	***CRR***	***FS***
1	Organic Clayey Silt	0.6	9	9	1.001	0.10	162	1.00	1.00	200	1.19	NL	
2	Organic Clayey Silt	1.2	18	18	0.995	0.10	146	1.00	1.00	200	1.19	NL	
3	Stiff Clayey silt	2.1	34	34	0.985	0.10	174	1.00	1.00	200	1.19	NL	
4	Stiff Clayey silt	3	50	50	0.974	0.09	158	1.00	1.00	200	1.19	0.13	1.35
5	Slightly Weat. Tuff	4.5	84	70	0.954	0.11	2470	1.00	1.00	200	1.19	NL	
6	Fresh Welded Tuff	7	146	107	0.915	0.12	3172	1.00	1.00	200	1.19	NL	
7	Soft silty sand	8	160	111	0.898	0.13	177	1.00	1.00	200	1.19	0.21	1.69
8	Soft silty sand	9	174	115	0.880	0.13	176	1.00	1.00	200	1.19	0.20	1.56
9	Soft silty sand	10	188	119	0.863	0.13	174	1.00	1.00	200	1.19	0.19	1.45
10	Soft silty sand	11	202	123	0.844	0.13	173	1.00	1.00	200	1.19	0.19	1.38
11	Soft silty sand	12	216	128	0.826	0.14	167	1.00	1.00	200	1.19	0.16	1.16
12	Soft silty sand	13	230	132	0.808	0.14	163	1.00	1.00	200	1.19	0.14	1.05
13	Soft silty sand	14	244	136	0.789	0.14	182	1.00	1.00	200	1.19	0.26	1.86
14	Soft silty sand	15	258	140	0.771	0.14	162	1.00	1.00	200	1.19	0.14	1.02
15	Soft silty sand	16	272	144	0.754	0.14	173	1.00	1.00	200	1.19	0.19	1.36
16	Soft silty sand	17	286	148	0.736	0.14	169	1.00	1.00	200	1.19	0.17	1.21
17	Soft silty sand	18	300	153	0.719	0.14	174	1.00	1.00	200	1.19	0.19	1.38
18	Soft silty sand	19	314	157	0.703	0.14	181	1.00	1.00	200	1.19	0.25	1.79
19	Soft silty sand	20	328	161	0.687	0.14	183	1.00	1.00	200	1.19	0.27	1.97

II) Based on geophysical data

The detailed liquefaction evaluation based on this analysis is presented in Appendix C. Amora-Gedel, HIP and Meskel square measured shear wave velocity exceeds the upper bound set by Andrus and Stoke 2004. As computed from FC of each site, the seismically measured and normalized shear wave velocity (V_{S1}) exceed the upper limit value of Andrus et al. (2004) at Amora-Gedel, HIP and Meskel Square sites. Hence VS based simplified approach based on the measured subsurface data reveals that they are safe against liquefaction. Typical outputs are presented from Table 4.22 to 4.25 for all sites.

Table.4.22 seismically measured Vs based simplified method liquefaction potential evaluation of Amora-Gedel site (Mw=7, a_{max} =0.27g)

Layer #	***Layer Name***	***Depth,m***	***σv***	***σ'v***	***rd***	***CSR***	***Vs1***	***Ka1***	***Ka2***	***VS1****	***MSF***	***CRR***	***FS***
1	Loose silty sand	1.0	18	18	1.000	0.18	212.9	1.0	1.0	200.0	1.19	NL	-
2	Loose silty sand	2.0	37	37	0.987	0.17	179.0	1.0	1.0	200.0	1.19	NL	-
3	Loose silty sand	3.3	60	60	0.970	0.17	157.6	1.0	1.0	200.0	1.19	NL	-
4	Ignimbrite	6.4	136	108	0.925	0.20		1.0			1.19	NL	-
5	M. dense silty sand	7.0	147	114	0.915	0.21	311.6	1.0	1.0	200.0	1.19	NL	-
6	M. dense silty sand	8.0	167	124	0.898	0.21	376.4	1.0	1.0	200.0	1.19	NL	-
7	M. dense silty sand	9.0	186	133	0.880	0.22	369.4	1.0	1.0	200.0	1.19	NL	-
8	M. dense silty sand	10.0	206	143	0.863	0.22	362.9	1.0	1.0	200.0	1.19	NL	-
9	M. dense silty sand	11.0	225	153	0.844	0.22	447.9	1.0	1.0	200.0	1.19	NL	-
10	M. dense silty sand	12.0	245	163	0.826	0.22	440.8	1.0	1.0	200.0	1.19	NL	-
11	M. dense silty sand	13.0	265	173	0.808	0.22	455.3	1.0	1.0	200.0	1.19	NL	-
12	M. dense silty sand	14.0	285	183	0.789	0.22	449.0	1.0	1.0	200.0	1.19	NL	-
13	M. dense silty sand	15.0	305	193	0.771	0.21	443.1	1.0	1.0	200.0	1.19	NL	-

Table.4.23 Measured Vs based simplified method liquefaction potential evaluation of HIP site (Mw=7, a_{max} = 0.235g)

Layer #	***Layer Name***	***Depth, m***	***σv***	***σ'v***	***rd***	***CSR***	***Vs1***	***Ka1***	***Ka2***	***VS1****	***MSF***	***CRR***	***FS***
1	Silty Sand	1	13	13	0.997	0.15	201.5	1.00	1.00	200	1.19	NL	-
2	Silty Sand	2	26	26	0.987	0.15	183.0	1.00	1.00	200	1.19	NL	-
3	Silty Sand	3	41	41	0.974	0.15	191.9	1.00	1.00	200	1.19	NL	-
4	Silty Sand	4	55	55	0.961	0.15	190.3	1.00	1.00	200	1.19	NL	-
5	Silty Sand	5	69	69	0.946	0.14	191.7	1.00	1.00	200	1.19	NL	-
6	Silty Sand	6	84	84	0.931	0.14	194.5	1.00	1.00	200	1.19	NL	-
7	Silty Sand	7	98	98	0.915	0.14	198.1	1.00	1.00	200	1.19	NL	-
8	Silty Sand	8	112	112	0.898	0.14	201.7	1.00	1.00	200	1.19	NL	-
9	Silty Sand	9	126	126	0.880	0.13	206.1	1.00	1.00	200	1.19	NL	-
10	Silty Sand	10	141	141	0.863	0.13	210.8	1.00	1.00	200	1.19	NL	-
11	Silty Sand	11	155	145	0.844	0.14	218.8	1.00	1.00	200	1.19	NL	-
12	Silty Sand	12	169	150	0.826	0.14	217.2	1.00	1.00	200	1.19	NL	-
13	Silty Sand	13	184	154	0.808	0.15	225.5	1.00	1.00	200	1.19	NL	-
14	Silty Sand	14	198	159	0.789	0.15	233.7	1.00	1.00	200	1.19	NL	-
15	Silty Sand	15	212	163	0.771	0.15	241.9	1.00	1.00	200	1.19	NL	-
16	Silty Sand	16	226	168	0.754	0.16	249.5	1.00	1.00	200	1.19	NL	-
17	Silty Sand	17	241	172	0.736	0.16	257.5	1.00	1.00	200	1.19	NL	-
18	Silty Sand	18	255	177	0.719	0.16	274.2	1.00	1.00	200	1.19	NL	-
19	Silty Sand	19	269	181	0.703	0.16	230.1	1.00	1.00	200	1.19	NL	-
20	Silty Sand	20	284	185	0.687	0.16	232.3	1.00	1.00	200	1.19	NL	-

Table.4.24 Measured Vs based simplified method liquefaction potential evaluation of Agricultural College site (Mw=7, a_{max} =0.215g)

Layer #	*Layer Name*	*Depth,m*	*σv*	*σ'v*	*rd*	*CSR*	*Vs1*	*Ka1*	*Ka2*	*VS1**	*MSF*	*CRR*	*FS*
1	silty sand (ash)	1.00	17	17	1.000	0.14	227	1.00	1.00	200	1.19	NL	-
2	silty sand (ash)	2.00	34	34	0.987	0.14	191	1.00	1.00	200	1.19	NL	-
3	silty sand (ash)	3.00	51	51	0.974	0.14	173	1.00	1.00	200	1.19	NL	-
4	silty sand (ash)	4.00	68	58	0.961	0.16	185	1.00	1.00	200	1.19	0.30	1.93
5	silty sand (ash)	5.00	85	65	0.946	0.17	180	1.00	1.00	200	1.19	0.24	1.38
6	Ignimbrite	6.40	92	58	0.925	0.20	2470				1.19	NL	-
7	M. dense silty sand	7.00	116	72	0.915	0.21	201	1.00	1.00	200	1.19	NL	-
8	M. dense silty sand	8.00	133	79	0.898	0.21	201	1.00	1.00	200	1.19	NL	-
9	M. dense silty sand	9.00	150	86	0.880	0.21	199	1.00	1.00	200	1.19	4.20	-
10	M. dense silty sand	10.00	167	94	0.863	0.21	195	1.00	1.00	200	1.19	0.79	3.66
11	M. dense silty sand	11.00	184	101	0.844	0.22	204	1.00	1.00	200	1.19	NL	-
12	M. dense silty sand	12.00	201	108	0.826	0.21	200	1.00	1.00	200	1.19	NL	-
13	M. dense silty sand	13.00	218	115	0.808	0.21	209	1.00	1.00	200	1.19	NL	-
14	M. dense silty sand	14.00	235	122	0.789	0.21	205	1.00	1.00	200	1.19	NL	-
15	M. dense silty sand	15.00	252	129	0.771	0.21	190	1.00	1.00	200	1.19	0.42	2.02
16	M. dense silty sand	16.00	269	137	0.754	0.21	188	1.00	1.00	200	1.19	0.35	1.68
17	M. dense silty sand	17.00	278	141	0.736	0.20	205	1.00	1.00	200	1.19	NL	-
18	M. dense silty sand	18.00	295	148	0.719	0.20	208	1.00	1.00	200	1.19	NL	-
19	M. dense silty sand	19.00	312	155	0.703	0.20	215	1.00	1.00	200	1.19	NL	-
20	M. dense silty sand	20.00	329	162	0.687	0.19	216	1.00	1.00	200	1.19	NL	-

Table.4.25 Measured shear-wave velocity based simplified method liquefaction potential evaluation of Meskel Square site (Mw=7, a_{max} = 0.17g)

Layer #	*Layer Name*	*Depth,m*	*σv*	*σ'v*	*rd*	*CSR*	*Vs1*	*Ka1*	*Ka2*	*VS1**	*MSF*	*CRR*	*FS*
1	Organic Clayey Silt	0.6	9	9	1.001	0.10	270	1.00	1.00	200	1.19	NL	-
2	Organic Clayey Silt	1.2	18	18	0.995	0.10	244	1.00	1.00	200	1.19	NL	-
3	Stiff Clayey silt	2.1	34	34	0.985	0.10	217	1.00	1.00	200	1.19	NL	-
4	Stiff Clayey silt	3	50	50	0.974	0.09	212	1.00	1.00	200	1.19	NL	-
5	Slightly Weath. Tuff	4.5	84	70	0.954	0.11	2470	1.00	1.00	200	1.19	NL	-
6	Fresh Welded Tuff	7	146	107	0.915	0.12	3172	1.00	1.00	200	1.19	NL	-
7	Soft silty sand	8	160	111	0.898	0.13	225	1.00	1.00	200	1.19	NL	-
8	Soft silty sand	9	174	115	0.880	0.13	241	1.00	1.00	200	1.19	NL	-
9	Soft silty sand	10	188	119	0.863	0.13	252	1.00	1.00	200	1.19	NL	-
10	Soft silty sand	11	202	123	0.844	0.13	262	1.00	1.00	200	1.19	NL	-
11	Soft silty sand	12	216	128	0.826	0.14	239	1.00	1.00	200	1.19	NL	-
12	Soft silty sand	13	230	132	0.808	0.14	239	1.00	1.00	200	1.19	NL	-
13	Soft silty sand	14	244	136	0.789	0.14	267	1.00	1.00	200	1.19	NL	-
14	Soft silty sand	15	258	140	0.771	0.14	237	1.00	1.00	200	1.19	NL	-
15	Soft silty sand	16	272	144	0.754	0.14	255	1.00	1.00	200	1.19	NL	-
16	Soft silty sand	17	286	148	0.736	0.14	253	1.00	1.00	200	1.19	NL	-
17	Soft silty sand	18	300	153	0.719	0.14	260	1.00	1.00	200	1.19	NL	-
18	Soft silty sand	19	314	157	0.703	0.14	268	1.00	1.00	200	1.19	NL	-
19	Soft silty sand	20	328	161	0.687	0.14	271	1.00	1.00	200	1.19	NL	-

Results are discussed in next chapter.

CHAPTER FIVE

RESULTS AND INTERPRETATIONS

A total of four sites are analyzed in this study. Seven selected bedrock motions have been used for EQL site response analyses to determine peak ground accelerations, which are used to compute CSR. Hence a total of 28 analyses were performed to determine earthquake loading interims of CSR for liquefaction analysis. In the simplified procedure of liquefaction potential assessment, the two common in-situ tests i.e. SPT and Shear- wave velocity methods are employed.

The results of the analyses for different moment magnitudes are presented in Figure 5.1 and Figure 5.2. As presented in the figures the results are compared with the minimum requirement of ES-EN 1998:2015 part 5 and BSSC 2000.

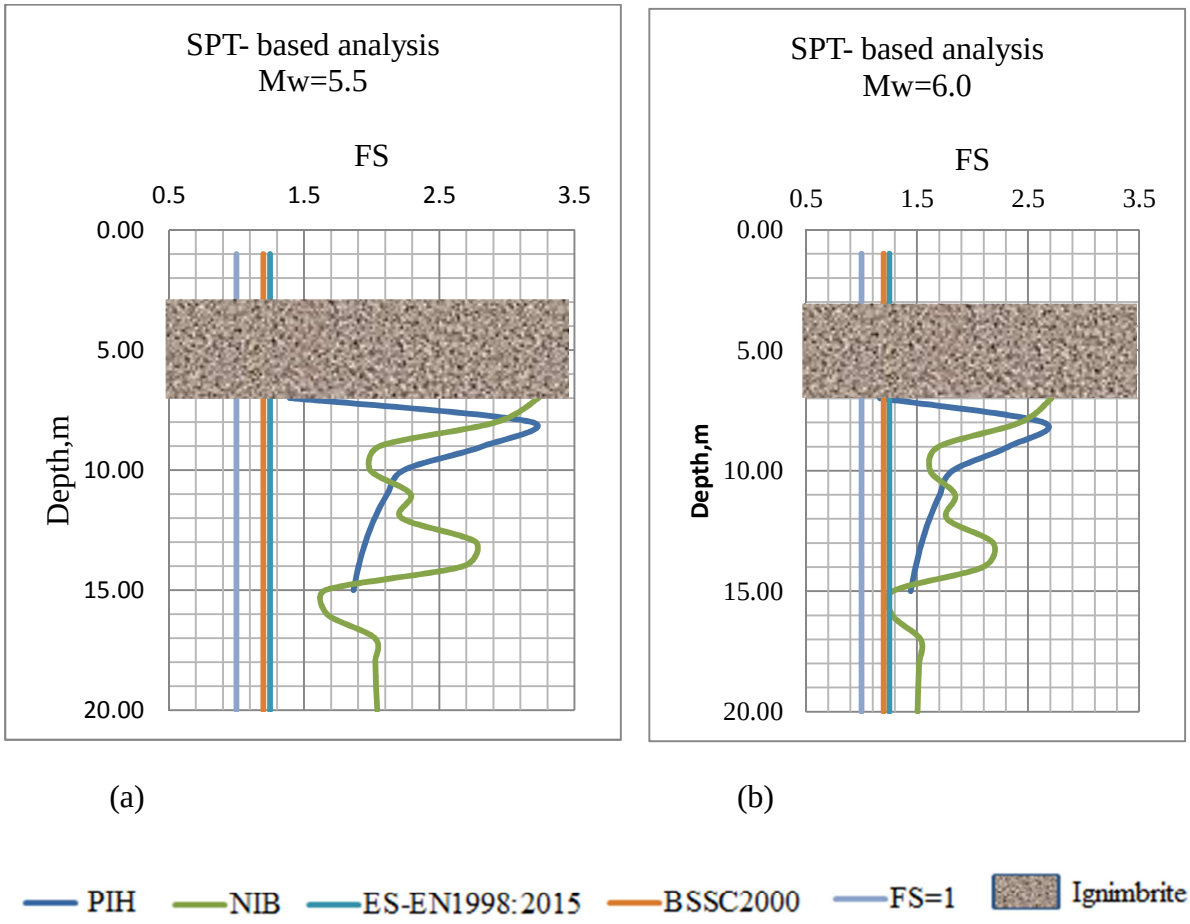

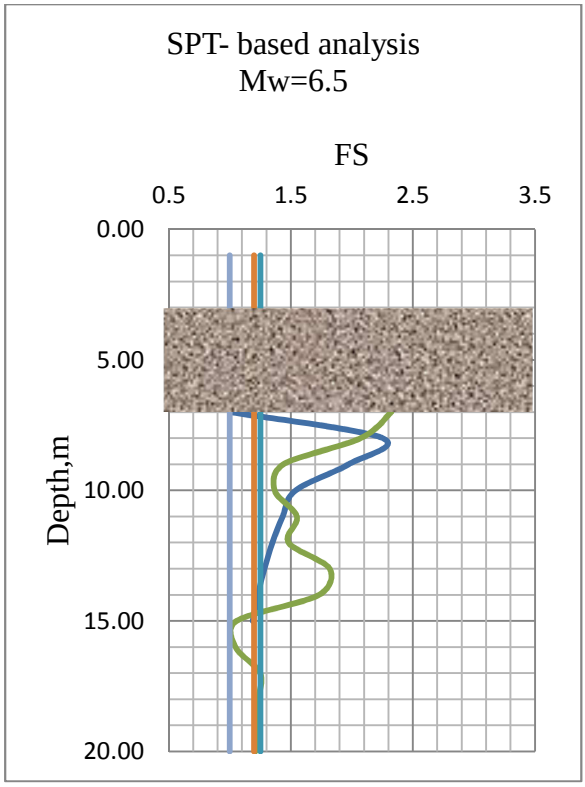

(c)

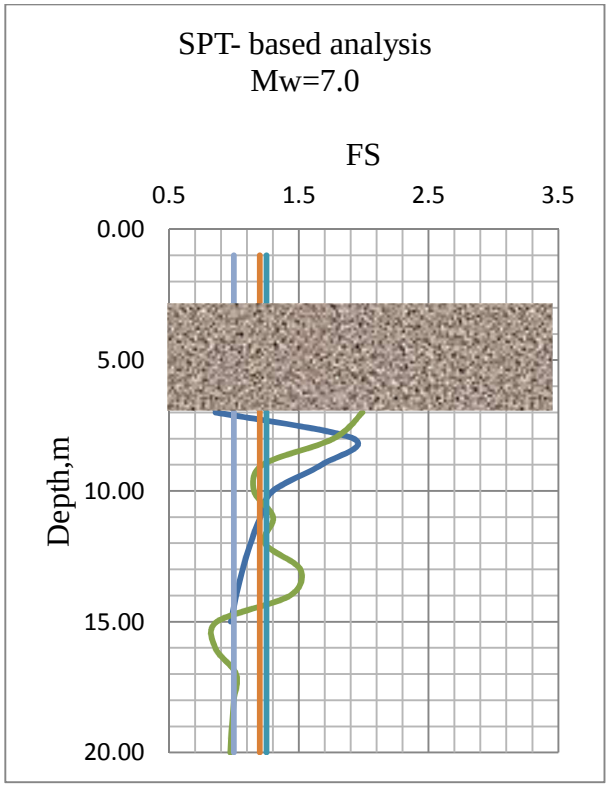

(d)

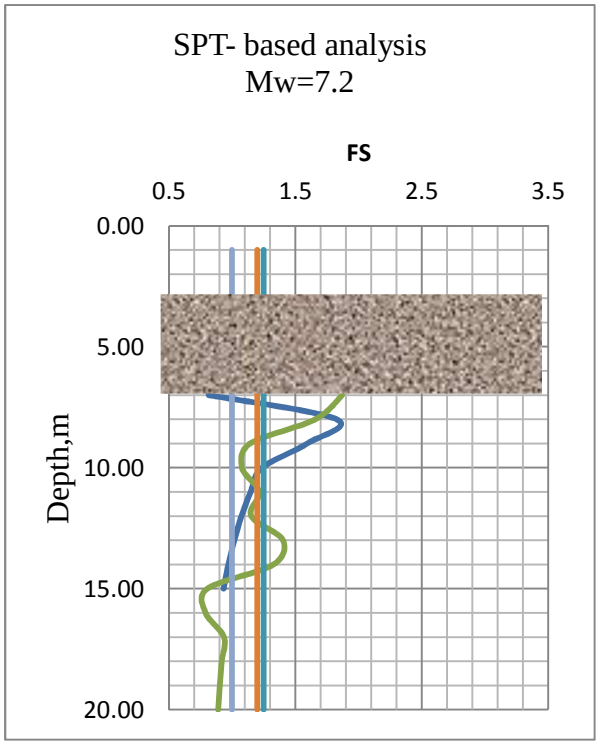

(e)

Figure 5.1 SPT based simplefied proceedure analyses result for different magnitudes for PIH and NIB sites

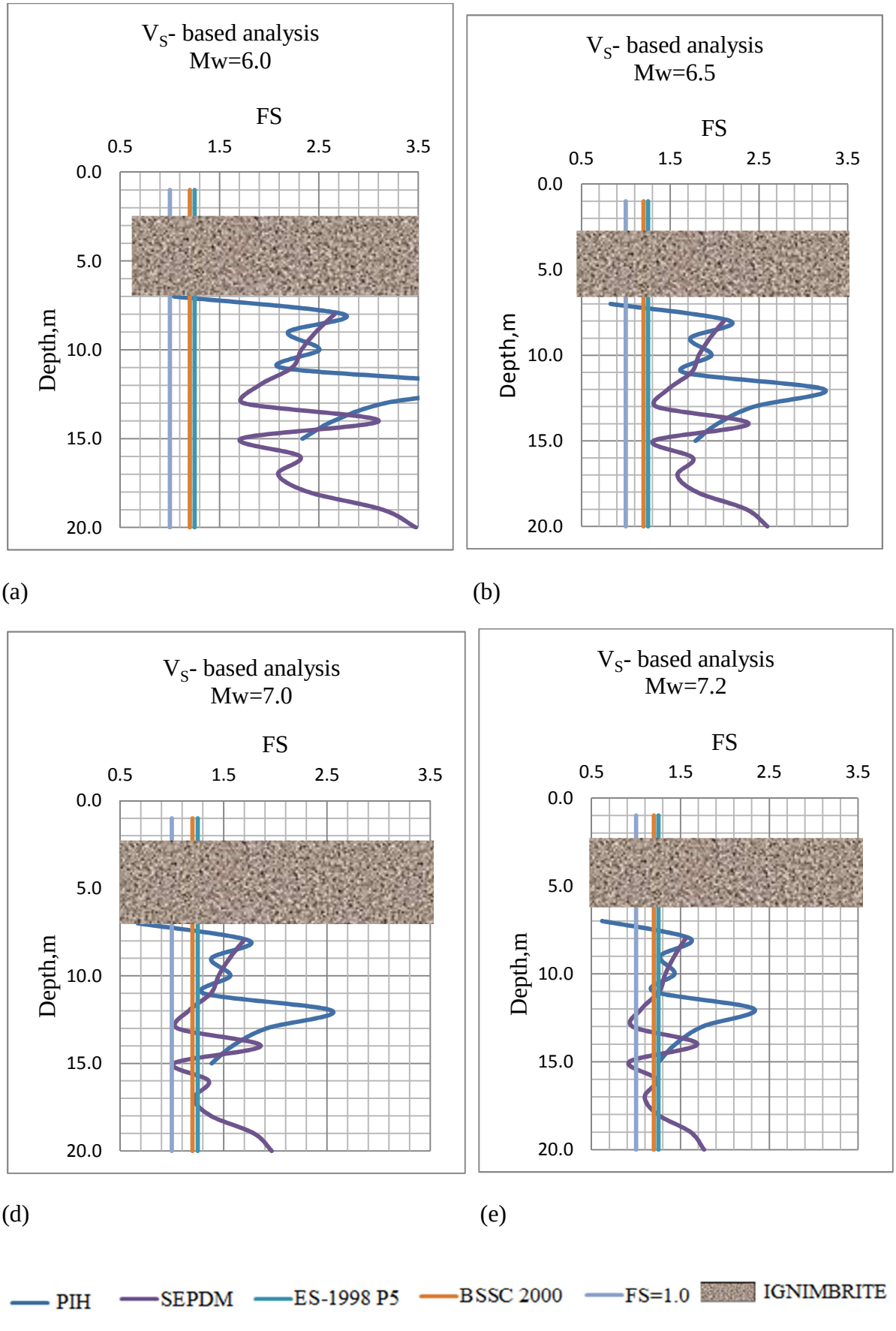

Figure 5.2 shear-wave velocity based simplefied proceedure analyses result for different magnitudes PIH and SEPDM sites

Amora-Gedel Site and PIH sites

As could be seen in Figure 5.1 (d) and (e) the layers below 10m depth from the ground surface have factor of safety less than the ES-EN1998:2015 recommended value for magnitudes 7 and 7.2. Additionally, a factor of safety less than 1.25 is observed in a thin layer of about 0.6m thickness at 7m from the ground surface with a lower magnitude. The Shear-wave velocity based analyses on shows similar trend at 7m depth (Figure 5.2). Eventhough the factor of safety is less than 1 by the insitu methods, One can notice that the thin layer below the weathered and fractured ignimbrite have minimal liquefaction vulnerability because generated excess pore pressures in thin layers dissipate quickly during earthquake owing to shorter drainage distances (Okamura et al. 2015).

HIP site

HIP ground water table is found at a depth of 10m. Hence, as it is observed in Appendix C, HIP site subsurface does not show liquefaction in all cases.

Agricultural College and NIB sites

The results presented in Figure 5.1 shows that the layers beneath 9m have a factor of safety less than 1.25, and less than 1 below 15m from the ground surface on a magnitude of 7.0 and 7.2. However, the shear- wave velocity analyses result in Figure 5.2 and Appendix C revealed that the entire profile is safe against liquefaction.

Meskel Square and SEPDM sites

The shear wave velocity based results shown in Figure 5.2 (c) and (d) reveal that the layers about 1m thick at 13m and 15m from the ground surface have a FS less than 1.25 for magnitudes of 7.00 and above. However the shear wave velocity based simplified procedure, which has been checked, based on the seismic survey; output in section 4.4.2. (II) and Appendix C confirms that it is safe against liquefaction.

CHAPTER SIX

CONCLUSIONS AND RECOMMENDATIONS

6.1 Conclusions

One can confidently say that soil formation is safe against liquefaction if the factor of safety in the analysis is greater than 1. If at any depth in the sediment profile, factor of safety is equal to or less than one, then there is a liquefaction hazard (BSSC 2000). BSSC 2000 recommends a factor of safety of 1.2 to 1.5 depending on the importance of structures. For buildings on shallow foundations, evaluation of the liquefaction susceptibility may be omitted when the saturated sandy soils are found at depths greater than 15 m from the ground surface (ES-EN1998:2015 part 5). Moreover the Ethiopian Code ES-EN 8-1998:2015 part 5 recommends factor of safety of 1.25.

Hence from the analyses results of the study, the following conclusions can be drawn:

- The study area is consistently safe against liquefaction up to a depth of about 9m from the surface with the range of anticipated earthquake magnitudes.
- Earthquakes of moment magnitudes below 6.5 do not pose liquefaction hazard at all depth of all sites.
- A higher magnitude of about 7 and above can potentially trigger liquefaction in Amora-Gedel and PIH sites area at depths below 10m.
- Hawassa Industry Park (HIP) area is safe against liquefaction up to a depth of 20m, leading to the conclusion that liquefaction is not a threat at that location.
- The Agricultural College and Nib bank area revealed that it has a vulnerable layer that liquefies at about 9m depth from the ground surface for magnitudes 7 and above. Though the geotechnical investigation reports revealed that the ground water table is found at 13.6m, the analyses have been performed with the projected GWT to 3m (owing to seasonal fluctuation) from the ground surface based on the resistivity contrast discussed in section 3.3.2.2. Liquefaction has been observed to be a possibility upon considering this seasonal fluctuation.
- The area around SEPDM and Meskel Square sites shows local susceptibility to liquefaction at a depth of about 12 to 13m from the ground surface. However, the depth can be assumed to be deep enough for liquefaction to not be considered a hazard for shallow founded structures, especially nothing the existence of ignimbrite at shallow depth.
- All analyses outputs based on the shear-wave velocity procedure from seismically measured subsurface data revealed that the study area is safe against liquefaction.
- Comparison of the results of this study with criteria of ES: EN1998:2015, part 5 indicates that the study area falls in less susceptible to marginally susceptible place to liquefaction for earthquakes of moment magnitude about 7.0 and above.

6.2 RECOMMENDATIONS

Seismic refraction survey has limitation to determine the shear wave velocity as discussed in Chapter 3. Its extent of investigation and reliability of data are more dependent on stratification. For sites like in Hawassa, having a layer of higher shear wave velocity interbedded between low velocity layers, the method is not the most preferred one. Hence, multiple techniques of survey such as uphole and downhole and crosshole methods shall be employed to get more reliable subsurface data.

It is recommended that site specific study shall be carried out for important structures based on multiple methods especially in the area at which liquefaction might be a threat.

REFERENCES

Ambraseys, N.N. and Menu, J.M. (1988). “Earthquake-induced ground displacements.” *Earthquake Engineering and Structural Dynamics*, 16, 985-1006.

Andrus, R.D., Stokoe K.H., and Juang C.H. (2004). “Guide for Shear-Wave-Based Liquefaction Potential Evaluation.” *Earthquake Engineering Research Institute Earthquake Spectra*, 20(2), 285–308.

Arango, I., Lewis, M. R., and Kramer, C., (2000). “Updated liquefaction potential analysis eliminates foundation retrofitting of two critical structure.” *Soil Dyn. Earthquake Eng.* 20, 17–25.

Atnafu Y. (2014) “Characterization of ground water –lake water interaction in Lake Hawassa basin.” MSc. Thesis, School of Civil and Environmental Engineering, Addis Ababa University, Addis Ababa.

Ayele, A. (2017) “Probabilistic seismic hazard analysis (PSHA) for Ethiopia and the neighboring region.” *Journal of African Earth Sciences*, 134, 257-264.

Beaty, M.H. and Byme, P.M (2001). “Observations on the San Fernando Dams.” *International Conferences on Recent Advances in Geotechnical Earthquake Engineering and Soil Dynamics*, 22.

Boore, D.M. (2004). “Estimating VS(30) (or NEHRP Site Classes) from shallow velocity models (depths <30m).” *Bull. Seismo. Am.*, 94(2), 591-597.

Boore, D.M., Thompson, E.M., and Cadet, H. (2011). “Regional Correlations of VS30 and Velocities Averaged Over Depths Less Than and Greater Than 30 Meters” *Bulletin of the Seismological Society of America*, 101(6), 3046–3059.

Boulanger, R.W., Idriss, I.M. (2006). “Liquefaction Susceptibility Criteria for Silts and Clays.” *Journal of Geotechnical and Geoenvironmental Engineering* 132(11),1413-1426.

BSSC (Building Seismic Safety Council). (2015) *2015 Edition NEHRP recommended Seismic Provisions for New Buildings and Other Structures*, FEMA P-1050-1 (Provisions and Commentary), Washington, D.C.

Chiou, B., Darragh, R., Gregor, N., and Silva, W. (2008). “NGA Project Strong-Motion Database.” *Earthquake Spectra*, 24(1), 23–44.

Choi, W.K. (2008). “Dynamic properties of Ash-Flow Tuffs.” PhD. dissertation, the University of Texas at Austin , TX.

Day R. W. (2002). *Geotechnical Earthquake Engineering Handbook* McGraw-Hill. NY.

Dessie, T. and Tesema, Z. (2003). *Hydrology and engineering geology of Awassa lake catchment*, Geological Survey of Ethiopia, Addis Ababa.

Essien, U.E., Akankpo, A.O. and Igboekwe, M.U. (2014). “Poisson’s Ratio of Surface Soils and Shallow Sediments Determined from Seismic Compressional and Shear Wave Velocities.” International Journal of Geosciences, 5, 1540-1546.

Gashaw A. (2012) “Shear modulus and damping ratio values of soils commonly found in Hawassa.” MSc. Thesis, School of Civil and Environmental Engineering, Addis Ababa University, Addis Ababa.

Giardini, D., Grünthal, G., Shedlock, K. M. and Zhang, P. (2003). “The GSHAP Global Seismic Hazard Map .In:Lee W. Kanamori H., Jennings, P., and Kisslinger,C.” *International Handbook of Earthquake & Engineering Seismology*, International Geophysics Series 81 B, Academic Press, Amsterdam, 1233-1239.

Gouin, P. (1979). Earthquake history of Ethiopia and the horn of Africa. IDRC. Ottawa, Ontario.

Haldar, A. and Tang, W.H. (1979). “Probabilistic evaluation of liquefaction potential.” *Journal of Geotechnical Engineering Division*, ASCE, 23(3), 313-318.

Haile, M. (1996). “Critical assessment of site effect parameters for strong ground motion prediction.” Ph.D. dissertation, Tokyo Institute of Technology, Tokyo.

Hanzawa, H., Itoh, Y., and Suzuki, K. (1979). “Shear characteristics of a quick sand in Arabian Gulf.” *Soils and Foundations*, 19(4), 1-15.

Hashash, Y.M.A., Philips, C. and Groholski, D. (2010). “Recent advances in non-linear site response analysis.” Fifth International Conference on Recent Advances in Geotechnical Earthquake Engineering and Soil Dynamics, OSP 4

Hashash, Y.M.A, Groholski, D.R., Phillips, C. A., Park, D, Musgrove, M. (2012). “DEEPSOIL 5.1, User Manual and Tutorial.” 107.

Housner, G.W. (1985). *Liquefaction of soils during earthquake.* Washington D.C.

Idriss, I.M. and Boulanger, R.W. (2010) *SPT-Based Liquefaction Triggering Procedures.* Center for Geotechnical Modeling, UCD/CGM-10/02, University of California at Davis.

Ishara, K. (1996). *Soil Behavior in Earthquake Geotechnics.* Oxford University Press. Engineering Science University of Tokyo.

JICA (Japan International Cooperation Agency) (2012). *The study on groundwater resources assessment in the rift valley lakes basic in the Federal Democratic Republic of Ethiopia*. Kokusai Kogyo Co., Ltd.

Kassegne, S.K, Engeda, S., Kebede, A., Tessema, E. (2012). “Notes and Proposed Guidelines on Updated Seismic Codes in Ethiopia - Implications for Large-Scale Infrastructures.” San Diego, CA.

Kebede, F. and van Eck, T. (1997) “Probabilistic seismic hazard assessment for the Horn of Africa based on seism-tectonic regionalization.” *Tectonophysics*, 270, 221-237.

Kramer, S.L. (1996). *Geotechnical Earthquake Engineering*. Prentice-Hall. Upper Saddle River.

Lamson-Hall, P., Degroot, D., Martin, R., Tafesse, T., Angel, S. (2015). “A new plan for African cities: The Ethiopia Urban Expansion Initiative.” *NYU Stern Urbanization Project report*, Marron Institute of Urban Management.

Luna, R. and Houda, J. (2000). “Determination of dynamic soil properties using geophysical methods.” *International Conference on the App. of Geophysical .and NDT methodologies to Transportation Facilities and Infrastructure*, St. Louis, MO.

Málek, J. (2014). “Seismic hazard of Southern Ethiopia,” *Institute of Rock Structure and Mechanics*, Academy of Sciences of the Czech Republic, Prague.

Martin, G.R. and Lew, M. (1999). “Guidelines for analysis and mitigation liquefaction in California”, Recommended procedures for implementation of DMG special Publication 117, *Southern California Earthquake Center*, University of Southern California.

Ministry of Construction (2015). Design of Structures for Earthquake Resistance, *Ethiopian Standards based on Euro Norms (ES EN 1998:2015)*, Addis Ababa.

Ni, S.H. and Fan, E.S. (2004). “Fine Content effects on liquefaction potential evaluation for sites liquefied during Chi-Chi earthquake, 1999.” *13th World Conference on Earthquake Engineering*, 2521, Vancouver, Canada.

Okamura, M., Nelson, F.C.(2015) “Liquefaction Assessment of Thin Sand Layers with Partially Drained Condition.” *6th International Conference on Earthquake Geotechnical Engineering*, Christchurch, New Zealand.

Ohta,Y., and Goto, N. (1978). “Empirical shear wave velocity equations in terms of characteristic soil indexes.” *Earthq. Eng. Struct. Dyn.*, 6, 167–187.

Polito, C. P., and Martin II, J. R. (2001). “Effects of nonplastic fines on the liquefaction resistance of sands.” *Journal of Geotechnical and Geoenvironmental Engineering*, ASCE, 127(5), 408-415.

Redpath, B.B. (1973). *Technical Report E-73-4: Seismic Refraction Exploration for Engineering Site Investigations.* U.S Army Engineer Waterway Experiment Station. Livermore, CA.

Seed,H.B. and Lee, K.L. (1966). “Liquefaction of saturated sands during cyclic loading.” *Journal of the Soil Mechanics and Foundation Division*, ASCE, 92(SM3), 25-28.

Seed, H.B. and Idriss, I.M. (1971). “Simplified procedure for evaluating soil liquefaction potential.” *Journal of Soil Mechanics and Foundation Division,* ASCE, 107(SM9), 1249-1274.

Sladen, J.A., Hollander, R.D. and Krahn, J. (1985), “The liquefaction of sands, a collapse surface approach.” *Canadian Geotechnical Journal*, 22, 564-578.

Stewart, J.P., Afshari, K. and Hashash, Y.M.A. (2014). “Guidelines for Performing Hazard-Consistent One-Dimensional Ground Response Analysis for Ground Motion Prediction.” Pacific Earthquake Engineering Research Center, University of California at Berkeley.

Suwal, L.P. and Kuwano, R. (2012). “Poisson’s Ratio Evaluation on Silty and Clayey Sands on Laboratory Specimens by Flat Disk Shaped Piezo-ceramic Transducer.” Bulletin of ERS, Institute of Industrial Science, 45, University of Tokyo.

Tekalign, A. (2013). “The impact of Unplanned Urban Waterfront Development on Lake Hawass.” MSc. Thesis, EiABC, Addis Ababa.

Telford, W.M., Geldart, L.P., and Sheriff, R.E. (1990). Applied Geophysics, Cambridge University Press, Cambridge, UK.

Uyanik, O. (2010). “Compressional and shear-wave velocity measurement in unconsolidated top-soil and comparison of the results.” *International Journal of the Physical Sciences,* 5(7), 1034-1039.

Vucetic, M. and Dobry, R. (1991). “Effect of Soil Plasticity on Cyclic Response.” ASCE, Journal of Geotechnical Engineering, 117(1), 89-107.

Wair, B.R., DeJong, J.T (2012). *Guidelines for Estimation of Shear-wave Velocity Profiles.* Department of Civil and Environmental Engineering University of California, Davis, PEER2012/08.

Water Works Design and Supervision Enterprise (1999). “The study of Awassa Lake level rise.” Vol. I-III. Addis Ababa.

Williams, F.M. (2016). *Understanding Ethiopia Geology and Scenery*, dept. of earth sciences, University of Adelaide, Adelaide, Australia, 178-196.

Yoshida, N. (2015). *Seismic Ground response Analysis*. Springer. Dordrecht.

Youd, T.L. and Idriss I. M. (2001). “Liquefaction resistance of soils: Summery report from the 1996 NCEER and 1998 NCEER/NSF workshops on evaluation of liquefaction resistance of soil.” *Journal of Geotechnical and Geo-environmental Engineering*, 297-313.

APPENDIX A

GEOTECHNICAL INVESTIGATION (SECONDARY DATA)

	Company Name: CONSTRUCTION DESIGN SCo.	Form No: OF/CDSCO/104
Title: Borehole Log Sheet		Issue No: 1 / Page No: Page 1 of 1

PROJECT HAWASSA HOTEL & RESORT (B+G+6) BORING TYPE Rotary Coring

LOCATION HAWASSA GROUND WATER LEVEL 3.60m

CLIENT PROGRESS INTERNATIONAL HOTEL P.L.C BH ELEVATION

DATE STARTED 12/04/2010 INCLINATION Vertical

DATE COMPLETED 13/04/2010

BH 9

DEPTH (m)	CASING SIZE (mm)	DRILLING SIZE (mm)	SAMPLE RECOVERY	SPT / SAMPLES	DEPTH (m)	PROFILE	TCR (%)	RQD (%)	STRATA DESCRIPTION	REMARK
0–3	116	116	2.80	10	0.00–3.00		100		Loose to medium dense, grey to pinkish grey, sand at the top, silty SAND	
3–6.4		100	4.70 SS		3.00–6.40	I I I I I I I I I I	100	0	Moderately strong to strong, grey to pink slightly weathered Ignimbrite	
6.4–15		75	8.20	22	6.40–15.00		100	30	Medium dense, grey, wet to pink SAND/silty SAND	
				23						
			12.60	21						
				21						

(Nc) CORE PENETRATION TEST
N BLOWS/30cm
SS ROCK SAMPLE
W WATER SAMPLE
TCR TOTAL CORE RECOVERY
RQD ROCK QUALITY DESIGNATION
DISTURBED SOIL SAMPLE
UNDISTURBED SOIL SAMPLE
SPT STANDARD PENETRATION
END OF DRILLING

CREW Bizuneh Adamu DRAWN BY Kassech zena

SUPERVISOR Tewodros Mako SIG

LOGGED BY Tewodros Mako SIG

CHECKED BY Getachew Teferi. SIG

PLEASE MAKE SURE THAT THIS IS THE CORRECT ISSUE BEFORE USE

(a)

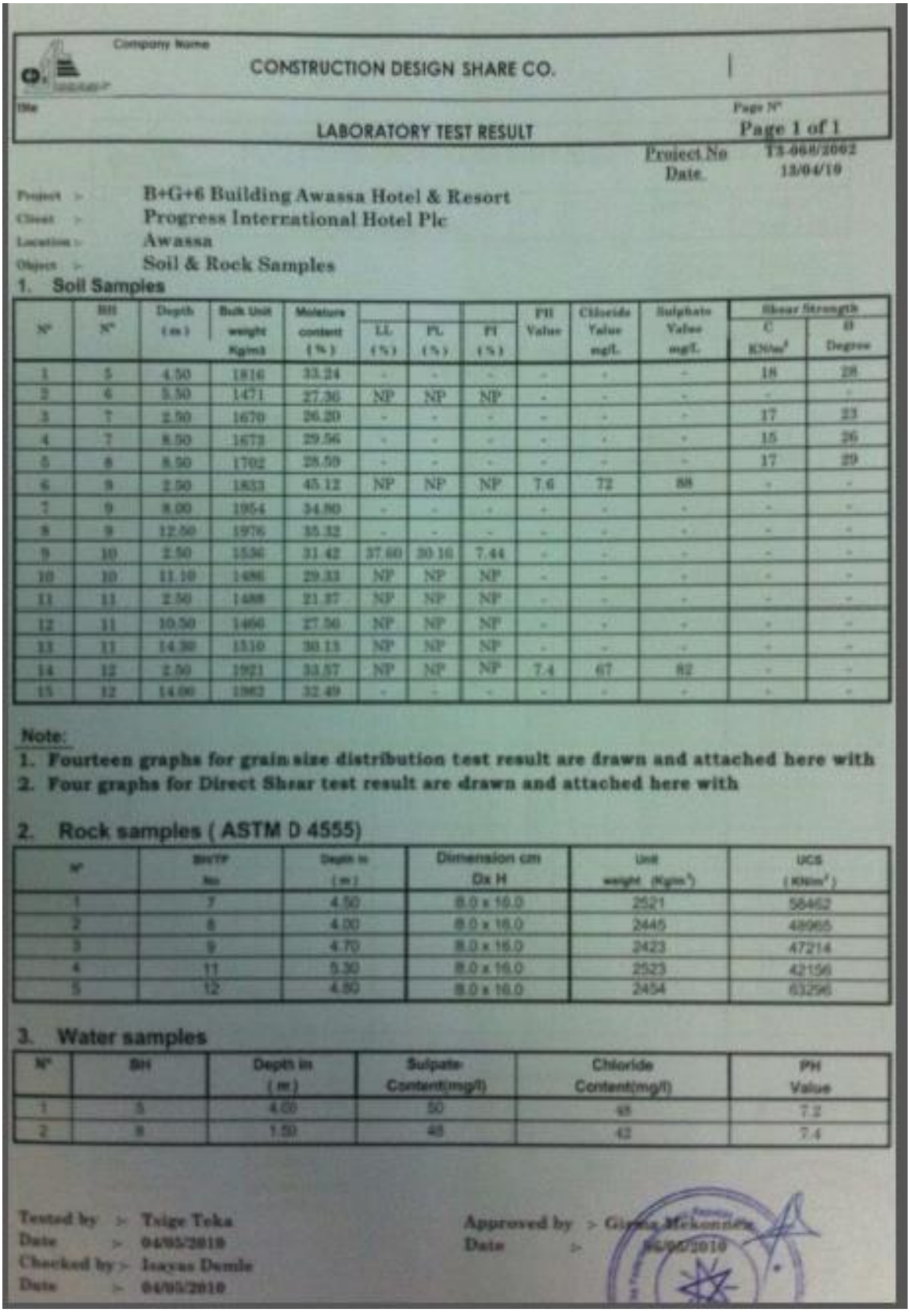

Company Name: CONSTRUCTION DESIGN SHARE CO.

Title: LABORATORY TEST RESULT

Page N°: Page 1 of 1

Project No: TS-068/2002

Date: 13/04/10

Project > B+G+6 Building Awassa Hotel & Resort
Client > Progress International Hotel Plc
Location > Awassa
Object > Soil & Rock Samples

1. Soil Samples

N°	BH N°	Depth (m)	Bulk Unit weight Kg/m3	Moisture content (%)	LL (%)	PL (%)	PI (%)	PH Value	Chloride Value mg/L	Sulphate Value mg/L	Shear Strength C KN/m²	Shear Strength Ø Degree
1	5	4.50	1816	33.24	-	-	-	-	-	-	18	28
2	6	5.50	1471	27.30	NP	NP	NP	-	-	-	-	-
3	7	2.50	1670	26.20	-	-	-	-	-	-	17	23
4	7	8.50	1673	29.56	-	-	-	-	-	-	15	26
5	8	8.50	1702	28.59	-	-	-	-	-	-	17	29
6	9	2.50	1833	45.12	NP	NP	NP	7.6	72	88	-	-
7	9	8.00	1954	34.80	-	-	-	-	-	-	-	-
8	9	12.50	1976	35.32	-	-	-	-	-	-	-	-
9	10	2.50	1536	31.42	37.60	30.16	7.44	-	-	-	-	-
10	10	11.10	1486	29.33	NP	NP	NP	-	-	-	-	-
11	11	2.50	1488	21.87	NP	NP	NP	-	-	-	-	-
12	11	10.50	1466	27.56	NP	NP	NP	-	-	-	-	-
13	11	14.30	1510	30.13	NP	NP	NP	-	-	-	-	-
14	12	2.50	1921	33.57	NP	NP	NP	7.4	67	82	-	-
15	12	14.00	1982	32.49	-	-	-	-	-	-	-	-

Note:

1. Fourteen graphs for grain size distribution test result are drawn and attached here with
2. Four graphs for Direct Shear test result are drawn and attached here with

2. Rock samples (ASTM D 4555)

N°	BH/TP No	Depth in (m)	Dimension cm Dx H	Unit weight (Kg/m³)	UCS (KN/m²)
1	7	4.50	8.0 x 16.0	2521	58462
2	8	4.00	8.0 x 16.0	2445	48965
3	9	4.70	8.0 x 16.0	2423	47214
4	11	5.30	8.0 x 16.0	2523	42156
5	12	4.80	8.0 x 16.0	2454	63296

3. Water samples

N°	BH	Depth in (m)	Sulpate Content(mg/l)	Chloride Content(mg/l)	PH Value
1	5	4.00	50	48	7.2
2	8	1.50	48	42	7.4

Tested by > Tsige Teka
Date > 04/05/2010
Checked by > Isayas Demle
Date > 04/05/2010

Approved by > Girma Mekonnen
Date > 04/05/2010

(b)

Figure A1 PIH geotechnical investigation report (a) BH -9 (b) Laboratory result of PIH (CDSco / ECDSWCo –BUDSW SECTOR OFFICE)

Company Name	Form No
CONSTRUCTION DESIGN SCo.	OF/CDSCO/104

Title	Issue No	Page No
Borehole Log Sheet	1	Page 1 of 1

PROJECT HAWASSA INDUSTRIAL PARK BORING TYPE ROTARY CORING

LOCATION HAWASSA GROUND WATER LEVEL NIL

CLIENT CCECC HAWASSA INDUSTRIAL PARK BH ELEVATION 1701.94m

DATE STARTED 14/12/2015 INCLINATION VERTICAL

DATE COMPLETED 14/12/2015 COORDINATE 781442.79E 444938.94N

BH B35C

DEPTH (m)	CASING SIZE (mm)	DRILLING SIZE (mm)	SAMPLE RECORD	S.P.T. (BLOWS/FT)	DEPTH (m)	PROFILE	TCR (%)	RQD (%)	STRATA DESCRIPTION	REMARK
0–1		116		8	0.00–1.00		100		Red ash	Fill material
1–10		100		15, 26, 28, 38	1.00–10.00		100		Medium dense to dense, variegated (grey to whitish) friable silty SAND/ sandy SILT with fine gravels (Tuff)	

(Ps) CONE PENETRATION TEST
N BLOWS/30cm
RS ROCK SAMPLE
W WATER SAMPLE
TCR TOTAL CORE RECOVERY
RQD ROCK QUALITY DESIGNATION
DISTURBED SOIL SAMPLE
UNDISTURBED SOIL SAMPLE
SPT STANDARD PENETRATION
END OF DRILLING

CREW Ibrahim Adem DRAWN BY Bezunesh W/Tsadik

SUPERVISOR Olana Bedasa SIG

LOGGED BY Olana Bedasa SIG

APPROVED BY Matewos Bekele SIG

PLEASE MAKE SURE THAT THIS IS THE CORRECT ISSUE BEFORE USE

(a)

	Company Name	Form N°
	CONSTRUCTION DESIGN SHARE SCo.	OF/CDSCo./123
Title		Issue NO
Grain Size Distribution		1

W.O/Proj. No	T7-016/2008
Date	17/12/2015

Sample ID:	GS/2014/512

Project :- Hawasa Industrial Park
Client :- CCECC Ethiopia Construction PLC
Location :- Hawasa
Description :- Dark Grey Silty Sand With Trace Clay
Test method :- ASTM D 422

BH B 32-C
Depth (m) 3.00

Specific gravity 2.60

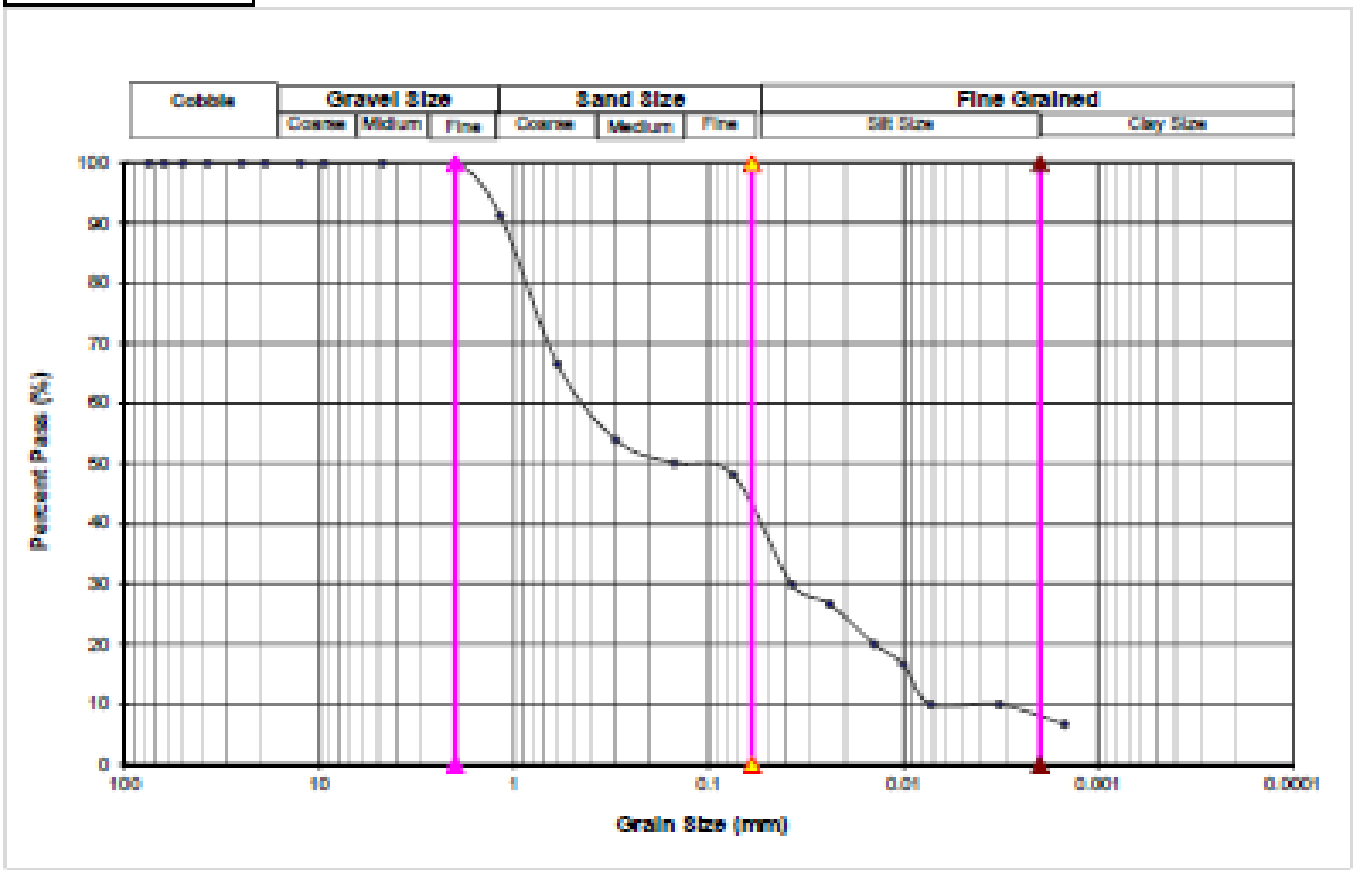

Tested by :- Tsige Teka
Date :- 04/01/2016
Checked by :- Abate Legesse
Date :- 13/01/2016

Approved by :- Biruk Abdi
Date :- 13/01/2016

(b)

Figure A2 HIP geotechnical investigation report (a) BH-35C (b) Grain size analysis report(CDSco / ECDSWCo –BUDSW SECTOR OFFICE)

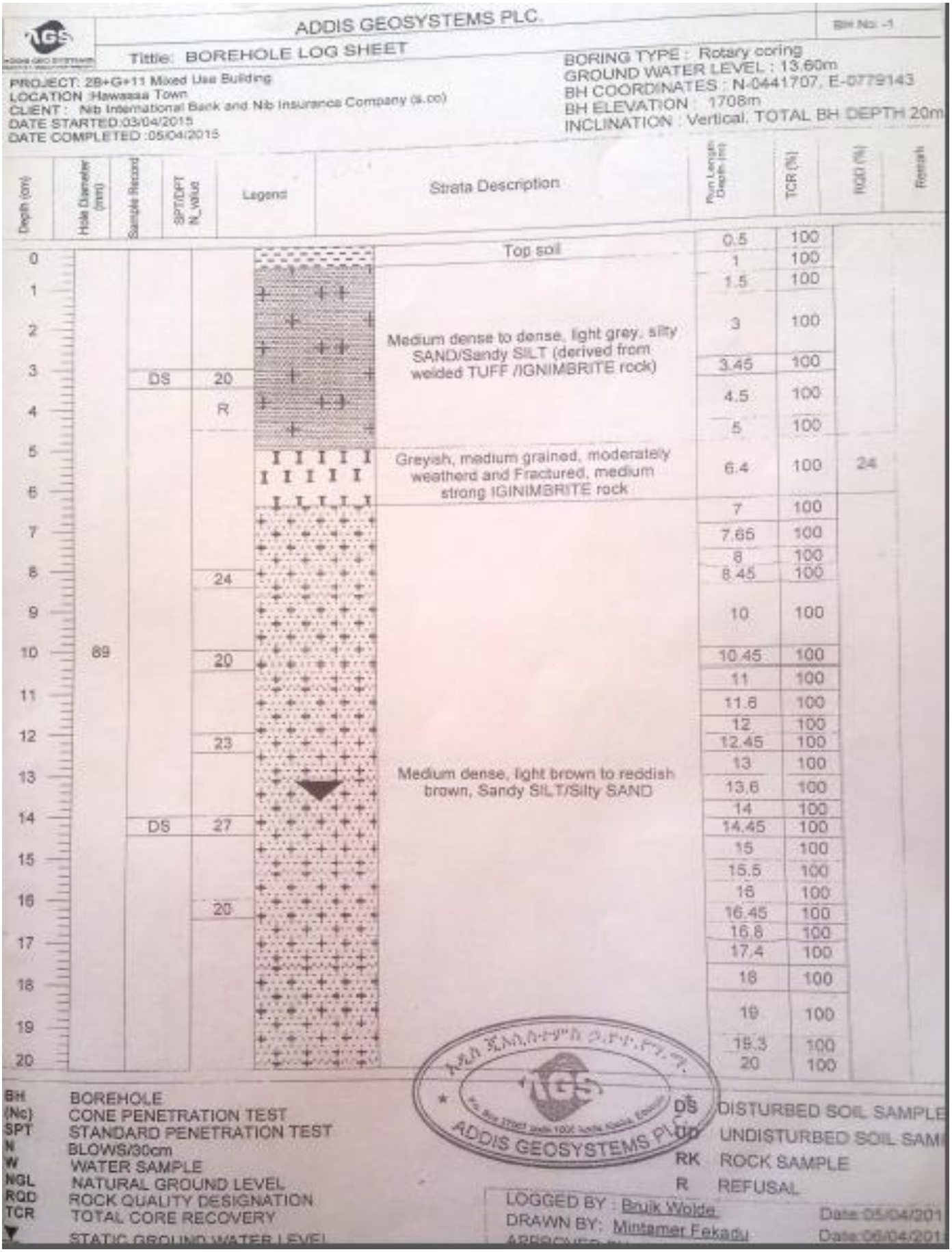

ADDIS GEOSYSTEMS PLC

BH No: -1

Tittle: BOREHOLE LOG SHEET

PROJECT: 2B+G+11 Mixed Use Building
LOCATION :Hawassa Town
CLIENT : Nib International Bank and Nib Insurance Company (s.cc)
DATE STARTED:03/04/2015
DATE COMPLETED :05/04/2015

BORING TYPE : Rotary coring
GROUND WATER LEVEL : 13.60m
BH COORDINATES : N-0441707, E-0779143
BH ELEVATION : 1708m
INCLINATION : Vertical, TOTAL BH DEPTH 20m

Depth (m)	Hole Diameter (mm)	Sample Record	SPT/DPT N_value	Legend	Strata Description	Run Length Depth (m)	TCR (%)	RQD (%)	Remark
0					Top soil	0.5	100		
1						1	100		
						1.5	100		
2					Medium dense to dense, light grey, silty SAND/Sandy SILT (derived from welded TUFF /IGNIMBRITE rock)	3	100		
3		DS	20			3.45	100		
						4.5	100		
4			R			5	100		
5					Greyish, medium grained, moderately weatherd and Fractured, medium strong IGINIMBRITE rock	6.4	100	24	
6						7	100		
7						7.65	100		
						8	100		
8			24			8.45	100		
9						10	100		
10	89		20			10.45	100		
						11	100		
11						11.8	100		
						12	100		
12			23			12.45	100		
13					Medium dense, light brown to reddish brown, Sandy SILT/Silty SAND	13	100		
						13.6	100		
14		DS	27			14	100		
						14.45	100		
15						15	100		
						15.5	100		
16			20			16	100		
						16.45	100		
17						16.8	100		
						17.4	100		
18						18	100		
19						19	100		
						19.3	100		
20						20	100		

BH (Nc) BOREHOLE
CONE PENETRATION TEST
SPT STANDARD PENETRATION TEST
N BLOWS/30cm
W WATER SAMPLE
NGL NATURAL GROUND LEVEL
RQD ROCK QUALITY DESIGNATION
TCR TOTAL CORE RECOVERY
STATIC GROUND WATER LEVEL

DS DISTURBED SOIL SAMPLE
UD UNDISTURBED SOIL SAM
RK ROCK SAMPLE
R REFUSAL

LOGGED BY : Bruk Wolde Date 05/04/201
DRAWN BY: Mintamer Fekadu Date 06/04/201

ADDIS GEOSYSTEMS PLC

(a)

ADDIS GEOSYSTEMS PLC
SOIL AND MATERIAL TESTING LABORATORY

Project :- 2B+G+11 Mixed Use Building
Client :- NIB International Bank & NIB Insurance Company (S.Co)
Location :- Hawassa Town
Test type :- Various

No	BH	Depth (M)	Soil Description	% Pass Sieve No-200	Specific Gravity	NMC (%)
1	1	3.00-3.45	Sandy Silt	57.68	2.45	35.65
2	1	14.00-14.45	Silty Sandy	44.85	2.65	45.06
3	2	3.00-3.45	-	-	-	38.51
4	2	11.00-11.45	Silty Sandy	44.02	2.45	45.95
5	3	4.00-4.45	Sandy Silt	65.38	2.45	60.76
6	4	4.00-4.45	-	-	-	17.81
7	4	14.00-14.45	Sandy Silt	68.53	3.50	43.37

Note :- 1. Five Graphs Of Grain Size Distribution test Results are drawn and attached here with

Tested By :- Helen Andemichael
Date :- 23/05/2013
Signature :-
Checked By :- Wossen Tadesse
Date :- 23/05/2013
Signature :-

Approved by :- Bal
Date :- 23/0
Signature :-

(b)

Figure A3 NIB geotechnical investigation report (a) BH 1 (b) Laboratory results report (ADDIS GEOSYSTEM PLC)

BOREHOLE LOG

BH 3

SHEET 1/1

PROJECT SPEDM HEAD OFFICE COMPLEX

CLIENT MH-ENGINEERING

LOCATION AWASSA GROUND WATER LEVEL 3.00m

BORING TYPE ROTARY CORING BH ELEVATION

DATE STARTED 09/01/97 INCLINATION VERTICAL

DATE COMPLETED 10/01/97

CASING SIZE (mm)	DRILLING RATE (min/m)	SAMPLE RECORD	SPT / N VALUE /	DEPTH (m)	PROFILE	TCR (%)	RQD (%)	STRATA DESCRIPTION	REMARK
116	116		4	1.20		100		Dark brown organic clayey SILT	
			15	3.00		100		Yellowish stiff clayey silt	
				4.50		100		whitish hard slightly weathered TUFF	
	75			5.00		100	25	Grey very strong fresh welded Tuff	
				7.00		100	86		
			12	10.00		100		Light brown soft friable silty SAND	

CONE PENETRATION TEST
BLOWS/20cm
ROCK SAMPLE
WATER SAMPLE
TOTAL CORE RECOVERY
ROCK QUALITY DESIGNATION
DISTURBED SOIL SAMPLE
UNDISTURBED SOIL SAMPLE
STANDARD PENETRATION
END OF DRILLING

CREW Asmake Bekele DRAWN BY Bezuneah W/Tsadik

SUPERVISOR Zerihun H/Selassie SIG

LOGGED BY Tadesse H/Mariam SIG

CHECKED BY Tadesse H/Mariam SIG

APPROVED BY Getachew Teferi SIG

(a)

(b)

Figure A4 SEPDM geotechnical investigation report (a) BH 3 (b) Grain size analysis report (CDSco / ECDSWCo –BUDSW SECTOR OFFICE)

APPENDIX B

INPUT MOTIONS

Table B1 Summary of data of selected records from PEER NGA West-2

RSN	**5%-95% Duration (Sec)**	**Earthquake Name**	**Year**	**Station Name**	**M_W**	**V_{S30} (m/Sec)**	**Horizontal Acc. Filename**
680	6.2	“Whittier Narrows-01”	1987	“Pasadena CIT Kresge Lab”	5.99	969.07	RSN680=WHITTIER.A_A-KRE360.AT2
797	14.2	“Loma Prieta”	1989	“SF-Rincon Hill”	6.93	873.10	RSN797_LOMAP_RIN090.AT2
4083	8.8	“Parkfield-02_CA”	2004	“Parkfield Turky Flat #1(om)”	6.0	906.96	RSN4083_PARK2004_36529270.AT2

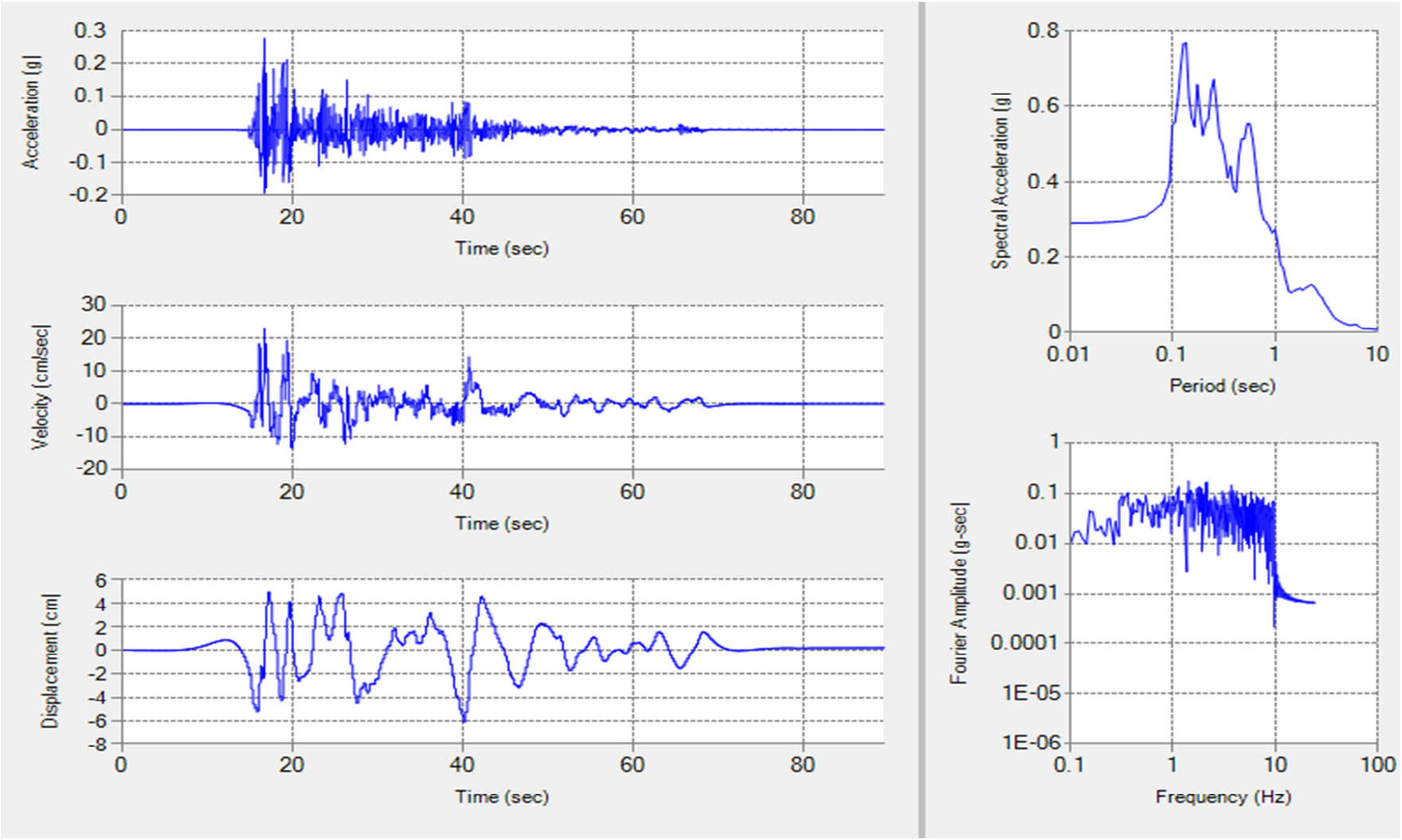

Figure B1uncalled Imperial valley EQ at Elcentro, 1940 input motion

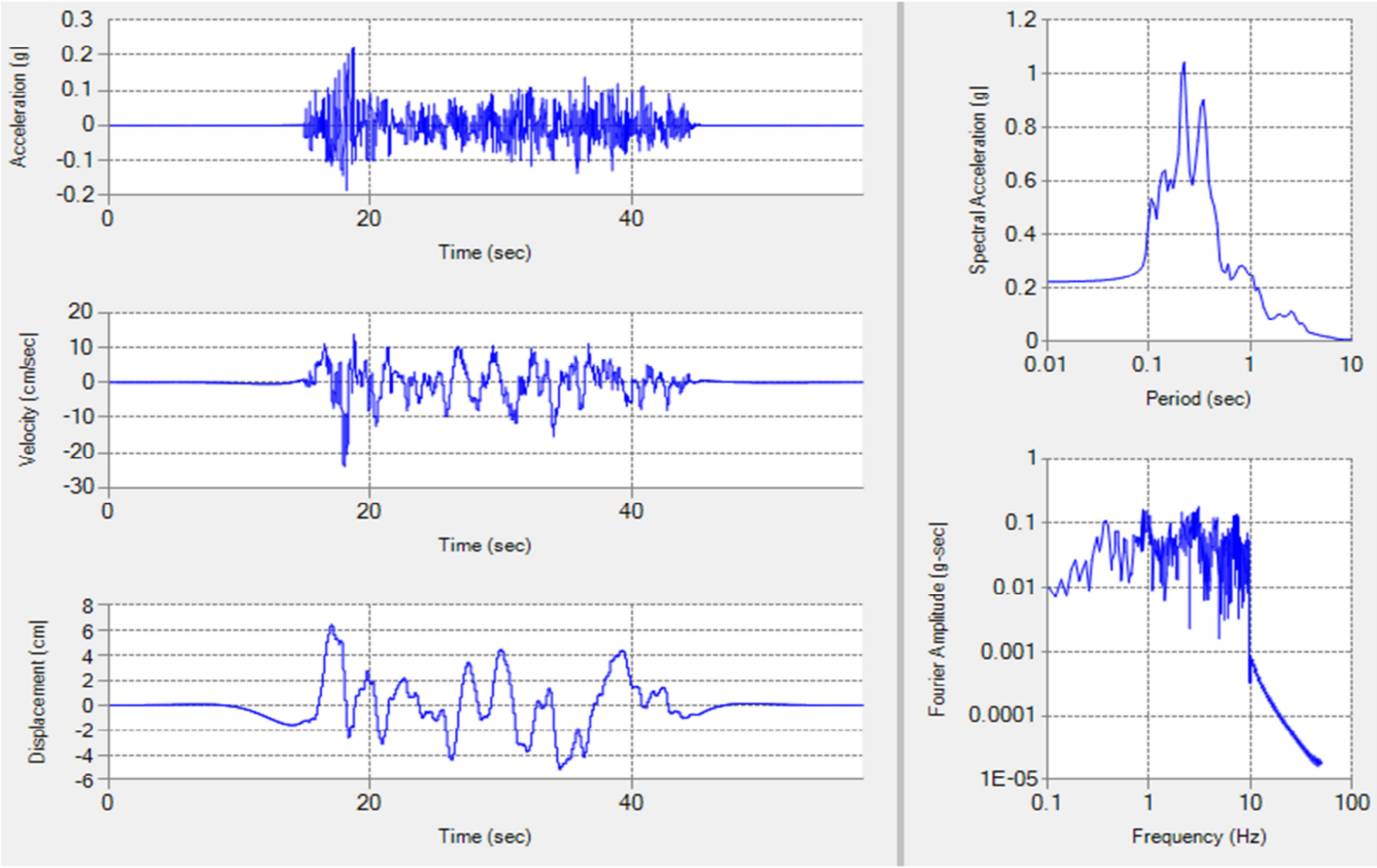

Figure B2 uncalled Tokachi-Oki EQ at Hachinohe,1968 input motion

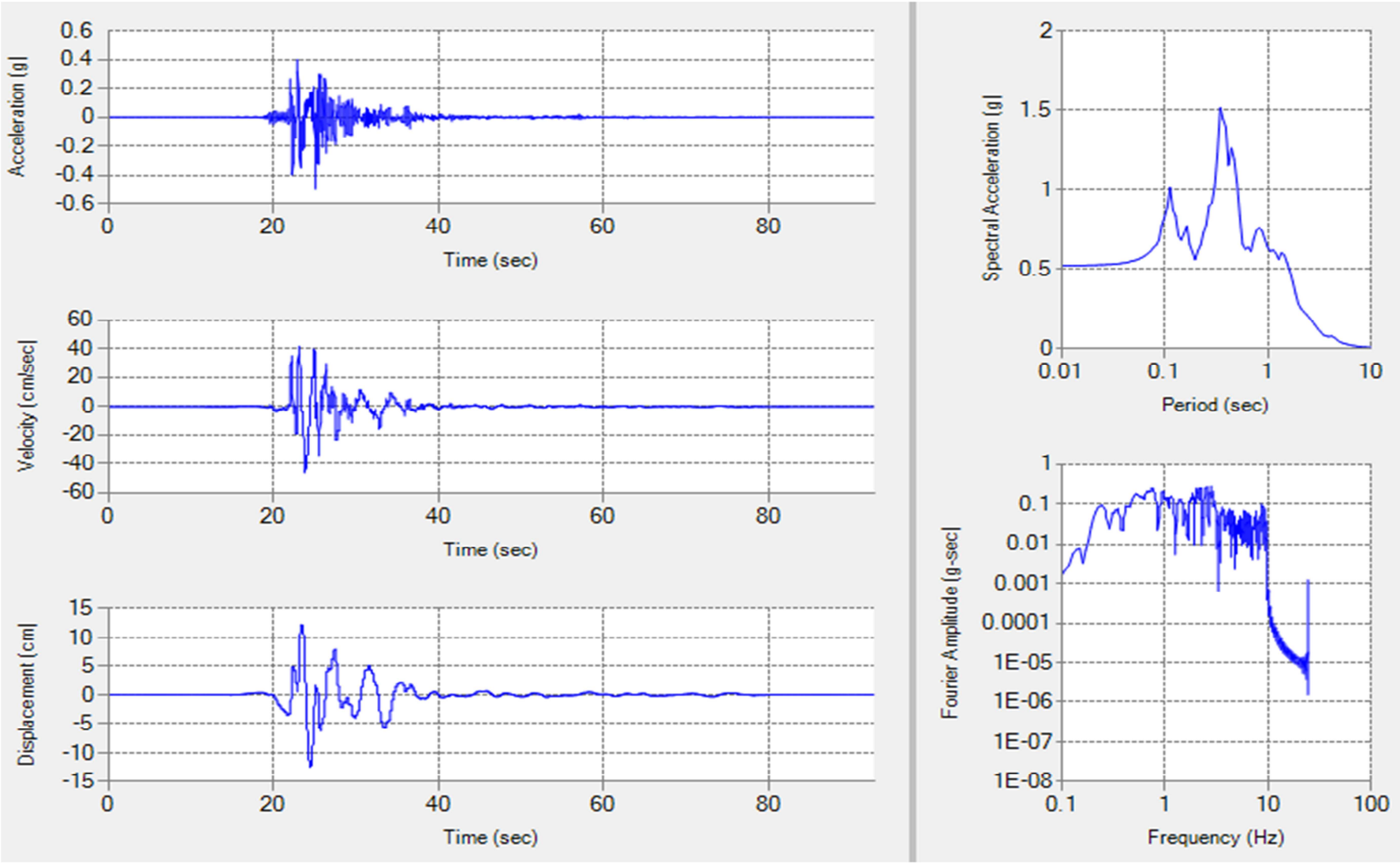

Figure B3 uncalled Hyogoken-nanbu Earthquake, Kobe university st. 1995 input motion

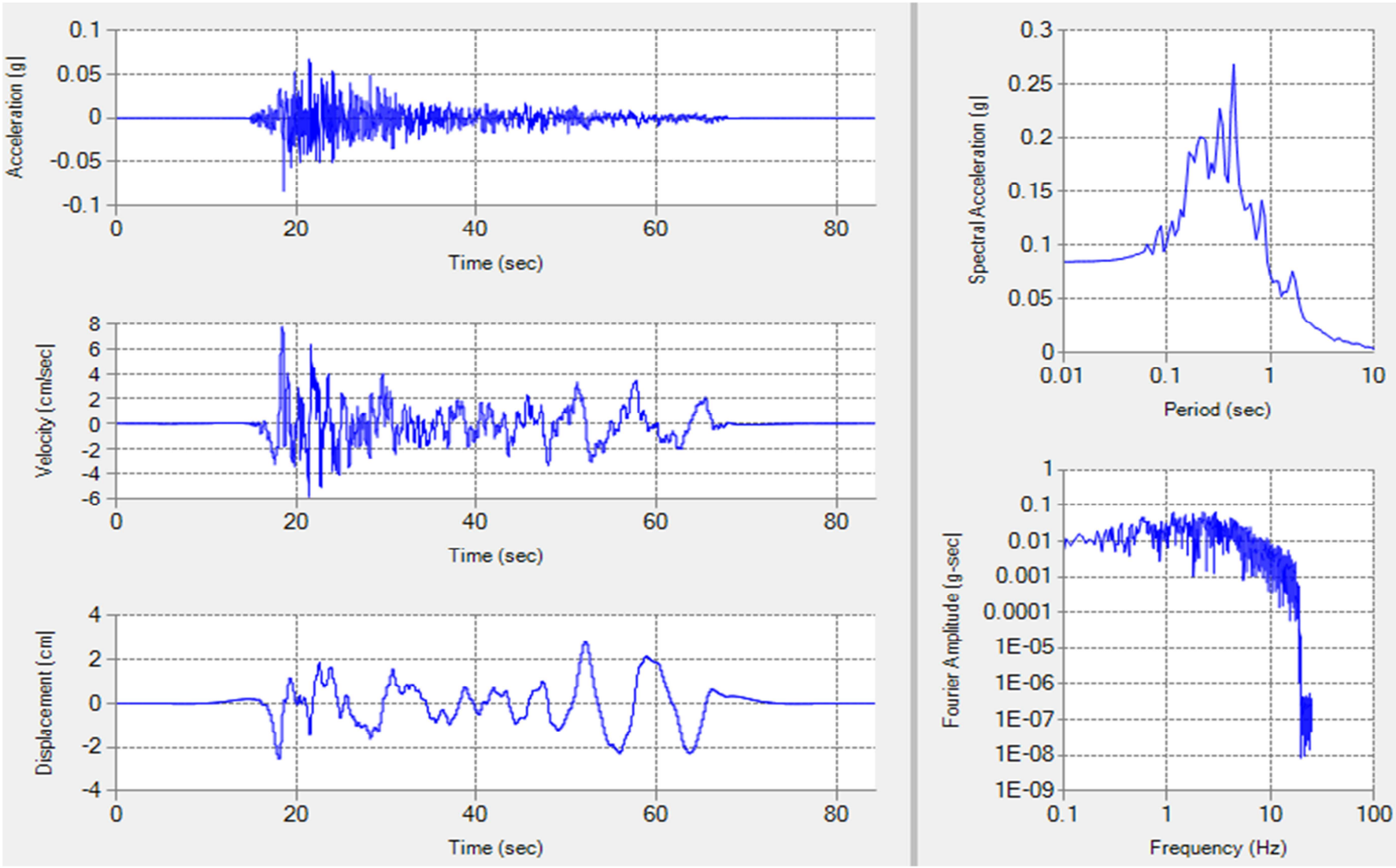

Figure B4 uncalled Kern County Earthquake, Taft Lincoln school St., 1952 input motion

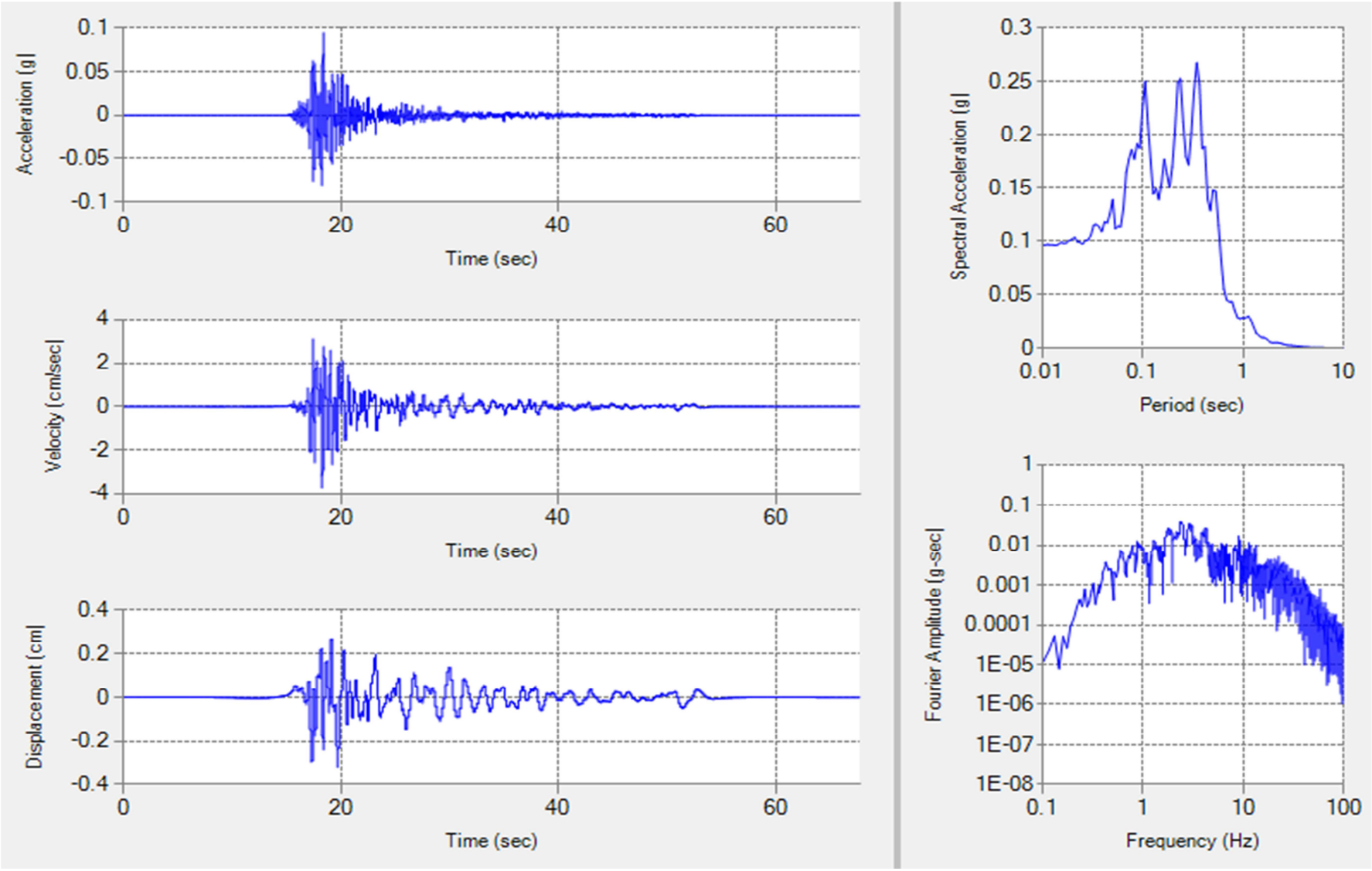

Figure B5 uncalled RSN 680- Whittier narrows-01 EQ recorded at St. Pasadena - CIT Kresge Lab input motion

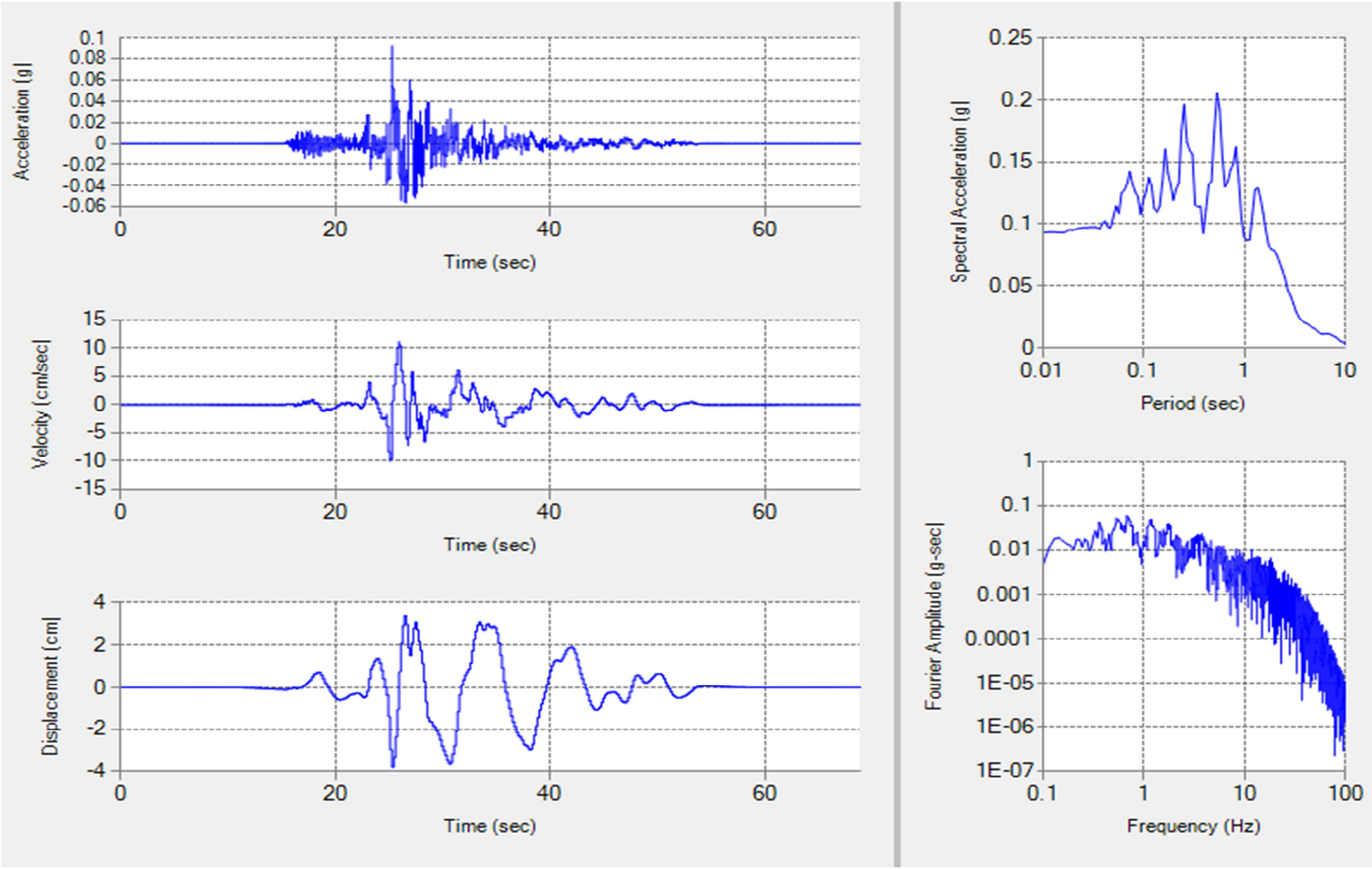

Figure B3 uncalled RSN 797 Loma prieta EQ recorded at St. SF - Rincon Hill input motion

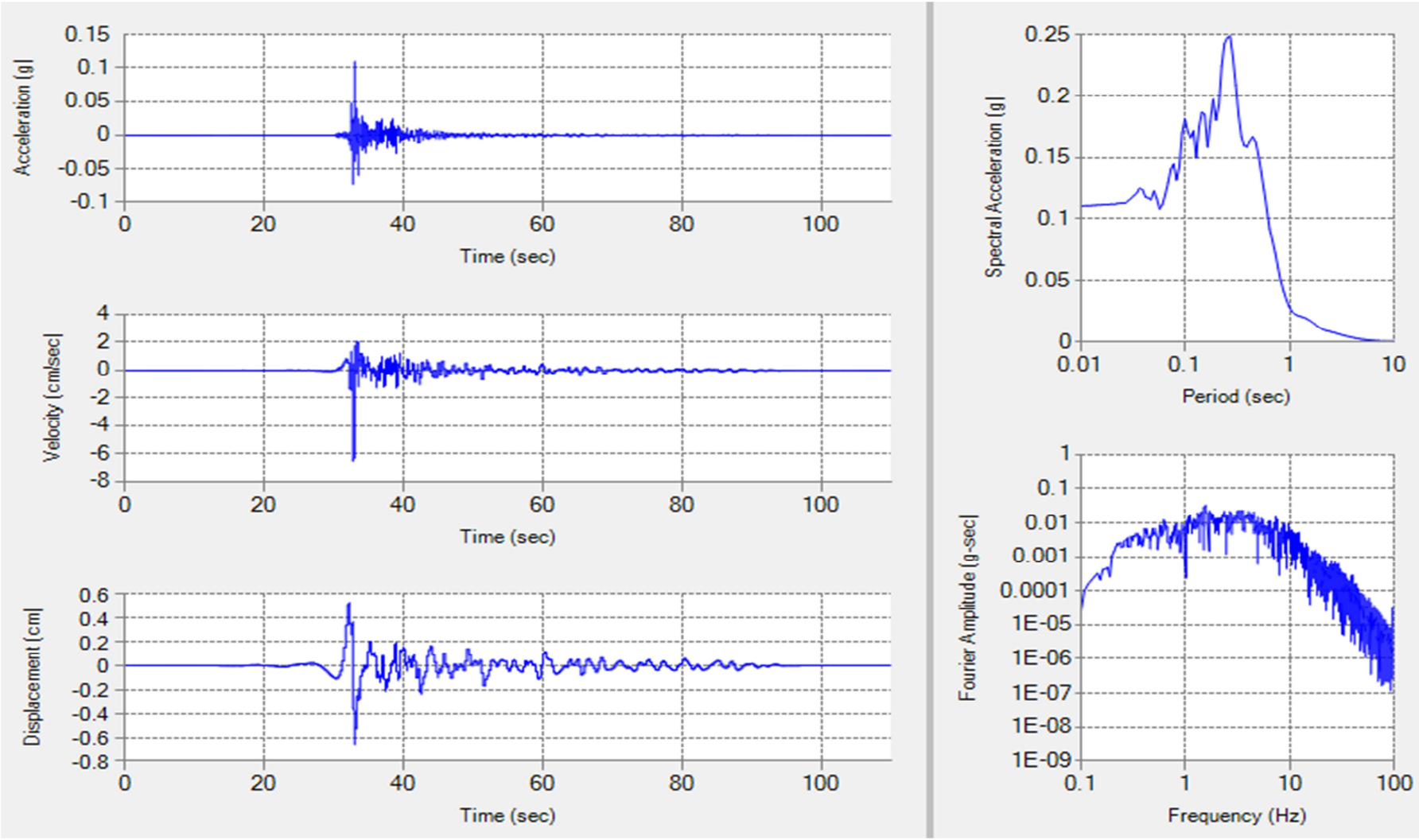

Figure B4 uncalled RSN 4083 Parkfield-02_ CA EQ recorded at ST. PARKFIELD input motion

APPENDIX C

Simplified procedure output

Table C1 and Table C2 are the output of SPT based simplified procedure (by Idriss and Boulanger 2010)

Table C1. SPT based analysis output of PIH for different magnitudes (amax=0.27g)

	Mw=	***5.5***												
Layer #	Layer Name	Depth, m	σv	σ'v	rd	CSR	FC ,%	Δ(N1) 60	(N1) 60	(N1) 60cs	MSF	Kσ	$CRR_{M=7.5, \sigma'v=1atm}$	$CRR_{M=7, \sigma'v}$	FS= CRR/CSR
1	Loose silty sand	1.00	18	18	1.000	0.18	65	6	17	22	1.69	0.97	0.23	0.38	
2	Loose silty sand	2.00	37	37	0.969	0.17	65	6	17	22	1.69	0.95	0.23	0.37	
3	Loose silty sand	3.30	60	60	0.937	0.16	65	6	13	18	1.69	0.92	0.19	0.29	
4	Ignimbrite	6.40	136	108	0.850	0.19					1.69				
5	M. Dense silty sand	7.00	147	114	0.832	0.19	65	6	12	18	1.69	0.86	0.18	0.26	1.39
6	M. Dense silty sand	8.00	167	124	0.802	0.19	65	6	24	30	1.69	0.75	0.48	0.60	3.18
7	M. Dense silty sand	9.00	186	133	0.771	0.19	65	6	23	29	1.69	0.74	0.43	0.53	2.83
8	M. Dense silty sand	10.00	206	143	0.741	0.19	65	6	21	26	1.69	0.75	0.33	0.42	2.24
9	M. Dense silty sand	11.00	225	153	0.710	0.18	65	6	20	26	1.69	0.74	0.31	0.39	2.12
10	M. Dense silty sand	12.00	245	163	0.681	0.18	65	6	20	25	1.69	0.73	0.29	0.36	2.02
11	M. Dense silty sand	13.00	265	173	0.652	0.18	65	6	19	25	1.69	0.72	0.28	0.34	1.96
12	M. Dense silty sand	14.00	285	183	0.624	0.17	65	6	18	24	1.69	0.71	0.27	0.32	1.90
13	M. Dense silty sand	15.00	305	193	0.597	0.17	65	6	18	24	1.69	0.70	0.26	0.31	1.87
	Mw=	***6***												
Layer #	Layer Name	Depth, m	σv	σ'v	rd	CSR	FC ,%	Δ(N1) 60	(N1) 60	(N1) 60cs	MSF	Kσ	$CRR_{M=7.5, \sigma'v=1atm}$	$CRR_{M=7, \sigma'v}$	FS= CRR/CSR
1	Loose silty sand	1.00	18	18	1.000	0.18	65	6	17	22	1.48	0.97	0.23	0.34	
2	Loose silty sand	2.00	37	37	0.978	0.17	65	6	17	22	1.48	0.95	0.23	0.33	
3	Loose silty sand	3.30	60	60	0.954	0.17	65	6	13	18	1.48	0.92	0.19	0.26	
4	Ignimbrite	6.40	136	108	0.887	0.20					1.48				
5	M. Dense silty sand	7.00	147	114	0.873	0.20	65	6	12	18	1.48	0.86	0.18	0.23	1.17
6	M. Dense silty sand	8.00	167	124	0.848	0.20	65	6	24	30	1.48	0.75	0.48	0.53	2.64
7	M. Dense silty sand	9.00	186	133	0.824	0.20	65	6	23	29	1.48	0.74	0.43	0.47	2.32
8	M. Dense silty sand	10.00	206	143	0.799	0.20	65	6	21	26	1.48	0.75	0.33	0.37	1.82
9	M. Dense silty sand	11.00	225	153	0.774	0.20	65	6	20	26	1.48	0.74	0.31	0.34	1.70
10	M. Dense silty sand	12.00	245	163	0.750	0.20	65	6	20	25	1.48	0.73	0.29	0.32	1.61
11	M. Dense silty sand	13.00	265	173	0.726	0.20	65	6	19	25	1.48	0.72	0.28	0.30	1.54
12	M. Dense silty sand	14.00	285	183	0.702	0.19	65	6	18	24	1.48	0.71	0.27	0.29	1.49
13	M. Dense silty sand	15.00	305	193	0.679	0.19	65	6	18	24	1.48	0.70	0.26	0.27	1.44
	Mw=	***6.5***												
Layer #	Layer Name	Depth, m	σv	σ'v	rd	CSR	FC ,%	Δ(N1) 60	(N1) 60	(N1) 60cs	MSF	Kσ	$CRR_{M=7.5, \sigma'v=1atm}$	$CRR_{M=7, \sigma'v}$	FS= CRR/CSR
1	Loose silty sand	1.00	18	18	1.000	0.18	65	6	17	22	1.30	0.97	0.23	0.30	

2	Loose silty sand	2.00	37	37	0.982	0.17	65	6	17	22	1.30	0.95	0.23	0.29	
3	Loose silty sand	3.30	60	60	0.962	0.17	65	6	13	18	1.30	0.92	0.19	0.23	
4	Ignimbrite	6.40	136	108	0.905	0.20					1.30				
5	M. Dense silty sand	7.00	147	114	0.893	0.20	65	6	12	18	1.30	0.86	0.18	0.20	1.00
6	M. Dense silty sand	8.00	167	124	0.873	0.21	65	6	24	30	1.30	0.75	0.48	0.47	2.25
7	M. Dense silty sand	9.00	186	133	0.852	0.21	65	6	23	29	1.30	0.74	0.43	0.41	1.97
8	M. Dense silty sand	10.00	206	143	0.830	0.21	65	6	21	26	1.30	0.75	0.33	0.32	1.54
9	M. Dense silty sand	11.00	225	153	0.809	0.21	65	6	20	26	1.30	0.74	0.31	0.30	1.43
10	M. Dense silty sand	12.00	245	163	0.787	0.21	65	6	20	25	1.30	0.73	0.29	0.28	1.35
11	M. Dense silty sand	13.00	265	173	0.766	0.21	65	6	19	25	1.30	0.72	0.28	0.26	1.28
12	M. Dense silty sand	14.00	285	183	0.744	0.20	65	6	18	24	1.30	0.71	0.27	0.25	1.23
13	M. Dense silty sand	15.00	305	193	0.724	0.20	65	6	18	24	1.30	0.70	0.26	0.24	1.19
	Mw=	***6.8***													
Layer #	Layer Name	Depth, m	σv	σ'v	rd	CSR	FC ,%	Δ(N1) 60	(N1) 60	(N1) 60cs	MSF	Kσ	$CRR_{M=7.5,\ \sigma'v=1atm}$	$CRR_{M=7,\ \sigma'v}$	FS= CRR/CSR
1	Loose silty sand	1.00	18	18	1.000	0.18	65	6	17	22	1.20	0.97	0.23	0.27	
2	Loose silty sand	2.00	37	37	0.985	0.17	65	6	17	22	1.20	0.95	0.23	0.27	
3	Loose silty sand	3.30	60	60	0.967	0.17	65	6	13	18	1.20	0.92	0.19	0.21	
4	Ignimbrite	6.40	136	108	0.917	0.20					1.20				
5	M. Dense silty sand	7.00	147	114	0.906	0.21	65	6	12	18	1.20	0.86	0.18	0.19	0.91
6	M. Dense silty sand	8.00	167	124	0.888	0.21	65	6	24	30	1.20	0.75	0.48	0.43	2.05
7	M. Dense silty sand	9.00	186	133	0.869	0.21	65	6	23	29	1.20	0.74	0.43	0.38	1.79
8	M. Dense silty sand	10.00	206	143	0.850	0.21	65	6	21	26	1.20	0.75	0.33	0.30	1.39
9	M. Dense silty sand	11.00	225	153	0.830	0.21	65	6	20	26	1.20	0.74	0.31	0.28	1.29
10	M. Dense silty sand	12.00	245	163	0.810	0.21	65	6	20	25	1.20	0.73	0.29	0.26	1.21
11	M. Dense silty sand	13.00	265	173	0.791	0.21	65	6	19	25	1.20	0.72	0.28	0.24	1.15
12	M. Dense silty sand	14.00	285	183	0.771	0.21	65	6	18	24	1.20	0.71	0.27	0.23	1.10
13	M. Dense silty sand	15.00	305	193	0.752	0.21	65	6	18	24	1.20	0.70	0.26	0.22	1.06
PIH	amax (g)														
	Mw=	***7***													
Layer #	Layer Name	Depth, m	σv	σ'v	rd	CSR	FC ,%	Δ(N1) 60	(N1) 60	(N1) 60cs	MSF	Kσ	$CRR_{M=7.5,\ \sigma'v=1atm}$	$CRR_{M=7,\ \sigma'v}$	FS= CRR/CSR
1	Loose silty sand	1.00	18	18	1.000	0.18	65	6	17	22	1.14	0.97	0.23	0.26	
2	Loose silty sand	2.00	37	37	0.987	0.17	65	6	17	22	1.14	0.95	0.23	0.25	
3	Loose silty sand	3.30	60	60	0.970	0.17	65	6	13	18	1.14	0.92	0.19	0.20	
4	Ignimbrite	6.40	136	108	0.925	0.20					1.14				
5	M. Dense silty sand	7.00	147	114	0.915	0.21	65	6	12	18	1.14	0.86	0.18	0.18	0.86
6	M. Dense silty sand	8.00	167	124	0.898	0.21	65	6	24	30	1.14	0.75	0.48	0.41	1.92
7	M. Dense silty sand	9.00	186	133	0.880	0.22	65	6	23	29	1.14	0.74	0.43	0.36	1.68
8	M. Dense silty sand	10.00	206	143	0.863	0.22	65	6	21	26	1.14	0.75	0.33	0.28	1.30
9	M. Dense silty sand	11.00	225	153	0.844	0.22	65	6	20	26	1.14	0.74	0.31	0.26	1.20
10	M. Dense silty sand	12.00	245	163	0.826	0.22	65	6	20	25	1.14	0.73	0.29	0.25	1.13
11	M. Dense silty sand	13.00	265	173	0.808	0.22	65	6	19	25	1.14	0.72	0.28	0.23	1.07
12	M. Dense silty sand	14.00	285	183	0.789	0.22	65	6	18	24	1.14	0.71	0.27	0.22	1.02
13	M. Dense silty sand	15.00	305	193	0.771	0.21	65	6	18	24	1.14	0.70	0.26	0.21	0.98

Layer #	Mw= 7.2 Layer Name	Depth, m	σv	σ'v	rd	CSR	FC ,%	Δ(N1) 60	(N1) 60	(N1) 60cs	MSF	Kσ	$CRR_{M=7.5, σ'v=1atm}$	$CRR_{M=7, σ'v}$	FS= CRR/CSR
1	Loose silty sand	1.00	18	18	0.997	0.18	65	6	17	22	1.08	0.97	0.23	0.25	
2	Loose silty sand	2.00	37	37	0.986	0.17	65	6	17	22	1.08	0.95	0.23	0.24	
3	Loose silty sand	3.30	60	60	0.970	0.17	65	6	13	18	1.08	0.92	0.19	0.19	
4	Ignimbrite	6.40	136	108	0.923	0.20					1.08				
5	M. Dense silty sand	7.00	147	114	0.913	0.21	65	6	12	18	1.08	0.86	0.18	0.17	0.82
6	M. Dense silty sand	8.00	167	124	0.895	0.21	65	6	24	30	1.08	0.75	0.48	0.39	1.83
7	M. Dense silty sand	9.00	186	133	0.878	0.22	65	6	23	29	1.08	0.74	0.43	0.34	1.60
8	M. Dense silty sand	10.00	206	143	0.859	0.22	65	6	21	26	1.08	0.75	0.33	0.27	1.24
9	M. Dense silty sand	11.00	225	153	0.841	0.22	65	6	20	26	1.08	0.74	0.31	0.25	1.15
10	M. Dense silty sand	12.00	245	163	0.822	0.22	65	6	20	25	1.08	0.73	0.29	0.23	1.08
11	M. Dense silty sand	13.00	265	173	0.803	0.22	65	6	19	25	1.08	0.72	0.28	0.22	1.02
12	M. Dense silty sand	14.00	285	183	0.785	0.21	65	6	18	24	1.08	0.71	0.27	0.21	0.97
13	M. Dense silty sand	15.00	305	193	0.766	0.21	65	6	18	24	1.08	0.70	0.26	0.20	0.93

Table C2. SPT based analysis output of NIB (amax=0.215g)

Layer #	Mw= 5.5 Layer Name	Depth, m	σv	σ'v	rd	CSR	FC ,%	Δ(N1) 60	(N1) 60	(N1) 60cs	MSF	Kσ	$CRR_{M=7.5, σ'v=1atm}$	$CRR_{M=7, σ'v}$	FS= CRR/CSR
1	silty sand (ash)	1.00	17	17	1.000	0.14	53	6	17	22	1.69	0.98	0.23	0.38	
2	silty sand (ash)	2.00	34	34	0.969	0.14	53	6	25	30	1.69	0.93	0.49	0.78	
3	silty sand (ash)	3.00	51	51	0.945	0.13	53	6	21	26	1.69	0.91	0.33	0.50	
4	silty sand (ash)	4.00	68	58	0.919	0.15	53	6	20	25	1.69	0.90	0.29	0.45	
5	silty sand (ash)	5.00	85	65	0.891	0.16	53	6	19	24	1.69	0.90	0.27	0.41	
6	Ignimbrite	6.40	117	83	0.850	0.17	53	6	0						
7	M. dense silty sand	7.00	127	88	0.832	0.17	53	6	22	28	1.69	0.84	0.39	0.54	3.23
8	M. dense silty sand	8.00	144	95	0.802	0.17	53	6	22	27	1.69	0.83	0.36	0.50	2.93
9	M. dense silty sand	9.00	161	102	0.771	0.17	53	6	17	23	1.69	0.85	0.24	0.35	2.06
10	M. dense silty sand	10.00	178	109	0.741	0.17	53	6	17	22	1.69	0.84	0.24	0.34	1.99
11	M. dense silty sand	11.00	195	116	0.710	0.17	53	6	19	24	1.69	0.82	0.28	0.38	2.29
12	M. dense silty sand	12.00	212	124	0.681	0.16	53	6	18	24	1.69	0.81	0.27	0.36	2.22
13	M. dense silty sand	13.00	229	131	0.652	0.16	53	6	21	27	1.69	0.77	0.34	0.44	2.77
14	M. dense silty sand	14.00	246	138	0.624	0.16	53	6	21	26	1.69	0.76	0.32	0.42	2.68
15	M. dense silty sand	15.00	263	145	0.597	0.15	53	6	12	18	1.69	0.82	0.18	0.25	1.66
16	M. dense silty sand	16.00	280	152	0.572	0.15	53	6	12	17	1.69	0.82	0.18	0.24	1.67
17	M. dense silty sand	17.00	297	160	0.547	0.14	53	6	15	21	1.69	0.78	0.22	0.29	2.02
18	M. dense silty sand	18.00	314	167	0.525	0.14	53	6	15	21	1.69	0.77	0.21	0.28	2.03
19	M. dense silty sand	19.00	331	174	0.503	0.13	53	6	15	20	1.69	0.76	0.21	0.27	2.03
20	M. dense silty sand	20.00	348	181	0.483	0.13	53	6	15	20	1.69	0.76	0.21	0.26	2.04

	Mw=	6												
Layer #	Layer Name	Depth, m	σv	σ'v	rd	CSR	FC ,%	Δ(N1)60	(N1)60	(N1) 60cs	MSF	Kσ	$CRR_{M=7.5, \sigma'v=1atm}$	$CRR_{M=7,\sigma'v}$	FS= CRR/CSR
1	silty sand (ash)	1.00	17	17	1.000	0.14	53	6	17	22	1.48	0.98	0.23	0.34	
2	silty sand (ash)	2.00	34	34	0.978	0.14	53	6	25	30	1.48	0.93	0.49	0.68	
3	silty sand (ash)	3.00	51	51	0.959	0.13	53	6	21	26	1.48	0.91	0.33	0.44	
4	silty sand (ash)	4.00	68	58	0.940	0.15	53	6	20	25	1.48	0.90	0.29	0.40	2.58
5	silty sand (ash)	5.00	85	65	0.918	0.17	53	6	19	24	1.48	0.90	0.27	0.36	2.17
6	Ignimbrite	6.40	117	83	0.887	0.17	53	6	0						
7	M. dense silty sand	7.00	127	88	0.873	0.18	53	6	22	28	1.48	0.84	0.39	0.48	2.71
8	M. dense silty sand	8.00	144	95	0.848	0.18	53	6	22	27	1.48	0.83	0.36	0.44	2.43
9	M. dense silty sand	9.00	161	102	0.824	0.18	53	6	17	23	1.48	0.85	0.24	0.31	1.70
10	M. dense silty sand	10.00	178	109	0.799	0.18	53	6	17	22	1.48	0.84	0.24	0.29	1.62
11	M. dense silty sand	11.00	195	116	0.774	0.18	53	6	19	24	1.48	0.82	0.28	0.33	1.84
12	M. dense silty sand	12.00	212	124	0.750	0.18	53	6	18	24	1.48	0.81	0.27	0.32	1.77
13	M. dense silty sand	13.00	229	131	0.726	0.18	53	6	21	27	1.48	0.77	0.34	0.39	2.19
14	M. dense silty sand	14.00	246	138	0.702	0.17	53	6	21	26	1.48	0.76	0.32	0.37	2.09
15	M. dense silty sand	15.00	263	145	0.679	0.17	53	6	12	18	1.48	0.82	0.18	0.22	1.28
16	M. dense silty sand	16.00	280	152	0.656	0.17	53	6	12	17	1.48	0.82	0.18	0.22	1.28
17	M. dense silty sand	17.00	297	160	0.635	0.17	53	6	15	21	1.48	0.78	0.22	0.25	1.53
18	M. dense silty sand	18.00	314	167	0.614	0.16	53	6	15	21	1.48	0.77	0.21	0.25	1.52
19	M. dense silty sand	19.00	331	174	0.595	0.16	53	6	15	20	1.48	0.76	0.21	0.24	1.51
20	M. dense silty sand	20.00	348	181	0.576	0.15	53	6	15	20	1.48	0.76	0.21	0.23	1.50
	Mw=	**6.5**												
Layer #	Layer Name	Depth, m	σv	σ'v	rd	CSR	FC ,%	Δ(N1)60	(N1)60	(N1) 60cs	MSF	Kσ	$CRR_{M=7.5, \sigma'v=1atm}$	$CRR_{M=7,\sigma'v}$	FS= CRR/CSR
1	silty sand (ash)	1.00	17	17	1.000	0.14	53	6	17	22	1.30	0.98	0.23	0.30	
2	silty sand (ash)	2.00	34	34	0.982	0.14	53	6	25	30	1.30	0.93	0.49	0.60	
3	silty sand (ash)	3.00	51	51	0.967	0.14	53	6	21	26	1.30	0.91	0.33	0.39	
4	silty sand (ash)	4.00	68	58	0.950	0.16	53	6	20	25	1.30	0.90	0.29	0.35	2.24
5	silty sand (ash)	5.00	85	65	0.932	0.17	53	6	19	24	1.30	0.90	0.27	0.32	1.88
6	Ignimbrite	6.40	117	83	0.905	0.18	53	6	0						
7	M. dense silty sand	7.00	127	88	0.893	0.18	53	6	22	28	1.30	0.84	0.39	0.42	2.32
8	M. dense silty sand	8.00	144	95	0.873	0.19	53	6	22	27	1.30	0.83	0.36	0.38	2.07
9	M. dense silty sand	9.00	161	102	0.852	0.19	53	6	17	23	1.30	0.85	0.24	0.27	1.44
10	M. dense silty sand	10.00	178	109	0.830	0.19	53	6	17	22	1.30	0.84	0.24	0.26	1.37
11	M. dense silty sand	11.00	195	116	0.809	0.19	53	6	19	24	1.30	0.82	0.28	0.29	1.55
12	M. dense silty sand	12.00	212	124	0.787	0.19	53	6	18	24	1.30	0.81	0.27	0.28	1.48
13	M. dense silty sand	13.00	229	131	0.766	0.19	53	6	21	27	1.30	0.77	0.34	0.34	1.82
14	M. dense silty sand	14.00	246	138	0.744	0.19	53	6	21	26	1.30	0.76	0.32	0.32	1.73
15	M. dense silty sand	15.00	263	145	0.724	0.18	53	6	12	18	1.30	0.82	0.18	0.19	1.06
16	M. dense silty sand	16.00	280	152	0.703	0.18	53	6	12	17	1.30	0.82	0.18	0.19	1.05
17	M. dense silty sand	17.00	297	160	0.684	0.18	53	6	15	21	1.30	0.78	0.22	0.22	1.25

18	M. dense silty sand	18.00	314	167	0.665	0.17	53	6	15	21	1.30	0.77	0.21	0.22	1.23
19	M. dense silty sand	19.00	331	174	0.647	0.17	53	6	15	20	1.30	0.76	0.21	0.21	1.22
20	M. dense silty sand	20.00	348	181	0.629	0.17	53	6	15	20	1.30	0.76	0.21	0.20	1.21
	Mw=	**6.8**													
Layer #	Layer Name	Depth, m	σv	σ'v	rd	CSR	FC ,%	Δ(N1)60	(N1)60	(N1) 60cs	MSF	Kσ	$CRR_{M=7.5, σ'v=1atm}$	$CRR_{M=7,σ'v}$	FS= CRR/CSR
1	silty sand (ash)	1.00	17	17	1.000	0.14	53	6	17	22	1.20	0.98	0.23	0.27	
2	silty sand (ash)	2.00	34	34	0.985	0.14	53	6	25	30	1.20	0.93	0.49	0.55	
3	silty sand (ash)	3.00	51	51	0.971	0.14	53	6	21	26	1.20	0.91	0.33	0.36	
4	silty sand (ash)	4.00	68	58	0.957	0.16	53	6	20	25	1.20	0.90	0.29	0.32	2.05
5	silty sand (ash)	5.00	85	65	0.941	0.17	53	6	19	24	1.20	0.90	0.27	0.29	1.72
6	Ignimbrite	6.40	117	83	0.917	0.18	53	6	0		1.20				
7	M. dense silty sand	7.00	127	88	0.906	0.18	53	6	22	28	1.20	0.84	0.39	0.39	2.12
8	M. dense silty sand	8.00	144	95	0.888	0.19	53	6	22	27	1.20	0.83	0.36	0.35	1.88
9	M. dense silty sand	9.00	161	102	0.869	0.19	53	6	17	23	1.20	0.85	0.24	0.25	1.30
10	M. dense silty sand	10.00	178	109	0.850	0.19	53	6	17	22	1.20	0.84	0.24	0.24	1.24
11	M. dense silty sand	11.00	195	116	0.830	0.19	53	6	19	24	1.20	0.82	0.28	0.27	1.40
12	M. dense silty sand	12.00	212	124	0.810	0.19	53	6	18	24	1.20	0.81	0.27	0.26	1.33
13	M. dense silty sand	13.00	229	131	0.791	0.19	53	6	21	27	1.20	0.77	0.34	0.31	1.63
14	M. dense silty sand	14.00	246	138	0.771	0.19	53	6	21	26	1.20	0.76	0.32	0.30	1.55
15	M. dense silty sand	15.00	263	145	0.752	0.19	53	6	12	18	1.20	0.82	0.18	0.18	0.94
16	M. dense silty sand	16.00	280	152	0.733	0.19	53	6	12	17	1.20	0.82	0.18	0.17	0.93
17	M. dense silty sand	17.00	297	160	0.715	0.19	53	6	15	21	1.20	0.78	0.22	0.21	1.10
18	M. dense silty sand	18.00	314	167	0.697	0.18	53	6	15	21	1.20	0.77	0.21	0.20	1.09
19	M. dense silty sand	19.00	331	174	0.680	0.18	53	6	15	20	1.20	0.76	0.21	0.19	1.07
20	M. dense silty sand	20.00	348	181	0.663	0.18	53	6	15	20	1.20	0.76	0.21	0.19	1.06
	Mw=	**7**													
Layer #	Layer Name	Depth, m	σv	σ'v	rd	CSR	FC ,%	Δ(N1)60	(N1)60	(N1) 60cs	MSF	Kσ	$CRR_{M=7.5, σ'v=1atm}$	$CRR_{M=7,σ'v}$	FS= CRR/CSR
1	silty sand (ash)	1.00	17	17	1.000	0.14	53	6	17	22	1.14	0.98	0.23	0.26	
2	silty sand (ash)	2.00	34	34	0.987	0.14	53	6	25	30	1.14	0.93	0.49	0.53	
3	silty sand (ash)	3.00	51	51	0.974	0.14	53	6	21	26	1.14	0.91	0.33	0.34	
4	silty sand (ash)	4.00	68	58	0.961	0.16	53	6	20	25	1.14	0.90	0.29	0.30	1.94
5	silty sand (ash)	5.00	85	65	0.946	0.17	53	6	19	24	1.14	0.90	0.27	0.28	1.62
6	Ignimbrite	6.40	117	83	0.925	0.18	53	6	0		1.14				
7	M. dense silty sand	7.00	127	88	0.915	0.19	53	6	22	28	1.14	0.84	0.39	0.37	1.99
8	M. dense silty sand	8.00	144	95	0.898	0.19	53	6	22	27	1.14	0.83	0.36	0.34	1.77
9	M. dense silty sand	9.00	161	102	0.880	0.19	53	6	17	23	1.14	0.85	0.24	0.24	1.22
10	M. dense silty sand	10.00	178	109	0.863	0.20	53	6	17	22	1.14	0.84	0.24	0.23	1.15
11	M. dense silty sand	11.00	195	116	0.844	0.20	53	6	19	24	1.14	0.82	0.28	0.26	1.30
12	M. dense silty sand	12.00	212	124	0.826	0.20	53	6	18	24	1.14	0.81	0.27	0.25	1.24
13	M. dense silty sand	13.00	229	131	0.808	0.20	53	6	21	27	1.14	0.77	0.34	0.30	1.51
14	M. dense silty sand	14.00	246	138	0.789	0.20	53	6	21	26	1.14	0.76	0.32	0.28	1.43

15	M. dense silty sand	15.00	263	145	0.771	0.20	53	6	12	18	1.14	0.82	0.18	0.17	0.87
16	M. dense silty sand	16.00	280	152	0.754	0.19	53	6	12	17	1.14	0.82	0.18	0.17	0.86
17	M. dense silty sand	17.00	297	160	0.736	0.19	53	6	15	21	1.14	0.78	0.22	0.19	1.02
18	M. dense silty sand	18.00	314	167	0.719	0.19	53	6	15	21	1.14	0.77	0.21	0.19	1.00
19	M. dense silty sand	19.00	331	174	0.703	0.19	53	6	15	20	1.14	0.76	0.21	0.18	0.98
20	M. dense silty sand	20.00	348	181	0.687	0.18	53	6	15	20	1.14	0.76	0.21	0.18	0.97
	Mw=	**7.2**													
Layer #	Layer Name	Depth, m	σv	σ'v	rd	CSR	FC ,%	Δ(N1)60	(N1)60	(N1) 60cs	MSF	Kσ	$CRR_{M=7.5, \sigma'v=1atm}$	$CRR_{M=7,\sigma'v}$	FS= CRR/CSR
1	silty sand (ash)	1.00	17	17	1.000	0.14	53	6	17	22	1.08	0.98	0.23	0.25	
2	silty sand (ash)	2.00	34	34	0.988	0.14	53	6	25	30	1.08	0.93	0.49	0.50	
3	silty sand (ash)	3.00	51	51	0.977	0.14	53	6	21	26	1.08	0.91	0.33	0.32	
4	silty sand (ash)	4.00	68	58	0.965	0.16	53	6	20	25	1.08	0.90	0.29	0.29	1.83
5	silty sand (ash)	5.00	85	65	0.952	0.17	53	6	19	24	1.08	0.90	0.27	0.26	1.53
6	Ignimbrite	6.40	117	83	0.932	0.18	53	6	0		1.08				
7	M. dense silty sand	7.00	127	88	0.924	0.19	53	6	22	28	1.08	0.84	0.39	0.35	1.87
8	M. dense silty sand	8.00	144	95	0.908	0.19	53	6	22	27	1.08	0.83	0.36	0.32	1.66
9	M. dense silty sand	9.00	161	102	0.892	0.20	53	6	17	23	1.08	0.85	0.24	0.22	1.14
10	M. dense silty sand	10.00	178	109	0.876	0.20	53	6	17	22	1.08	0.84	0.24	0.22	1.08
11	M. dense silty sand	11.00	195	116	0.859	0.20	53	6	19	24	1.08	0.82	0.28	0.24	1.21
12	M. dense silty sand	12.00	212	124	0.842	0.20	53	6	18	24	1.08	0.81	0.27	0.23	1.15
13	M. dense silty sand	13.00	229	131	0.825	0.20	53	6	21	27	1.08	0.77	0.34	0.28	1.40
14	M. dense silty sand	14.00	246	138	0.808	0.20	53	6	21	26	1.08	0.76	0.32	0.27	1.33
15	M. dense silty sand	15.00	263	145	0.791	0.20	53	6	12	18	1.08	0.82	0.18	0.16	0.80
16	M. dense silty sand	16.00	280	152	0.775	0.20	53	6	12	17	1.08	0.82	0.18	0.16	0.79
17	M. dense silty sand	17.00	297	160	0.758	0.20	53	6	15	21	1.08	0.78	0.22	0.18	0.94
18	M. dense silty sand	18.00	314	167	0.742	0.20	53	6	15	21	1.08	0.77	0.21	0.18	0.92
19	M. dense silty sand	19.00	331	174	0.727	0.19	53	6	15	20	1.08	0.76	0.21	0.17	0.90
20	M. dense silty sand	20.00	348	181	0.712	0.19	53	6	15	20	1.08	0.76	0.21	0.17	0.89

Table C3 to Table C6 are the output of simplified procedure (Andrus and stoke 2004) based on geotechnical investigation report

Table C3. Shear wave velocity based analysis output of PIH (amax =0.27g)

	Mw=	***5.5***														
Layer #	Layer Name	Depth, m	σv	σ'v	rd	CSR	FC , %	VS rec.(m/s)	CN	Vs1	Ka1	Ka2	VS1*	MSF	CRR	FS= CRR/CSR
1	Loose silty sand	1.0	18	18	1.000	0.18	65	138	1.5	211	1.0	1.0	200	2.21	NL	
2	Loose silty sand	2.0	37	37	0.969	0.17	65	138	1.3	177	1.0	1.0	200	2.21	NL	
3	Loose silty sand	3.3	60	60	0.937	0.16	65	138	1.1	156	1.0	1.0	200	2.21	NL	
4	Ignimbrite	6.4	136	108	0.850	0.19		3035			1.0				NL	
5	M. dense silty sand	7.0	147	114	0.832	0.19	65	167	1.0	162	1.0	1.0	200	2.21	0.26	1.36
6	M. dense silty sand	8.0	167	124	0.802	0.19	65	199	0.9	189	1.0	1.0	200	2.21	0.69	3.63
7	M. dense silty sand	9.0	186	133	0.771	0.19	65	199	0.9	185	1.0	1.0	200	2.21	0.55	2.92
8	M. dense silty sand	10.0	206	143	0.741	0.19	65	205	0.9	187	1.0	1.0	200	2.21	0.63	3.38
9	M. dense silty sand	11.0	225	153	0.710	0.18	65	205	0.9	184	1.0	1.0	200	2.21	0.53	2.88
10	M. dense silty sand	12.0	245	163	0.681	0.18	65	218	0.9	193	1.0	1.0	200	2.21	1.03	5.74
11	M. dense silty sand	13.0	265	173	0.652	0.18	65	218	0.9	190	1.0	1.0	200	2.21	0.77	4.41
12	M. dense silty sand	14.0	285	183	0.624	0.17	65	218	0.9	187	1.0	1.0	200	2.21	0.64	3.72
13	M. dense silty sand	15.0	305	193	0.597	0.17	65	218	0.8	185	1.0	1.0	200	2.21	0.55	3.32
	Mw=	**6**								EST. VS1						
Layer #	Layer Name	Depth, m	σv	σ'v	rd	CSR	FC , %	VS rec.(m/s)	CN	Vs1	Ka1	Ka2	VS1*	MSF	CRR	FS
1	Loose silty sand	1.0	18	18	1.000	0.18	65	138	1.5	211	1.0	1.0	200	1.77	NL	
2	Loose silty sand	2.0	37	37	0.978	0.17	65	138	1.3	177	1.0	1.0	200	1.77	NL	
3	Loose silty sand	3.3	60	60	0.954	0.17	65	138	1.1	156	1.0	1.0	200	1.77	NL	
4	Ignimbrite	6.4	136	108	0.887	0.20		3035			1.0				NL	
5	M. dense silty sand	7.0	147	114	0.873	0.20	65	167	1.0	162	1.0	1.0	200	1.77	0.21	1.04
6	M. dense silty sand	8.0	167	124	0.848	0.20	65	199	0.9	189	1.0	1.0	200	1.77	0.55	2.75
7	M. dense silty sand	9.0	186	133	0.824	0.20	65	199	0.9	185	1.0	1.0	200	1.77	0.44	2.19
8	M. dense silty sand	10.0	206	143	0.799	0.20	65	205	0.9	187	1.0	1.0	200	1.77	0.51	2.51
9	M. dense silty sand	11.0	225	153	0.774	0.20	65	205	0.9	184	1.0	1.0	200	1.77	0.42	2.12
10	M. dense silty sand	12.0	245	163	0.750	0.20	65	218	0.9	193	1.0	1.0	200	1.77	0.83	4.17
11	M. dense silty sand	13.0	265	173	0.726	0.20	65	218	0.9	190	1.0	1.0	200	1.77	0.62	3.17
12	M. dense silty sand	14.0	285	183	0.702	0.19	65	218	0.9	187	1.0	1.0	200	1.77	0.51	2.65
13	M. dense silty sand	15.0	305	193	0.679	0.19	65	218	0.8	185	1.0	1.0	200	1.77	0.44	2.34
	Mw=	**6.5**														
Layer #	Layer Name	Depth, m	σv	σ'v	rd	CSR	FC , %	VS rec.(m/s)	CN	Vs1	Ka1	Ka2	VS1*	MSF	CRR	FS
1	Loose silty sand	1.0	18	18	1.000	0.18	65	138	1.5	211	1.0	1.0	200	1.44	NL	
2	Loose silty sand	2.0	37	37	0.982	0.17	65	138	1.3	177	1.0	1.0	200	1.44	NL	
3	Loose silty sand	3.3	60	60	0.962	0.17	65	138	1.1	156	1.0	1.0	200	1.44	NL	
4	Ignimbrite	6.4	136	108	0.905	0.20		3035			1.0				NL	

5	M. dense silty sand	7.0	147	114	0.893	0.20	65	167	1.0	162	1.0	1.0	200	1.44	0.17	0.83
6	M. dense silty sand	8.0	167	124	0.873	0.21	65	199	0.9	189	1.0	1.0	200	1.44	0.45	2.18
7	M. dense silty sand	9.0	186	133	0.852	0.21	65	199	0.9	185	1.0	1.0	200	1.44	0.36	1.73
8	M. dense silty sand	10.0	206	143	0.830	0.21	65	205	0.9	187	1.0	1.0	200	1.44	0.41	1.97
9	M. dense silty sand	11.0	225	153	0.809	0.21	65	205	0.9	184	1.0	1.0	200	1.44	0.35	1.65
10	M. dense silty sand	12.0	245	163	0.787	0.21	65	218	0.9	193	1.0	1.0	200	1.44	0.67	3.24
11	M. dense silty sand	13.0	265	173	0.766	0.21	65	218	0.9	190	1.0	1.0	200	1.44	0.50	2.45
12	M. dense silty sand	14.0	285	183	0.744	0.20	65	218	0.9	187	1.0	1.0	200	1.44	0.41	2.04
13	M. dense silty sand	15.0	305	193	0.724	0.20	65	218	0.8	185	1.0	1.0	200	1.44	0.36	1.78
	Mw=	**6.8**														
Layer #	Layer Name	Depth, m	σv	σ'v	rd	CSR	FC , %	VS rec.(m/s)	CN	Vs1	Ka1	Ka2	VS1*	MSF	CRR	FS
1	Loose silty sand	1.0	18	18	1.000	0.18	65	138	1.5	211	1.0	1.0	200	1.28	NL	
2	Loose silty sand	2.0	37	37	0.985	0.17	65	138	1.3	177	1.0	1.0	200	1.28	NL	
3	Loose silty sand	3.3	60	60	0.967	0.17	65	138	1.1	156	1.0	1.0	200	1.28	NL	
4	Ignimbrite	6.4	136	108	0.917	0.20		3035			1.0			1.28	NL	
5	M. dense silty sand	7.0	147	114	0.906	0.21	65	167	1.0	162	1.0	1.0	200	1.28	0.15	0.73
6	M. dense silty sand	8.0	167	124	0.888	0.21	65	199	0.9	189	1.0	1.0	200	1.28	0.40	1.91
7	M. dense silty sand	9.0	186	133	0.869	0.21	65	199	0.9	185	1.0	1.0	200	1.28	0.32	1.51
8	M. dense silty sand	10.0	206	143	0.850	0.21	65	205	0.9	187	1.0	1.0	200	1.28	0.37	1.71
9	M. dense silty sand	11.0	225	153	0.830	0.21	65	205	0.9	184	1.0	1.0	200	1.28	0.31	1.43
10	M. dense silty sand	12.0	245	163	0.810	0.21	65	218	0.9	193	1.0	1.0	200	1.28	0.60	2.80
11	M. dense silty sand	13.0	265	173	0.791	0.21	65	218	0.9	190	1.0	1.0	200	1.28	0.45	2.11
12	M. dense silty sand	14.0	285	183	0.771	0.21	65	218	0.9	187	1.0	1.0	200	1.28	0.37	1.75
13	M. dense silty sand	15.0	305	193	0.752	0.21	65	218	0.8	185	1.0	1.0	200	1.28	0.32	1.53
	Mw=	**7**														
Layer #	Layer Name	Depth, m	σv	σ'v	rd	CSR	FC , %	VS rec.(m/s)	CN	Vs1	Ka1	Ka2	VS1*	MSF	CRR	FS
1	Loose silty sand	1.0	18	18	1.000	0.18	65	138	1.5	211	1.0	1.0	200	1.19	NL	
2	Loose silty sand	2.0	37	37	0.987	0.17	65	138	1.3	177	1.0	1.0	200	1.19	NL	
3	Loose silty sand	3.3	60	60	0.970	0.17	65	138	1.1	156	1.0	1.0	200	1.19	NL	
4	Ignimbrite	6.4	136	108	0.925	0.20		3035			1.0			1.19	NL	
5	M. dense silty sand	7.0	147	114	0.915	0.21	65	167	1.0	162	1.0	1.0	200	1.19	0.14	0.67
6	M. dense silty sand	8.0	167	124	0.898	0.21	65	199	0.9	189	1.0	1.0	200	1.19	0.37	1.75
7	M. dense silty sand	9.0	186	133	0.880	0.22	65	199	0.9	185	1.0	1.0	200	1.19	0.30	1.38
8	M. dense silty sand	10.0	206	143	0.863	0.22	65	205	0.9	187	1.0	1.0	200	1.19	0.34	1.56
9	M. dense silty sand	11.0	225	153	0.844	0.22	65	205	0.9	184	1.0	1.0	200	1.19	0.29	1.31
10	M. dense silty sand	12.0	245	163	0.826	0.22	65	218	0.9	193	1.0	1.0	200	1.19	0.56	2.55
11	M. dense silty sand	13.0	265	173	0.808	0.22	65	218	0.9	190	1.0	1.0	200	1.19	0.42	1.92
12	M. dense silty sand	14.0	285	183	0.789	0.22	65	218	0.9	187	1.0	1.0	200	1.19	0.34	1.59
13	M. dense silty sand	15.0	305	193	0.771	0.21	65	218	0.8	185	1.0	1.0	200	1.19	0.30	1.38
	Mw=	**7.2**														
Layer #	Layer Name	Depth, m	σv	σ'v	rd	CSR	FC , %	VS rec.(m/s)	CN	Vs1	Ka1	Ka2	VS1*	MSF	CRR	FS
1	Loose silty sand	1.0	18	18	1.000	0.18	65	138	1.5	211	1.0	1.0	200	1.11	NL	

2	Loose silty sand	2.0	37	37	0.988	0.17	65	138	1.3	177	1.0	1.0	200	1.11	NL	
3	Loose silty sand	3.3	60	60	0.974	0.17	65	138	1.1	156	1.0	1.0	200	1.11	NL	
4	Ignimbrite	6.4	136	108	0.932	0.21		3035			1.0			1.11	NL	
5	M. dense silty sand	7.0	147	114	0.924	0.21	65	167	1.0	162	1.0	1.0	200	1.11	0.13	0.62
6	M. dense silty sand	8.0	167	124	0.908	0.21	65	199	0.9	189	1.0	1.0	200	1.11	0.35	1.61
7	M. dense silty sand	9.0	186	133	0.892	0.22	65	199	0.9	185	1.0	1.0	200	1.11	0.28	1.27
8	M. dense silty sand	10.0	206	143	0.876	0.22	65	205	0.9	187	1.0	1.0	200	1.11	0.32	1.43
9	M. dense silty sand	11.0	225	153	0.859	0.22	65	205	0.9	184	1.0	1.0	200	1.11	0.27	1.20
10	M. dense silty sand	12.0	245	163	0.842	0.22	65	218	0.9	193	1.0	1.0	200	1.11	0.52	2.33
11	M. dense silty sand	13.0	265	173	0.825	0.22	65	218	0.9	190	1.0	1.0	200	1.11	0.39	1.75
12	M. dense silty sand	14.0	285	183	0.808	0.22	65	218	0.9	187	1.0	1.0	200	1.11	0.32	1.44
13	M. dense silty sand	15.0	305	193	0.791	0.22	65	218	0.8	185	1.0	1.0	200	1.11	0.28	1.26

Table C4. Shear wave velocity based analysis output of HIP (geotechnical inv. Data) (amax=0.235g)

		Mw=	***5.5***													
Layer #	Layer Name		Depth, m	σv	σ'v	rd	CSR	FC ,%	V_S rec. (m/s)	CN	Vs1	Ka1	Ka2	VS1*	MSF	CRR	FS= CRR/CSR
1	Silty Sand		1	13	13	0.991	0.15	53	113	1.67	189	1.0	1.0	200	2.21	NL	
2	Silty Sand		2	26	26	0.969	0.15	53	129	1.40	180	1.0	1.0	200	2.21	NL	
3	Silty Sand		3	41	41	0.945	0.14	53	145	1.25	182	1.0	1.0	200	2.21	NL	
4	Silty Sand		4	55	55	0.919	0.14	53	185	1.16	215	1.0	1.0	200	2.21	NL	
5	Silty Sand		5	69	69	0.891	0.14	53	185	1.10	203	1.0	1.0	200	2.21	NL	
6	Silty Sand		6	84	84	0.862	0.13	53	185	1.05	194	1.0	1.0	200	2.21	NL	
7	Silty Sand		7	98	98	0.832	0.13	53	196	1.01	197	1.0	1.0	200	2.21	NL	
8	Silty Sand		8	112	112	0.802	0.12	53	209	0.97	203	1.0	1.0	200	2.21	NL	
9	Silty Sand		9	126	126	0.771	0.12	53	221	0.94	208	1.0	1.0	200	2.21	NL	
10	Silty Sand		10	141	141	0.741	0.11	53	221	0.92	203	1.0	1.0	200	2.21	NL	
11	Silty Sand		11	155	145	0.710	0.12	53	217	0.91	198	1.0	1.0	200	2.21	3.34	28.80
12	Silty Sand		12	169	150	0.681	0.12	53	214	0.90	193	1.0	1.0	200	2.21	1.05	8.96
13	Silty Sand		13	184	154	0.652	0.12	53	213	0.90	191	1.0	1.0	200	2.21	0.86	7.26
14	Silty Sand		14	198	159	0.624	0.12	53	239	0.89	213	1.0	1.0	200	2.21	NL	
15	Silty Sand		15	212	163	0.597	0.12	53	215	0.88	190	1.0	1.0	200	2.21	0.78	6.60
16	Silty Sand		16	226	168	0.572	0.12	53	232	0.88	204	1.0	1.0	200	2.21	NL	
17	Silty Sand		17	241	172	0.547	0.12	53	230	0.87	201	1.0	1.0	200	2.21	NL	
18	Silty Sand		18	255	177	0.525	0.12	53	238	0.87	207	1.0	1.0	200	2.21	NL	
19	Silty Sand		19	269	181	0.503	0.11	53	248	0.86	214	1.0	1.0	200	2.21	NL	
20	Silty Sand		20	284	185	0.483	0.11	53	252	0.86	216	1.0	1.0	200	2.21	NL	
		Mw=	**6**													
Layer #	Layer Name		Depth, m	σv	σ'v	rd	CSR	FC ,%	V_S rec. (m/s)	CN	Vs1	Ka1	Ka2	VS1*	MSF	CRR	FS= CRR/CSR
1	Silty Sand		1	13	13	0.994	0.15	53	113	1.67	189	1.0	1.0	200	1.77	NL	
2	Silty Sand		2	26	26	0.978	0.15	53	129	1.40	180	1.0	1.0	200	1.77	NL	

3	Silty Sand		3	41	41	0.959	0.15	53	145	1.25	182	1.0	1.0	200	1.77	NL	
4	Silty Sand		4	55	55	0.940	0.14	53	185	1.16	215	1.0	1.0	200	1.77	NL	
5	Silty Sand		5	69	69	0.918	0.14	53	185	1.10	203	1.0	1.0	200	1.77	NL	
6	Silty Sand		6	84	84	0.896	0.14	53	185	1.05	194	1.0	1.0	200	1.77	NL	
7	Silty Sand		7	98	98	0.873	0.13	53	196	1.01	197	1.0	1.0	200	1.77	NL	
8	Silty Sand		8	112	112	0.848	0.13	53	209	0.97	203	1.0	1.0	200	1.77	NL	
9	Silty Sand		9	126	126	0.824	0.13	53	221	0.94	208	1.0	1.0	200	1.77	NL	
10	Silty Sand		10	141	141	0.799	0.12	53	221	0.92	203	1.0	1.0	200	1.77	NL	
11	Silty Sand		11	155	145	0.774	0.13	53	217	0.91	198	1.0	1.0	200	1.77	2.67	21.14
12	Silty Sand		12	169	150	0.750	0.13	53	214	0.90	193	1.0	1.0	200	1.77	0.84	6.51
13	Silty Sand		13	184	154	0.726	0.13	53	213	0.90	191	1.0	1.0	200	1.77	0.69	5.22
14	Silty Sand		14	198	159	0.702	0.13	53	239	0.89	213	1.0	1.0	200	1.77	NL	
15	Silty Sand		15	212	163	0.679	0.13	53	215	0.88	190	1.0	1.0	200	1.77	0.63	4.64
16	Silty Sand		16	226	168	0.656	0.14	53	232	0.88	204	1.0	1.0	200	1.77	NL	
17	Silty Sand		17	241	172	0.635	0.14	53	230	0.87	201	1.0	1.0	200	1.77	NL	
18	Silty Sand		18	255	177	0.614	0.14	53	238	0.87	207	1.0	1.0	200	1.77	NL	
19	Silty Sand		19	269	181	0.595	0.14	53	248	0.86	214	1.0	1.0	200	1.77	NL	
20	Silty Sand		20	284	185	0.576	0.13	53	252	0.86	216	1.0	1.0	200	1.77	NL	
		Mw=	**6.5**														
Layer #	Layer Name		Depth, m	σv	σ'v	rd	CSR	FC ,%	V_S rec. (m/s)	CN	Vs1	Ka1	Ka2	VS1*	MSF	CRR	FS= CRR/CSR
1	Silty Sand		1	13	13	0.996	0.15	53	113	1.67	189	1.0	1.0	200	1.44	NL	
2	Silty Sand		2	26	26	0.982	0.15	53	129	1.40	180	1.0	1.0	200	1.44	NL	
3	Silty Sand		3	41	41	0.967	0.15	53	145	1.25	182	1.0	1.0	200	1.44	NL	
4	Silty Sand		4	55	55	0.950	0.15	53	185	1.16	215	1.0	1.0	200	1.44	NL	
5	Silty Sand		5	69	69	0.932	0.14	53	185	1.10	203	1.0	1.0	200	1.44	NL	
6	Silty Sand		6	84	84	0.913	0.14	53	185	1.05	194	1.0	1.0	200	1.44	NL	
7	Silty Sand		7	98	98	0.893	0.14	53	196	1.01	197	1.0	1.0	200	1.44	NL	
8	Silty Sand		8	112	112	0.873	0.13	53	209	0.97	203	1.0	1.0	200	1.44	NL	
9	Silty Sand		9	126	126	0.852	0.13	53	221	0.94	208	1.0	1.0	200	1.44	NL	
10	Silty Sand		10	141	141	0.830	0.13	53	221	0.92	203	1.0	1.0	200	1.44	NL	
11	Silty Sand		11	155	145	0.809	0.13	53	217	0.91	198	1.0	1.0	200	1.44	2.18	16.49
12	Silty Sand		12	169	150	0.787	0.14	53	214	0.90	193	1.0	1.0	200	1.44	0.69	5.05
13	Silty Sand		13	184	154	0.766	0.14	53	213	0.90	191	1.0	1.0	200	1.44	0.56	4.03
14	Silty Sand		14	198	159	0.744	0.14	53	239	0.89	213	1.0	1.0	200	1.44	NL	
15	Silty Sand		15	212	163	0.724	0.14	53	215	0.88	190	1.0	1.0	200	1.44	0.51	3.55
16	Silty Sand		16	226	168	0.703	0.15	53	232	0.88	204	1.0	1.0	200	1.44	NL	
17	Silty Sand		17	241	172	0.684	0.15	53	230	0.87	201	1.0	1.0	200	1.44	NL	
18	Silty Sand		18	255	177	0.665	0.15	53	238	0.87	207	1.0	1.0	200	1.44	NL	
19	Silty Sand		19	269	181	0.647	0.15	53	248	0.86	214	1.0	1.0	200	1.44	NL	
20	Silty Sand		20	284	185	0.629	0.15	53	252	0.86	216	1.0	1.0	200	1.44	NL	
		Mw=	**6.8**														
Layer #	Layer Name		Depth, m	σv	σ'v	rd	CSR	FC ,%	V_S rec. (m/s)	CN	Vs1	Ka1	Ka2	VS1*	MSF	CRR	FS= CRR/CSR
1	Silty Sand		1	13	13	0.997	0.15	53	113	1.67	189	1.0	1.0	200	1.28	NL	

2	Silty Sand		2	26	26	0.985	0.15	53	129	1.40	180	1.0	1.0	200	1.28	NL	
3	Silty Sand		3	41	41	0.971	0.15	53	145	1.25	182	1.0	1.0	200	1.28	NL	
4	Silty Sand		4	55	55	0.957	0.15	53	185	1.16	215	1.0	1.0	200	1.28	NL	
5	Silty Sand		5	69	69	0.941	0.14	53	185	1.10	203	1.0	1.0	200	1.28	NL	
6	Silty Sand		6	84	84	0.924	0.14	53	185	1.05	194	1.0	1.0	200	1.28	NL	
7	Silty Sand		7	98	98	0.906	0.14	53	196	1.01	197	1.0	1.0	200	1.28	NL	
8	Silty Sand		8	112	112	0.888	0.14	53	209	0.97	203	1.0	1.0	200	1.28	NL	
9	Silty Sand		9	126	126	0.869	0.13	53	221	0.94	208	1.0	1.0	200	1.28	NL	
10	Silty Sand		10	141	141	0.850	0.13	53	221	0.92	203	1.0	1.0	200	1.28	NL	
11	Silty Sand		11	155	145	0.830	0.14	53	217	0.91	198	1.0	1.0	200	1.28	1.94	14.32
12	Silty Sand		12	169	150	0.810	0.14	53	214	0.90	193	1.0	1.0	200	1.28	0.61	4.37
13	Silty Sand		13	184	154	0.791	0.14	53	213	0.90	191	1.0	1.0	200	1.28	0.50	3.48
14	Silty Sand		14	198	159	0.771	0.15	53	239	0.89	213	1.0	1.0	200	1.28	NL	
15	Silty Sand		15	212	163	0.752	0.15	53	215	0.88	190	1.0	1.0	200	1.28	0.45	3.04
16	Silty Sand		16	226	168	0.733	0.15	53	232	0.88	204	1.0	1.0	200	1.28	NL	
17	Silty Sand		17	241	172	0.715	0.15	53	230	0.87	201	1.0	1.0	200	1.28	NL	
18	Silty Sand		18	255	177	0.697	0.15	53	238	0.87	207	1.0	1.0	200	1.28	NL	
19	Silty Sand		19	269	181	0.680	0.15	53	248	0.86	214	1.0	1.0	200	1.28	NL	
20	Silty Sand		20	284	185	0.663	0.15	53	252	0.86	216	1.0	1.0	200	1.28	NL	
		Mw=	**7**														
Layer #	Layer Name		Depth, m	σv	σ'v	rd	CSR	FC ,%	V_S rec. (m/s)	CN	Vs1	Ka1	Ka2	VS1*	MSF	CRR	FS= CRR/CSR
1	Silty Sand		1	13	13	0.997	0.15	53	113	1.67	189	1.0	1.0	200	1.19	NL	
2	Silty Sand		2	26	26	0.987	0.15	53	129	1.40	180	1.0	1.0	200	1.19	NL	
3	Silty Sand		3	41	41	0.974	0.15	53	145	1.25	182	1.0	1.0	200	1.19	NL	
4	Silty Sand		4	55	55	0.961	0.15	53	185	1.16	215	1.0	1.0	200	1.19	NL	
5	Silty Sand		5	69	69	0.946	0.14	53	185	1.10	203	1.0	1.0	200	1.19	NL	
6	Silty Sand		6	84	84	0.931	0.14	53	185	1.05	194	1.0	1.0	200	1.19	NL	
7	Silty Sand		7	98	98	0.915	0.14	53	196	1.01	197	1.0	1.0	200	1.19	NL	
8	Silty Sand		8	112	112	0.898	0.14	53	209	0.97	203	1.0	1.0	200	1.19	NL	
9	Silty Sand		9	126	126	0.880	0.13	53	221	0.94	208	1.0	1.0	200	1.19	NL	
10	Silty Sand		10	141	141	0.863	0.13	53	221	0.92	203	1.0	1.0	200	1.19	NL	
11	Silty Sand		11	155	145	0.844	0.14	53	217	0.91	198	1.0	1.0	200	1.19	1.80	13.07
12	Silty Sand		12	169	150	0.826	0.14	53	214	0.90	193	1.0	1.0	200	1.19	0.57	3.98
13	Silty Sand		13	184	154	0.808	0.15	53	213	0.90	191	1.0	1.0	200	1.19	0.46	3.16
14	Silty Sand		14	198	159	0.789	0.15	53	239	0.89	213	1.0	1.0	200	1.19	NL	
15	Silty Sand		15	212	163	0.771	0.15	53	215	0.88	190	1.0	1.0	200	1.19	0.42	2.75
16	Silty Sand		16	226	168	0.754	0.16	53	232	0.88	204	1.0	1.0	200	1.19	NL	
17	Silty Sand		17	241	172	0.736	0.16	53	230	0.87	201	1.0	1.0	200	1.19	NL	
18	Silty Sand		18	255	177	0.719	0.16	53	238	0.87	207	1.0	1.0	200	1.19	NL	
19	Silty Sand		19	269	181	0.703	0.16	53	248	0.86	214	1.0	1.0	200	1.19	NL	
20	Silty Sand		20	284	185	0.687	0.16	53	252	0.86	216	1.0	1.0	200	1.19	NL	
		Mw=	**7.2**														
Layer #	Layer Name		Depth, m	σv	σ'v	rd	CSR	FC ,%	V_S rec. (m/s)	CN	Vs1	Ka1	Ka2	VS1*	MSF	CRR	FS= CRR/CSR

1	Silty Sand	1	13	13	0.998	0.15	53	113	1.67	189	1.0	1.0	200	1.11	NL	
2	Silty Sand	2	26	26	0.988	0.15	53	129	1.40	180	1.0	1.0	200	1.11	NL	
3	Silty Sand	3	41	41	0.977	0.15	53	145	1.25	182	1.0	1.0	200	1.11	NL	
4	Silty Sand	4	55	55	0.965	0.15	53	185	1.16	215	1.0	1.0	200	1.11	NL	
5	Silty Sand	5	69	69	0.952	0.15	53	185	1.10	203	1.0	1.0	200	1.11	NL	
6	Silty Sand	6	84	84	0.938	0.14	53	185	1.05	194	1.0	1.0	200	1.11	NL	
7	Silty Sand	7	98	98	0.924	0.14	53	196	1.01	197	1.0	1.0	200	1.11	NL	
8	Silty Sand	8	112	112	0.908	0.14	53	209	0.97	203	1.0	1.0	200	1.11	NL	
9	Silty Sand	9	126	126	0.892	0.14	53	221	0.94	208	1.0	1.0	200	1.11	NL	
10	Silty Sand	10	141	141	0.876	0.13	53	221	0.92	203	1.0	1.0	200	1.11	NL	
11	Silty Sand	11	155	145	0.859	0.14	53	217	0.91	198	1.0	1.0	200	1.11	1.67	11.95
12	Silty Sand	12	169	150	0.842	0.15	53	214	0.90	193	1.0	1.0	200	1.11	0.53	3.63
13	Silty Sand	13	184	154	0.825	0.15	53	213	0.90	191	1.0	1.0	200	1.11	0.43	2.88
14	Silty Sand	14	198	159	0.808	0.15	53	239	0.89	213	1.0	1.0	200	1.11	NL	
15	Silty Sand	15	212	163	0.791	0.16	53	215	0.88	190	1.0	1.0	200	1.11	0.39	2.50
16	Silty Sand	16	226	168	0.775	0.16	53	232	0.88	204	1.0	1.0	200	1.11	NL	
17	Silty Sand	17	241	172	0.758	0.16	53	230	0.87	201	1.0	1.0	200	1.11	NL	
18	Silty Sand	18	255	177	0.742	0.16	53	238	0.87	207	1.0	1.0	200	1.11	NL	
19	Silty Sand	19	269	181	0.727	0.17	53	248	0.86	214	1.0	1.0	200	1.11	NL	
20	Silty Sand	20	284	185	0.712	0.17	53	252	0.86	216	1.0	1.0	200	1.11	NL	

Table C5 Shear wave velocity based analysis output of NIB (amax=0.215g)

	Mw=	***5.5***														
Layer #	Layer Name	Depth, m	σv	σ'v	rd	CSR	FC,%	Vs rec. (m/s)	CN	Vs1	Ka1	Ka2	VS1*	MSF	CRR	FS= CRR/CSR
1	silty sand (ash)	1.00	17	17	0.991	0.14	53	146	1.56	227	1.00	1.00	200	2.21	NL	
2	silty sand (ash)	2.00	34	34	0.969	0.14	53	146	1.31	191	1.00	1.00	200	2.21	NL	
3	silty sand (ash)	3.00	51	51	0.945	0.13	53	146	1.18	173	1.00	1.00	200	2.21	NL	
4	silty sand (ash)	4.00	68	58	0.919	0.15	53	162	1.14	185	1.00	1.00	200	2.21	0.56	3.75
5	silty sand (ash)	5.00	85	65	0.891	0.16	53	162	1.11	180	1.00	1.00	200	2.21	0.44	2.71
6	Ignimbrite	6.40	92	58	0.850	0.19	53	2470								
7	M. dense silty sand	7.00	116	72	0.832	0.19	53	185	1.09	201	1.00	1.00	200	2.21	NL	
8	M. dense silty sand	8.00	133	79	0.802	0.19	53	190	1.06	201	1.00	1.00	200	2.21	NL	
9	M. dense silty sand	9.00	150	86	0.771	0.19	53	192	1.04	199	1.00	1.00	200	2.21	7.78	
10	M. dense silty sand	10.00	167	94	0.741	0.18	53	192	1.02	195	1.00	1.00	200	2.21	1.46	7.90
11	M. dense silty sand	11.00	184	101	0.710	0.18	53	204	1.00	204	1.00	1.00	200	2.21	NL	
12	M. dense silty sand	12.00	201	108	0.681	0.18	53	204	0.98	200	1.00	1.00	200	2.21	NL	
13	M. dense silty sand	13.00	218	115	0.652	0.17	53	216	0.97	209	1.00	1.00	200	2.21	NL	
14	M. dense silty sand	14.00	235	122	0.624	0.17	53	216	0.95	205	1.00	1.00	200	2.21	NL	
15	M. dense silty sand	15.00	252	129	0.597	0.16	53	203	0.94	190	1.00	1.00	200	2.21	0.78	4.84
16	M. dense silty sand	16.00	269	137	0.572	0.16	53	203	0.92	188	1.00	1.00	200	2.21	0.65	4.12
17	M. dense silty sand	17.00	278	141	0.547	0.15	53	224	0.92	205	1.00	1.00	200	2.21	NL	

18	M. dense silty sand	18.00	295	148	0.525	0.15	53	230	0.91	208	1.00	1.00	200	2.21	NL	
19	M. dense silty sand	19.00	312	155	0.503	0.14	53	240	0.90	215	1.00	1.00	200	2.21	NL	
20	M. dense silty sand	20.00	329	162	0.483	0.14	53	244	0.89	216	1.00	1.00	200	2.21	NL	
	Mw=	**6.0**														
Layer #	Layer Name	Depth, m	σv	σ'v	rd	CSR	FC,%	Vs rec. (m/s)	CN	Vs1	Ka1	Ka2	VS1*	MSF	CRR	FS= CRR/CSR
1	silty sand (ash)	1.00	17	17	0.994	0.14	53	146	1.56	227	1.00	1.00	200	1.77	NL	
2	silty sand (ash)	2.00	34	34	0.978	0.14	53	146	1.31	191	1.00	1.00	200	1.77	NL	
3	silty sand (ash)	3.00	51	51	0.959	0.13	53	146	1.18	173	1.00	1.00	200	1.77	NL	
4	silty sand (ash)	4.00	68	58	0.940	0.15	53	162	1.14	185	1.00	1.00	200	1.77	0.45	2.94
5	silty sand (ash)	5.00	85	65	0.918	0.17	53	162	1.11	180	1.00	1.00	200	1.77	0.35	2.11
6	Ignimbrite	6.40	92	58	0.887	0.19	53	2470								
7	M. dense silty sand	7.00	116	72	0.873	0.20	53	185	1.09	201	1.00	1.00	200	1.77	NL	
8	M. dense silty sand	8.00	133	79	0.848	0.20	53	190	1.06	201	1.00	1.00	200	1.77	NL	
9	M. dense silty sand	9.00	150	86	0.824	0.20	53	192	1.04	199	1.00	1.00	200	1.77	6.23	
10	M. dense silty sand	10.00	167	94	0.799	0.20	53	192	1.02	195	1.00	1.00	200	1.77	1.17	5.86
11	M. dense silty sand	11.00	184	101	0.774	0.20	53	204	1.00	204	1.00	1.00	200	1.77	NL	
12	M. dense silty sand	12.00	201	108	0.750	0.19	53	204	0.98	200	1.00	1.00	200	1.77	NL	
13	M. dense silty sand	13.00	218	115	0.726	0.19	53	216	0.97	209	1.00	1.00	200	1.77	NL	
14	M. dense silty sand	14.00	235	122	0.702	0.19	53	216	0.95	205	1.00	1.00	200	1.77	NL	
15	M. dense silty sand	15.00	252	129	0.679	0.18	53	203	0.94	190	1.00	1.00	200	1.77	0.63	3.40
16	M. dense silty sand	16.00	269	137	0.656	0.18	53	203	0.92	188	1.00	1.00	200	1.77	0.52	2.87
17	M. dense silty sand	17.00	278	141	0.635	0.18	53	224	0.92	205	1.00	1.00	200	1.77	NL	
18	M. dense silty sand	18.00	295	148	0.614	0.17	53	230	0.91	208	1.00	1.00	200	1.77	NL	
19	M. dense silty sand	19.00	312	155	0.595	0.17	53	240	0.90	215	1.00	1.00	200	1.77	NL	
20	M. dense silty sand	20.00	329	162	0.576	0.16	53	244	0.89	216	1.00	1.00	200	1.77	NL	
	Mw=	**6.5**														
Layer #	Layer Name	Depth, m	σv	σ'v	rd	CSR	FC,%	Vs rec. (m/s)	CN	Vs1	Ka1	Ka2	VS1*	MSF	CRR	FS= CRR/CSR
1	silty sand (ash)	1.00	17	17	0.996	0.14	53	146	1.56	227	1.00	1.00	200	1.44	NL	
2	silty sand (ash)	2.00	34	34	0.982	0.14	53	146	1.31	191	1.00	1.00	200	1.44	NL	
3	silty sand (ash)	3.00	51	51	0.967	0.14	53	146	1.18	173	1.00	1.00	200	1.44	NL	
4	silty sand (ash)	4.00	68	58	0.950	0.16	53	162	1.14	185	1.00	1.00	200	1.44	0.37	2.37
5	silty sand (ash)	5.00	85	65	0.932	0.17	53	162	1.11	180	1.00	1.00	200	1.44	0.29	1.69
6	Ignimbrite	6.40	92	58	0.905	0.20	53	2470								
7	M. dense silty sand	7.00	116	72	0.893	0.20	53	185	1.09	201	1.00	1.00	200	1.44	NL	
8	M. dense silty sand	8.00	133	79	0.873	0.20	53	190	1.06	201	1.00	1.00	200	1.44	NL	
9	M. dense silty sand	9.00	150	86	0.852	0.21	53	192	1.04	199	1.00	1.00	200	1.44	5.07	
10	M. dense silty sand	10.00	167	94	0.830	0.21	53	192	1.02	195	1.00	1.00	200	1.44	0.95	4.59
11	M. dense silty sand	11.00	184	101	0.809	0.21	53	204	1.00	204	1.00	1.00	200	1.44	NL	
12	M. dense silty sand	12.00	201	108	0.787	0.20	53	204	0.98	200	1.00	1.00	200	1.44	NL	
13	M. dense silty sand	13.00	218	115	0.766	0.20	53	216	0.97	209	1.00	1.00	200	1.44	NL	
14	M. dense silty sand	14.00	235	122	0.744	0.20	53	216	0.95	205	1.00	1.00	200	1.44	NL	
15	M. dense silty sand	15.00	252	129	0.724	0.20	53	203	0.94	190	1.00	1.00	200	1.44	0.51	2.60
16	M. dense silty sand	16.00	269	137	0.703	0.19	53	203	0.92	188	1.00	1.00	200	1.44	0.42	2.18

17	M. dense silty sand		17.00	278	141	0.684	0.19	53	224	0.92	205	1.00	1.00	200	1.44	NL	
18	M. dense silty sand		18.00	295	148	0.665	0.19	53	230	0.91	208	1.00	1.00	200	1.44	NL	
19	M. dense silty sand		19.00	312	155	0.647	0.18	53	240	0.90	215	1.00	1.00	200	1.44	NL	
20	M. dense silty sand		20.00	329	162	0.629	0.18	53	244	0.89	216	1.00	1.00	200	1.44	NL	
		Mw=	**6.8**														
Layer #	Layer Name		Depth, m	σv	σ'v	rd	CSR	FC,%	Vs rec. (m/s)	CN	Vs1	Ka1	Ka2	VS1*	MSF	CRR	FS= CRR/CSR
1	silty sand (ash)		1.00	17	17	0.997	0.14	53	146	1.56	227	1.00	1.00	200	1.28	NL	
2	silty sand (ash)		2.00	34	34	0.985	0.14	53	146	1.31	191	1.00	1.00	200	1.28	NL	
3	silty sand (ash)		3.00	51	51	0.971	0.14	53	146	1.18	173	1.00	1.00	200	1.28	NL	
4	silty sand (ash)		4.00	68	58	0.957	0.16	53	162	1.14	185	1.00	1.00	200	1.28	0.33	2.09
5	silty sand (ash)		5.00	85	65	0.941	0.17	53	162	1.11	180	1.00	1.00	200	1.28	0.26	1.49
6	Ignimbrite		6.40	92	58	0.917	0.20	53	2470								
7	M. dense silty sand		7.00	116	72	0.906	0.20	53	185	1.09	201	1.00	1.00	200	1.28	NL	
8	M. dense silty sand		8.00	133	79	0.888	0.21	53	190	1.06	201	1.00	1.00	200	1.28	NL	
9	M. dense silty sand		9.00	150	86	0.869	0.21	53	192	1.04	199	1.00	1.00	200	1.28	4.52	21.49
10	M. dense silty sand		10.00	167	94	0.850	0.21	53	192	1.02	195	1.00	1.00	200	1.28	0.85	4.00
11	M. dense silty sand		11.00	184	101	0.830	0.21	53	204	1.00	204	1.00	1.00	200	1.28	NL	
12	M. dense silty sand		12.00	201	108	0.810	0.21	53	204	0.98	200	1.00	1.00	200	1.28	NL	
13	M. dense silty sand		13.00	218	115	0.791	0.21	53	216	0.97	209	1.00	1.00	200	1.28	NL	
14	M. dense silty sand		14.00	235	122	0.771	0.21	53	216	0.95	205	1.00	1.00	200	1.28	NL	
15	M. dense silty sand		15.00	252	129	0.752	0.20	53	203	0.94	190	1.00	1.00	200	1.28	0.46	2.23
16	M. dense silty sand		16.00	269	137	0.733	0.20	53	203	0.92	188	1.00	1.00	200	1.28	0.38	1.86
17	M. dense silty sand		17.00	278	141	0.715	0.20	53	224	0.92	205	1.00	1.00	200	1.28	NL	
18	M. dense silty sand		18.00	295	148	0.697	0.19	53	230	0.91	208	1.00	1.00	200	1.28	NL	
19	M. dense silty sand		19.00	312	155	0.680	0.19	53	240	0.90	215	1.00	1.00	200	1.28	NL	
20	M. dense silty sand		20.00	329	162	0.663	0.19	53	244	0.89	216	1.00	1.00	200	1.28	NL	
		Mw=	**7.0**														
Layer #	Layer Name		Depth, m	σv	σ'v	rd	CSR	FC,%	Vs rec. (m/s)	CN	Vs1	Ka1	Ka2	VS1*	MSF	CRR	FS= CRR/CSR
1	silty sand (ash)		1.00	17	17	0.998	0.14	53	146	1.56	227	1.00	1.00	200	1.19	NL	
2	silty sand (ash)		2.00	34	34	0.987	0.14	53	146	1.31	191	1.00	1.00	200	1.19	NL	
3	silty sand (ash)		3.00	51	51	0.974	0.14	53	146	1.18	173	1.00	1.00	200	1.19	NL	
4	silty sand (ash)		4.00	68	58	0.961	0.16	53	162	1.14	185	1.00	1.00	200	1.19	0.30	1.93
5	silty sand (ash)		5.00	85	65	0.946	0.17	53	162	1.11	180	1.00	1.00	200	1.19	0.24	1.38
6	Ignimbrite		6.40	92	58	0.925	0.20	53	2470								
7	M. dense silty sand		7.00	116	72	0.915	0.21	53	185	1.09	201	1.00	1.00	200	1.19	NL	
8	M. dense silty sand		8.00	133	79	0.898	0.21	53	190	1.06	201	1.00	1.00	200	1.19	NL	
9	M. dense silty sand		9.00	150	86	0.880	0.21	53	192	1.04	199	1.00	1.00	200	1.19	4.20	
10	M. dense silty sand		10.00	167	94	0.863	0.21	53	192	1.02	195	1.00	1.00	200	1.19	0.79	3.66
11	M. dense silty sand		11.00	184	101	0.844	0.22	53	204	1.00	204	1.00	1.00	200	1.19	NL	
12	M. dense silty sand		12.00	201	108	0.826	0.21	53	204	0.98	200	1.00	1.00	200	1.19	NL	
13	M. dense silty sand		13.00	218	115	0.808	0.21	53	216	0.97	209	1.00	1.00	200	1.19	NL	
14	M. dense silty sand		14.00	235	122	0.789	0.21	53	216	0.95	205	1.00	1.00	200	1.19	NL	
15	M. dense silty sand		15.00	252	129	0.771	0.21	53	203	0.94	190	1.00	1.00	200	1.19	0.42	2.02

16	M. dense silty sand	16.00	269	137	0.754	0.21	53	203	0.92	188	1.00	1.00	200	1.19	0.35	1.68
17	M. dense silty sand	17.00	278	141	0.736	0.20	53	224	0.92	205	1.00	1.00	200	1.19	NL	
18	M. dense silty sand	18.00	295	148	0.719	0.20	53	230	0.91	208	1.00	1.00	200	1.19	NL	
19	M. dense silty sand	19.00	312	155	0.703	0.20	53	240	0.90	215	1.00	1.00	200	1.19	NL	
20	M. dense silty sand	20.00	329	162	0.687	0.19	53	244	0.89	216	1.00	1.00	200	1.19	NL	
	Mw=	**7.2**														
Layer #	Layer Name	Depth, m	σv	σ'v	rd	CSR	FC,%	Vs rec. (m/s)	CN	Vs1	Ka1	Ka2	VS1*	MSF	CRR	FS= CRR/CSR
1	silty sand (ash)	1.00	17	17	0.998	0.14	53	146	1.56	227	1.00	1.00	200	1.11	NL	
2	silty sand (ash)	2.00	34	34	0.988	0.14	53	146	1.31	191	1.00	1.00	200	1.11	NL	
3	silty sand (ash)	3.00	51	51	0.977	0.14	53	146	1.18	173	1.00	1.00	200	1.11	NL	
4	silty sand (ash)	4.00	68	58	0.965	0.16	53	162	1.14	185	1.00	1.00	200	1.11	0.28	1.79
5	silty sand (ash)	5.00	85	65	0.952	0.17	53	162	1.11	180	1.00	1.00	200	1.11	0.22	1.27
6	Ignimbrite	6.40	92	58	0.932	0.20	53	2470								
7	M. dense silty sand	7.00	116	72	0.924	0.21	53	185	1.09	201	1.00	1.00	200	1.11	NL	
8	M. dense silty sand	8.00	133	79	0.908	0.21	53	190	1.06	201	1.00	1.00	200	1.11	NL	
9	M. dense silty sand	9.00	150	86	0.892	0.22	53	192	1.04	199	1.00	1.00	200	1.11	3.91	
10	M. dense silty sand	10.00	167	94	0.876	0.22	53	192	1.02	195	1.00	1.00	200	1.11	0.73	3.35
11	M. dense silty sand	11.00	184	101	0.859	0.22	53	204	1.00	204	1.00	1.00	200	1.11	NL	
12	M. dense silty sand	12.00	201	108	0.842	0.22	53	204	0.98	200	1.00	1.00	200	1.11	NL	
13	M. dense silty sand	13.00	218	115	0.825	0.22	53	216	0.97	209	1.00	1.00	200	1.11	NL	
14	M. dense silty sand	14.00	235	122	0.808	0.22	53	216	0.95	205	1.00	1.00	200	1.11	NL	
15	M. dense silty sand	15.00	252	129	0.791	0.21	53	203	0.94	190	1.00	1.00	200	1.11	0.39	1.83
16	M. dense silty sand	16.00	269	137	0.775	0.21	53	203	0.92	188	1.00	1.00	200	1.11	0.32	1.52
17	M. dense silty sand	17.00	278	141	0.758	0.21	53	224	0.92	205	1.00	1.00	200	1.11	NL	
18	M. dense silty sand	18.00	295	148	0.742	0.21	53	230	0.91	208	1.00	1.00	200	1.11	NL	
19	M. dense silty sand	19.00	312	155	0.727	0.20	53	240	0.90	215	1.00	1.00	200	1.11	NL	
20	M. dense silty sand	20.00	329	162	0.712	0.20	53	244	0.89	216	1.00	1.00	200	1.11	NL	

Table C6 shear wave velocity based analysis output of SEPDM (amax=0.15g)

	Mw=	*5.5*														
Layer #	Layer Name	Depth, m	σv	σ'v	rd	CSR	FC,%	Vs rec. (m/s)	CN	Vs1	Ka1	Ka2	VS1*	MSF	CRR	FS= CRR/CSR
1	Organic Clayey Silt	0.6	9	9	0.995	0.10	72	95	1.70	162	1.0	1.0	200	2.21	NL	
2	Organic Clayey Silt	1.2	18	18	0.991	0.10	72	95	1.54	146	1.0	1.0	200	2.21	NL	
3	Stiff Clayey silt	2.1	34	34	0.984	0.10	72	133	1.31	174	1.0	1.0	200	2.21	NL	
4	Stiff Clayey silt	3	50	50	0.977	0.10	72	133	1.19	158	1.0	1.0	200	2.21	0.24	2.49
5	Slightly Weath.Tuff	4.5	84	70	0.966	0.11	72	2470		2470	1.0	1.0	200	2.21	NL	
6	Fresh Welded Tuff	7	146	107	0.946	0.13	72	3172		3172	1.0	1.0	200	2.21	NL	
7	Soft silty sand	8	160	111	0.939	0.13	72	182	0.97	177	1.0	1.0	200	2.21	0.40	3.00
8	Soft silty sand	9	174	115	0.931	0.14	72	182	0.97	176	1.0	1.0	200	2.21	0.37	2.73
9	Soft silty sand	10	188	119	0.907	0.14	72	182	0.96	174	1.0	1.0	200	2.21	0.36	2.56

10	Soft silty sand	11	202	123	0.880	0.14	72	182	0.95	173	1.0	1.0	200	2.21	0.34	2.45
11	Soft silty sand	12	216	128	0.854	0.14	72	178	0.94	167	1.0	1.0	200	2.21	0.29	2.08
12	Soft silty sand	13	230	132	0.827	0.14	72	175	0.93	163	1.0	1.0	200	2.21	0.27	1.91
13	Soft silty sand	14	244	136	0.800	0.14	72	197	0.93	182	1.0	1.0	200	2.21	0.48	3.40
14	Soft silty sand	15	258	140	0.774	0.14	72	177	0.92	162	1.0	1.0	200	2.21	0.26	1.88
15	Soft silty sand	16	272	144	0.747	0.14	72	190	0.91	173	1.0	1.0	200	2.21	0.35	2.54
16	Soft silty sand	17	286	148	0.720	0.14	72	187	0.91	169	1.0	1.0	200	2.21	0.31	2.30
17	Soft silty sand	18	300	153	0.693	0.13	72	193	0.90	174	1.0	1.0	200	2.21	0.35	2.65
18	Soft silty sand	19	314	157	0.667	0.13	72	203	0.89	181	1.0	1.0	200	2.21	0.46	3.50
19	Soft silty sand	20	328	161	0.640	0.13	72	206	0.89	183	1.0	1.0	200	2.21	0.50	3.91

Mw= 6

Layer #	Layer Name	Depth, m	σv	σ'v	rd	CSR	FC,%	Vs rec. (m/s)	CN	Vs1	Ka1	Ka2	VS1*	MSF	CRR	FS= CRR/CSR
1	Organic Clayey Silt	0.6	9	9	1.000	0.10	72	95	1.70	162	1.0	1.0	200	1.77	NL	
2	Organic Clayey Silt	1.2	18	18	0.991	0.10	72	95	1.54	146	1.0	1.0	200	1.77	NL	
3	Stiff Clayey silt	2.1	34	34	0.976	0.10	72	133	1.31	174	1.0	1.0	200	1.77	NL	
4	Stiff Clayey silt	3	50	50	0.959	0.09	72	133	1.19	158	1.0	1.0	200	1.77	0.19	2.03
5	Slightly Weath. Tuff	4.5	84	70	0.929	0.11	72	2470		2470	1.0	1.0	200	1.77	NL	
6	Fresh Welded Tuff	7	146	107	0.873	0.12	72	3172		3172	1.0	1.0	200	1.77	NL	
7	Soft silty sand	8	160	111	0.848	0.12	72	182	0.97	177	1.0	1.0	200	1.77	0.32	2.66
8	Soft silty sand	9	174	115	0.824	0.12	72	182	0.97	176	1.0	1.0	200	1.77	0.30	2.47
9	Soft silty sand	10	188	119	0.799	0.12	72	182	0.96	174	1.0	1.0	200	1.77	0.29	2.32
10	Soft silty sand	11	202	123	0.774	0.12	72	182	0.95	173	1.0	1.0	200	1.77	0.28	2.23
11	Soft silty sand	12	216	128	0.750	0.12	72	178	0.94	167	1.0	1.0	200	1.77	0.23	1.90
12	Soft silty sand	13	230	132	0.726	0.12	72	175	0.93	163	1.0	1.0	200	1.77	0.21	1.74
13	Soft silty sand	14	244	136	0.702	0.12	72	197	0.93	182	1.0	1.0	200	1.77	0.38	3.10
14	Soft silty sand	15	258	140	0.679	0.12	72	177	0.92	162	1.0	1.0	200	1.77	0.21	1.72
15	Soft silty sand	16	272	144	0.656	0.12	72	190	0.91	173	1.0	1.0	200	1.77	0.28	2.31
16	Soft silty sand	17	286	148	0.635	0.12	72	187	0.91	169	1.0	1.0	200	1.77	0.25	2.09
17	Soft silty sand	18	300	153	0.614	0.12	72	193	0.90	174	1.0	1.0	200	1.77	0.28	2.39
18	Soft silty sand	19	314	157	0.595	0.12	72	203	0.89	181	1.0	1.0	200	1.77	0.36	3.14
19	Soft silty sand	20	328	161	0.576	0.11	72	206	0.89	183	1.0	1.0	200	1.77	0.40	3.48

Mw= 6.5

Layer #	Layer Name	Depth, m	σv	σ'v	rd	CSR	FC,%	Vs rec. (m/s)	CN	Vs1	Ka1	Ka2	VS1*	MSF	CRR	FS= CRR/CSR
1	Organic Clayey Silt	0.6	9	9	1.001	0.10	72	95	1.70	162	1.0	1.0	200	1.44	NL	
2	Organic Clayey Silt	1.2	18	18	0.993	0.10	72	95	1.54	146	1.0	1.0	200	1.44	NL	
3	Stiff Clayey silt	2.1	34	34	0.981	0.10	72	133	1.31	174	1.0	1.0	200	1.44	NL	
4	Stiff Clayey silt	3	50	50	0.967	0.09	72	133	1.19	158	1.0	1.0	200	1.44	0.15	1.64
5	Slightly Weath. Tuff	4.5	84	70	0.941	0.11	72	2470		2470	1.0	1.0	200	1.44	NL	
6	Fresh Welded Tuff	7	146	107	0.893	0.12	72	3172		3172	1.0	1.0	200	1.44	NL	
7	Soft silty sand	8	160	111	0.873	0.12	72	182	0.97	177	1.0	1.0	200	1.44	0.26	2.10
8	Soft silty sand	9	174	115	0.852	0.13	72	182	0.97	176	1.0	1.0	200	1.44	0.24	1.95

9	Soft silty sand	10	188	119	0.830	0.13	72	182	0.96	174	1.0	1.0	200	1.44	0.23	1.82
10	Soft silty sand	11	202	123	0.809	0.13	72	182	0.95	173	1.0	1.0	200	1.44	0.22	1.74
11	Soft silty sand	12	216	128	0.787	0.13	72	178	0.94	167	1.0	1.0	200	1.44	0.19	1.47
12	Soft silty sand	13	230	132	0.766	0.13	72	175	0.93	163	1.0	1.0	200	1.44	0.18	1.34
13	Soft silty sand	14	244	136	0.744	0.13	72	197	0.93	182	1.0	1.0	200	1.44	0.31	2.38
14	Soft silty sand	15	258	140	0.724	0.13	72	177	0.92	162	1.0	1.0	200	1.44	0.17	1.31
15	Soft silty sand	16	272	144	0.703	0.13	72	190	0.91	173	1.0	1.0	200	1.44	0.23	1.76
16	Soft silty sand	17	286	148	0.684	0.13	72	187	0.91	169	1.0	1.0	200	1.44	0.20	1.58
17	Soft silty sand	18	300	153	0.665	0.13	72	193	0.90	174	1.0	1.0	200	1.44	0.23	1.80
18	Soft silty sand	19	314	157	0.647	0.13	72	203	0.89	181	1.0	1.0	200	1.44	0.30	2.36
19	Soft silty sand	20	328	161	0.629	0.12	72	206	0.89	183	1.0	1.0	200	1.44	0.32	2.59

Mw= 6.8

Layer #	Layer Name	Depth, m	σv	σ'v	rd	CSR	FC,%	Vs rec. (m/s)	CN	Vs1	Ka1	Ka2	VS1*	MSF	CRR	FS= CRR/CSR
1	Organic Clayey Silt	0.6	9	9	1.001	0.10	72	95	1.70	162	1.0	1.0	200	1.28	NL	
2	Organic Clayey Silt	1.2	18	18	0.994	0.10	72	95	1.54	146	1.0	1.0	200	1.28	NL	
3	Stiff Clayey silt	2.1	34	34	0.983	0.10	72	133	1.31	174	1.0	1.0	200	1.28	NL	
4	Stiff Clayey silt	3	50	50	0.971	0.09	72	133	1.19	158	1.0	1.0	200	1.28	0.14	1.45
5	Slightly Weath. Tuff	4.5	84	70	0.949	0.11	72	2470		2470	1.0	1.0	200	1.28	NL	
6	Fresh Welded Tuff	7	146	107	0.906	0.12	72	3172		3172	1.0	1.0	200	1.28	NL	
7	Soft silty sand	8	160	111	0.888	0.12	72	182	0.97	177	1.0	1.0	200	1.28	0.23	1.84
8	Soft silty sand	9	174	115	0.869	0.13	72	182	0.97	176	1.0	1.0	200	1.28	0.22	1.70
9	Soft silty sand	10	188	119	0.850	0.13	72	182	0.96	174	1.0	1.0	200	1.28	0.21	1.59
10	Soft silty sand	11	202	123	0.830	0.13	72	182	0.95	173	1.0	1.0	200	1.28	0.20	1.51
11	Soft silty sand	12	216	128	0.810	0.13	72	178	0.94	167	1.0	1.0	200	1.28	0.17	1.28
12	Soft silty sand	13	230	132	0.791	0.13	72	175	0.93	163	1.0	1.0	200	1.28	0.16	1.16
13	Soft silty sand	14	244	136	0.771	0.13	72	197	0.93	182	1.0	1.0	200	1.28	0.28	2.05
14	Soft silty sand	15	258	140	0.752	0.13	72	177	0.92	162	1.0	1.0	200	1.28	0.15	1.13
15	Soft silty sand	16	272	144	0.733	0.13	72	190	0.91	173	1.0	1.0	200	1.28	0.20	1.50
16	Soft silty sand	17	286	148	0.715	0.13	72	187	0.91	169	1.0	1.0	200	1.28	0.18	1.35
17	Soft silty sand	18	300	153	0.697	0.13	72	193	0.90	174	1.0	1.0	200	1.28	0.20	1.53
18	Soft silty sand	19	314	157	0.680	0.13	72	203	0.89	181	1.0	1.0	200	1.28	0.26	2.00
19	Soft silty sand	20	328	161	0.663	0.13	72	206	0.89	183	1.0	1.0	200	1.28	0.29	2.19

Mw= 7

Layer #	Layer Name	Depth, m	σv	σ'v	rd	CSR	FC,%	Vs rec. (m/s)	CN	Vs1	Ka1	Ka2	VS1*	MSF	CRR	FS= CRR/CSR
1	Organic Clayey Silt	0.6	9	9	1.001	0.10	72	95	1.70	162	1.0	1.0	200	1.19	NL	
2	Organic Clayey Silt	1.2	18	18	0.995	0.10	72	95	1.54	146	1.0	1.0	200	1.19	NL	
3	Stiff Clayey silt	2.1	34	34	0.985	0.10	72	133	1.31	174	1.0	1.0	200	1.19	NL	
4	Stiff Clayey silt	3	50	50	0.974	0.09	72	133	1.19	158	1.0	1.0	200	1.19	0.13	1.35
5	Slightly Weath. Tuff	4.5	84	70	0.954	0.11	72	2470		2470	1.0	1.0	200	1.19	NL	
6	Fresh Welded Tuff	7	146	107	0.915	0.12	72	3172		3172	1.0	1.0	200	1.19	NL	
7	Soft silty sand	8	160	111	0.898	0.13	72	182	0.97	177	1.0	1.0	200	1.19	0.21	1.69

8	Soft silty sand	9	174	115	0.880	0.13	72	182	0.97	176	1.0	1.0	200	1.19	0.20	1.56
9	Soft silty sand	10	188	119	0.863	0.13	72	182	0.96	174	1.0	1.0	200	1.19	0.19	1.45
10	Soft silty sand	11	202	123	0.844	0.13	72	182	0.95	173	1.0	1.0	200	1.19	0.19	1.38
11	Soft silty sand	12	216	128	0.826	0.14	72	178	0.94	167	1.0	1.0	200	1.19	0.16	1.16
12	Soft silty sand	13	230	132	0.808	0.14	72	175	0.93	163	1.0	1.0	200	1.19	0.14	1.05
13	Soft silty sand	14	244	136	0.789	0.14	72	197	0.93	182	1.0	1.0	200	1.19	0.26	1.86
14	Soft silty sand	15	258	140	0.771	0.14	72	177	0.92	162	1.0	1.0	200	1.19	0.14	1.02
15	Soft silty sand	16	272	144	0.754	0.14	72	190	0.91	173	1.0	1.0	200	1.19	0.19	1.36
16	Soft silty sand	17	286	148	0.736	0.14	72	187	0.91	169	1.0	1.0	200	1.19	0.17	1.21
17	Soft silty sand	18	300	153	0.719	0.14	72	193	0.90	174	1.0	1.0	200	1.19	0.19	1.38
18	Soft silty sand	19	314	157	0.703	0.14	72	203	0.89	181	1.0	1.0	200	1.19	0.25	1.79
19	Soft silty sand	20	328	161	0.687	0.14	72	206	0.89	183	1.0	1.0	200	1.19	0.27	1.97

Mw= 7.2

Layer #	Layer Name	Depth, m	σv	σ'v	rd	CSR	FC,%	Vs rec. (m/s)	CN	Vs1	Ka1	Ka2	VS1*	MSF	CRR	FS= CRR/CSR
1	Organic Clayey Silt	0.6	9	9	1.002	0.10	72	95	1.70	162	1.0	1.0	200	1.11	NL	
2	Organic Clayey Silt	1.2	18	18	0.996	0.10	72	95	1.54	146	1.0	1.0	200	1.11	NL	
3	Stiff Clayey silt	2.1	34	34	0.987	0.10	72	133	1.31	174	1.0	1.0	200	1.11	NL	
4	Stiff Clayey silt	3	50	50	0.977	0.10	72	133	1.19	158	1.0	1.0	200	1.11	0.12	1.25
5	Slightly Weath. Tuff	4.5	84	70	0.959	0.11	72	2470		2470	1.0	1.0	200	1.11	NL	
6	Fresh Welded Tuff	7	146	107	0.924	0.12	72	3172		3172	1.0	1.0	200	1.11	NL	
7	Soft silty sand	8	160	111	0.908	0.13	72	182	0.97	177	1.0	1.0	200	1.11	0.20	1.56
8	Soft silty sand	9	174	115	0.892	0.13	72	182	0.97	176	1.0	1.0	200	1.11	0.19	1.43
9	Soft silty sand	10	188	119	0.876	0.13	72	182	0.96	174	1.0	1.0	200	1.11	0.18	1.33
10	Soft silty sand	11	202	123	0.859	0.14	72	182	0.95	173	1.0	1.0	200	1.11	0.17	1.26
11	Soft silty sand	12	216	128	0.842	0.14	72	178	0.94	167	1.0	1.0	200	1.11	0.15	1.06
12	Soft silty sand	13	230	132	0.825	0.14	72	175	0.93	163	1.0	1.0	200	1.11	0.13	0.96
13	Soft silty sand	14	244	136	0.808	0.14	72	197	0.93	182	1.0	1.0	200	1.11	0.24	1.69
14	Soft silty sand	15	258	140	0.791	0.14	72	177	0.92	162	1.0	1.0	200	1.11	0.13	0.92
15	Soft silty sand	16	272	144	0.775	0.14	72	190	0.91	173	1.0	1.0	200	1.11	0.17	1.23
16	Soft silty sand	17	286	148	0.758	0.14	72	187	0.91	169	1.0	1.0	200	1.11	0.16	1.10
17	Soft silty sand	18	300	153	0.742	0.14	72	193	0.90	174	1.0	1.0	200	1.11	0.18	1.24
18	Soft silty sand	19	314	157	0.727	0.14	72	203	0.89	181	1.0	1.0	200	1.11	0.23	1.61
19	Soft silty sand	20	328	161	0.712	0.14	72	206	0.89	183	1.0	1.0	200	1.11	0.25	1.77

Table C7 to Table C10 are the output of shear wave velocity simplified procedure (Andrus and stoke 2004). The analyses were performed with geophysical survey measured subsurface data reported in Chapter Three.

Table C7. Shear wave velocity based analysis output of Amora-Gedel (amax=0.27g)

		Mw=	***5.5***													
Layer #	Layer Name		Depth, m	σv	σ'v	rd	CSR	FC , %	Vs rec. (m/sec)	CN	Vs1	Ka1	Ka2	VS1*	MSF	CRR	FS= CRR/CSR
1	Loose silty sand		1.0	18	18	1.000	0.18	65	139	1.53	213	1.0	1.0	200	2.21	NL	
2	Loose silty sand		2.0	37	37	0.969	0.17	65	139	1.29	179	1.0	1.0	200	2.21	NL	
3	Loose silty sand		3.3	60	60	0.937	0.16	65	139	1.13	158	1.0	1.0	200	2.21	NL	
4	Ignimbrite		6.4	136	108	0.850	0.19		3035			1.0				NL	
5	M. dense silty sand		7.0	147	114	0.832	0.19	65	322	0.97	312	1.0	1.0	200	2.21	NL	
6	M. dense silty sand		8.0	167	124	0.802	0.19	65	397	0.95	376	1.0	1.0	200	2.21	NL	
7	M. dense silty sand		9.0	186	133	0.771	0.19	65	397	0.93	369	1.0	1.0	200	2.21	NL	
8	M. dense silty sand		10.0	206	143	0.741	0.19	65	397	0.91	363	1.0	1.0	200	2.21	NL	
9	M. dense silty sand		11.0	225	153	0.710	0.18	65	498	0.90	448	1.0	1.0	200	2.21	NL	
10	M. dense silty sand		12.0	245	163	0.681	0.18	65	498	0.89	441	1.0	1.0	200	2.21	NL	
11	M. dense silty sand		13.0	265	173	0.652	0.18	65	522	0.87	455	1.0	1.0	200	2.21	NL	
12	M. dense silty sand		14.0	285	183	0.624	0.17	65	522	0.86	449	1.0	1.0	200	2.21	NL	
13	M. dense silty sand		15.0	305	193	0.597	0.17	65	522	0.85	443	1.0	1.0	200	2.21	NL	
		Mw=	**6**													
Layer #	Layer Name		Depth, m	σv	σ'v	rd	CSR	FC , %	Vs rec. (m/sec)	CN	Vs1	Ka1	Ka2	VS1*	MSF	CRR	FS= CRR/CSR
1	Loose silty sand		1.0	18	18	1.000	0.18	65	139	1.53	213	1.0	1.0	200	1.77	NL	
2	Loose silty sand		2.0	37	37	0.978	0.17	65	139	1.29	179	1.0	1.0	200	1.77	NL	
3	Loose silty sand		3.3	60	60	0.954	0.17	65	139	1.13	158	1.0	1.0	200	1.77	NL	
4	Ignimbrite		6.4	136	108	0.887	0.20		3035			1.0				NL	
5	M. dense silty sand		7.0	147	114	0.873	0.20	65	322	0.97	312	1.0	1.0	200	1.77	NL	
6	M. dense silty sand		8.0	167	124	0.848	0.20	65	397	0.95	376	1.0	1.0	200	1.77	NL	
7	M. dense silty sand		9.0	186	133	0.824	0.20	65	397	0.93	369	1.0	1.0	200	1.77	NL	
8	M. dense silty sand		10.0	206	143	0.799	0.20	65	397	0.91	363	1.0	1.0	200	1.77	NL	
9	M. dense silty sand		11.0	225	153	0.774	0.20	65	498	0.90	448	1.0	1.0	200	1.77	NL	
10	M. dense silty sand		12.0	245	163	0.750	0.20	65	498	0.89	441	1.0	1.0	200	1.77	NL	
11	M. dense silty sand		13.0	265	173	0.726	0.20	65	522	0.87	455	1.0	1.0	200	1.77	NL	
12	M. dense silty sand		14.0	285	183	0.702	0.19	65	522	0.86	449	1.0	1.0	200	1.77	NL	
13	M. dense silty sand		15.0	305	193	0.679	0.19	65	522	0.85	443	1.0	1.0	200	1.77	NL	
		Mw=	**6.5**													
Layer #	Layer Name		Depth, m	σv	σ'v	rd	CSR	FC , %	Vs rec. (m/sec)	CN	Vs1	Ka1	Ka2	VS1*	MSF	CRR	FS= CRR/CSR
1	Loose silty sand		1.0	18	18	1.000	0.18	65	139	1.53	213	1.0	1.0	200	1.44	NL	
2	Loose silty sand		2.0	37	37	0.982	0.17	65	139	1.29	179	1.0	1.0	200	1.44	NL	
3	Loose silty sand		3.3	60	60	0.962	0.17	65	139	1.13	158	1.0	1.0	200	1.44	NL	
4	Ignimbrite		6.4	136	108	0.905	0.20		3035			1.0				NL	

5	M. dense silty sand		7.0	147	114	0.893	0.20	65	322	0.97	312	1.0	1.0	200	1.44	NL	
6	M. dense silty sand		8.0	167	124	0.873	0.21	65	397	0.95	376	1.0	1.0	200	1.44	NL	
7	M. dense silty sand		9.0	186	133	0.852	0.21	65	397	0.93	369	1.0	1.0	200	1.44	NL	
8	M. dense silty sand		10.0	206	143	0.830	0.21	65	397	0.91	363	1.0	1.0	200	1.44	NL	
9	M. dense silty sand		11.0	225	153	0.809	0.21	65	498	0.90	448	1.0	1.0	200	1.44	NL	
10	M. dense silty sand		12.0	245	163	0.787	0.21	65	498	0.89	441	1.0	1.0	200	1.44	NL	
11	M. dense silty sand		13.0	265	173	0.766	0.21	65	522	0.87	455	1.0	1.0	200	1.44	NL	
12	M. dense silty sand		14.0	285	183	0.744	0.20	65	522	0.86	449	1.0	1.0	200	1.44	NL	
13	M. dense silty sand		15.0	305	193	0.724	0.20	65	522	0.85	443	1.0	1.0	200	1.44	NL	
		Mw=	**6.8**														
Layer #	Layer Name		Depth, m	σv	σ'v	rd	CSR	FC , %	Vs rec. (m/sec)	CN	Vs1	Ka1	Ka2	VS1*	MSF	CRR	FS= CRR/CSR
1	Loose silty sand		1.0	18	18	1.000	0.18	65	139	1.53	213	1.0	1.0	200	1.28	NL	
2	Loose silty sand		2.0	37	37	0.985	0.17	65	139	1.29	179	1.0	1.0	200	1.28	NL	
3	Loose silty sand		3.3	60	60	0.967	0.17	65	139	1.13	158	1.0	1.0	200	1.28	NL	
4	Ignimbrite		6.4	136	108	0.917	0.20		3035			1.0			1.28	NL	
5	M. dense silty sand		7.0	147	114	0.906	0.21	65	322	0.97	312	1.0	1.0	200	1.28	NL	
6	M. dense silty sand		8.0	167	124	0.888	0.21	65	397	0.95	376	1.0	1.0	200	1.28	NL	
7	M. dense silty sand		9.0	186	133	0.869	0.21	65	397	0.93	369	1.0	1.0	200	1.28	NL	
8	M. dense silty sand		10.0	206	143	0.850	0.21	65	397	0.91	363	1.0	1.0	200	1.28	NL	
9	M. dense silty sand		11.0	225	153	0.830	0.21	65	498	0.90	448	1.0	1.0	200	1.28	NL	
10	M. dense silty sand		12.0	245	163	0.810	0.21	65	498	0.89	441	1.0	1.0	200	1.28	NL	
11	M. dense silty sand		13.0	265	173	0.791	0.21	65	522	0.87	455	1.0	1.0	200	1.28	NL	
12	M. dense silty sand		14.0	285	183	0.771	0.21	65	522	0.86	449	1.0	1.0	200	1.28	NL	
13	M. dense silty sand		15.0	305	193	0.752	0.21	65	522	0.85	443	1.0	1.0	200	1.28	NL	
		Mw=	**7**														
Layer #	Layer Name		Depth, m	σv	σ'v	rd	CSR	FC , %	Vs rec. (m/sec)	CN	Vs1	Ka1	Ka2	VS1*	MSF	CRR	FS= CRR/CSR
1	Loose silty sand		1.0	18	18	1.000	0.18	65	139	1.53	213	1.0	1.0	200	1.19	NL	
2	Loose silty sand		2.0	37	37	0.987	0.17	65	139	1.29	179	1.0	1.0	200	1.19	NL	
3	Loose silty sand		3.3	60	60	0.970	0.17	65	139	1.13	158	1.0	1.0	200	1.19	NL	
4	Ignimbrite		6.4	136	108	0.925	0.20		3035			1.0			1.19	NL	
5	M. dense silty sand		7.0	147	114	0.915	0.21	65	322	0.97	312	1.0	1.0	200	1.19	NL	
6	M. dense silty sand		8.0	167	124	0.898	0.21	65	397	0.95	376	1.0	1.0	200	1.19	NL	
7	M. dense silty sand		9.0	186	133	0.880	0.22	65	397	0.93	369	1.0	1.0	200	1.19	NL	
8	M. dense silty sand		10.0	206	143	0.863	0.22	65	397	0.91	363	1.0	1.0	200	1.19	NL	
9	M. dense silty sand		11.0	225	153	0.844	0.22	65	498	0.90	448	1.0	1.0	200	1.19	NL	
10	M. dense silty sand		12.0	245	163	0.826	0.22	65	498	0.89	441	1.0	1.0	200	1.19	NL	
11	M. dense silty sand		13.0	265	173	0.808	0.22	65	522	0.87	455	1.0	1.0	200	1.19	NL	
12	M. dense silty sand		14.0	285	183	0.789	0.22	65	522	0.86	449	1.0	1.0	200	1.19	NL	
13	M. dense silty sand		15.0	305	193	0.771	0.21	65	522	0.85	443	1.0	1.0	200	1.19	NL	
		Mw=	**7.2**														
Layer #	Layer Name		Depth, m	σv	σ'v	rd	CSR	FC , %	Vs rec. (m/sec)	CN	Vs1	Ka1	Ka2	VS1*	MSF	CRR	FS= CRR/CSR
1	Loose silty sand		1.0	18	18	1.000	0.18	65	139	1.53	213	1.0	1.0	200	1.11	NL	

2	Loose silty sand	2.0	37	37	0.988	0.17	65	139	1.29	179	1.0	1.0	200	1.11	NL	
3	Loose silty sand	3.3	60	60	0.974	0.17	65	139	1.13	158	1.0	1.0	200	1.11	NL	
4	Ignimbrite	6.4	136	108	0.932	0.21		3035			1.0			1.11	NL	
5	M. dense silty sand	7.0	147	114	0.924	0.21	65	322	0.97	312	1.0	1.0	200	1.11	NL	
6	M. dense silty sand	8.0	167	124	0.908	0.21	65	397	0.95	376	1.0	1.0	200	1.11	NL	
7	M. dense silty sand	9.0	186	133	0.892	0.22	65	397	0.93	369	1.0	1.0	200	1.11	NL	
8	M. dense silty sand	10.0	206	143	0.876	0.22	65	397	0.91	363	1.0	1.0	200	1.11	NL	
9	M. dense silty sand	11.0	225	153	0.859	0.22	65	498	0.90	448	1.0	1.0	200	1.11	NL	
10	M. dense silty sand	12.0	245	163	0.842	0.22	65	498	0.89	441	1.0	1.0	200	1.11	NL	
11	M. dense silty sand	13.0	265	173	0.825	0.22	65	522	0.87	455	1.0	1.0	200	1.11	NL	
12	M. dense silty sand	14.0	285	183	0.808	0.22	65	522	0.86	449	1.0	1.0	200	1.11	NL	
13	M. dense silty sand	15.0	305	193	0.791	0.22	65	522	0.85	443	1.0	1.0	200	1.11	NL	

Table C8. Shear wave velocity based analysis output of HIP (seismic sur.) (amax=0.235g)

		Mw=	***5.5***													
Layer #	Layer Name		Depth,m	σv	σ'v	rd	CSR	FC ,%	Vs Rec. (m/S)	CN	Vs1	Ka1	Ka2	VS1*	MSF	CRR	FS= CRR/CSR
1	Silty Sand		1	13	13	0.991	0.15	53	121	1.67	202	1.0	1.0	200	2.21	NL	
2	Silty Sand		2	26	26	0.969	0.15	53	131	1.40	183	1.0	1.0	200	2.21	NL	
3	Silty Sand		3	41	41	0.945	0.14	53	153	1.25	192	1.0	1.0	200	2.21	NL	
4	Silty Sand		4	55	55	0.919	0.14	53	164	1.16	190	1.0	1.0	200	2.21	NL	
5	Silty Sand		5	69	69	0.891	0.14	53	175	1.10	192	1.0	1.0	200	2.21	NL	
6	Silty Sand		6	84	84	0.862	0.13	53	186	1.05	194	1.0	1.0	200	2.21	NL	
7	Silty Sand		7	98	98	0.832	0.13	53	197	1.01	198	1.0	1.0	200	2.21	NL	
8	Silty Sand		8	112	112	0.802	0.12	53	208	0.97	202	1.0	1.0	200	2.21	NL	
9	Silty Sand		9	126	126	0.771	0.12	53	219	0.94	206	1.0	1.0	200	2.21	NL	
10	Silty Sand		10	141	141	0.741	0.11	53	230	0.92	211	1.0	1.0	200	2.21	NL	
11	Silty Sand		11	155	145	0.710	0.12	53	240	0.91	219	1.0	1.0	200	2.21	NL	
12	Silty Sand		12	169	150	0.681	0.12	53	240	0.90	217	1.0	1.0	200	2.21	NL	
13	Silty Sand		13	184	154	0.652	0.12	53	251	0.90	225	1.0	1.0	200	2.21	NL	
14	Silty Sand		14	198	159	0.624	0.12	53	262	0.89	234	1.0	1.0	200	2.21	NL	
15	Silty Sand		15	212	163	0.597	0.12	53	273	0.88	242	1.0	1.0	200	2.21	NL	
16	Silty Sand		16	226	168	0.572	0.12	53	284	0.88	250	1.0	1.0	200	2.21	NL	
17	Silty Sand		17	241	172	0.547	0.12	53	295	0.87	258	1.0	1.0	200	2.21	NL	
18	Silty Sand		18	255	177	0.525	0.12	53	316	0.87	274	1.0	1.0	200	2.21	NL	
19	Silty Sand		19	269	181	0.503	0.11	53	267	0.86	230	1.0	1.0	200	2.21	NL	
20	Silty Sand		20	284	185	0.483	0.11	53	271	0.86	232	1.0	1.0	200	2.21	NL	
		Mw=	**6**													
Layer #	Layer Name		Depth,m	σv	σ'v	rd	CSR	FC ,%	Vs Rec. (m/S)	CN	Vs1	Ka1	Ka2	VS1*	MSF	CRR	FS= CRR/CSR
1	Silty Sand		1	13	13	0.994	0.15	53	121	1.67	202	1.0	1.0	200	1.77	NL	
2	Silty Sand		2	26	26	0.978	0.15	53	131	1.40	183	1.0	1.0	200	1.77	NL	

3	Silty Sand		3	41	41	0.959	0.15	53	153	1.25	192	1.0	1.0	200	1.77	NL	
4	Silty Sand		4	55	55	0.940	0.14	53	164	1.16	190	1.0	1.0	200	1.77	NL	
5	Silty Sand		5	69	69	0.918	0.14	53	175	1.10	192	1.0	1.0	200	1.77	NL	
6	Silty Sand		6	84	84	0.896	0.14	53	186	1.05	194	1.0	1.0	200	1.77	NL	
7	Silty Sand		7	98	98	0.873	0.13	53	197	1.01	198	1.0	1.0	200	1.77	NL	
8	Silty Sand		8	112	112	0.848	0.13	53	208	0.97	202	1.0	1.0	200	1.77	NL	
9	Silty Sand		9	126	126	0.824	0.13	53	219	0.94	206	1.0	1.0	200	1.77	NL	
10	Silty Sand		10	141	141	0.799	0.12	53	230	0.92	211	1.0	1.0	200	1.77	NL	
11	Silty Sand		11	155	145	0.774	0.13	53	240	0.91	219	1.0	1.0	200	1.77	NL	
12	Silty Sand		12	169	150	0.750	0.13	53	240	0.90	217	1.0	1.0	200	1.77	NL	
13	Silty Sand		13	184	154	0.726	0.13	53	251	0.90	225	1.0	1.0	200	1.77	NL	
14	Silty Sand		14	198	159	0.702	0.13	53	262	0.89	234	1.0	1.0	200	1.77	NL	
15	Silty Sand		15	212	163	0.679	0.13	53	273	0.88	242	1.0	1.0	200	1.77	NL	
16	Silty Sand		16	226	168	0.656	0.14	53	284	0.88	250	1.0	1.0	200	1.77	NL	
17	Silty Sand		17	241	172	0.635	0.14	53	295	0.87	258	1.0	1.0	200	1.77	NL	
18	Silty Sand		18	255	177	0.614	0.14	53	316	0.87	274	1.0	1.0	200	1.77	NL	
19	Silty Sand		19	269	181	0.595	0.14	53	267	0.86	230	1.0	1.0	200	1.77	NL	
20	Silty Sand		20	284	185	0.576	0.13	53	271	0.86	232	1.0	1.0	200	1.77	NL	
		Mw=	**6.5**														
Layer #	Layer Name		Depth,m	σv	σ'v	rd	CSR	FC ,%	Vs Rec. (m/S)	CN	Vs1	Ka1	Ka2	VS1*	MSF	CRR	FS= CRR/CSR
1	Silty Sand		1	13	13	0.996	0.15	53	121	1.67	202	1.0	1.0	200	1.44	NL	
2	Silty Sand		2	26	26	0.982	0.15	53	131	1.40	183	1.0	1.0	200	1.44	NL	
3	Silty Sand		3	41	41	0.967	0.15	53	153	1.25	192	1.0	1.0	200	1.44	NL	
4	Silty Sand		4	55	55	0.950	0.15	53	164	1.16	190	1.0	1.0	200	1.44	NL	
5	Silty Sand		5	69	69	0.932	0.14	53	175	1.10	192	1.0	1.0	200	1.44	NL	
6	Silty Sand		6	84	84	0.913	0.14	53	186	1.05	194	1.0	1.0	200	1.44	NL	
7	Silty Sand		7	98	98	0.893	0.14	53	197	1.01	198	1.0	1.0	200	1.44	NL	
8	Silty Sand		8	112	112	0.873	0.13	53	208	0.97	202	1.0	1.0	200	1.44	NL	
9	Silty Sand		9	126	126	0.852	0.13	53	219	0.94	206	1.0	1.0	200	1.44	NL	
10	Silty Sand		10	141	141	0.830	0.13	53	230	0.92	211	1.0	1.0	200	1.44	NL	
11	Silty Sand		11	155	145	0.809	0.13	53	240	0.91	219	1.0	1.0	200	1.44	NL	
12	Silty Sand		12	169	150	0.787	0.14	53	240	0.90	217	1.0	1.0	200	1.44	NL	
13	Silty Sand		13	184	154	0.766	0.14	53	251	0.90	225	1.0	1.0	200	1.44	NL	
14	Silty Sand		14	198	159	0.744	0.14	53	262	0.89	234	1.0	1.0	200	1.44	NL	
15	Silty Sand		15	212	163	0.724	0.14	53	273	0.88	242	1.0	1.0	200	1.44	NL	
16	Silty Sand		16	226	168	0.703	0.15	53	284	0.88	250	1.0	1.0	200	1.44	NL	
17	Silty Sand		17	241	172	0.684	0.15	53	295	0.87	258	1.0	1.0	200	1.44	NL	
18	Silty Sand		18	255	177	0.665	0.15	53	316	0.87	274	1.0	1.0	200	1.44	NL	
19	Silty Sand		19	269	181	0.647	0.15	53	267	0.86	230	1.0	1.0	200	1.44	NL	
20	Silty Sand		20	284	185	0.629	0.15	53	271	0.86	232	1.0	1.0	200	1.44	NL	
		Mw=	**6.8**														
Layer #	Layer Name		Depth,m	σv	σ'v	rd	CSR	FC ,%	Vs Rec. (m/S)	CN	Vs1	Ka1	Ka2	VS1*	MSF	CRR	FS= CRR/CSR
1	Silty Sand		1	13	13	0.997	0.15	53	121	1.67	202	1.0	1.0	200	1.28	NL	

2	Silty Sand		2	26	26	0.985	0.15	53	131	1.40	183	1.0	1.0	200	1.28	NL	
3	Silty Sand		3	41	41	0.971	0.15	53	153	1.25	192	1.0	1.0	200	1.28	NL	
4	Silty Sand		4	55	55	0.957	0.15	53	164	1.16	190	1.0	1.0	200	1.28	NL	
5	Silty Sand		5	69	69	0.941	0.14	53	175	1.10	192	1.0	1.0	200	1.28	NL	
6	Silty Sand		6	84	84	0.924	0.14	53	186	1.05	194	1.0	1.0	200	1.28	NL	
7	Silty Sand		7	98	98	0.906	0.14	53	197	1.01	198	1.0	1.0	200	1.28	NL	
8	Silty Sand		8	112	112	0.888	0.14	53	208	0.97	202	1.0	1.0	200	1.28	NL	
9	Silty Sand		9	126	126	0.869	0.13	53	219	0.94	206	1.0	1.0	200	1.28	NL	
10	Silty Sand		10	141	141	0.850	0.13	53	230	0.92	211	1.0	1.0	200	1.28	NL	
11	Silty Sand		11	155	145	0.830	0.14	53	240	0.91	219	1.0	1.0	200	1.28	NL	
12	Silty Sand		12	169	150	0.810	0.14	53	240	0.90	217	1.0	1.0	200	1.28	NL	
13	Silty Sand		13	184	154	0.791	0.14	53	251	0.90	225	1.0	1.0	200	1.28	NL	
14	Silty Sand		14	198	159	0.771	0.15	53	262	0.89	234	1.0	1.0	200	1.28	NL	
15	Silty Sand		15	212	163	0.752	0.15	53	273	0.88	242	1.0	1.0	200	1.28	NL	
16	Silty Sand		16	226	168	0.733	0.15	53	284	0.88	250	1.0	1.0	200	1.28	NL	
17	Silty Sand		17	241	172	0.715	0.15	53	295	0.87	258	1.0	1.0	200	1.28	NL	
18	Silty Sand		18	255	177	0.697	0.15	53	316	0.87	274	1.0	1.0	200	1.28	NL	
19	Silty Sand		19	269	181	0.680	0.15	53	267	0.86	230	1.0	1.0	200	1.28	NL	
20	Silty Sand		20	284	185	0.663	0.15	53	271	0.86	232	1.0	1.0	200	1.28	NL	
		Mw=	**7.0**														
Layer #	Layer Name		Depth,m	σv	σ'v	rd	CSR	FC ,%	Vs Rec. (m/S)	CN	Vs1	Ka1	Ka2	VS1*	MSF	CRR	FS= CRR/CSR
1	Silty Sand		1	13	13	0.997	0.15	53	121	1.67	202	1.0	1.0	200	1.19	NL	
2	Silty Sand		2	26	26	0.987	0.15	53	131	1.40	183	1.0	1.0	200	1.19	NL	
3	Silty Sand		3	41	41	0.974	0.15	53	153	1.25	192	1.0	1.0	200	1.19	NL	
4	Silty Sand		4	55	55	0.961	0.15	53	164	1.16	190	1.0	1.0	200	1.19	NL	
5	Silty Sand		5	69	69	0.946	0.14	53	175	1.10	192	1.0	1.0	200	1.19	NL	
6	Silty Sand		6	84	84	0.931	0.14	53	186	1.05	194	1.0	1.0	200	1.19	NL	
7	Silty Sand		7	98	98	0.915	0.14	53	197	1.01	198	1.0	1.0	200	1.19	NL	
8	Silty Sand		8	112	112	0.898	0.14	53	208	0.97	202	1.0	1.0	200	1.19	NL	
9	Silty Sand		9	126	126	0.880	0.13	53	219	0.94	206	1.0	1.0	200	1.19	NL	
10	Silty Sand		10	141	141	0.863	0.13	53	230	0.92	211	1.0	1.0	200	1.19	NL	
11	Silty Sand		11	155	145	0.844	0.14	53	240	0.91	219	1.0	1.0	200	1.19	NL	
12	Silty Sand		12	169	150	0.826	0.14	53	240	0.90	217	1.0	1.0	200	1.19	NL	
13	Silty Sand		13	184	154	0.808	0.15	53	251	0.90	225	1.0	1.0	200	1.19	NL	
14	Silty Sand		14	198	159	0.789	0.15	53	262	0.89	234	1.0	1.0	200	1.19	NL	
15	Silty Sand		15	212	163	0.771	0.15	53	273	0.88	242	1.0	1.0	200	1.19	NL	
16	Silty Sand		16	226	168	0.754	0.16	53	284	0.88	250	1.0	1.0	200	1.19	NL	
17	Silty Sand		17	241	172	0.736	0.16	53	295	0.87	258	1.0	1.0	200	1.19	NL	
18	Silty Sand		18	255	177	0.719	0.16	53	316	0.87	274	1.0	1.0	200	1.19	NL	
19	Silty Sand		19	269	181	0.703	0.16	53	267	0.86	230	1.0	1.0	200	1.19	NL	
20	Silty Sand		20	284	185	0.687	0.16	53	271	0.86	232	1.0	1.0	200	1.19	NL	
		Mw=	**7.2**														
Layer #	Layer Name		Depth,m	σv	σ'v	rd	CSR	FC ,%	Vs Rec. (m/S)	CN	Vs1	Ka1	Ka2	VS1*	MSF	CRR	FS= CRR/CSR

1	Silty Sand	1	13	13	0.998	0.15	53	121	1.67	202	1.0	1.0	200	1.11	NL
2	Silty Sand	2	26	26	0.988	0.15	53	131	1.40	183	1.0	1.0	200	1.11	NL
3	Silty Sand	3	41	41	0.977	0.15	53	153	1.25	192	1.0	1.0	200	1.11	NL
4	Silty Sand	4	55	55	0.965	0.15	53	164	1.16	190	1.0	1.0	200	1.11	NL
5	Silty Sand	5	69	69	0.952	0.15	53	175	1.10	192	1.0	1.0	200	1.11	NL
6	Silty Sand	6	84	84	0.938	0.14	53	186	1.05	194	1.0	1.0	200	1.11	NL
7	Silty Sand	7	98	98	0.924	0.14	53	197	1.01	198	1.0	1.0	200	1.11	NL
8	Silty Sand	8	112	112	0.908	0.14	53	208	0.97	202	1.0	1.0	200	1.11	NL
9	Silty Sand	9	126	126	0.892	0.14	53	219	0.94	206	1.0	1.0	200	1.11	NL
10	Silty Sand	10	141	141	0.876	0.13	53	230	0.92	211	1.0	1.0	200	1.11	NL
11	Silty Sand	11	155	145	0.859	0.14	53	240	0.91	219	1.0	1.0	200	1.11	NL
12	Silty Sand	12	169	150	0.842	0.15	53	240	0.90	217	1.0	1.0	200	1.11	NL
13	Silty Sand	13	184	154	0.825	0.15	53	251	0.90	225	1.0	1.0	200	1.11	NL
14	Silty Sand	14	198	159	0.808	0.15	53	262	0.89	234	1.0	1.0	200	1.11	NL
15	Silty Sand	15	212	163	0.791	0.16	53	273	0.88	242	1.0	1.0	200	1.11	NL
16	Silty Sand	16	226	168	0.775	0.16	53	284	0.88	250	1.0	1.0	200	1.11	NL
17	Silty Sand	17	241	172	0.758	0.16	53	295	0.87	258	1.0	1.0	200	1.11	NL
18	Silty Sand	18	255	177	0.742	0.16	53	316	0.87	274	1.0	1.0	200	1.11	NL
19	Silty Sand	19	269	181	0.727	0.17	53	267	0.86	230	1.0	1.0	200	1.11	NL
20	Silty Sand	20	284	185	0.712	0.17	53	271	0.86	232	1.0	1.0	200	1.11	NL

Table C9. Shear wave velocity based analysis output of Agricultural College (amax=0.215g)

	Mw=	***5.5***													
Layer #	Layer Name	Depth, m	σv	σ'v	rd	CSR	FC ,%	Vs, Rec. (m/s)	CN	Vs1	Ka1	Ka2	VS1*	MSF	CRR	FS= CRR/CSR
1	silty sand (ash)	1.00	17	17	1.000	0.14	53	143	1.56	223	1.0	1.0	200	2.21	NL	
2	silty sand (ash)	2.00	34	34	0.969	0.14	53	143	1.31	187	1.0	1.0	200	2.21	NL	
3	silty sand (ash)	3.00	51	51	0.945	0.13	53	143	1.18	169	1.0	1.0	200	2.21	NL	
4	silty sand (ash)	4.00	68	58	0.919	0.15	53	153	1.14	175	1.0	1.0	200	2.21	0.37	2.45
5	silty sand (ash)	5.00	85	65	0.891	0.16	53	163	1.11	181	1.0	1.0	200	2.21	0.46	2.84
6	Ignimbrite	6.40	92	58	0.850	0.19	53	2470			1.0	1.0				
7	M. dense silty sand	7.00	116	72	0.832	0.19	53	203	1.09	220	1.0	1.0	200	2.21	NL	
8	M. dense silty sand	8.00	133	79	0.802	0.19	53	233	1.06	247	1.0	1.0	200	2.21	NL	
9	M. dense silty sand	9.00	150	86	0.771	0.19	53	294	1.04	305	1.0	1.0	200	2.21	NL	
10	M. dense silty sand	10.00	167	94	0.741	0.18	53	324	1.02	329	1.0	1.0	200	2.21	NL	
11	M. dense silty sand	11.00	184	101	0.710	0.18	53	354	1.00	353	1.0	1.0	200	2.21	NL	
12	M. dense silty sand	12.00	201	108	0.681	0.18	53	384	0.98	377	1.0	1.0	200	2.21	NL	
13	M. dense silty sand	13.00	218	115	0.652	0.17	53	414	0.97	400	1.0	1.0	200	2.21	NL	
14	M. dense silty sand	14.00	235	122	0.624	0.17	53	278	0.95	264	1.0	1.0	200	2.21	NL	
15	M. dense silty sand	15.00	252	129	0.597	0.16	53	250	0.94	234	1.0	1.0	200	2.21	NL	
16	M. dense silty sand	16.00	269	137	0.572	0.16	53	270	0.92	250	1.0	1.0	200	2.21	NL	
17	M. dense silty sand	17.00	278	141	0.547	0.15	53	279	0.92	256	1.0	1.0	200	2.21	NL	

18	M. dense silty sand	18.00	295	148	0.525	0.15	53	290	0.91	263	1.0	1.0	200	2.21	NL	
19	M. dense silty sand	19.00	312	155	0.503	0.14	53	295	0.90	264	1.0	1.0	200	2.21	NL	
20	M. dense silty sand	20.00	329	162	0.483	0.14	53	307	0.89	272	1.0	1.0	200	2.21	NL	
	Mw=	**6.0**														
Layer #	Layer Name	Depth, m	σv	σ'v	rd	CSR	FC ,%	Vs, Rec. (m/s)	CN	Vs1	Ka1	Ka2	VS1*	MSF	CRR	FS= CRR/CSR
1	silty sand (ash)	1.00	17	17	1.000	0.14	53	146	1.56	227	1.0	1.0	200	1.77	NL	
2	silty sand (ash)	2.00	34	34	0.978	0.14	53	146	1.31	191	1.0	1.0	200	1.77	NL	
3	silty sand (ash)	3.00	51	51	0.959	0.13	53	146	1.18	173	1.0	1.0	200	1.77	NL	
4	silty sand (ash)	4.00	68	58	0.940	0.15	53	162	1.14	185	1.0	1.0	200	1.77	0.45	2.94
5	silty sand (ash)	5.00	85	65	0.918	0.17	53	162	1.11	180	1.0	1.0	200	1.77	0.35	2.11
6	Ignimbrite	6.40	92	58	0.887	0.19	53	2470		2470	1.0	1.0		1.77	NL	
7	M. dense silty sand	7.00	116	72	0.873	0.20	53	185	1.09	201	1.0	1.0	200	1.77	NL	
8	M. dense silty sand	8.00	133	79	0.848	0.20	53	190	1.06	201	1.0	1.0	200	1.77	NL	
9	M. dense silty sand	9.00	150	86	0.824	0.20	53	192	1.04	199	1.0	1.0	200	1.77	6.23	
10	M. dense silty sand	10.00	167	94	0.799	0.20	53	192	1.02	195	1.0	1.0	200	1.77	1.17	5.86
11	M. dense silty sand	11.00	184	101	0.774	0.20	53	204	1.00	204	1.0	1.0	200	1.77	NL	
12	M. dense silty sand	12.00	201	108	0.750	0.19	53	204	0.98	200	1.0	1.0	200	1.77	NL	
13	M. dense silty sand	13.00	218	115	0.726	0.19	53	216	0.97	209	1.0	1.0	200	1.77	NL	
14	M. dense silty sand	14.00	235	122	0.702	0.19	53	216	0.95	205	1.0	1.0	200	1.77	NL	
15	M. dense silty sand	15.00	252	129	0.679	0.18	53	203	0.94	190	1.0	1.0	200	1.77	0.63	3.40
16	M. dense silty sand	16.00	269	137	0.656	0.18	53	203	0.92	188	1.0	1.0	200	1.77	0.52	2.87
17	M. dense silty sand	17.00	278	141	0.635	0.18	53	224	0.92	205	1.0	1.0	200	1.77	NL	
18	M. dense silty sand	18.00	295	148	0.614	0.17	53	230	0.91	208	1.0	1.0	200	1.77	NL	
19	M. dense silty sand	19.00	312	155	0.595	0.17	53	240	0.90	215	1.0	1.0	200	1.77	NL	
20	M. dense silty sand	20.00	329	162	0.576	0.16	53	244	0.89	216	1.0	1.0	200	1.77	NL	
	Mw=	**6.5**														
Layer #	Layer Name	Depth, m	σv	σ'v	rd	CSR	FC ,%	Vs, Rec. (m/s)	CN	Vs1	Ka1	Ka2	VS1*	MSF	CRR	FS= CRR/CSR
1	silty sand (ash)	1.00	17	17	1.000	0.14	53	146	1.56	227	1.0	1.0	200	1.44	NL	
2	silty sand (ash)	2.00	34	34	0.982	0.14	53	146	1.31	191	1.0	1.0	200	1.44	NL	
3	silty sand (ash)	3.00	51	51	0.967	0.14	53	146	1.18	173	1.0	1.0	200	1.44	NL	
4	silty sand (ash)	4.00	68	58	0.950	0.16	53	162	1.14	185	1.0	1.0	200	1.44	0.37	2.37
5	silty sand (ash)	5.00	85	65	0.932	0.17	53	162	1.11	180	1.0	1.0	200	1.44	0.29	1.69
6	Ignimbrite	6.40	92	58	0.905	0.20	53	2470		2470	1.0	1.0		1.44	NL	
7	M. dense silty sand	7.00	116	72	0.893	0.20	53	185	1.09	201	1.0	1.0	200	1.44	NL	
8	M. dense silty sand	8.00	133	79	0.873	0.20	53	190	1.06	201	1.0	1.0	200	1.44	NL	
9	M. dense silty sand	9.00	150	86	0.852	0.21	53	192	1.04	199	1.0	1.0	200	1.44	5.07	
10	M. dense silty sand	10.00	167	94	0.830	0.21	53	192	1.02	195	1.0	1.0	200	1.44	0.95	4.59
11	M. dense silty sand	11.00	184	101	0.809	0.21	53	204	1.00	204	1.0	1.0	200	1.44	NL	
12	M. dense silty sand	12.00	201	108	0.787	0.20	53	204	0.98	200	1.0	1.0	200	1.44	NL	
13	M. dense silty sand	13.00	218	115	0.766	0.20	53	216	0.97	209	1.0	1.0	200	1.44	NL	
14	M. dense silty sand	14.00	235	122	0.744	0.20	53	216	0.95	205	1.0	1.0	200	1.44	NL	
15	M. dense silty sand	15.00	252	129	0.724	0.20	53	203	0.94	190	1.0	1.0	200	1.44	0.51	2.60
16	M. dense silty sand	16.00	269	137	0.703	0.19	53	203	0.92	188	1.0	1.0	200	1.44	0.42	2.18

17	M. dense silty sand	17.00	278	141	0.684	0.19	53	224	0.92	205	1.0	1.0	200	1.44	NL	
18	M. dense silty sand	18.00	295	148	0.665	0.19	53	230	0.91	208	1.0	1.0	200	1.44	NL	
19	M. dense silty sand	19.00	312	155	0.647	0.18	53	240	0.90	215	1.0	1.0	200	1.44	NL	
20	M. dense silty sand	20.00	329	162	0.629	0.18	53	244	0.89	216	1.0	1.0	200	1.44	NL	
	Mw=	**6.8**														
Layer #	Layer Name	Depth, m	σv	σ'v	rd	CSR	FC ,%	Vs, Rec. (m/s)	CN	Vs1	Ka1	Ka2	VS1*	MSF	CRR	FS= CRR/CSR
1	silty sand (ash)	1.00	17	17	1.000	0.14	53	146	1.56	227	1.0	1.0	200	1.28	NL	
2	silty sand (ash)	2.00	34	34	0.985	0.14	53	146	1.31	191	1.0	1.0	200	1.28	NL	
3	silty sand (ash)	3.00	51	51	0.971	0.14	53	146	1.18	173	1.0	1.0	200	1.28	NL	
4	silty sand (ash)	4.00	68	58	0.957	0.16	53	162	1.14	185	1.0	1.0	200	1.28	0.33	2.09
5	silty sand (ash)	5.00	85	65	0.941	0.17	53	162	1.11	180	1.0	1.0	200	1.28	0.26	1.49
6	Ignimbrite	6.40	92	58	0.917	0.20	53	2470		2470	1.0	1.0		1.28	NL	
7	M. dense silty sand	7.00	116	72	0.906	0.20	53	185	1.09	201	1.0	1.0	200	1.28	NL	
8	M. dense silty sand	8.00	133	79	0.888	0.21	53	190	1.06	201	1.0	1.0	200	1.28	NL	
9	M. dense silty sand	9.00	150	86	0.869	0.21	53	192	1.04	199	1.0	1.0	200	1.28	4.52	21.49
10	M. dense silty sand	10.00	167	94	0.850	0.21	53	192	1.02	195	1.0	1.0	200	1.28	0.85	4.00
11	M. dense silty sand	11.00	184	101	0.830	0.21	53	204	1.00	204	1.0	1.0	200	1.28	NL	
12	M. dense silty sand	12.00	201	108	0.810	0.21	53	204	0.98	200	1.0	1.0	200	1.28	NL	
13	M. dense silty sand	13.00	218	115	0.791	0.21	53	216	0.97	209	1.0	1.0	200	1.28	NL	
14	M. dense silty sand	14.00	235	122	0.771	0.21	53	216	0.95	205	1.0	1.0	200	1.28	NL	
15	M. dense silty sand	15.00	252	129	0.752	0.20	53	203	0.94	190	1.0	1.0	200	1.28	0.46	2.23
16	M. dense silty sand	16.00	269	137	0.733	0.20	53	203	0.92	188	1.0	1.0	200	1.28	0.38	1.86
17	M. dense silty sand	17.00	278	141	0.715	0.20	53	224	0.92	205	1.0	1.0	200	1.28	NL	
18	M. dense silty sand	18.00	295	148	0.697	0.19	53	230	0.91	208	1.0	1.0	200	1.28	NL	
19	M. dense silty sand	19.00	312	155	0.680	0.19	53	240	0.90	215	1.0	1.0	200	1.28	NL	
20	M. dense silty sand	20.00	329	162	0.663	0.19	53	244	0.89	216	1.0	1.0	200	1.28	NL	
	Mw=	**7.0**														
Layer #	Layer Name	Depth, m	σv	σ'v	rd	CSR	FC ,%	Vs, Rec. (m/s)	CN	Vs1	Ka1	Ka2	VS1*	MSF	CRR	FS= CRR/CSR
1	silty sand (ash)	1.00	17	17	1.000	0.14	53	146	1.56	227	1.0	1.0	200	1.19	NL	
2	silty sand (ash)	2.00	34	34	0.987	0.14	53	146	1.31	191	1.0	1.0	200	1.19	NL	
3	silty sand (ash)	3.00	51	51	0.974	0.14	53	146	1.18	173	1.0	1.0	200	1.19	NL	
4	silty sand (ash)	4.00	68	58	0.961	0.16	53	162	1.14	185	1.0	1.0	200	1.19	0.30	1.93
5	silty sand (ash)	5.00	85	65	0.946	0.17	53	162	1.11	180	1.0	1.0	200	1.19	0.24	1.38
6	Ignimbrite	6.40	92	58	0.925	0.20	53	2470		2470	1.0	1.0		1.19	NL	
7	M. dense silty sand	7.00	116	72	0.915	0.21	53	185	1.09	201	1.0	1.0	200	1.19	NL	
8	M. dense silty sand	8.00	133	79	0.898	0.21	53	190	1.06	201	1.0	1.0	200	1.19	NL	
9	M. dense silty sand	9.00	150	86	0.880	0.21	53	192	1.04	199	1.0	1.0	200	1.19	4.20	
10	M. dense silty sand	10.00	167	94	0.863	0.21	53	192	1.02	195	1.0	1.0	200	1.19	0.79	3.66
11	M. dense silty sand	11.00	184	101	0.844	0.22	53	204	1.00	204	1.0	1.0	200	1.19	NL	
12	M. dense silty sand	12.00	201	108	0.826	0.21	53	204	0.98	200	1.0	1.0	200	1.19	NL	
13	M. dense silty sand	13.00	218	115	0.808	0.21	53	216	0.97	209	1.0	1.0	200	1.19	NL	
14	M. dense silty sand	14.00	235	122	0.789	0.21	53	216	0.95	205	1.0	1.0	200	1.19	NL	
15	M. dense silty sand	15.00	252	129	0.771	0.21	53	203	0.94	190	1.0	1.0	200	1.19	0.42	2.02

16	M. dense silty sand	16.00	269	137	0.754	0.21	53	203	0.92	188	1.0	1.0	200	1.19	0.35	1.68
17	M. dense silty sand	17.00	278	141	0.736	0.20	53	224	0.92	205	1.0	1.0	200	1.19	NL	
18	M. dense silty sand	18.00	295	148	0.719	0.20	53	230	0.91	208	1.0	1.0	200	1.19	NL	
19	M. dense silty sand	19.00	312	155	0.703	0.20	53	240	0.90	215	1.0	1.0	200	1.19	NL	
20	M. dense silty sand	20.00	329	162	0.687	0.19	53	244	0.89	216	1.0	1.0	200	1.19	NL	
	Mw=	**7.2**														
Layer #	Layer Name	Depth, m	σv	σ'v	rd	CSR	FC ,%	Vs, Rec. (m/s)	CN	Vs1	Ka1	Ka2	VS1*	MSF	CRR	FS= CRR/CSR
1	silty sand (ash)	1.00	17	17	1.000	0.14	53	146	1.56	227	1.0	1.0	200	1.11	NL	
2	silty sand (ash)	2.00	34	34	0.988	0.14	53	146	1.31	191	1.0	1.0	200	1.11	NL	
3	silty sand (ash)	3.00	51	51	0.977	0.14	53	146	1.18	173	1.0	1.0	200	1.11	NL	
4	silty sand (ash)	4.00	68	58	0.965	0.16	53	162	1.14	185	1.0	1.0	200	1.11	0.28	1.79
5	silty sand (ash)	5.00	85	65	0.952	0.17	53	162	1.11	180	1.0	1.0	200	1.11	0.22	1.27
6	Ignimbrite	6.40	92	58	0.932	0.20	53	2470		2470	1.0	1.0		1.11	NL	
7	M. dense silty sand	7.00	116	72	0.924	0.21	53	185	1.09	201	1.0	1.0	200	1.11	NL	
8	M. dense silty sand	8.00	133	79	0.908	0.21	53	190	1.06	201	1.0	1.0	200	1.11	NL	
9	M. dense silty sand	9.00	150	86	0.892	0.22	53	192	1.04	199	1.0	1.0	200	1.11	3.91	
10	M. dense silty sand	10.00	167	94	0.876	0.22	53	192	1.02	195	1.0	1.0	200	1.11	0.73	3.35
11	M. dense silty sand	11.00	184	101	0.859	0.22	53	204	1.00	204	1.0	1.0	200	1.11	NL	
12	M. dense silty sand	12.00	201	108	0.842	0.22	53	204	0.98	200	1.0	1.0	200	1.11	NL	
13	M. dense silty sand	13.00	218	115	0.825	0.22	53	216	0.97	209	1.0	1.0	200	1.11	NL	
14	M. dense silty sand	14.00	235	122	0.808	0.22	53	216	0.95	205	1.0	1.0	200	1.11	NL	
15	M. dense silty sand	15.00	252	129	0.791	0.21	53	203	0.94	190	1.0	1.0	200	1.11	0.39	1.83
16	M. dense silty sand	16.00	269	137	0.775	0.21	53	203	0.92	188	1.0	1.0	200	1.11	0.32	1.52
17	M. dense silty sand	17.00	278	141	0.758	0.21	53	224	0.92	205	1.0	1.0	200	1.11	NL	
18	M. dense silty sand	18.00	295	148	0.742	0.21	53	230	0.91	208	1.0	1.0	200	1.11	NL	
19	M. dense silty sand	19.00	312	155	0.727	0.20	53	240	0.90	215	1.0	1.0	200	1.11	NL	
20	M. dense silty sand	20.00	329	162	0.712	0.20	53	244	0.89	216	1.0	1.0	200	1.11	NL	

Table C10. Shear wave velocity based analysis output of Meskel Square (amax=0.15g)

	Mw=	***5.5***													
Layer #	Layer Name	Depth,m	σv	σ'v	rd	CSR	FC ,%	Vs, Rec. (m/s)	CN	Vs1	Ka1	Ka2	VS1*	MSF	CRR	FS= CRR/CSR
1	Organic Clayey Silt	0.6	9	9	0.995	0.10	72	159	1.70	270	1.0	1.0	200	2.21	NL	
2	Organic Clayey Silt	1.2	18	18	0.991	0.10	72	159	1.54	244	1.0	1.0	200	2.21	NL	
3	Stiff Clayey silt	2.1	34	34	0.984	0.10	72	166	1.31	217	1.0	1.0	200	2.21	NL	
4	Stiff Clayey silt	3.0	50	50	0.977	0.10	72	179	1.19	212	1.0	1.0	200	2.21	NL	
5	Slightly Weath. Tuff	4.5	84	70	0.966	0.11	72	2470		2470	1.0	1.0	200	2.21	NL	
6	Fresh Welded Tuff	7.0	146	107	0.946	0.13	72	3172		3172	1.0	1.0	200	2.21	NL	
7	Soft silty sand	8.0	160	111	0.939	0.13	72	231	0.97	225	1.0	1.0	200	2.21	NL	
8	Soft silty sand	9.0	174	115	0.931	0.14	72	250	0.97	241	1.0	1.0	200	2.21	NL	
9	Soft silty sand	10.0	188	119	0.907	0.14	72	263	0.96	252	1.0	1.0	200	2.21	NL	

10	Soft silty sand	11.0	202	123	0.880	0.14	72	276	0.95	262	1.0	1.0	200	2.21	NL	
11	Soft silty sand	12.0	216	128	0.854	0.14	72	254	0.94	239	1.0	1.0	200	2.21	NL	
12	Soft silty sand	13.0	230	132	0.827	0.14	72	256	0.93	239	1.0	1.0	200	2.21	NL	
13	Soft silty sand	14.0	244	136	0.800	0.14	72	288	0.93	267	1.0	1.0	200	2.21	NL	
14	Soft silty sand	15.0	258	140	0.774	0.14	72	258	0.92	237	1.0	1.0	200	2.21	NL	
15	Soft silty sand	16.0	272	144	0.747	0.14	72	279	0.91	255	1.0	1.0	200	2.21	NL	
16	Soft silty sand	17.0	286	148	0.720	0.14	72	279	0.91	253	1.0	1.0	200	2.21	NL	
17	Soft silty sand	18.0	300	153	0.693	0.13	72	289	0.90	260	1.0	1.0	200	2.21	NL	
18	Soft silty sand	19.0	314	157	0.667	0.13	72	300	0.89	268	1.0	1.0	200	2.21	NL	
19	Soft silty sand	20.0	328	161	0.640	0.13	72	305	0.89	271	1.0	1.0	200	2.21	NL	
	Mw=	**6**														
Layer #	Layer Name	Depth,m	σv	σ'v	rd	CSR	FC ,%	Vs, (m/s)	CN	Vs1	Ka1	Ka2	VS1*	MSF	CRR	FS= CRR/CSR
1	Organic Clayey Silt	0.6	9	9	1.000	0.10	72	159	1.70	270	1.0	1.0	200	1.77	NL	
2	Organic Clayey Silt	1.2	18	18	0.991	0.10	72	159	1.54	244	1.0	1.0	200	1.77	NL	
3	Stiff Clayey silt	2.1	34	34	0.976	0.10	72	166	1.31	217	1.0	1.0	200	1.77	NL	
4	Stiff Clayey silt	3.0	50	50	0.959	0.09	72	179	1.19	212	1.0	1.0	200	1.77	NL	
5	Slightly Weathered Tuff	4.5	84	70	0.929	0.11	72	2470		2470	1.0	1.0	200	1.77	NL	
6	Fresh Welded Tuff	7.0	146	107	0.873	0.12	72	3172		3172	1.0	1.0	200	1.77	NL	
7	Soft silty sand	8.0	160	111	0.848	0.12	72	231	0.97	225	1.0	1.0	200	1.77	NL	
8	Soft silty sand	9.0	174	115	0.824	0.12	72	250	0.97	241	1.0	1.0	200	1.77	NL	
9	Soft silty sand	10.0	188	119	0.799	0.12	72	263	0.96	252	1.0	1.0	200	1.77	NL	
10	Soft silty sand	11.0	202	123	0.774	0.12	72	276	0.95	262	1.0	1.0	200	1.77	NL	
11	Soft silty sand	12.0	216	128	0.750	0.12	72	254	0.94	239	1.0	1.0	200	1.77	NL	
12	Soft silty sand	13.0	230	132	0.726	0.12	72	256	0.93	239	1.0	1.0	200	1.77	NL	
13	Soft silty sand	14.0	244	136	0.702	0.12	72	288	0.93	267	1.0	1.0	200	1.77	NL	
14	Soft silty sand	15.0	258	140	0.679	0.12	72	258	0.92	237	1.0	1.0	200	1.77	NL	
15	Soft silty sand	16.0	272	144	0.656	0.12	72	279	0.91	255	1.0	1.0	200	1.77	NL	
16	Soft silty sand	17.0	286	148	0.635	0.12	72	279	0.91	253	1.0	1.0	200	1.77	NL	
17	Soft silty sand	18.0	300	153	0.614	0.12	72	289	0.90	260	1.0	1.0	200	1.77	NL	
18	Soft silty sand	19.0	314	157	0.595	0.12	72	300	0.89	268	1.0	1.0	200	1.77	NL	
19	Soft silty sand	20.0	328	161	0.576	0.11	72	305	0.89	271	1.0	1.0	200	1.77	NL	
	Mw=	**6.5**														
Layer #	Layer Name	Depth,m	σv	σ'v	rd	CSR	FC ,%	Vs, (m/s)	CN	Vs1	Ka1	Ka2	VS1*	MSF	CRR	FS= CRR/CSR
1	Organic Clayey Silt	0.6	9	9	1.001	0.10	72	159	1.70	270	1.0	1.0	200	1.44	NL	
2	Organic Clayey Silt	1.2	18	18	0.993	0.10	72	159	1.54	244	1.0	1.0	200	1.44	NL	
3	Stiff Clayey silt	2.1	34	34	0.981	0.10	72	166	1.31	217	1.0	1.0	200	1.44	NL	
4	Stiff Clayey silt	3.0	50	50	0.967	0.09	72	179	1.19	212	1.0	1.0	200	1.44	NL	
5	Slightly Weathered Tuff	4.5	84	70	0.941	0.11	72	2470		2470	1.0	1.0	200	1.44	NL	
6	Fresh Welded Tuff	7.0	146	107	0.893	0.12	72	3172		3172	1.0	1.0	200	1.44	NL	
7	Soft silty sand	8.0	160	111	0.873	0.12	72	231	0.97	225	1.0	1.0	200	1.44	NL	
8	Soft silty sand	9.0	174	115	0.852	0.13	72	250	0.97	241	1.0	1.0	200	1.44	NL	

9	Soft silty sand	10.0	188	119	0.830	0.13	72	263	0.96	252	1.0	1.0	200	1.44	NL	
10	Soft silty sand	11.0	202	123	0.809	0.13	72	276	0.95	262	1.0	1.0	200	1.44	NL	
11	Soft silty sand	12.0	216	128	0.787	0.13	72	254	0.94	239	1.0	1.0	200	1.44	NL	
12	Soft silty sand	13.0	230	132	0.766	0.13	72	256	0.93	239	1.0	1.0	200	1.44	NL	
13	Soft silty sand	14.0	244	136	0.744	0.13	72	288	0.93	267	1.0	1.0	200	1.44	NL	
14	Soft silty sand	15.0	258	140	0.724	0.13	72	258	0.92	237	1.0	1.0	200	1.44	NL	
15	Soft silty sand	16.0	272	144	0.703	0.13	72	279	0.91	255	1.0	1.0	200	1.44	NL	
16	Soft silty sand	17.0	286	148	0.684	0.13	72	279	0.91	253	1.0	1.0	200	1.44	NL	
17	Soft silty sand	18.0	300	153	0.665	0.13	72	289	0.90	260	1.0	1.0	200	1.44	NL	
18	Soft silty sand	19.0	314	157	0.647	0.13	72	300	0.89	268	1.0	1.0	200	1.44	NL	
19	Soft silty sand	20.0	328	161	0.629	0.12	72	305	0.89	271	1.0	1.0	200	1.44	NL	
	Mw=	**6.8**														
Layer #	Layer Name	Depth,m	σv	σ'v	rd	CSR	FC ,%	Vs, (m/s)	CN	Vs1	Ka1	Ka2	VS1*	MSF	CRR	FS= CRR/CSR
1	Organic Clayey Silt	0.6	9	9	1.001	0.10	72	159	1.70	270	1.0	1.0	200	1.28	NL	
2	Organic Clayey Silt	1.2	18	18	0.994	0.10	72	159	1.54	244	1.0	1.0	200	1.28	NL	
3	Stiff Clayey silt	2.1	34	34	0.983	0.10	72	166	1.31	217	1.0	1.0	200	1.28	NL	
4	Stiff Clayey silt	3.0	50	50	0.971	0.09	72	179	1.19	212	1.0	1.0	200	1.28	NL	
5	Slightly Weathered Tuff	4.5	84	70	0.949	0.11	72	2470		2470	1.0	1.0	200	1.28	NL	
6	Fresh Welded Tuff	7.0	146	107	0.906	0.12	72	3172		3172	1.0	1.0	200	1.28	NL	
7	Soft silty sand	8.0	160	111	0.888	0.12	72	231	0.97	225	1.0	1.0	200	1.28	NL	
8	Soft silty sand	9.0	174	115	0.869	0.13	72	250	0.97	241	1.0	1.0	200	1.28	NL	
9	Soft silty sand	10.0	188	119	0.850	0.13	72	263	0.96	252	1.0	1.0	200	1.28	NL	
10	Soft silty sand	11.0	202	123	0.830	0.13	72	276	0.95	262	1.0	1.0	200	1.28	NL	
11	Soft silty sand	12.0	216	128	0.810	0.13	72	254	0.94	239	1.0	1.0	200	1.28	NL	
12	Soft silty sand	13.0	230	132	0.791	0.13	72	256	0.93	239	1.0	1.0	200	1.28	NL	
13	Soft silty sand	14.0	244	136	0.771	0.13	72	288	0.93	267	1.0	1.0	200	1.28	NL	
14	Soft silty sand	15.0	258	140	0.752	0.13	72	258	0.92	237	1.0	1.0	200	1.28	NL	
15	Soft silty sand	16.0	272	144	0.733	0.13	72	279	0.91	255	1.0	1.0	200	1.28	NL	
16	Soft silty sand	17.0	286	148	0.715	0.13	72	279	0.91	253	1.0	1.0	200	1.28	NL	
17	Soft silty sand	18.0	300	153	0.697	0.13	72	289	0.90	260	1.0	1.0	200	1.28	NL	
18	Soft silty sand	19.0	314	157	0.680	0.13	72	300	0.89	268	1.0	1.0	200	1.28	NL	
19	Soft silty sand	20.0	328	161	0.663	0.13	72	305	0.89	271	1.0	1.0	200	1.28	NL	
	Mw=	**7**														
Layer #	Layer Name	Depth,m	σv	σ'v	rd	CSR	FC ,%	Vs, (m/s)	CN	Vs1	Ka1	Ka2	VS1*	MSF	CRR	FS= CRR/CSR
1	Organic Clayey Silt	0.6	9	9	1.001	0.10	72	159	1.70	270	1.0	1.0	200	1.19	NL	
2	Organic Clayey Silt	1.2	18	18	0.995	0.10	72	159	1.54	244	1.0	1.0	200	1.19	NL	
3	Stiff Clayey silt	2.1	34	34	0.985	0.10	72	166	1.31	217	1.0	1.0	200	1.19	NL	
4	Stiff Clayey silt	3.0	50	50	0.974	0.09	72	179	1.19	212	1.0	1.0	200	1.19	NL	
5	Slightly Weathered Tuff	4.5	84	70	0.954	0.11	72	2470		2470	1.0	1.0	200	1.19	NL	
6	Fresh Welded Tuff	7.0	146	107	0.915	0.12	72	3172		3172	1.0	1.0	200	1.19	NL	
7	Soft silty sand	8.0	160	111	0.898	0.13	72	231	0.97	225	1.0	1.0	200	1.19	NL	

8	Soft silty sand	9.0	174	115	0.880	0.13	72	250	0.97	241	1.0	1.0	200	1.19	NL	
9	Soft silty sand	10.0	188	119	0.863	0.13	72	263	0.96	252	1.0	1.0	200	1.19	NL	
10	Soft silty sand	11.0	202	123	0.844	0.13	72	276	0.95	262	1.0	1.0	200	1.19	NL	
11	Soft silty sand	12.0	216	128	0.826	0.14	72	254	0.94	239	1.0	1.0	200	1.19	NL	
12	Soft silty sand	13.0	230	132	0.808	0.14	72	256	0.93	239	1.0	1.0	200	1.19	NL	
13	Soft silty sand	14.0	244	136	0.789	0.14	72	288	0.93	267	1.0	1.0	200	1.19	NL	
14	Soft silty sand	15.0	258	140	0.771	0.14	72	258	0.92	237	1.0	1.0	200	1.19	NL	
15	Soft silty sand	16.0	272	144	0.754	0.14	72	279	0.91	255	1.0	1.0	200	1.19	NL	
16	Soft silty sand	17.0	286	148	0.736	0.14	72	279	0.91	253	1.0	1.0	200	1.19	NL	
17	Soft silty sand	18.0	300	153	0.719	0.14	72	289	0.90	260	1.0	1.0	200	1.19	NL	
18	Soft silty sand	19.0	314	157	0.703	0.14	72	300	0.89	268	1.0	1.0	200	1.19	NL	
19	Soft silty sand	20.0	328	161	0.687	0.14	72	305	0.89	271	1.0	1.0	200	1.19	NL	
	Mw=	**7.2**														
Layer #	Layer Name	Depth,m	σv	σ'v	rd	CSR	FC ,%	Vs, (m/s)	CN	Vs1	Ka1	Ka2	VS1*	MSF	CRR	FS= CRR/CSR
1	Organic Clayey Silt	0.6	9	9	1.002	0.10	72	159	1.70	270	1.0	1.0	200	1.11	NL	
2	Organic Clayey Silt	1.2	18	18	0.996	0.10	72	159	1.54	244	1.0	1.0	200	1.11	NL	
3	Stiff Clayey silt	2.1	34	34	0.987	0.10	72	166	1.31	217	1.0	1.0	200	1.11	NL	
4	Stiff Clayey silt	3.0	50	50	0.977	0.10	72	179	1.19	212	1.0	1.0	200	1.11	NL	
5	Slightly Weathered Tuff	4.5	84	70	0.959	0.11	72	2470		2470	1.0	1.0	200	1.11	NL	
6	Fresh Welded Tuff	7.0	146	107	0.924	0.12	72	3172		3172	1.0	1.0	200	1.11	NL	
7	Soft silty sand	8.0	160	111	0.908	0.13	72	231	0.97	225	1.0	1.0	200	1.11	NL	
8	Soft silty sand	9.0	174	115	0.892	0.13	72	250	0.97	241	1.0	1.0	200	1.11	NL	
9	Soft silty sand	10.0	188	119	0.876	0.13	72	263	0.96	252	1.0	1.0	200	1.11	NL	
10	Soft silty sand	11.0	202	123	0.859	0.14	72	276	0.95	262	1.0	1.0	200	1.11	NL	
11	Soft silty sand	12.0	216	128	0.842	0.14	72	254	0.94	239	1.0	1.0	200	1.11	NL	
12	Soft silty sand	13.0	230	132	0.825	0.14	72	256	0.93	239	1.0	1.0	200	1.11	NL	
13	Soft silty sand	14.0	244	136	0.808	0.14	72	288	0.93	267	1.0	1.0	200	1.11	NL	
14	Soft silty sand	15.0	258	140	0.791	0.14	72	258	0.92	237	1.0	1.0	200	1.11	NL	
15	Soft silty sand	16.0	272	144	0.775	0.14	72	279	0.91	255	1.0	1.0	200	1.11	NL	
16	Soft silty sand	17.0	286	148	0.758	0.14	72	279	0.91	253	1.0	1.0	200	1.11	NL	
17	Soft silty sand	18.0	300	153	0.742	0.14	72	289	0.90	260	1.0	1.0	200	1.11	NL	
18	Soft silty sand	19.0	314	157	0.727	0.14	72	300	0.89	268	1.0	1.0	200	1.11	NL	
19	Soft silty sand	20.0	328	161	0.712	0.14	72	305	0.89	271	1.0	1.0	200	1.11	NL	